Gauge/gravity duality:
From quantum phase transitions towards out-of-equilibrium physics

Dissertation der Fakultät für Physik
der
Ludwig-Maximilians-Universität München

vorgelegt von HAI **NGO THANH**
aus Hanoi, Vietnam

München, 2. Mai 2011

Dissertation

by Ngô Thanh Hai
born on February 19th, 1981 in Hà Nội, Việt Nam

supervised by PD Dr. Johanna Karen Erdmenger
Max-Planck-Institut für Physik, München

1st Referee: PD Dr. Johanna Karen Erdmenger
2nd Referee: Prof. Dr. Dieter Lüst

Date of oral examination: July 14th, 2011

Contents

Zusammenfassung

Diese Dissertation beschäftigt sich mit den Anwendungen der AdS/CFT-Korrespondenz, die in ihren Erweiterungen durch eine Dualität zwischen einer nicht-abelschen Eichtheorie und einer Gravitationstheorie verallgemeinert wird, und auch Eichtheorie/ Gravitations-Dualität oder Holographie genannt wird. Mittels dieser Dualität ist es möglich, störungstheoretische Berechnungen im Rahmen einer schwach wechselwirkenden Gravitationstheorie in Observablen einer stark gekoppelten Quantenfeldtheorie zu übersetzen. Von besonderem Interesse für die vorliegende Arbeit sind Phänomene wie Quantenphasenübergänge, quantenkritische Punkte (QKP), elektrischer Ladungstransport bei starker Kopplung und der Thermalisierungsprozess von stark gekoppelten Systemen. Die in dieser Arbeit diskutierten Themen können als Modelle zur Beschreibung der Physik der kondensierten Materie in einer supraleitenden Phase in der Umgebung eines quantenkritischen Punktes oder zur Beschreibung der Eigenschaften des Quark-Gluon-Plasmas (QGP) benutzt werden.

Der QKP tritt auf, wenn Phasenübergänge am absoluten Nullpunkt kontinuierlich ablaufen. Am quantenkritischen Punkt wird der Phasenübergang durch Quantenfluktuationen ausgelöst, nicht durch thermische Fluktuationen wie beim herkömmlichen Phasenübergang. Durch das Zusammenspiel thermischer Anregungen mit der Quantenkritikalität ergeben sich weitreichende Konsequenzen für grosse Bereiche im Phasendiagram in einer Umgebung des QKPs, sogar bei endlichen Temperaturen. Diese Bereiche werden als quantenkritische Region bezeichnet. Es wird vermutet, dass das Phänomen der Hochtemperatursupraleitung in Verbindung mit der quantenkritischen Region gebracht werden kann.

Das Quark-Gluon-Plasma ist ein Aggregatzustand, der in Experimenten an Schwerionenbeschleunigern realisiert wurde, wenn auch nur für sehr kurze Zeitspannen. Es handelt sich um stark wechselwirkende Quarks und Gluonen, die nicht in Hadronen eingeschlossen sind. Das QGP ist damit besonders gut für Anwendungen der Eichtheorie/Gravitations-Dualität geeignet, um interessante Eigenschaften stark gekoppelter Systeme zu untersuchen.

In der vorliegenden Arbeit untersuchen wir mittels der Eichtheorie/Gravitations-Dualität Phänomene, die in einem stark gekoppelten System auftauchen, welches sich in einem thermischen Gleichtgewicht befindet, nur eine kleine Störung des Gleichgewichts beschreibt oder sogar weit vom Gleichgewicht entfernt ist.

Wir beginnen mit Systemen im Gleichgewicht und konstruieren holographische Supraflüssigkeit bei endlicher Baryon- und Isospinladungsdichte. Zu diesem Zweck benutzen wir zwei Ansätze, nämlich den 'bottom-up-Ansatz' mit einer $U(2)$ Einstein-

Yang-Mills Theorie unter Berücksichtigung der Rückwirkung der eingeschalteten Felder auf die Hintergrundgeometrie und den 'top-down-Ansatz' mit einer D3/D7 Brane-Konfiguration mit zwei koinzidenten D7-Probebranen, d. h. ohne Rückwirkung auf die Geometrie. In beiden Fällen beobachten wir Phasenübergänge von einer normalleitenden zu einer supraleitenden Phase, sowohl bei endlichen Temperaturen als auch beim absoluten Nullpunkt. Wir untersuchen die Ordnungen der Phasenübergänge am absoluten Nullpunkt und stellen fest, dass in der D3/D7 Brane-Konfiguration der Phasenübergang immer von zweiter Ordnung ist, während der Phasenübergang bei der $U(2)$ Einstein-Yang-Mills Theorie – abhängig von der Stärke der Rückwirkung – entweder von erster oder von höheren Ordnungen ist.

Wir gehen dann zu Systemen über, die leicht aus dem Gleichgewicht sind. Dafür benutzen wir eine D3/D7 Brane-Konfiguration mit koinzidenten D7-Probebranen und berechnen die elektrische Leitfähigkeit der massiven $\mathcal{N} = 2$ supersymmetrischen Hypermultiplettfelder, d. h. der fundamentalen Flavorfelder, die durch ein $\mathcal{N} = 4$ Super- Yang-Mills Plasma propagieren. Dazu führen wir eine baryonische Ladungsdichte und konstante elektromagnetische Felder ein. Diese Konfiguration beschreibt ein Modell für das Propagieren von geladenen Quarks durch das QGP. Wir berechnen alle Komponenten des Leitfähigkeitstensors, die dem Transport von baryonischen Ladungsträgern zugehörig sind. Wir bestimmen den Beitrag von Flavorfeldern zum gesamten Energie-Impuls-Tensor und können die Energie- und Impuls-Verlustraten der Flavorfeldern an das umgebende Plasma identifizieren. Wir finden einen Strom, der Anomalien aufweist, wenn das Magnetfeld eine zum elektrischen Feld parallel gerichtete Komponente hat. Dieser Strom kann benutzt werden, um Ladungstransport in der Anwesenheit von Anomalien zu untersuchen.

Hinsichtlich der Systeme, die sich im starken Ungleichgewicht befinden, untersuchen wir eine zeitabhängige Hintergrundgeometrie, welche durch einen sich bewegenden Spiegel im Anti-de Sitter Raum dargestellt wird. Dieser Hintergrund kann als einfaches Modell gesehen werden, das für die Formulierung eines holographischen Thermalisierungsprozesses von Relevanz ist. Für diese Konfiguration entwickeln wir eine Vorschrift für die Berechnung von zeitabhängigen Zweipunktfunktionen von skalaren Fluktuationen, die auf einer WKB-Näherungsmethode basiert. Wir testen unsere Vorschrift für zwei Klassen von Spiegeltrajektorien und stellen fest, dass die Singularitätsstruktur der Zweipunktfunktionen in Übereinstimmung mit der geometrischen Optik ist.

Diese Dissertation wurde in der Arbeitsgruppe von PD Dr. J. K. Erdmenger am Max-Planck-Institut für Physik (Werner-Heisenberg-Institut) in München angefertigt. Die in dieser Dissertation dargelegten neuen Erkenntnisse wurden in folgenden Publikationen veröffentlicht.

[1] M. Ammon, T. H. Ngo, A. O'Bannon, *Holographic Flavor Transport in Arbitrary Constant Background Fields*, JHEP **10** (2009) 027, arXiv:0908.2625.

[2] J. Erdmenger, S. Lin, T. H. Ngo, *A moving mirror in AdS space as a toy model for holographic thermalization*, JHEP **04** (2011) 035, arXiv:1101.5505.

[3] J. Erdmenger, P. Kerner, V. Grass, T. H. Ngo, *Holographic Superfluidity in Imbalanced Mixtures*, arXiv:1103.4145.

Abstract

In this dissertation we use gauge/gravity duality to investigate various phenomena of strongly coupled field theories. Of special interest are quantum phase transitions, quantum critical points, transport phenomena of charges and the thermalization process of strongly coupled medium. The systems studied in this thesis might be used as models for describing condensed matter physics in a superfluid phase near the quantum critical point and the physics of quark-gluon plasma (QGP), a deconfinement phase of QCD, which has been recently created at the Relativistic Heavy Ion Collider (RHIC).

Moreover, we follow the line of considering different gravity setups whose dual field descriptions show interesting phenomena of systems in thermal equilibrium, slightly out-of-equilibrium and far-from-equilibrium.

We first focus on systems in equilibrium and construct holographic superfluids at finite baryon and isospin charge densities. For that we use two different approaches, the bottom-up with an $U(2)$ Einstein-Yang-Mills theory with back-reaction and the top-down approach with a D3/D7 brane setup with two coincident D7-brane probes. In both cases we observe phase transitions from a normal to a superfluid phase at finite and also at zero temperature. In our setup, the gravity duals of superfluids are Anti-de Sitter black holes which develop vector-hair. Studying the order of phase transitions at zero temperature, in the D3/D7 brane setup we always find a second order phase transition, while in the Einstein-Yang-Mills theory, depending on the strength of the back-reaction, we obtain a continuous or first order transition.

We then move to systems which are slightly out-of-equilibrium. Using the D3/D7 brane setup with N_c coincident D3-branes and N_f coincident D7-brane probes, we compute transport coefficients associated with massive $\mathcal{N} = 2$ supersymmetric hypermultiplet fields propagating through an $\mathcal{N} = 4$ $SU(N_c)$ super Yang-Mills plasma in the limit of $N_f \ll N_c$. Introducing a baryon number density and arbitrary constant electric and magnetic fields, we compute all components of the conductivity tensor associated with transport of baryon number charge. Determining the contribution that the flavor degrees of freedom make to the stress-energy tensor, we are able to identify the rates of energy and momentum loss of the flavor field to the plasma. We find one current which is anomalous when the magnetic field has a component parallel to the electric field. This current may be related to the study of charge transport in the presence of anomalies.

Going towards systems far-from-equilibrium, we investigate a time-dependent geometry consisting of a mirror moving in the bulk of the Anti-de Sitter space. This geometry can be seen as a toy model which is relevant to the formulation of holographic

thermalization in strongly coupled field theory. For this configuration, we establish a procedure for calculating time-dependent two-point functions of scalar fluctuations, based on a WKB approximation. We test our method on two sample trajectories for the mirror, and find that the singularity structure of the two-point functions is in agreement with geometric optics.

The main results presented in this thesis have been obtained by the author in collaboration with various members of the group of PD Dr. J. K. Erdmenger at the Max-Planck-Institut für Physik (Werner-Heisenberg-Institut) in Munich, Germany during the time from May 2008 to April 2011. The relevant publications are listed below [1–3].

[1] M. Ammon, T. H. Ngo, A. O'Bannon, *Holographic Flavor Transport in Arbitrary Constant Background Fields*, JHEP **10** (2009) 027, arXiv:0908.2625.

[2] J. Erdmenger, S. Lin, T. H. Ngo, *A moving mirror in AdS space as a toy model for holographic thermalization*, JHEP **04** (2011) 035, arXiv:1101.5505.

[3] J. Erdmenger, P. Kerner, V. Grass, T. H. Ngo, *Holographic Superfluidity in Imbalanced Mixtures*, arXiv:1103.4145.

Introduction and overview

Particle physics has been driven by the quest for a unified theory of all fundamental interactions between elementary particles in nature. A particularly promising candidate is string theory which predicts all types of particles and interactions within a single theoretical framework. However, string theory has recently lead also to new relations between different branches of physics. This is due to the AdS/CFT correspondence which arises in the context of studying D-branes in superstring theory. It describes a conjecture of a duality between a superstring theory and a superconformal field theory. We comment on some developments and recent applications of the correspondence on strong coupling problems of real-world physics, which are even of interest to condensed matter physics, and thereby present the motivation for this dissertation. Finally, we give an overview of the thesis where we follow the line of studying phenomena of strongly coupled systems in equilibrium towards systems out-of-equilibrium using AdS/CFT methods.

1.1 The dream of a complete theory of physics

In nature there are four known fundamental interactions between elementary particles: the electromagnetic one which acts between electrically charged particles, the weak interaction which is responsible for nuclear phenomena such as beta decay, the strong interaction which holds together the subatomic particles e. g. of the nucleus and the gravity which is described by attractive forces between massive particles.

One of the great ambitions in theoretical particle physics is to unify all fundamental forces and relationships between elementary particles in terms of a single theoretical framework. Here, one basic concept of representing fundamental interactions is based on the principle that fundamental forces can be described by exchange particles, the mediating gauge bosons. So far, besides gravity the remaining three interactions are successfully formulated by a theory known as the standard model (SM) of particle physics. The SM in the current formulation has been completed in the mid 1970s. It is a quantum field theory. The general relativity published by Einstein in 1916, however, is not formulated as a quantum theory, it is a classical theory of gravitation.

The gauge group of the standard model is $SU(3)_c \times SU(2)_I \times U(1)_Y$. There are twelve mediating gauge *bosons* representing different force carriers: the eight gluons for the strong color force, the W^+, W^- and Z^0 for the weak force, and the photon γ for the electromagnetic force. The unification of the electromagnetic and weak interaction to *electroweak* interaction is accomplished under the group $SU(2)_I \times U(1)_Y$. Starting with four massless gauge bosons, a process of spontaneous symmetry breaking from $SU(2)_I \times U(1)_Y$ to $U(1)_{em}$ caused by the Higgs mechanism gives mass to the carriers of the weak force $W^\pm$ and Z^0. The particle that remains massless is the photon γ which is the force carrier of the electromagnetic interaction. The theory of strong interactions is governed by a $SU(3)_c$ Yang-Mills theory which is known as quantum chromodynamics (QCD). While all force carriers are bosons, all matter particles in the SM are *fermions*. Matter particles are divided in two types: leptons and quarks. To each charged lepton, there is a corresponding neutral lepton, the neutrino. Including the anti-particles, there are twelve leptons in total. While charged leptons – electron, myon and tau – are subject to electromagnetic and weak interactions, the neutrinos only participate in weak interactions. The quarks carry color charge, electric charge and also participate to weak interaction. There are six different types of quarks denoted by six different flavors, i.e. up, down, strange, charm, bottom and top. Each quark comes in three colors, hence there exist eighteen different kinds of quarks. Adding the leptons and quarks together and including the anti-particles, the number of matter particles sums up to forty-eight. The SM has been tested extensively in a large number of experiments at many particle accelerators. Up to the energy of about 100 GeV, there is no experimental result which contradicts the standard model. In year 2000, with the discovery of the tau-neutrino [4] the last matter particle of the standard model has been observed directly. The only missing particle of the SM is the hypothetical Higgs boson which is responsible for giving mass to all elementary particles. The mass of the Higgs particle is expected to be between $115 - 185$ GeV, depending on the different models used. It is widely believed that the Higgs boson should be observed at the Large Hadron Collider (LHC) within a few years.

Up to the present day the standard model summarizes completely the present knowledge of particle physics, however, it is not a complete theory of physics because of two reasons: It does not include gravity and it contains about twenty free parameters that cannot be calculated within its framework and have to be put into the model by hand [5]. For improving the situation concerning the latter reason, there have been many efforts in formulating a Grand Unified Theory (GUT) which would unify the electroweak and the strong forces, and reduce the number of independent input parameters. Despite of many impressive progress, a breakthrough in this direction is still expected. Another possibility is the enlargement of the SM by including supersymmetry (SUSY). It is a symmetry that relates fermions to bosons and vice versa, thus SUSY unifies matter and forces. In a theory with supersymmetry, bosons and fermions appear in pairs of equal mass. The fact that no superpartner of any elementary particle in the SM has been observed so far might be explained by the spontaneous supersymmetry breaking at low energies which gives greater mass to the superparticles. Many physicists believe that if supersymmetry exists in nature, the superparticles will eventually be discovered at the LHC within this decade.

At present, GUT and SUSY appear to be two necessary, but eventually optional, steps towards constructing a complete theory of physics. The crucial step, however, is the incorporating of gravity into the elementary particle physics framework. Here, the major difficulty is that while the standard model is described by a quantum field theory, general relativity is described by a classical one. Given the successes of the standard model, Einstein's general relativity should be turned into a quantum field theory, but all efforts so far yield theories of quantum gravity which are either incalculable or totally unpredictive [5]. Among different approaches, superstring theory seems to be one of the brightest candidate for a unified theory of all four known fundamental forces in nature.

1.2 String theory and the AdS/CFT correspondence

In string theory, see e.g. [5,6], elementary point-like particles with their corresponding properties are represented by various vibrational modes of a microscopic one-dimensional object called elementary string. There is only one dimensionful parameter which can be chosen to be the characteristic string length which sets the scale in which the theory operates. String theory is said to have no adjustable parameter, i.e. no dimensionless parameter is needed to formulate the theory. The string coupling, for instance, is rather a dynamical parameter which is determined by the value of the dilaton field. This is an ideal property in a unified theory of all interactions, because the string coupling might be calculable. In string theory there are open and closed strings. The strings interact via the process of joining and splitting, thus open strings can close to form closed strings, and in general we do not consider theories with only open strings. The key argument why string theory might be an appropriate candidate for a unified theory of physics is due to the fact that graviton arises naturally when closed strings are quantized. This means that string theory is a *quantum theory of gravity*. Unfortunately, string theory has been not well understood so far. Arising in the late 1960s, up to the present day it has been remained an unfinished theory and is still considered to be at an early stage of development. String theory, moreover, requires extra dimensions. So far there has been no experimental verification of string theory, but nevertheless, it is believed that recent developments at Tevatron and future developments at LHC might help for finding signatures predicted by string theory [7,8].

Motivated by experimental data relevant to hadronic scattering, bosonic string theory was invented in the late 1960s as an attempt to describe the strong nuclear force which binds the quarks together. This bosonic string theory is consistent only in 26 space-time dimensions and suffered from several unphysical features like the absence of fermions and the presence of a tachyon [5]. During the 1970s supersymmetry has been built into string theory to form *superstring theory*, which is free of tachyons and consistent in 10-dimensional space-time [6]. Moreover, its spectrum contains bosons and fermions, thus SUSY serves as a very important ingredient in string theory. By the mids 1980s there are five known superstring theories: type I theory of open and closed *unoriented* strings; type IIA and IIB of closed *oriented* strings; heterotic string theory with gauge group $E_8 \times E_8$; and heterotic string theory with gauge group $SO(32)$. At that time some relationships between the five theories were known, but only after the

discovery of the 11-dimensional M-theory[1] as the large coupling limit of type IIA in the late 1990s, a clearer picture emerged. The five superstring theories and the M-theory are all related by transformations which are combinations of the so-called S-, T- and U-dualities, see e.g. [9]. This discovery implies that the five superstring theories and the M-theory might be just different limits of one unique theory which still remains mysterious to the present day.

String theory in the contemporary formulation is not only a theory of one-dimensional strings, it also contains higher-dimensional objects called D-branes. There are two descriptions of D-branes, namely D-branes as solitonic solutions to the low-energy effective action of type II supertrings and D-branes as dynamical spatial extended objects[2] where open strings can end. Using the latter description, it is possible to construct the standard model since the dynamics of open strings on the D-branes gives rise to effective world-volume field theories. The gauge group of the SM is realized by a specific configuration of stacks of coincident D-branes, and gauge and matter particles arise from vibrations of open strings that stretch between D-branes[3]. Combining the study of field theories on the world-volume of a stack of N_c coincident D3-branes and the study of D3-branes as solitonic solutions of type IIB supergravity, a low-energy effective action of type IIB superstring, Maldacena came to a conjecture in 1997 which states that the superconformal $\mathcal{N} = 4$ $\mathrm{SU}(N_c)$ super Yang-Mills (SYM) theory in $(3+1)$- dimensions describes the same physics as type IIB superstring theory on an $\mathrm{AdS}_5 \times \mathrm{S}^5$ background (AdS). Here AdS_5 denotes the five-dimensional Anti-de Sitter space, S^5 a five-sphere, N_c the number of the colors of the field theory and $\mathcal{N} = 4$ the number of the supercharges [10]. This formulation is the prototype of the so-called AdS/CFT correspondence which is a *holographic* duality, since it claims a physical equivalence between a four-dimensional gauge theory and a ten-dimensional closed superstring theory.

Soon after the formulation of the conjecture presented in [10], the duality has been elaborated by Witten, Gubser et al. [11, 12], where the correspondence is given explicitly by the mappings between the parameters and the generating functional of correlation functions of the two theories. There are plenty of arguments and tests supporting the correctness of the correspondence, see section 2.1.5 for more detail and [13, 14] for a review. Since the string partition function of type IIB superstring on $\mathrm{AdS}_5 \times \mathrm{S}^5$ is not well understood, most subsequent developments of the duality are in the limits of *large N_c and large 't Hooft coupling constant*, where type IIB superstring reduces to type IIB supergravity, hence making explicit computations on the gravity side feasible. Furthermore, in these limits the AdS/CFT describes a duality between a *weakly* coupled gravity theory and a *strongly* coupled field theory. Thus it provides a powerful tool by means of using gravity to study field theories at strong coupling

---

[1]M-theory is not a string theory. It is a theory of membranes. In M-theory, there are 2-branes and 5-branes. They should not be confused with D-branes.

[2]A Dp-brane is a p-spatial extended object in string theory. The world-volume of a Dp-brane is $(p + 1)$-dimensional.

[3]Our 4-dimensional world is part of the D-branes, but these D-branes happen to have more than three spatial dimensions. The extra dimensions are wrapped on compact spaces. Depending on the detail of the wrapping, there exists a huge number of string models which are consistent with the SM. Because of this possiblity string theory suffers from its predictive power [5].

where conventional perturbative methods fail to hold. Morever, the idea of AdS/CFT has been generalized to cases which are more relevant to real-world physics. These generalizations are referred to as gauge/gravity duality.

Using the methods developed in gauge/gravity duality, it is expected to gain new insights in phenomena arising at strongly coupled field theory systems. Recently, there has been many efforts in applying gauge/gravity duality for the studies of strong coupling problems in condensed matter physics such as the pairing mechanism in high T_c superconductors or transport phenomena of charges near the quantum critical point known as the quantum critical region. As a first step towards studying high T_c superconductivity, prescriptions for constructing holographic systems which resemble signatures of superconductors or superfluids are needed. So far there are two known approaches for constructing holographic systems which show transitions from a normal to a superconducting phase, namely the *bottom-up* approach where the dual field theory is not specified [15, 16] and the *top-down* approach where the dual field theory is explicitly known [17, 18]. More technical details about these two approaches will be discussed later in section 3.2.2. For more information about the recent developments utilizing these ideas presented in [15–18] we refer to the reviews [19–23]. Looking for universal features of quantum critical transport, where the transport coefficients are not determined by collision rate, but by universal constants of nature [24], it is desirable to study systems which possess a quantum critical point and hence a quantum critical region. A quantum point occurs if the phase transition at zero temperature, i.e. quantum phase transition, is at least of second order, i.e. continuous. So far there are only a few known holographic systems which seem to have such a quantum critical point [25–28]. In chapter 3 we will consider two gravity setups which are dual to holographic superfluids and study the quantum phase transitions in these systems.

Another prominent example of strongly interacting matter is the quark-gluon plasma (QGP) which has been created at the Relativistic Heavy Ion Collider (RHIC) [29–31]. QGP is a phase of QCD at extremely high temperatures and densities where quarks and gluons are no longer confined in hadrons. The fact that QGP does not behave like a dilute gas of quasi-particles, but rather follows the laws of hydrodynamics like a perfect fluid has been predicted by calculations using methods from AdS/CFT [32]. The famous result of $1/4\pi$ for the ratio the shear viscosity over entropy density for the QGP, which is assumed to be a nearly perfect fluid, has been confirmed to be of the same range with experimental data. This value is a universal of for a large class of strongly interacting quantum field theories and serves as a lower bound for quantum perfect fluids [33]. Within the framework of the AdS/CFT correspondence, the quark-gluon plasma near-equilibrium is quite well understood. In this regime the dynamics of QGP is governed by hydrodynamics which is mapped to the study of perturbations of AdS black hole geometry, see [34] for a review. In particular, some near-equilibrium phenomena like transport of charge, jet quenching due to parton energy loss, quarkonium suppression and drag force within the plasma can be found in [35–39]. In chapter 4 of this thesis, we will present a gravity setup which serves as a model to study transport properties such as conductivity, momentum and energy loss rates of partons moving through the QGP. While the near-equilibrium properties of QGP is well described by gauge/gravity duality, the complete thermalization process

of quark-gluon plasma requires the understanding of strongly coupled field theory far-from-equilibrium. Using the methods from AdS/CFT correspondence, it is at least in principle possible to describe such a process. The AdS/CFT states that while a strongly coupled field theory at zero temperature corresponds to an AdS background, a field theory at finite temperature is dual to an AdS black hole metric. Thus it is expected that a process of forming a black hole horizon on the gravity side will correspond to a process of thermalization in the dual field theory. Some works along this direction include gravity models which are obtained analytically in the limit of quasi-equilibrium [40, 41] and numerically at far-from-equilibrium stages of thermalization [42–44]. Some further approaches towards describing holographic thermalization will be discussed later in chapter 5 when we study a moving mirror in AdS space as a toy model for holographic thermalization.

1.3 Overview of the thesis

In this thesis we discuss four different gravity setups which are motivated by using the methods developed in gauge/gravity duality for exploring phenomena of strongly coupled field theory. In particular, we begin with systems in thermal equilibrium, then move to near-equilibrium systems and finally consider an example which is relevant for far-from-equilibrium physics.

The first two gravity setups presented in chapter 3 are related to phenomena of strongly coupled systems in *equilibrium* such as quantum phase transitions and quantum critical points. Here, both the bottom-up and top-down approaches mentioned in 1.2 and later in 3.2.2 are used for the construction of holographic superfluids. In both setups we use two physically independent tuning parameters for reproducing the phase diagram. We study the quantum phase transitions and search for the presence of a possible quantum critical point.

In the third gravity setup presented in chapter 4, we study *near-equilibrium* phenomena such as transport of charges, energy and momentum loss of charge carriers moving through a conducting medium. This setup serves a model for describing partons moving in the *near-equilibrium* QGP. In order to study transport phenomena, we need to disturb the system, thus bring the system to an out-of-equilibrium state, and study its responses on external perturbations. In particular, using a method from gauge/gravity duality, we can study effects beyond linear response theory.

In the last gravity setup in chapter 5, we study a time-dependent process in the $AdS_5 \times S^5$ background by considering a mirror moving in the bulk of the AdS space. This setup should be seen as a first step towards a larger program, e.g. later replacing the arbitrary mirror trajectory by a more physical trajectory determined by gravitational collapse processes in AdS black hole geometries. The ultimate aim of such a program would be a holographic formulation of thermalization where the physics at different stages from *far-from-equilibrium* to *equilibrium* might be studied analytically.

In the following paragraphs, we give a detail description of the main content of the thesis which can be roughly divided in three parts, namely quantum phase transitions in holographic superfluids, flavor transport in $\mathcal{N} = 4$ SYM plasma and moving mirror as a toy model for holographic thermalization.

Quantum phase transitions in holographic superfluids   This part of the thesis is motivated by phenomena in *thermal equilibrium* which arise in quantum critical theories. In particular, it is the quantum critical point (QCP) which is represented by a continuous phase transition at zero temperature [24]. The physics of the quantum critical region near the QCP may be described by a critical theory even at finite temperature [45–47]. There are speculations that quantum phase transitions might be important in describing high T_c-superconductors like cuprates, non-Fermi liquids or superconducting-insulator transitions in thin metallic films, see e.g. [19, 20, 46, 47].

On the other hand gauge/gravity duality provides a novel method for studying strongly correlated systems at finite temperature and densities. Recently, there are many efforts in applying gauge/gravity to study strongly coupled condensed matter physics at low temperatures, including phenomena like superconductivity and superfluidity. Using the gauge/gravity duality it is possible to construct physical systems which show a phase transition from a normal to a superconducting phase, see e.g. the reviews [19–22]. Thus it is of great interest to study whether it is possible to construct holographic models which show phase transitions at zero temperature, and eventually also a quantum critical point.

So far most of studied systems showing the transition to a holographic *superfluid* have only been considered with one control parameter, usually the ratio of the temperature to the isospin chemical potential. In such systems the phase transition is at a finite temperature and thus these systems have no quantum phase transition, see e.g. [17, 48]. In chapter 3 we construct gravity systems which resemble a p-wave superfluid with continuous phase transitions at zero temperature and thus possess quantum critical points. Compared to [17, 48], that can be done by introducing a further chemical potential, the baryon chemical potential, as a second control parameter. Here, another motivation for studying quantum phase transitions at finite baryon and isospin chemical potential using gauge/gravity methods is that there are also studies about quantum phase transitions at finite baryon and isospin chemical potential from QCD [49, 50]. We can use them to compare with our results obtained from gravity models.

In sections 3.3 and 3.4 we use two different approaches to construct holographic superfluids, the bottom-up [15, 16] and the top-down approach [17, 18]. More precisely, in the bottom-up approach, we consider the $\mathrm{U}(2)$ Einstein-Yang-Mills (EYM) theory and allow the gauge fields to back-react on the geometry in order to get a coupling between the overall $\mathrm{U}(1)$ and the $\mathrm{SU}(2)$ gauge fields whose time-components give rise to the baryon and isospin chemical, respectively. In the top-down approach in section 3.4, we consider the D3/D7 brane setup with two coincident D7-brane probes which feature the $\mathrm{U}(2)$ gauge theory. In this model the interaction between the overall $\mathrm{U}(1)$ and the $\mathrm{SU}(2)$ gauge fields is obtained by the Dirac-Born-Infeld action.

In both models we found quantum phase transitions, but different behavior in the phase diagrams and different behavior concerning the presence of the quantum critical point. We argue that one of the reason for the differences might depend on the type of the interactions between the $\mathrm{U}(1)$ and the $\mathrm{SU}(2)$ gauge fields. Compared the results obtained in sections 3.3 and 3.4 with those from QCD [49, 50], we find interesting similarities and differences which are discussed later in section 3.4.4. As a technical comment we want to stress that while most of the results in section 3.4 have been

obtained via a numerical method, many results in section 3.3 can be expressed in analytical terms, for instance, the position of the quantum critical point in the phase diagram (3.54).

The main results of this part have been published in [3].

Flavor transport in $\mathcal{N} = 4$ SYM plasma   Studying transport properties of holographic flavor fields, we make a *small step* to move from studying phenomena of strongly coupled systems in thermal equilibrium towards phenomena in *non-equilibrium*. We consider a D3/D7 brane setup at finite temperature which is dual to $\mathcal{N} = 4$ SYM plasma with the presence of fundamental fields, see section 2.2.2. This gravity setup can be seen as a model for describing quarks moving through a quark-gluon plasma (QGP) which has been created at RHIC, since it is generally believed that the $\mathcal{N} = 4$ SYM plasma and QGP share common properties, e.g. broken SUSY and no confinement at high temperatures.

In order to study conductivity we need a description of charge density which on the gravity side can be provided by the time component of the $U(1)_B$ gauge potential on the D7-branes, see section 2.2.2. Moreover, we need to *disturb* the system and study the response of the system on external perturbations. For this purpose we will turn on an external electromagnetic field which is given by the spatial components of the $U(1)_B$ gauge potential. The presence of the electromagnetic field will drive the system to an out-of-equilibrium state, since the charge carriers will be accelerated and loss momentum and energy to the surrounding medium.

This part of the thesis is motivated by the works in [51] and [52–54]. In [51] it was shown that scaling arguments lead to universal non-linearities in transport such as in conductivity if the system is *near the quantum critical point*. Typically in linear response theory, the conductivity tensor components are extracted from a low-frequency limit of the two-point functions using the Kubo formula. This method cannot be applied for studying non-linear effects in conductivity. In [52, 53] an alternative strategy has been developed to study non-linear effects of electrical conductivity. Instead of calculating two-point functions for extracting the conductivity tensor, using the methods presented in [52, 53], it is sufficient to determine the one-point function corresponding to the expectation value of the induced current. Using the Ohm's law, the conductivity tensor σ_{ij} measuring the electrical response of a conducting medium to externally applied fields is defined by

$$\langle J_i \rangle = \sigma_{ij} \, E_j \,,$$

where E_j are the component of the externally applied electric field and $\langle J_i \rangle$ are the electrical currents induced in the medium. In general σ_{ij} will depend on the components of the electromagnetic field. As a key result found in [52, 53], there are two types of charge carriers contributing to the currents, namely the charge carriers which are introduced explicitly in $\langle J^t \rangle$ and also charge carriers coming from pair-production at strong coupling which differs from the usual Schwinger pair production in the dependence on the electrical field $\vec{E}$.

In [54], the momentum and energy loss rates of massive flavor fields to the SYM theory plasma in the presence external electric and magnetic fields have been studied

for the setups in [52, 53]. The loss rates appear explicitly in the components the stress-energy tensor [54] which can be obtained by a *holographic method*[4]. In particular, they consider the case where the electric and magnetic field are *perpendicular* to each other [53].

Our goal in this part of the thesis is to generalize the results in [52–54] by considering *arbitrary orientations* between the constant electric and magnetic field. We compute the full conductivity tensor as well as the contribution to the stress-energy tensor associated with massive flavor fields propagating through an $\mathcal{N} = 4$ SYM theory plasma at finite temperature. For an arbitrary configuration of constant electric and magnetic fields, we may sum all the electric fields into a single vector, and similarly for the magnetic fields. The most general configuration is thus an electric field $\vec{E}$ pointing in some direction, which we will take to be $\hat{x}$, and a magnetic field $\vec{B}$ that may be decomposed into two components, one along $\hat{x}$, which we call B_x, and one perpendicular to it, along the $\hat{z}$ direction, which we call B_z. Stated simply, then, we will generalize the results of refs. [52–54] to include a magnetic field with non-zero $\hat{x}$ component, or equivalently a non-zero $\vec{E} \cdot \vec{B} \sim F \wedge F$, where F is the field strength tensor.

For vanishing B_x as in [52–54], only σ_{xx} and σ_{xy} can be obtained. With non-zero B_x, we expect an additional current $\langle J^z \rangle$, and hence we can compute a transport coefficient σ_{xz} which is new to [52, 53]. Furthermore, we can compute the entire conductivity tensor and determine its dependence on B_x. We generalize the results in [54] by calculating the contribution of the flavor fields to the stress-energy tensor and determine the energy and momentum loss rates for the most general configuration of the electric and magnetic fields. As mentioned in [54], we can also find an observer who sees no loss rates, but only when $\vec{E} \cdot \vec{B} = 0$. When $\vec{E} \cdot \vec{B} \neq 0$, the observer measures a current with non-zero divergence $J^2 (\vec{E} \cdot \vec{B})$. The identity of this observer was left as an open question in [54]. Here we find that this observer's four-vector is in fact the magnetic field as measured by the moving charges.

The main results of this part have been published in [1].

Moving mirror as a toy model for thermalization   While many properties of quark-gluon plasma near equilibrium are well described by methods of gauge/gravity duality, see e. g. [34] for a review, looking for a theoretical description of the thermalization process for QGP still remains a great challenge. It is because the early stages of the thermalization require the understanding of strongly coupled field theory *far-from-equilibrium*. Another obstacle is due to the time-dependence of the process. As a further step towards studying strongly coupled system far-from-equilibrium, in this part of the thesis, we consider a time-dependent process in the bulk of AdS space which is relevant for the thermalization of strongly coupled field theory.

There has been many efforts in formulating the process of thermalization using gauge/gravity duality, for instance, the study of collisions of gravitational shock waves in AdS space [55–66], but information other than the one-point function of

---

[4]By holographic method we mean that we do the calculations on the gravity side of the duality, and afterwards we map the obtained results to expectation values of field theory quantities via the so-called AdS/CFT dictionary which is presented in section 2.1.4.

the stress tensor are extremely difficult to obtain due to the complexity of the metric resulting from the collisions. An alternative approach is to consider collapses in AdS spaces [40–44, 67, 68], since the gravity picture of thermalization is expected to describe the dynamical process of black hole formation from some initially regular space-time. In this approach, the collapsing geometry can be probed by external fields, but usually the responses given by the two-point correlators can be approximated only at late times, i.e. at a near-equilibrium stage, in the quasi-static limit.

Looking for a method for evaluating time-dependent two-point functions, we consider a simple toy model for a time-dependent geometry. This model consists of a mirror moving in the bulk of AdS space. We impose Dirichlet boundary conditions at the position of the mirror and calculate the two-point function of a scalar field in this geometry. For mirror trajectories preserving the scaling symmetry of the AdS space, we compute the two-point functions based on an eigenmode decomposition and find that the singularity structure of the two-point correlator is related to the physics of bouncing light ray between the moving mirror and the AdS boundary, see figs. 5.1 and 5.2. More precisely, the singularity structure of the correlator is determined by a *geometric optics picture*, a result which is known so far only to the case of static mirror [69] .

We explore the geometric optics limit in more detail with a WKB analysis, which leads to a prescription for calculating two-point correlator for *arbitrary trajectories* of the mirror along the radial direction of the AdS space (5.52). The final formula for the correlator (5.52) is expressed as a Mellin transform involving the ratio of incoming and outgoing waves for each component in the eigenmode decomposition. We test this correlator prescription using two sample trajectories of the mirror, constant moving and spacelike trajectories, with success.

The main results of this part have been published in [2].

In summary, in this thesis we study quantum phase transitions, electrical transport of charges and the process of thermalization, which are of relevance for applications to the quark-gluon plasma and to condensed matter physics. We construct two gravity setups where we find quantum phase transitions from a normal to a superfluid phase. In both setups we find a quantum critical point. In another model we study electrical conductivity of flavor fields moving through a SYM plasma in the most general configuration of an electromagnetic field and compute a new coefficient of the conductivity tensor. In a last setup we study a simple time-dependent geometry which is of relevance to the formulation of holographic thermalization.

Giving a resumé of the content of the thesis, in the context of gauge/gravity duality we consider different gravity setups with the intention to study various subjects of strongly coupled systems in real-world physics, ranking from phenomena in thermal equilibrium like quantum phase transitions in condensed matter physics over transport phenomena of flavor fields in a near-equilibrium system to far-from-equilibrium phenomena such as the process of thermalization in quark-gluon plasma.

In chapter 2 we give a brief review the original AdS/CFTcorrespondence 2.1 as it has been conjectured by Maldacena and provide some theoretical concepts which are of direct relevance to the formulation of the correspondence. In section 2.2 we presents

some of its extensions and generalizations leading to the so-called gauge/gravity duality.

In chapter 3 we construct gravity models which resemble p-wave superfluids at finite baryon and isospin chemical potential. Studying the phase diagrams, we observe quantum phase transitions from a normal to a superfluid phase. We apply two approaches: a bottom-up approach in section 3.3 using an $U(2)$ Einstein-Yang-Mills theory with back-reaction and a top-down approach in section 3.4 using a D3/D7 model setup.

In chapter 4 we study transport properties of holographic flavor fields moving in a $\mathcal{N} = 4$ SYM plasma using another D3/D7 brane setup. In section 4.2 we determine the full conductivity tensor of flavor fields in the presence of a constant but arbitrary electromagnetic field using a method beyond linear response. In section 4.3, we compute the stress-energy tensor of flavor fields and identify the energy and momentum loss rates of flavor fields to the surrounding medium.

In chapter 5 we consider a moving mirror in AdS space as a simple model for a time-dependent geometry, which may be of relevance for the formulation of holographic thermalization. In section 5.3 we derive a procedure for obtaining time-dependent two-point functions of scalar fields for the case of mirror trajectories which respect the scaling symmetry of AdS space. In section 5.4 we extend the procedure for arbitrary mirror trajectories along the radial direction of AdS space.

The conclusions and outlook of the thesis are in chapter 6. Some detail calculations in the thesis are moved to the appendices A and B.

AdS/CFT correspondence

The AdS/CFT correspondence and its applications are the main subjects of this thesis. This chapter serves as a review of the correspondence and presents some of its extensions and generalizations. In section 2.1 we explain the duality in detail by providing some basic knowledge which should support the understanding of the correspondence. In the section 2.2 we introduce certain extensions and generalizations to the original correspondence and discuss some arguments, evidence and tests for the correctness of the conjecture. This chapter contains all the basic information for the applications of the AdS/CFT correspondence presented in chapter 3, 4 and 5.

2.1 The original AdS/CFT correspondence

The AdS/CFT correspondence has been conjectured by Maldacena [10] in 1997 and originally states that the $\mathcal{N} = 4\,\mathrm{SU}(N_\mathrm{c})$ super Yang-Mills (SYM) theory[1] in $(3 + 1)$-dimensions describes the same physics as type IIB superstring theory on an $\mathrm{AdS}_5 \times \mathrm{S}^5$ background, where AdS_5 is the five-dimensional Anti-de Sitter space and S^5 a five-sphere. N_c denotes the number of the colors of the theory and $\mathcal{N} = 4$ the number of the supercharges. In section 2.1.1 and 2.1.2 we will give a very brief introduction to the $\mathcal{N} = 4\,\mathrm{SU}(N_\mathrm{c})$ SYM theory and type IIB superstring theory. In section 2.1.3 we review the physics of D-branes from two different perspectives which play a crucial role for the formulation of the conjecture. We close this section by studying the conjecture in three different forms and emphasize that all applications of the AdS/CFT presented in this thesis are worked out in a special limit of the correspondence which is described in the last part of section 2.1.4.

2.1.1 $\mathcal{N} = 4$ super Yang-Mills theory

In this section we will give a brief description of the $\mathcal{N} = 4\,\mathrm{SU}(N_\mathrm{c})$ SYM theory and its properties relevant for this thesis. We closely follow the work in [14].

---

[1]The gauge group $\mathrm{U}(N_\mathrm{c})$ can be written as $\mathrm{SU}(N_\mathrm{c}) \times \mathrm{U}(1)$ and the center group $\mathrm{U}(1)$ is identified to describe the center of mass motion of the stack of coincident N_c D3-branes, thus fixing the position of the stack of the D3-branes.

The $\mathcal{N} = 4$ $\mathrm{SU}(N_c)$ SYM theory is a superconformal quantum field theory with $\mathcal{N} = 4$ supercharges rotating under the $\mathrm{SU}(4)_R$ R-symmetry. Its field content consists of one gauge field A_μ with μ denoting the Lorentz indices in (3+1) space-time dimensions, four Weyl fermions λ^a with $a = 1, ..., \mathcal{N}$ and six real scalars X^i with $i = 1, 2, ..., 6$. Under the $\mathrm{SU}(4)_R$ symmetry, A_μ is a singlet, λ^a is a **4** and the scalars X^i are a rank 2 anti-symmetric **6**, where the indices i and a are related to the representations of the $\mathrm{SU}(4)_R$. All the fields are in the adjoint representation of the color group $\mathrm{SU}(N_c)$, i.e. we have e.g. for the scalar field $(X^i)^m{}_n = X^{i(k)}(T^{(k)})^m{}_n$ with $k = 1, 2, \ldots, N_c^2 - 1$ and $m, n = 1, 2, \ldots, N_c$. The whole field content can be arranged in one supersymmetry multiplet, the $\mathcal{N} = 4$ gauge multiplet. Its Lagrangian can be described by [14]

$$\mathcal{L} = \mathrm{Tr}\left\{ \; -\frac{1}{2g_{\mathrm{YM}}^2}F_{\mu\nu}F^{\mu\nu} + \frac{\theta_I}{8\pi^2}F_{\mu\nu}\star F^{\mu\nu} - \sum_a i\bar{\lambda}^a\bar{\tau}^\mu D_\mu\lambda_a \right.$$
$$- \sum_i D_\mu X^i D^\mu X^i + g_{\mathrm{YM}}\sum_{a,b,i} C_i^{ab}\lambda_a[X^i,\lambda_b]$$
$$\left. + \; g_{\mathrm{YM}}\sum_{a,b,i}\bar{C}_{iab}\bar{\lambda}^a[X^i,\bar{\lambda}^b] + \frac{g_{\mathrm{YM}}^2}{2}\sum_{i,j}[X^i,X^j]^2 \right\}, \qquad (2.1)$$

where g_{YM} is the gauge coupling, θ_I is the instanton angle, the field strength is $F_{\mu\nu} = \partial_\mu A_\nu - \partial_\nu A_\mu + i\,g_{\mathrm{YM}}[A_\mu, A_\nu]$, $\star F_{\mu\nu} = \frac{1}{2}\epsilon_{\mu\nu\rho\sigma}F^{\rho\sigma}$ is the Hodge dual of F, D_μ denote the covariant derivatives acting on λ as $D_\mu\lambda = \partial_\mu\lambda + i\,g_{\mathrm{YM}}[A_\mu, \lambda]$ and on X as $D_\mu X = \partial_\mu X + i\,g_{\mathrm{YM}}[A_\mu, X]$. Furthermore, τ^μ are components of the four vector $(\mathbf{1}, -\tau^i)$ of 2×2 matrices with the standard Pauli matrices τ^i and the constants C_i^{ab} are the Lie algebra structure constants of the symmetry group $\mathrm{SO}(6)_R \sim \mathrm{SU}(4)_R$.

The theory is believed to be UV finite because, upon perturbative quantization, $\mathcal{N} = 4$ SYM theory exhibits no ultraviolet divergences in the correlation functions and the instanton corrections also lead to finite contributions.

The theory has two parameters, the number of colors N_c and the gauge coupling g_{YM}. It is scale invariant, hence from the mass dimension analysis in 4 dim. the energy dimension of the fields and couplings are determined to be

$$[A_\mu] = [X^i] = 1 \qquad [\lambda_a] = \frac{3}{2} \qquad [g] = [\theta_I] = 0\,. \qquad (2.2)$$

$\mathcal{N} = 4$ SYM theory is a superconformal field theory with vanishing beta function, i.e. the Lagrangian above is invariant under action of the conformal group in (3+1) dimensions $\mathrm{SO}(2,4)$ and also respects the $\mathcal{N} = 4$ Poincaré symmetry described by the $\mathrm{SU}(4)_R$ group. The combination of conformal invariance and $\mathcal{N} = 4$ Poincaré supersymmetry produces a larger superconformal symmetry given by the supergroup $\mathrm{PSU}(2,2|4)$.

For the Lagrangian (2.1) there is an additional symmetry related to the Montonen-Olive or S-duality conjecture, see e.g. [6,9]. This invariance can be stated by combining the real coupling g_{YM} and the real instanton angle θ_I into a single complex coupling

$$\tau \equiv \frac{\theta_I}{2\pi} + \frac{4\pi i}{g_{\mathrm{YM}}^2}\,. \qquad (2.3)$$

The theory is invariant under $\tau \to \tau + 1$. The Montonen-Olive conjecture states that $\mathcal{N} = 4$ SYM theory is also invariant under the transformation $\tau \to -1/\tau$. The combination of both symmetries yields the S-duality group SL(2, $\mathbb{Z}$), generated by

$$\tau \to \frac{a\tau + b}{c\tau + d}, \qquad ad - bc = 1, \quad a, b, c, d \in \mathbb{Z}. \tag{2.4}$$

When $\theta_I = 0$, the S-duality transformation with $a = d = 0$ and $b = -c = 1$ maps $g_{\mathrm{YM}} \to 4\pi/g_{\mathrm{YM}}$. That is remarkable because it exchanges strong and weak coupling region of the same theory. Note, however, that S-duality is a useful symmetry only in the strongest form of the AdS/CFT conjecture for arbitrary g_{YM} and N_{c}. As soon as one takes some limits, e.g. taking $N_{\mathrm{c}} \to \infty$ while keeping $g_{\mathrm{YM}}^2 N_{\mathrm{c}}$ fixed, the S-duality no longer has a consistent action.

2.1.2 Type IIB superstrings and type IIB supergravity

Type IIB superstring theory is a superstring theory of closed oriented superstrings, which contains a *finite* number of massless fields, including the graviton, the dilaton and the Kalb-Ramond antisymmetric 2-form. Furthermore it contains the fermionic superpartners and an infinite number of massive string excitations. The terminology II refers to the fact that the theory has two gravitinos in the spectrum, and the terminology B is used to distinguish type IIB from type IIA superstring theory concerning different chiralities within the spectrum. The closed string spectrum is a product of two copies of the open string spectrum with right- and left-moving levels matched. While the spectrum of type IIA superstring is formed by right-movers and left-movers transforming under separate space-time supersymmetries with opposite chiralities, the spectrum of type IIB superstring is formed by right-movers and left-movers transforming under separate space-time supersymmetries with the same chirality, e.g. the two gravitinos of type IIA are of opposite chiralities and the two gravitinos of type IIB are of the same chirality.

Next, we will give a brief description of type IIB superstring theory and consider type IIB supergravity as its low-energy effective action. Due to the complexity of the subject, the content of the discussion below is not self-contained. The following paragraphs in this section are intended to:

- first, briefly explain what type IIB superstring theory and type IIB supergravity are;

- and second, discuss relevant properties of superstring theories and supergravity which are important for this thesis, in particular, the low-energy effective action and the low-energy field content of these theories.

More details about supergravity, bosonic and superstring theories can be found in [5, 6, 70].

Ramond-Neveu-Schwarz formalism of open superstrings The incorporating of supersymmetry into bosonic string theory removes the theory's inconsistency due to

the occurrence of tachyonic modes in the closed string spectrum. Moreover, with super-symmetry as a new ingredient the field content of the bosonic string was enlarged by fermionic fields which are necessary for describing fundamental interactions in nature. Before discussing type IIB superstrings, we first review open oriented superstrings in D-dimensional Minkowski space-time [9]. The superstring world-sheet action reads

$$S = -\frac{1}{4\pi\alpha'} \int_\Sigma d\tau d\sigma \{\partial^\alpha X^A \partial_\alpha X_A + \bar{\psi}^A \gamma^\alpha \partial_\alpha \psi_A\}, \tag{2.5}$$

where $\tau \in (-\infty, \infty)$ and $\sigma \in [0, \pi]$ parameterize the world-sheet time and spatial coordinate, respectively. $X^A(\tau, \sigma)$ are the bosonic fields of the two dimensional world-sheet theory with $A \in \{1, 2, \cdots, D\}$ and $\psi^A(\tau, \sigma)$ are their fermionic partners, which can be described by the two-component Marojana-Weyl spinors on the world-sheet,

$$\psi^A = \begin{pmatrix} \psi_-^A \\ \psi_+^A \end{pmatrix} \quad \text{with} \quad \bar{\psi} = i\gamma^0 \psi^T. \tag{2.6}$$

Moreover, ψ^A can be seen as vector in the D-dimensional Minkowski space-time which transforms in the vector representation of the Lorentz group $SO(D-1, 1)$. The γ^α with $\alpha \in \{0, 1\}$ represent the two-dimensional Dirac matrices obeying $\{\gamma^\alpha, \gamma^\beta\} = 2\eta^{\alpha\beta}\mathbb{1}$. The only free parameter in this action is α' which is related to the length of the string $l_s = \sqrt{\alpha'}$. The action (2.5) is invariant under supersymmetric transformations mixing bosonic and fermionic fields.

Going to the light-cone coordinates $\sigma^\pm = \tau \pm \sigma$, the equations of motion for the two spinor components are the Dirac equations

$$\partial_+ \psi_-^A = 0 \quad \text{and} \quad \partial_- \psi_+^A = 0 \tag{2.7}$$

whose solutions $\psi_-^A(\tau + \sigma)$ and $\psi_+^A(\tau - \sigma)$ describe left-moving and right-moving waves. By considering the variation of the fields $\psi_\pm^A$ it can be shown that the action (2.5) is stationary if the equations of motion (2.7) are satisfied. The condition that the boundary terms in the variation of the fermionic part of the action vanish leads to the requirement at $\sigma = 0$ and $\sigma = \pi$ parametrizing the two ends of the open string,

$$\delta(\psi_+^A)^2 = \delta(\psi_-^A)^2. \tag{2.8}$$

Since the overall sign of the components is a matter of convention, without loss of generality, we fix the relative sign between the components at one end of the string by demanding

$$\psi_+^A(\tau, 0) = \psi_-^A(\tau, 0). \tag{2.9}$$

With this choice the boundary condition at $\sigma = \pi$ allows two options for the components of world-sheet fermions which will be referred to the Ramond (R) sector and the Neveu-Schwarz (NS) sector of the theory,

$$\begin{aligned} \text{R} &: \psi_+^A(\tau, \pi) = +\psi_-^A(\tau, \pi), \\ \text{NS} &: \psi_+^A(\tau, \pi) = -\psi_-^A(\tau, \pi). \end{aligned} \tag{2.10}$$

The mode decomposition of the components of the fermionic fields in different sectors take the form

$$
\begin{aligned}
\text{R} \ &: \psi_\pm^A(\tau, \sigma) = \frac{1}{\sqrt{2}} \sum_{n \in \mathbb{Z}} d_n^A e^{-in\sigma^\pm}, \\
\text{NS} \ &: \psi_\pm^A(\tau, \sigma) = \frac{1}{\sqrt{2}} \sum_{r \in \mathbb{Z}+\frac{1}{2}} b_r^A e^{-ir\sigma^\pm},
\end{aligned}
\tag{2.11}
$$

where d_n^A and b_r^A are Grassmann numbers which after quantization of the strings will be used to construct different string states from the ground states in each sector. While the Ramond boundary conditions give rise to space-time fermions at all mass levels, the Neveu-Schwarz boundary conditions give rise to space-time bosons.

The ground state of the NS sector is a scalar in space-time. It has negative mass squared, hence a tachyon, but this state will be eliminated from the spectrum by the so called GSO projection introduced by Gliozzi, Scherk and Olive, see e.g. [6, 9]The GSO projection also ensures the equal number of bosons and fermions at each mass level which is a necessary condition for space-time supersymmetry. The first excited state in the NS sector is a massless space-time vector which is classified by its $SO(8)$ representation under Lorentz rotations that leave the momentum invariant. It is created by acting the operators $b_{-1/2}^i$ on the ground state. Here, the index i takes values in $\{1, \cdots, \mathrm{D}-2\}$ denoting the eight transverse directions to the world-sheet. Hence, there are eight polarization states, as required for a massless vector in ten dimensions. After performing the GSO projection, this massless vector boson becomes the physical ground state of the NS sector which transforms in the eight-dimensional vector representation $\mathbf{8_v}$ of the $SO(8)$.

The ground state of the R sector is massless and can be described by a 32×32-component spinor. In ten dimensions spinors can be restricted by Majorana and Weyl conditions[2] which lead to two alternative ground states corresponding to the two possible ten-dimensional chiralities. Furthermore, a minimal possibility for a Ramond ground state corresponding to an irreducible spinor of $Spin(8)$ can be obtained by a further restriction due to the Dirac-Ramond equation, a stringy generalization of the Dirac equation. The GSO projection amounts to projecting spinors onto states of a given chirality, thus after the GSO projection the spinors in the R sector will have definite parity depending on the chirality of the spinor ground state. In the following we will denote the representation of the GSO-projected ground state spinor with definite chirality as $\mathbf{8_s}$ of the $SO(8)$. If only one R sector is considered, the choice of the chirality is purely a matter of convention. However, when two R sectors are needed to form the spectrum of closed superstrings, different choices of chirality in each of the two R sectors will lead to different type II superstrings.

Type IIB superstrings The closed string spectrum is a product of two copies of the open string spectrum with left- and right-moving levels matched. Since both left-moving and right-moving fermionic components of the spinor ψ^A can either be

---

[2]A Weyl spinor always has a definite chirality.

in the R or in the NS sector, there are four possible sectors of the spectrum of closed superstrings: R-R, R-NS, NS-R and NS-NS.

While the spectrum of closed superstrings in R-NS, NS-R and NS-NS sector is quite straightforward construct, the situation for the R-R sector is more subtle due to two possible choices of chiralities for the ground state of the R-sector. If the left- and right-moving R sector have the different chiralities, this will lead to type IIA superstring theory which is non-chiral. Otherwise if they share the same chirality, we end up with type IIB superstring theory which is chiral. At this point it is worth mentioning that type IIA and type IIB theories can be related by T-duality, and since they have different R-R fields, T-duality should transform one set of the fields into the other.

According to the prescription described above, the massless spectrum of type IIB strings are constructed by the tensor products of the $\mathbf{8_v}$ of the $SO(8)$ for massless vector boson in the NS sector and the $\mathbf{8_s}$ of the $SO(8)$ for the GSO-projected ground state spinor. For definiteness we chose one chirality for all R sectors, and the type IIB massless spectrum reads

$$(\mathbf{8_v} \oplus \mathbf{8_s}) \otimes (\mathbf{8_v} \oplus \mathbf{8_s}) \,. \tag{2.12}$$

In different sectors, the various products are

$$
\begin{aligned}
\text{NS-NS} \;:\quad & \mathbf{8_v} \otimes \mathbf{8_v} = \mathbf{1} \oplus \mathbf{28} \oplus \mathbf{35} = \Phi \oplus B_{\mu\nu} \oplus G_{\mu\nu} \,, \\
\text{NS-R} \;:\quad & \mathbf{8_v} \otimes \mathbf{8_s} = \mathbf{8_c} \oplus \mathbf{56_s} \,, \\
\text{R-NS} \;:\quad & \mathbf{8_s} \otimes \mathbf{8_v} = \mathbf{8_c} \oplus \mathbf{56_s} \,, \\
\text{R-R} \;:\quad & \mathbf{8_s} \otimes \mathbf{8_s} = \mathbf{1} \oplus \mathbf{28} \oplus \mathbf{35}_+ = [0] \oplus [2] \oplus [4]_+ = C_0 \oplus C_2 \oplus C_4 \,,
\end{aligned}
$$
$$\tag{2.13}$$

where $\mathbf{8_c}$ is another tensor representation of $SO(8)$ which differs from $\mathbf{8_s}$ only by a space-time parity redefinition, and $[n]$ denotes the n-times anti-symmetrized representation of $SO(8)$, with $[4]_+$ being self-dual. There are 64 states in each of the four massless sectors, that we summarize as:

- The NS-NS spectrum contains a scalar Φ called the dilaton (one state), an antisymmetric two-form Kalb-Ramond field B_2 (28 states) and a symmetric traceless rank-two tensor $G_{\mu\nu}$, the graviton (35 states);

- Each of the NS-R and R-NS sectors contains a spin 1/2 fermion called the dilatino (eight states) and a spin 3/2 gravitino (56 states). The dilatinos and gravitinos in both sectors have the same chirality;

- The states in the R-R sector are bosons obtained by tensoring a pair of Majorana-Weyl spinors, namely one zero-form gauge potential C_0 (one state), a two-form gauge potential C_2 (28 states) and a four-form gauge potential C_4 with a self-dual field strength (35 states).

The NS-NS and R-R sectors are space-time bosons and the NS-R and R-NS sectors are space-time fermions, so there are equal number of bosonic and fermionic degrees of

freedom, as required for unbroken space-time supersymmetry. Note that the massless spectrum of the type IIB string theories contains two Majorana-Weyl gravitinos with the same chirality which form $\mathcal{N} = 2$ supergravity multiplets.

Type IIB supergravity There is no known general consistent formulation for a type IIB theory at all mass levels. At low energy, where only massless degrees of freedom are considered, type IIB string theories can effectively be described by type IIB $\mathcal{N} = 2$ supergravity Type IIB $\mathcal{N} = 2$ supergravity and type IIB string theory have identical field content at massless level. In general it is difficult to find Lorentz covariant actions for self-dual tensors. One approach to circumvent this difficulty is imposing the self-duality condition as a constraint. As stated in [6] the following low-energy effective action written in string frame should come close to a covariant formulation,

$$
\begin{aligned}
S_{\text{IIB}} =& \frac{1}{2\kappa_{10}^2} \int \mathrm{d}^{10}x \, \sqrt{-\det|G|} \left\{ e^{-2\Phi} \left(\mathcal{R} + 4 \, \partial^\mu \Phi \partial_\mu \Phi - \frac{1}{2} |H_3|^2 \right) \right. \\
& \left. - \frac{1}{2} \left(|F_1|^2 + |\tilde{F}_3|^2 + \frac{1}{2} |\tilde{F}_5|^2 \right) \right\} - \frac{1}{4\kappa_{10}^2} \int C_4 \wedge H_3 \wedge F_3 \,,
\end{aligned}
\tag{2.14}
$$

with the constraint

$$
\star \tilde{F}_5 = \tilde{F}_5 \,,
\tag{2.15}
$$

where $\star$ denotes the ten-dimensional Hodge star operator. In (2.14) fields in the fermionic R-R sectors are not shown, κ_{10} is related to the Newton gravitational constant in 10 dimensions, $G_{\text{N}}^{(10)}$, and the string coupling constant g_s by

$$
2\kappa_{10}^2 g_s^2 = 16\pi G_{\text{N}}^{(10)} = (2\pi)^7 \alpha'^4 g_s^2 \,,
\tag{2.16}
$$

$\mathcal{R}$ is the Ricci scalar and the following differential form notations have been used

$$
\begin{aligned}
& H_3 = \mathrm{d}B_2 \,, \quad F_1 = \mathrm{d}C_0 \,, \quad F_3 = \mathrm{d}C_2 \,, \quad F_5 = \mathrm{d}C_4 \,, \\
& \tilde{F}_3 = F_3 - C_0 \wedge H_3 \,, \quad \tilde{F}_5 = F_5 - \frac{1}{2} C_2 \wedge H_3 + \frac{1}{2} B_2 \wedge F_3 \,.
\end{aligned}
\tag{2.17}
$$

The action (2.14) possesses a $\mathrm{SL}(2,\mathbb{R})$ symmetry which can be seen best when it is displayed in the Einstein frame [6]. Let us define

$$
\begin{aligned}
& G_{\mu\nu_E} = e^{\Phi/2} G_{\mu\nu} \,, \quad \tilde{\tau} \equiv C_0 + i e^{-\Phi} \,, \\
& \mathcal{M}_{ij} \equiv \frac{1}{\mathrm{Im}\,\tilde{\tau}} \begin{bmatrix} |\tilde{\tau}|^2 & -\mathrm{Re}\,\tilde{\tau} \\ -\mathrm{Re}\,\tilde{\tau} & 1 \end{bmatrix} \,, \quad F_3^i = \begin{bmatrix} H_3 \\ F_3 \end{bmatrix} \,,
\end{aligned}
\tag{2.18}
$$

then the action (2.14) reads

$$
\begin{aligned}
S_{IIB}^E =& \frac{1}{2\kappa_{10}^2} \int \mathrm{d}^{10}x \, \sqrt{-\det|G_E|} \left(\mathcal{R}_E - \frac{\partial_\mu \bar{\tilde{\tau}} \partial^\mu \tilde{\tau}}{2(\mathrm{Im}\,\tilde{\tau})^2} - \frac{\mathcal{M}_{ij}}{2} F_3^i F_3^j - \frac{1}{4} |\tilde{F}_5|^2 \right) \\
& - \frac{\epsilon_{ij}}{8\kappa_{10}^2} \int C_4 \wedge F_3^i \wedge F_3^j \,,
\end{aligned}
$$

$$(2.19)$$

with the Einstein metric being used everywhere. The action (2.19) is invariant under the following $\mathrm{SL}(2, \mathbb{R})$ symmetry:

$$\tilde{\tau} \to \frac{a\tilde{\tau} + b}{c\tilde{\tau} + d}\,; \quad \tilde{F}_5 \to \tilde{F}_5\,; \qquad G_{\mu\nu_E} \to G_{\mu\nu_E}\,;$$

$$F_3^i \to \Lambda_j^i F_3^j, \quad \Lambda_j^i = \begin{bmatrix} d & c \\ b & a \end{bmatrix}\,, \quad \{a, b, c, d \in \mathbb{R} \mid ad - bc = 1\}\,.$$

$$(2.20)$$

There are some interesting remarks on this symmetry.

- The $\mathrm{SL}(2, \mathbb{R})$ symmetry is just an accidental symmetry of the low energy theory. For the full type IIB string theory, the continuous $\mathrm{SL}(2, \mathbb{R})$ symmetry is broken to the discrete group $\mathrm{SL}(2, \mathbb{Z})$ due to charge quantization.

- The closed string coupling constant is given by $g_s = e^{\Phi}$. Using the $\mathrm{SL}(2, \mathbb{R})$ symmetry, e^{Φ} can be transformed to $e^{-\Phi}$, e.g. for $C_0 = 0$, $a = d = 0$ and $b = -c = 1$, thus this transformation is also known as S-duality relating g_s to $1/g_s$.

- The $\mathrm{SL}(2, \mathbb{R})$ symmetry mixes the field strength tensors H_3 and F_3 coming from the two-form gauge potentials B_2 and C_2, respectively. Because a fundamental string carries only one unit of B_2 charge, only the NS-NS two-form B_2 couples to the string and the R-R two-form C_2 does not. Since in type IIB superstrings there are non-perturbatives objects like D-branes which only couple to potential forms coming from the R-R sector and not to those from the NS-NS sector, the $\mathrm{SL}(2, \mathbb{R})$ symmetry suggests a connection between D-branes and fundamental strings. Indeed, a general $\mathrm{SL}(2, \mathbb{Z})$ transformation will map the fundamental string to a bound state (p, q) carrying p units of NS-NS charge and q units of R-R charge.

2.1.3 Physics of D-branes

The AdS/CFT correspondence describes a duality between $\mathrm{SU}(N_c)\,\mathcal{N} = 4$ SYM in flat four space-time dimensions and type IIB supertring theory in $\mathrm{AdS}_5 \times \mathrm{S}^5$. To this point we have given a very brief description of the $\mathrm{SU}(N_c)\,\mathcal{N} = 4$ SYM theory and its dual counterpart type IIB supertrings whose low-energy effective action is described by type IIB $\mathcal{N} = 2$ supergravity. The type IIB superstring theory presented in the last section, however, is formulated in ten-dimensional Minkowski space-time which differs much from the curved $\mathrm{AdS}_5 \times \mathrm{S}^5$. To this day a covariant superstring theory formulation in $\mathrm{AdS}_5 \times \mathrm{S}^5$ is not known, hence the question arises how Maldacena could make such a persuasive conjecture relating two traditionally disparate theories, even though one of them is very poorly understood. Explanations for that come from the study of D-branes.

There are two descriptions of the low energy dynamics of the branes. One description uses the collective dynamics of the effective world-volume field theory, and the other one treats the brane as a soliton-like source of various low energy closed string

fields in superstring theory. In this section we will study the physics of D-branes from these two points of view which provide many hints for the existence of the AdS/CFT correspondence.

D-branes as dynamical objects in superstring theories From this point of view D-branes are non-perturbative objects in string theory. They are p-spatial extended objects where open strings can end. In the presence of D-branes, some symmetries of the string vacuum are broken, e.g. in type IIB superstring theory in Minkowski vacuum a Dp-brane breaks the $\mathrm{SO}(1,9)$ Lorentz symmetry to $\mathrm{SO}(1,p) \times \mathrm{SO}(9-p)$. Moreover, massless open strings give rise to vector supermultiplets with 16 or fewer conserved supercharges, hence D-branes are BPS objects in superstring theories [9].

The world-volume Σ of Dp-branes is $(p+1)$ dimensional, thus they naturally couple to the R-R form fields C_{p+1} by pulling back the forms on the manifold Σ

$$\mu_p \int_{\Sigma_{p+1}} \mathcal{P}[C_{p+1}], \tag{2.21}$$

which leads to consistent open-closed string interactions [71]. The R-R p-form charge μ_p corresponding to the Dp-brane is related to the brane tension τ_p by

$$T_p = g_s \tau_p = \frac{\sqrt{\pi}}{\kappa_{10}} (4\pi^2 \alpha')^{\frac{3-p}{2}} = (2\pi)^{-p} \alpha'^{-\frac{p+1}{2}} = \mu_p, \tag{2.22}$$

where T_p is the brane tension in units of the string coupling constant g_s. The expression for the brane tension arises from comparing the results in field theory and string theory which ensures that there is no force between static parallel BPS objects of the same charge. For this case in particular, the vanishing of the force comes about from a cancellation between attraction due to the graviton and dilation and repulsion due to the R-R tensor [6]. The equality between the tension - mass per unit volume - and the charge μ_p is just a consequence of the BPS-mechanism.

For the form fields in the R-R sector of type IIB superstrings, the electric-magnetic duality known as Poincaré duality[3],

$$\mathrm{d}C_{p+1} = F_{p+2} = \star F_{8-p} = \star \mathrm{d}C_{7-p}, \tag{2.23}$$

relates C_{p+1} and C_{7-p}, hence the possible Dp-branes in type IIB superstring theory are D(−1), D1, D3, D5, D7 and D9. D(−1) imposes Dirichlet boundary conditions in time and all spatial directions. It is a point-like object in spacetime and often called as D-instanton. D9 is a space-time filling brane. The D3-brane is special in the sense that it is self-dual under electric-magnetic duality. D3-branes couple electrically to C_4 via (2.21), but due to (2.23) this can also be seen as a magnetic coupling to C_{7-3}, thus D3-branes are both the electric and magnetic source of the five-form field strength, hence $F_5 = \star F_5$.

The massless excitations of open strings give rise to scalar, gauge fields and their fermionic superpartners. Quantization of open strings in the presence of a Dp-brane

---

[3]This duality exchanges the Maxwell equation $\mathrm{d}\star F = 0$ with the Bianchi identity $\mathrm{d}F = 0$.
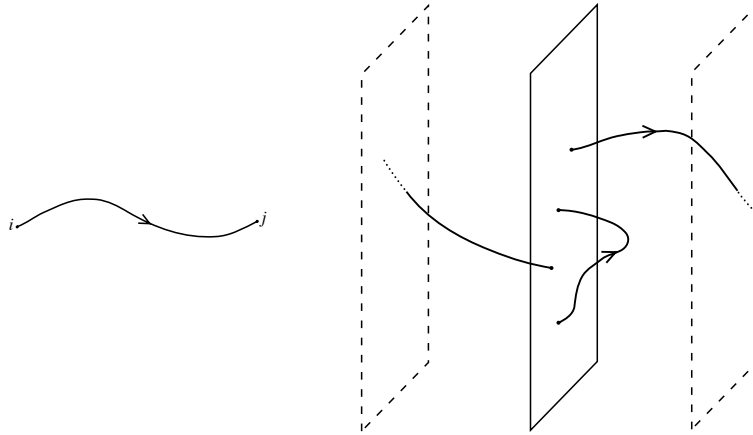
FIGURE 2.1: A cartoon of open strings and D-branes. In superstring theory, the endpoints of open strings are attached to D-branes. Open strings extending from brane i to brane j can be labeled by the Chan-Paton indices $[ij]$. Massless open strings, i.e. strings of zero length, give rise to gauge fields living on the world-volume of the D-branes. For N coincident D-branes, the $N \times N$ massless open strings $[ij]$ can be used to form the adjoint of the $U(N)$ gauge group. If none of the N D-branes coincides with another, there is one massless sector for each D-brane giving the $U(1)^N$ gauge group. The figures in 2.1 are taken from [72].

embedded in D space-time dimensions gives rise to $(D - p - 1)$ massless scalar fields – the transverse fluctuations – describing the transverse position of the Dp-brane. The scalar fields break the translation invariance in the $(9 - p)$ transversal directions. A single D-brane also supports a single $U(1)$ multiplet on its world-volume whose massless vector arises from zero-length strings starting and ending at the same position on the brane. In the presence of N branes, open strings extending from brane i to brane j can be labeled by $[ij]$ with $i, j \in \{1 \cdots N\}$. The discrete labels i, j used to label the branes are called *Chan-Paton* indices [5]. Each end of the strings carries a Chan-Paton label of the gauge group. That is an index in the fundamental representation, thus the $U(1)$ vector multiplet field is labelled with a fundamental and an anti-fundamental index (ingoing and outcoming), hence can be seen as adjoint fields.

If there are N D-branes and none of the D-branes coincides with another, there is one massless vector each, or $U(1)^N$ in all. If N D-branes coincide, there are $N \times N$ massless states on the world-volume corresponding to $N \times N$ possibilities of labelling a string with vanishing length. The $N \times N$ massless vectors can be used to form the adjoint of the $U(N)$ gauge group. It was found that the low energy effective action of N coincident D-branes is the $U(N)$ supersymmetric gauge theory which is dimensionally reduced from ten-dimensional down to $(p + 1)$-dimensional world-volume of the D-brane [72, 73]. The last statement can be made more precise by the σ-model approach to string theory [74]. Considering the σ-model action with Dirichlet and Neumann conditions for the branes, consistency conditions required by the conformal invariance can be derived. These consistency conditions imply equations of motion of the Born-Infeld action which is taken as the low energy effective description of the D-brane. In the non-abelian situation, the effective action of a D-brane can be approximated by the dimensional reduction of 10-dimensional $\mathcal{N} = 1$ $U(N)$-SYM theory. Interestingly,

for a stack of coincident N D3-branes the reduction gives rise to $\mathcal{N} = 4$ $\mathrm{U}(N)$ SYM theory. Usually, the central group $\mathrm{U}(1) = \mathrm{U}(N)/\mathrm{SU}(N)$ corresponding to the overall position of the branes can be ignored if only the dynamics on the branes is considered, thereby leaving only a $\mathrm{SU}(N)$ gauge symmetry [75].

In the following we will discuss the low energy effective action of a single D-brane. D-branes can source closed strings and are able to interact with closed string fields in the background space-time. Moreover, the fluctuations of D-branes are described by field theories living on their world-volume whose gauge fields arise from open strings ending on them [4]. The low energy effective action is defined as the result of integrating out all massive modes and massless modes circulating in loops. For type IIB superstrings the massless fields are given by the massless spectrum in (2.13) and the massless excitations of open superstrings ending on Dp-branes which are the world-volume gauge fields A^a with $a \in \{0, \cdots p\}$, the transverse scalars ϕ^i with $i \in \{p+1, \cdots \mathrm{D}\}$ and their fermionic superpartners. For the abelian case, where only one D-brane is considered, the bosonic part of the effective action for the fields coupling to a Dp brane can be obtained to all orders in α'. This action consists of two contributions: the Dirac-Born-Infeld (DBI) term and the Wess-Zumino (WZ) term. The Dirac-Born-Infeld [76] action reads

$$S_{\mathrm{DBI}} = -T_p \int \mathrm{d}^{p+1}\xi \, e^{-\Phi} \sqrt{-\det\left(\mathcal{P}[\mathrm{G} + \mathrm{B}]_{\mathrm{ab}} + 2\pi\alpha'\mathrm{F}_{\mathrm{ab}}\right)}, \qquad (2.24)$$

where T_p denotes the D-brane tension from (2.22), G the background metric, B the NS-NS 2-form, Φ the dilaton and $F = \mathrm{d}A$ the field strength of the $\mathrm{U}(1)$ gauge field A^a living on the brane. The determinant is taken over the D-brane world-volume coordinates $\{a, b\}$, and

$$\mathcal{P}[T]_{a_1 \dots a_n} = \frac{\partial X^{A_1}}{\partial \xi^{a_1}} \cdots \frac{\partial X^{A_n}}{\partial \xi^{a_n}} T_{A_1 \cdots A_n} \qquad (2.25)$$

denotes the pullback of the tensor T on the D-brane world-volume. The scalar fields ϕ^i fixing the position of the D-brane in the target space-time are incorporated in the embedding functions $X^A(\xi)$.

Let us study (2.24) in the limits of vanishing Kalb-Ramond field B, constant dilation and small field strengths $2\pi\alpha'F_{ab} \ll 1$. Then the DBI action can be written as a series expansion in α', namely

$$S_{\mathrm{DBI}} = -\frac{T_p}{g_s} \int \mathrm{d}^{p+1}\xi \, \sqrt{-\det\left(\mathcal{P}[\mathrm{G}]_{\mathrm{ab}}\right)} \left(1 + \pi^2\alpha'^2 F^2 + \mathcal{O}\left(F^4\right)\right). \quad (2.26)$$

The leading term in (2.26) corresponds to the Nambu-Goto action which minimizes the world-volume of the Dp-brane embedded into background metric G. The next leading term is the Maxwell action for an $\mathrm{U}(1)$ field theory in $(p+1)$ space-time dimensions. Comparing this to the canonically normalized Yang-Mills action

$$S_{\mathrm{YM}} = -\frac{1}{4g_{\mathrm{YM}}^2} \sqrt{-\det\left(\mathcal{P}[\mathrm{G}]_{\mathrm{ab}}\right)} F_{cd}F^{cd}, \qquad (2.27)$$

---

[4]Since D-branes are dynamical massive objects, they couple to gravity and curve space-time. This property will be discussed in the next paragraph.

and using (2.22) one finds a relation between the string coupling constant g_s and the Yang-Mills coupling constant g_{YM} in $(p+1)$ dimensions [76],

$$g_{\text{YM}}^2 = (2\pi)^{p-2}(\alpha')^{\frac{p-3}{2}} g_s \,. \tag{2.28}$$

This relation is remarkable since it can be used to give the correct relation between gauge theory couplings and string quanties. The string coupling g_s is dimensionless, thus g_{YM} is also dimensionless for $p = 3$. This is as expected since in this case the field theory lives on the four dimensional world-volume of the D3-brane.

At this point we want to mention that in the presence of a stack of N coincident Dp-branes, the field theory living on their world-volume becomes non-abelian with the gauge group $\text{SU}(N)$, hence the abelian DBI action (2.24) has to be generalized to the non-abelian one which will be discussed later in section 3.4.2.

The second contribution to the bosonic part of the low energy effective action for a single Dp-brane is the Wess-Zumino term. It describes the coupling of the Dp-brane to the R-R fields C_q with q even for type IIB, as well as to the NS-NS Kalb-Ramond two-form B and the gauge fields A^a. The interactions are given by

$$S_{\text{WZ}} = \mu_p \sum_q \int_{\Sigma_{p+1}} \mathcal{P}\left[C_q e^B\right] e^{2\pi\alpha'F}, \tag{2.29}$$

where μ_p is the R-R p-form charge from (2.22). The above formula should be interpreted as follows: (i) The multiplication operations in expanding the exponential function are of the wedge product form, i.e.

$$e^{\mathcal{P}[B]+2\pi\alpha'F} = \sum_{n=0}^{\infty} \frac{1}{n!} \underbrace{\left(\mathcal{P}\left[B\right] + 2\pi\alpha'F\right) \wedge \cdots \wedge \left(\mathcal{P}\left[B\right] + 2\pi\alpha'F\right)}_{n \text{ times}}; \tag{2.30}$$

(ii) Taking a C_q field with even q for type IIB, we select from the expansion of the exponentials the form with dimension $(p + 1 - q)$ such that integrations over the world-volume of the Dp-brane are well defined. Since the number of forms in the R-R sector are finite, the expansion in (2.30) also collapses to finite number of terms. Note that the coupling of the C_{p+1} potential to the world-volume of the Dp-brane (2.21) is recovered as the leading term in α' expansion of the WZ action.

D-branes as solutions of type IIB supergravity In this paragraph we study D-branes as massive and charged objects which couple to gravity and curve space-time. The pioneer work in this direction was the construction of black p-brane solutions in flat space-time [77]. If we restrict to constructing a black Dp-brane which does not carry lower-dimensional brane charge, only the R-R gauge potential C_{p+1} is needed in type II supergravity action, since the coupling of Dp-branes to this gauge potential guarantees the presence of the R-R form charge μ_p described in (2.21). If we further restrict to type IIB supergravity, i.e. p odd, the action (2.14) now reads,

$$S_{\text{IIB}}^{(p)} = \frac{1}{2\kappa_{10}^2} \int \mathrm{d}^{10}x \, \sqrt{-\det|G|} \left\{ e^{-2\Phi} \left(\mathcal{R} + 4\,\partial^\mu\Phi\partial_\mu\Phi\right) - \frac{1}{2}|F_{p+2}|^2 \right\}. \tag{2.31}$$

The BPS Dp-brane solution with the $\text{SO}(1,p) \times \text{SO}(9-p)$ symmetry are given by

$$\text{d}s^2 = H_p(r)^{-1/2}\eta^{ab}\text{d}x_a\text{d}x_b + H_p(r)^{1/2}\delta^{ij}\,\text{d}y_i\text{d}y_j\,,$$
$$e^\phi = g_s H_p(r)^{(3-p)/4}\,,$$
$$C_{p+1} = \left(\frac{1}{H_p(r)} - 1\right)\text{d}x_0 \wedge \cdots \wedge \text{d}x_p\,, \tag{2.32}$$

with $a,b \in \{0,\cdots p\}$ denoting the indices for the Dp-brane world-volume coordinates and $i,j \in \{p+1,\cdots \text{D}\}$ the indices for the transverse coordinates. The harmonic function H_p is given by

$$H_p(r) = 1 + \left(\frac{R_p}{r}\right)^{7-p}\,, \quad r^2 = \sum_{i=p+1}^{9} y_i^2\,, \tag{2.33}$$

where R_p satisfies the relation

$$R_p^{7-p} = (4\pi)^{\frac{5-p}{2}}\, \Gamma\left(\frac{7-p}{2}\right) g_s N \left(\alpha'\right)^{\frac{7-p}{2}}\,, \tag{2.34}$$

and N denotes the total R-R charges which is determined by the number of coincident Dp-branes. Due to charge conservation, the integration of the dual $(p+2)$-form field strength over the S^{8-p}-sphere surrounding the Dp-branes in the transverse directions gives

$$\int_{S^{8-p}} \star F_{p+2} = N\,. \tag{2.35}$$

Again, the case of D3-branes is special. Its world-volume has 4-dimensional Poincaré invariance. Only for $p = 3$ the dilation is constant, leading to constant string coupling $g_s = e^\Phi$. The five-form field strength is self-dual and can be expressed as

$$F_5 = q_3(\omega_5 + \star\omega_5)\,, \tag{2.36}$$

where q_3 is the D3-brane charge and ω_5 the volume form for the unit five-sphere. For a stack of N coincident D3-branes, the near-horizon limit $r \ll 1$ of the metric in the solution takes the form of the $\text{AdS}_5 \times \text{S}^5$ geometry,

$$R_3^4 = 4\pi g_s N \alpha'^2 \equiv R^4\,,$$
$$\text{d}s^2 = \frac{r^2}{R^2}\eta^{ab}\text{d}x_a\text{d}x_b + \frac{R^2}{r^2}\text{d}r^2 + R^2\text{d}\Omega_5^2\,, \quad a,b \in \{0,\cdots,3\}\,. \tag{2.37}$$

As a concluding statement for this section, at this point, it seems appropriate first to repeat the original AdS/CFT duality which states a correspondence between $\text{SU}(N_c)$ $\mathcal{N} = 4$ SYM in flat four space-time dimensions and type IIB superstring theory in $\text{AdS}_5 \times \text{S}^5$. Second, during the study of the two different perpectives of Dp-branes in this section it was mentioned for the special of $p = 3$ that

- the field theory living on the 4-dimensional world-volume of a stack of N coincident D3-branes is the $\mathcal{N} = 4$ SYM with the gauge group $\mathrm{U}(N) = \mathrm{SU}(N) \times \mathrm{U}(1)$ whose low energy effective action is given by the DBI and WZ terms;

- and a stack of N coincident D3-branes describes a solution of type IIB supergravity, the low energy limit of type IIB superstring theory, consisting of an $\mathrm{AdS}_5 \times \mathrm{S}^5$ geometry in the near horizon limit, a constant dilation and a self-dual R-R five-form field strength.

These observations are crucial for the establishing of the AdS/CFT duality conjecture which is going to be elaborated in the next section.

2.1.4 The conjecture in different limits

In the preceding sections, we have discussed in general the $\mathcal{N} = 4$ SYM theory, type IIB superstring theory, type IIB supergravity and two different points of view on the physics of Dp-branes. The case of a stack of N_c coincident D3-branes in supergravity and superstring theory gives hints for a possible connection between $\mathcal{N} = 4$ SYM theory in 4 dimensions and type IIB superstring theory in $\mathrm{AdS}_5 \times \mathrm{S}^5$. In this section, we discuss the Maldacena's heuristic argument which leads to the AdS/CFT conjecture. We present the conjecture in three different limits: the Maldacena limit, the 't Hooft limit and the so-called large 't Hooft coupling limit of the $\mathcal{N} = 4$ SYM. We also give the dictionary for the correspondence which precisely maps the parameters and the correlation functions of the two theories. Here, we closely follow the reviews [13, 14]. More details on the original formulation of the AdS/CFT correspondence can be found in [10–12].

The Maldacena limit and a heuristic argument To motivate the duality, let us first consider the excitations around the ground state of type IIB superstring theory in the presence of N_c coincident D3-branes in flat, ten dimensional Minkowski space-time. The D3-branes are extended along a $(3+1)$ dimensional plane in ten dimensional space-time. The excitations of the system consist of open and closed strings in interaction with each other. Quantization of the superstrings leads to a spectrum containing a massless $\mathcal{N} = 4$ vector multiplet plus a tower of massive string excitations. Since the open string endpoints are attached to the D3-branes, all the massless modes arising from zero-length strings propagate in the four dimensional world-volume of these branes. Similarly, quantization of closed strings provides a massless graviton supermultiplet plus a tower of massive string modes, all propagating in flat, ten dimensional space-time.

At energies smaller than the string scale $1/l_s$, where $l_s = \sqrt{\alpha'}$ denotes the string length, only massless string states can be excited. Additionally taking the Maldacena limit, i.e. sending α' to zero while keeping the energy and all the dimensionless parameters like the string coupling constant g_s and the number of D3-branes N_c fixed, one-dimensional fundamental strings can be seen as point particles with different boundary conditions for open and closed strings. In the AdS/CFT context, the

low-energy limit together with the Maldacena limit is sometimes referred to as the decoupling limit, where the justification for this choice of name will be explained in what follows.

Massless closed superstring modes are effectively described by supergravity. The strength of interactions in gravity is determined by the value of Newton gravitational constant which in ten dimensions is given by (2.16) and thus proportional to $g_s^2 \alpha'^4$. Hence in the decoupling limit the closed strings become non-interacting. Interactions between open strings are controlled by the Yang-Mills coupling constant $g_{\text{YM}}^2 = 2\pi g_s$. In the preceding sections, it was mentioned that the dynamics of open string states living on the world-volume of a stack of N_c D3-branes are governed by the Lagrangian of $\mathcal{N} = 4$ SU(N_c) SYM theory [73]. There is no interaction between massless closed and open strings, hence in the decoupling limit the effective action for massless string excitations in the presence of N_c coincident D3-branes in ten-dimensional Minkowski space-time is left with two decoupled systems: the free gravity in the ten-dimensional bulk; and the superconformal $\mathcal{N} = 4$ SU(N_c) gauge theory in four dimensions.

Next, let us examine the Maldacena limit from the supergravity description of D-branes. Here, the low-energy limit consists of focusing on excitations that have arbitrarily low energy with respect to an observer in the asymptotically flat Minkowski region. As discussed in the last section, since D-branes are massive charged objects they deform their embedding space-time. For the special case of N_c coincident D3-branes, the general supergravity solution (2.32) for Dp-branes is reduced to

$$
\begin{aligned}
\mathrm{d}s^2 &= H^{-1/2}(-\mathrm{d}x_0^2 + \mathrm{d}x_1^2 + \mathrm{d}x_2^2 + \mathrm{d}x_3^2) + H^{1/2}(\mathrm{d}r^2 + r^2 \mathrm{d}\Omega_5^2)\,, \qquad (2.38) \\
H &= 1 + \frac{R^4}{r^4}\,, \quad \int_{\mathrm{S}^5} F_5 = N_c\,, \quad F_5 = (1 + \star)\, \mathrm{d}x_0^2 \wedge \mathrm{d}x_1 \wedge \mathrm{d}x_2 \wedge \mathrm{d}x_3 \wedge \mathrm{d}H^{-1}.
\end{aligned}
$$

The metric component g_{tt} is r-dependent, hence the energy E_r of an object measured by an observer at the constant position r and the energy E_∞ measured by an observer at infinity are related by the redshift factor

$$
E_\infty = \sqrt{g_{00}}\, E_r\,. \qquad (2.39)
$$

From the point of view of an observer at $r \to \infty$, there are two kinds of possible excitations which can be considered to be in the low-energy regime: the massless graviton supermultiplet propagating at the ten-dimensional Minkowski region (bulk region); and massive string excitations in the region close to $r = 0$ (near-horizon region) which for an observer at infinity appear to have arbitrarily low energy due to the redshift effect.

Considering the Maldacena limit by taking the $\alpha' \to 0$ while keeping the energy fixed, the ten-dimensional Newton constant (2.16) goes to zero. Hence the massless particles propagating in the bulk become non-interacting and are described by free gravity. Moreover, there are no interactions between the near-horizon modes and the bulk modes. At low energies the wave length of bulk modes becomes much larger than the size of the curvature radius R in the near-horizon region, thus they cannot propagate in this region. Similarly, the modes living near the D3-branes cannot escape to infinity, since otherwise they have to climb up an infinite gravitational potential. As

a result, the configuration is again well approximated by two decoupled systems: free gravity in flat ten-dimensional spacetime and interacting closed strings of type IIB in the near-horizon region, whose geometry for $r \ll R$ is $\mathrm{AdS}_5 \times \mathrm{S}^5$,

$$\mathrm{d}s^2 = \frac{r^2}{R^2}(-\mathrm{d}x_0^2 + \mathrm{d}x_1^2 + \mathrm{d}x_2^2 + \mathrm{d}x_3^2) + \frac{R^2}{r^2}\mathrm{d}r^2 + R^2\mathrm{d}\Omega_5^2\,. \qquad (2.40)$$

In the decoupling limit, the effective action for the open and closed strings massless modes in the two different descriptions of D3-branes can be summarized in the following table.

	brane world-volume/ near-horizon region	bulk at infinity/ asymptotic region
N_c D3-branes in string theory	$\mathcal{N} = 4$ SYM with the gauge group $\mathrm{SU}(N_\mathrm{c})$	free gravity in flat 10d Minkowski
N_c D3-branes as solution of supergravity	type IIB superstring theory in $\mathrm{AdS}_5 \times \mathrm{S}^5$	free gravity in flat 10d Minkowski

Since in both descriptions of D3-branes there is a decoupled subsystem of free closed strings in flat ten-dimensional Minkowski space-time, it is tempting to conjecture a duality between [10]

- the $\mathcal{N} = 4$ SYM theory in (3+1)-dimensions with the gauge group $\mathrm{SU}(N_\mathrm{c})$ and the coupling constant g_YM;

- and type IIB superstring theory on $\mathrm{AdS}_5 \times \mathrm{S}^5$ where both AdS_5 and S^5 have the same radius R. This theory has one parameter, the string coupling g_s, and there is a five-form flux $\int_{\mathrm{S}^5} F_5 = N_\mathrm{c}$.

The conjecture describes a holographic duality, since the field theory lives in the four-dimensional Minkowski space-time which can be seen as the conformal boundary of the ten-dimensional $\mathrm{AdS}_5 \times \mathrm{S}^5$ where closed strings of type IIB propagate.

For concreteness, the duality is formulated by the so-called AdS/CFT dictionary which precisely maps physical quantities on both sides of the correspondence. The dictionary can be summarized in two relations which identify the parameters and the generating functionals for correlation functions among the two theories [11, 12]. The first relation identifies the parameters of the SYM theory, the number of colors N_c and the gauge coupling constant g_YM, with the parameters of the string theory given by the string coupling constant g_s and the size of the AdS_5 and S^5 space determined by R, namely

$$g_\mathrm{YM}^2 = 2\pi g_s, \quad g_\mathrm{YM}^2 N_\mathrm{c} = \frac{R^4}{\alpha'^2}\,. \qquad (2.41)$$

The second relation, first proposed in [11, 12], maps the generating functional for correlation functions on the field theory side and the string partition function on the string theory side,

$$\left\langle e^{\int d^4x \phi_0(\vec{x})\mathcal{O}(\vec{x})} \right\rangle_{\mathrm{CFT}} = \mathcal{Z}_{\mathrm{string}}\left[\phi\left(\vec{x}, r\right)|_{r\to\infty} = \phi_0\left(\vec{x}\right)\right]\,, \qquad (2.42)$$

where $\mathcal{O}(\vec{x})$ describes a gauge-invariant local operator which couples to the source $\phi_0(\vec{x})$. On the string theory side $\phi_0(\vec{x})$ is the boundary values of the bulk field $\phi(\vec{x}, r)$. There is no first principle to ensure which operator corresponds to which field. The necessary conditions for the mapping, however, require that fields and their dual operators must have the same quantum numbers, e.g. spin, global symmetries,... Moreover, there is a relation between the five (ten)-dimensional mass of the field and the conformal dimension of the dual operator depending on the spin, which will be discussed later in section 2.1.5, where we also provide some examples for (2.42).

The strongest form of the conjecture states that the identifications (2.41) and (2.42) should hold for all values of g_{YM} and N_c. To the present day the AdS/CFT still has the status of a conjecture. Due to the difficulty of quantizing superstrings on curved space-times, the string partition function on $AdS_5 \times S^5$ cannot be constructed explicitly, hence looking for a proof of the conjecture seems not to be a promising task. Nevertheless, some progress towards proving the AdS/CFT correspondence has been achieved during the last decade which are known in the context of AdS/CFT integrability in the planar $\mathcal{N} = 4$ SYM/ free type IIB superstrings sector, see [78] for an overview. In the next two paragraphs, two further limits of the correspondence will be considered in which the Maldacena conjecture becomes more tractable but still remains non-trivial.

The 't Hooft limit and the gauge-string theory connection The 't Hooft limit consists of taking the number of colors N_c to infinity while keeping the so-called 't Hooft coupling

$$\lambda \equiv g_{YM}^2 N_c = 2\pi g_s N_c \qquad (2.43)$$

fixed. In this limit, Feynman diagrams can be arranged in a perturbative expansion in $1/N_c$, in which field theory re-organizes itself topologically [79]. On the AdS side, the string coupling constant g_s becomes small as N_c is sent to infinity while keeping λ fixed, thus the 't Hooft limit corresponds to weak coupling string perturbation theory which is classical type IIB string theory in $AdS_5 \times S^5$ with diagrams arranged in g_s string loop expansion. In the strict $N_c \to \infty$ limit, this becomes a free string theory, since string interactions are suppressed.

For elucidating the connection between large N_c field theory and string theory, we discuss a simple model [13]

$$\mathcal{L} \sim \text{Tr}\left[\partial\Phi_i \, \partial\Phi_i\right] + \text{Tr}\left[g_{YM} c^{ijk} \Phi_i \Phi_j \Phi_k\right] + \text{Tr}\left[g_{YM}^2 d^{ijkl} \Phi_i \Phi_j \Phi_k \Phi_l\right] \qquad (2.44)$$

where $(\Phi_i)^a{}_b = (\Phi_i^A)(T^A)^a{}_b$ with $A = 1, 2, \ldots, N_c^2 - 1$ and $a, b = 1, 2, \ldots, N_c$ are fields in the adjoint representation of $SU(N_c)$. The Lagrangian is constructed in such a way that three-point vertices are proportional to g_{YM} and four-point vertices proportional to g_{YM}^2. The constants c^{ijk} and d^{ijkl} ensure that the action is $SU(N_c)$-invariant. Introducing $\tilde{\Phi}_i = g_{YM}\Phi_i$, the Lagrangian takes the form

$$\mathcal{L} \sim \frac{1}{g_{YM}^2} \left\{ \text{Tr}\left[\partial\tilde{\Phi}_i \, \partial\tilde{\Phi}_i\right] + \text{Tr}\left[c^{ijk} \tilde{\Phi}_i \tilde{\Phi}_j \tilde{\Phi}_k\right] + \text{Tr}\left[d^{ijkl} \tilde{\Phi}_i \tilde{\Phi}_j \tilde{\Phi}_k \tilde{\Phi}_l\right] \right\}. \qquad (2.45)$$
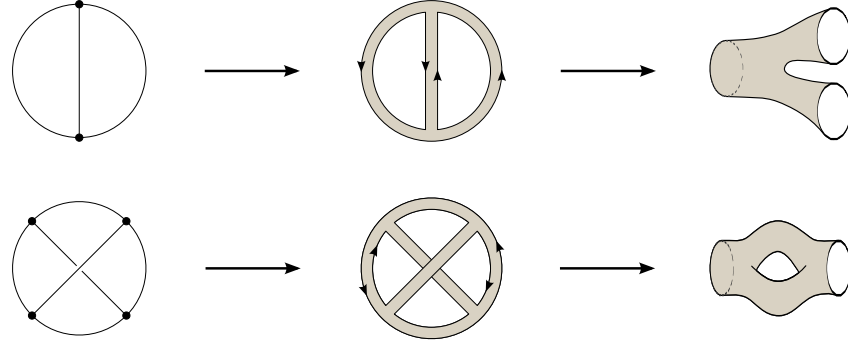
FIGURE 2.2: The Feynman diagrams (left) can be translated to double line diagrams (middle), which in turn can be interpreted as Riemann surfaces of well defined topology (shaded). These surfaces (deformed to the shape on the right) can be interpreted as stringy Feynman diagrams. While the upper diagrams are planar, the lower diagrams are non-planar of genus $g = 1$. This figure is taken from [80].

Using the double line notation introduced by 't Hooft [79], in which fundamental and anti-fundamental fields are represented by directed lines with the color indices at both ends and an adjoint field may be seen as a direct product of a fundamental and an anti-fundamental field, the propagator

$$\left\langle \left(\Phi_i^A(x)\right) \left(T^A\right)^a{}_b \left(\Phi_j^B(x')\right) \left(T^B\right)^a{}_b \right\rangle = \delta^{AB} D_{ij}(x - x') \left(\frac{1}{2} \delta_d^a \delta_b^c - \frac{1}{2N_c} \delta_b^a \delta_d^c \right)$$

(2.46)

in the limit of $N_c \to \infty$ can be represented by two parallel lines. In figure 2.2 the double line graphs for three-point vertices are displayed in the center.

One of the great advantages of the double line notation is that it provides a very simple way to keep track of the color index contractions in Feynman diagrams. Moreover, all Feynman diagrams can be written as a sum of double line graphs and can be seen as the sum of surfaces obtained by gluing polygons together at the double lines. In this language, a generic vacuum Feynman diagram, i.e. a connected vacuum graph with no external legs, defines a two-dimensional surface with F faces (color loops), E edges (propagators) and V vertices. The Feynman counting rules for such diagrams are:

- Each loop yields a factor of N_c due to the trace over the color indices;

- There is a factor of g_{YM}^2 for each propagator;

- The Lagrangian (2.45) assigns to each vertex a factor of $1/g_{YM}^2$.

Using these rules, a generic diagram with F faces, E edges and V vertices is of order

$$N_c^F g_{YM}^{2(E-V)} = N_c^{F-E+V} \lambda^{E-V} = N_c^\chi \lambda^{E-V} ,$$

(2.47)

where $\lambda = g_{YM}^2 N_c$ is the 't Hooft coupling and $\chi = F - E + V = 2 - 2g$ is the Euler characteristic, a topological invariant, which for a closed oriented surface is

completely determined by the genus g, the number of handles, of the surface. Hence in the 't Hooft limit, the leading contribution consists of diagrams with the lowest genus $g = 0$, i.e. diagrams which can be drawn on a plane or a sphere, thus all order N_c^2 graphs are planar diagrams. The next to leading order consists of diagrams on a torus with genus $g = 1$ which is suppressed by powers of $1/N_c^2$ relative to the leading order. In general, diagrams with topologies of higher genus $g \geqslant 1$ are suppressed by powers of N_c^{-2g}, and the $1/N_c$ perturbative expansion series of field theory can be written as the sum over all diagrams with topology g

$$\sum_{g=0}^{\infty} N_c^{2-2g} f_g(\lambda) \,, \tag{2.48}$$

where $f_g(\lambda)$ is some polynomial in λ which is determined by the diagrams relevant to physical processes with topology g with different structures concerning the difference of edges and vertices.

The topological $1/N_c$ expansion of field theory at large N_c is very similar to the perturbative expansion of closed string theories with string coupling g_s. More precisely, this can be seen by rewriting (2.47) as

$$N_c^F g_{YM}^{2(E-V)} = (g_{YM}^2 N_c)^F g_{YM}^{2(E-V-F)} = \lambda^F (2\pi g_s)^{2g-2} \,. \tag{2.49}$$

Summing over all diagrams at each topology g, the perturbative expansion of large N_c field theory can be written also as

$$\sum_{g=0}^{\infty} g_s^{2g-2} f_g'(\lambda) \,, \tag{2.50}$$

where $f_g'(\lambda)$ is some polynomial in λ which is determined by the diagrams relevant to physical processes with topology g with different structures concerning the number of faces (loops). This version clearly resembles the form of perturbative expansion series of closed string theories with small string coupling g_s.

As a concluding statement for this paragraph, it should be emphasized that although the above analysis was made for a general theory (2.44), it is true for any gauge theory coupled to adjoint matter fields, including the $\mathcal{N} = 4$ SYM theory [13], and the 't Hooft limit exhibits the original AdS/CFT conjecture in a weaker form, namely a correspondence between classical weak coupling string theory in $AdS_5 \times S^5$ and the large N_c limit of the $\mathcal{N} = 4$ SYM $SU(N_c)$ gauge theories.

The large λ limit The large λ limit consists of sending $\lambda \to \infty$ after the 't Hooft limit has been taken. The main motivation for studying this limit stems from the fact that classical type IIB string theory on $AdS_5 \times S^5$ reduces to classical type IIB supergravity on $AdS_5 \times S^5$ which is well understood. The reduction can be seen from the mapping (2.41) which implies that large $\lambda = g_{YM}^2 N_c = R^4/\alpha'^2$ corresponds to small $\alpha' = l_s^2$, hence in the large λ limit one-dimensional strings can be considered as point particles.

In this limit physical quantities can be described by the effective action of type IIB supergravity which may be written as an expansion in powers of α'. On the field theory side, this expansion corresponds to a $1/\sqrt{\lambda}$ expansion. The mapping between the generating functional for correlation functions on the field theory side and the string partition function on the string theory side (2.42) reduces to

$$\left\langle e^{\int d^4x \phi_0(\vec{x})\mathcal{O}(\vec{x})} \right\rangle_{\text{CFT}} = \mathcal{Z}_{\text{string}} \left[\phi(\vec{x}, r)|_{r\to\infty} = \phi_0(\vec{x})\right] \approx e^{-S_{\text{sugra}}[\phi_0(\vec{x})]}. \quad (2.51)$$

Since it is known how to calculate S_{sugra}, many physical quantities in strongly coupled, i.e. large λ, field theory can be obtained via doing calculations in classical gravity. The computation of correlation functions on the field theory side is mapped to the problem of solving the equations of motion for the dual fields, since the correlators can be given by

$$\langle \mathcal{O}(\vec{x}_1) \cdots \mathcal{O}(\vec{x}_n) \rangle = \frac{\delta^n e^{-S_{\text{sugra}}[\phi_0(\vec{x})]}}{\delta \phi_0(\vec{x}_1) \cdots \delta \phi_0(\vec{x}_n)}|_{\phi_0=0}. \quad (2.52)$$

At this point it is worth mentioning that this prescription is referred to as the so-called Euclidean signature of the AdS/CFT correspondence. In the Minkowski signature of the correspondence, however, the recipe for how to obtain correct two-point correlation functions is described in [81], where the authors of [81] point out that taking different boundary conditions for the considered fields will lead to different kind of correlators, namely retarted or advanced.

Up to this date, the large λ limit is the best understood part of the conjecture. It proves to be a powerful tool for studying strongly coupled field theories, since physical quantities can be computed on the gravity side which can be translated to field theory quantities via the AdS/CFT dictionary. A summary of different limits of the AdS/CFT correspondence can be found in the table presented below.

	Field theory side	String theory side
Maldacena limit (all N_c, g_{YM})	$\mathcal{N} = 4$ SU(N_c) SYM field theory	type IIB superstring theory in AdS
't Hooft limit ($N_c \gg 1$, $\lambda = \text{const}$)	$\mathcal{N} = 4$ SU(N_c) SYM with $1/N_c$ expansion	classical type IIB superstring in AdS with g_s expansion
large λ limit ($N_c \gg 1$, $\lambda \gg 1$)	$\mathcal{N} = 4$ SU(N_c) SYM with $1/\sqrt{\lambda}$ expansion	classical type IIB supergravity in AdS with α' expansion

2.1.5 Symmetry argument and some tests for the conjecture

In the last sections some arguments for the credibility of the duality conjecture have been discussed. Amongst others there are the large N_c argument, the Maldacena's heuristic argument, different descriptions of the same physical object D3-brane, the matching of low-energy field spectrum of theories from both sides, and we also mention the matching of the global symmetry of type IIB superstring theory in $\text{AdS}_5 \times \text{S}^5$ and the $\mathcal{N} = 4$ SYM with gauge group SU(N_c).

Below, the symmetry argument, which is often considered as the strongest argument for the conjecture, will be discussed in detail. In this section, we also provide

some early tests for the original AdS/CFT correspondence which includes matching of the spectrum of the operators, the computation of the AdS propagators and the calculation of expectation value of the Wilson loop, from which static quark anti-quark potential in the conformal phase can be read off.

I. The symmetry argument

It was mentioned in section 2.1.1 and 2.1.2 that both the $\mathcal{N} = 4$ SYM in four-dimensional Minkowski space-time and type IIB superstring theory in $\mathrm{AdS}_5 \times \mathrm{S}^5$ have the same global symmetry described by the supergroup $\mathrm{PSU}(2,2|4)$. Moreover, as it was pointed out in equation (2.4) and (2.20), they are both invariant under the S-duality $\mathrm{SL}(2, \mathbb{Z})$.

In the following, we will comment on how the symmetry described by the supergroup $\mathrm{PSU}(2,2|4)$ emerges on both sides of the correspondence. In general, the superconformal algebra $\mathfrak{psu}(2,2|4)$ is decomposed into space-time and internal symmetry, whose generators can be given by

$$
\begin{aligned}
\text{conformal algebra } \mathfrak{so}(2,4) : & \overbrace{M_{\mu\nu}, P_\mu}^{\text{Poincaré}}, \overbrace{K_\mu}^{\text{spec. conf.}}, \overbrace{D}^{\text{dilatation}}, \\
& \mu, \nu \in \{0, 1, 2, 3\}, \\
\text{R-symmetry } \mathfrak{su}(4) : & \mathfrak{R}_b^a, \quad a, b \in \{1, 2, 3, 4\}, \\
\text{supersymmetry operators} : & Q_\alpha^a, \bar{Q}_{\dot\alpha a}, \\
\text{conformal superalgebra generators} : & S_{\alpha a}, \bar{S}_{\dot\alpha}^a, \quad \alpha, \dot\alpha \in \{1, 2\},
\end{aligned}
\tag{2.53}
$$

where the full commutation relations among the generators can be found e.g. in [82] or in the compact form in the appendix of [83].

Superconformal $\mathcal{N} = 4$ **SYM** Conformal field theories are invariant under the action of the conformal group. In general, conformal transformations leave the metric invariant up to a scale factor

$$
g_{\mu\nu}(x) \to \Omega^2(x) g_{\mu\nu}(x),
\tag{2.54}
$$

and thereby preserve all angles. For $\Omega^2(x) = 1$, the metric remains invariant and the transformations are given by the generators of the Poincaré group which is composed of the Lorentz and the translation group. The most general conformal group in d-dimensions is the Poincaré group with the translation generators P_μ and rotation generators $M_{\mu\nu}$ extended by the scale transformation $D : x^\mu \to \Lambda x^\mu$ and the special conformal transformation $K_\mu : x^\mu \to (x^\mu + a^\mu x^2)/(1 + 2x^\nu a_\nu + a^2 x^2)$ with $\mu, \nu \in \{0, \cdots, d-1\}$. The generators of the conformal group satisfy the algebra

$$
[M_{\mu\nu}, P_\rho] = -i(\eta_{\mu\rho} P_\nu - \eta_{\nu\rho} P_\mu),
\tag{2.55}
$$
$$
[M_{\mu\nu}, K_\rho] = -i(\eta_{\mu\rho} K_\nu - \eta_{\nu\rho} K_\mu),
$$
$$
[M_{\mu\nu}, M_{\rho\sigma}] = -i\eta_{\mu\rho} M_{\nu\sigma} \pm \text{permutations}, \qquad [M_{\mu\nu}, D] = 0,
$$
$$
[D, K_\mu] = iK_\mu, \qquad [D, P_\mu] = -iP_\mu, \qquad [P_\mu, K_\nu] = 2iM_{\mu\nu} - 2i\eta_{\mu\nu} D,
$$

with all other commutators vanishing. Defining the generators J_{MN} with $M, N \in \{0, \cdots, d+1\}$ as follows

$$J_{\mu\nu} = M_{\mu\nu}, \quad J_{\mu d} = \frac{1}{2}(K_\mu - P_\mu), \quad J_{\mu(d+1)} = \frac{1}{2}(K_\mu + P_\mu), \quad J_{(d+1)d} = D,$$
(2.56)

the commutator $[J_{MN}, J_{RS}]$ displays the algebra structure of $\mathrm{SO}(2, d)$

$$[J_{MN}, J_{RS}] = -i(\eta_{MR} J_{NS} + \eta_{NS} J_{MR} - \eta_{NR} J_{MS} - \eta_{MS} J_{NR}) \quad (2.57)$$

with signature $\eta_{MN} = (-, +, +, \cdots, +, -)$. Thus the conformal group in flat $d = 4$ dimensional space-time is given by the group $\mathrm{SO}(2, 4)$.

By construction the $\mathcal{N} = 4$ SYM Lagrangian (2.1) is not only invariant under the conformal group $\mathrm{SO}(2, 4)$ but also invariant under $\mathcal{N} = 4$ Poincaré supersymmetry. The Poincaré supersymmetry enlarges the Poincaré algebra by including spinor supercharges Q_α^a transforming as left Weyl spinors of $\mathrm{SO}(1, 3)$ and their complex conjugates $(Q_\alpha^a)^\dagger = \bar{Q}_{\dot\alpha a}$ transforming as right Weyl spinors of $\mathrm{SO}(1, 3)$, where $\alpha, \dot\alpha \in \{1, 2\}$ denotes the spinor indices and $a \in \{1, \cdots, \mathcal{N}\}$ the number of supercharges Q. The supercharges commute with translations and satisfy the SUSY structure relations

$$\{Q_\alpha^a, \bar{Q}_{\dot\beta b}\} = 2\tau_{\alpha\dot\beta}^\mu P_\mu \delta_b^a, \qquad \{Q_\alpha^a, Q_\beta^b\} = 2\epsilon_{\alpha\beta} Z^{ab}, \qquad (2.58)$$

where the central charges Z^{ab}, which commute with all generators of the supersymmetry algebra, are anti-symmetric in the indices by construction, and the τ^μ are components of the four vector $(\mathbb{1}, -\tau^i)$ of 2×2 matrices with the standard Pauli matrices τ^i.

The supersymmetry algebra is invariant under the rotations of supercharges into one another under the unitary group $\mathrm{SU}(\mathcal{N})_R$, see e.g. [70], which is known as the R-symmetry group. For $\mathcal{N} = 4$ SYM, the R-symmetry group is $\mathrm{SU}(4)_R$. The supercharges Q_α^a transform under the $\mathbf{4}$ and $\bar{Q}_{\dot\alpha a}$ under the $\bar{\mathbf{4}}$ of $\mathrm{SU}(4)_R$.

The Poincaré supersymmetries and the special conformal transformations K_μ do not commute. Since both are symmetries, their commutator is also a symmetry. These symmetries are generated by $S_{\alpha a}$ and $\bar{S}_{\dot\alpha}^a$ which transform under the $\bar{\mathbf{4}}$ and under the $\mathbf{4}$ of $\mathrm{SU}(4)_R$, respectively.

Collecting all the symmetry groups discussed above, we conclude that the full symmetry algebra of the $\mathcal{N} = 4$ SYM theory is the superconformal algebra $\mathfrak{psu}(2, 2|4)$ whose generator are listed in (2.53).

Isometries of AdS On the other side of the correspondence, strings of type IIB string theory propagate on $\mathrm{AdS}_5 \times \mathrm{S}^5$. The conformal group in (3+1) dimensions $\mathrm{SO}(2, 4)$ is identified with the isometry group of AdS_5. This can be seen by embedding the hyperboloid of radius R

$$-X_{-1}^2 - X_0^2 + X_1^2 + X_2^2 + X_3^2 + X_4^2 = -R^2 \qquad (2.59)$$

in a flat six-dimensional space-time with the metric $\eta = \text{diag}(-1, -1, 1, 1, 1, 1)$. By the change of variables

$$
\begin{aligned}
r &= X_{-1} + X_4 \\
v &= X_{-1} - X_4 = \frac{R^2}{r} + \frac{x^2 r}{R^2} \\
x_\mu &= \frac{X_\mu R}{r}, \qquad \mu = 0, 1, 2, 3
\end{aligned}
\tag{2.60}
$$

the induced metric on the hyperboloid, which has the isometry $\text{SO}(2, 4)$, takes exactly the form of the AdS_5-part of (2.40), namely

$$
\mathrm{d}s_{\text{ind.}}^2 = \frac{r^2}{R^2}(-\mathrm{d}x_0^2 + \mathrm{d}x_1^2 + \mathrm{d}x_2^2 + \mathrm{d}x_3^2) + \frac{R^2}{r^2}\mathrm{d}r^2\,,
\tag{2.61}
$$

where in the intermediate step the relation

$$
\mathrm{d}v = \left(-\frac{R^2}{r^2} + \frac{x^2}{R^2}\right)\mathrm{d}r + 2\frac{xr}{R^2}\,\mathrm{d}x\,.
\tag{2.62}
$$

has been used. In addition, the isometries of S^5 form the group $\text{SO}(6) \sim \text{SU}(4)$ which is identified with the R-symmetry of the $\mathcal{N} = 4$ SYM theory. Hence, the full isometry group of $\text{AdS}_5 \times \text{S}^5$ is $\text{SO}(2, 4) \times \text{SO}(6)$ which is isomorphic to $\text{SU}(2, 2) \times \text{SU}(4)$. After including the supercharges transforming in the $(\mathbf{4}, \mathbf{4}) + (\overline{\mathbf{4}}, \overline{\mathbf{4}})$ of $\text{SU}(2, 2) \times \text{SU}(4)$, the full isometry supergroup of the $\text{AdS}_5 \times \text{S}^5$ background is $\text{PSU}(2, 2|4)$.

At this point it is interesting to note that the metric is invariant under the action of the dilatation operator $D : x^\mu \to \Lambda x^\mu$ accompanied by the rescaling $r \to r/\Lambda$, where Λ is a constant. Since $\mathcal{N} = 4$ $\text{SU}(N)$ SYM describes a conformal theory, it is also invariant under the action of D. Hence, the correspondence states that short-distance physics in gauge theory is associated to physics near the AdS boundary ($r \to \infty$) and the long-distance physics in gauge theory to the physics near the horizon ($r \to 0$) of AdS.

II. Some tests for the correspondence

Up to this date, there are a huge number of tests for the correspondence in the original and extended versions. So far no contradiction has been found, see e. g. [84] for a short summary. Since the correspondence always describes a weak/strong coupling duality, physical quantities like BPS objects, whose expectation values do not depend on the coupling, are of special interest for the purpose of comparison. Their correlators are also independent of the coupling constant λ, thus results obtained from field theory calculations at weak coupling can be directly compared to results at strong coupling obtained from supergravity calculations on $\text{AdS}_5 \times \text{S}^5$ background. In what follows, some evidence and tests for the original correspondence to leading order at large N_c or equivalently string tree-level will be discussed, among others the spectrum

of the operators, correlation functions and the non-local gauge invariant Wilson loops. This part of the thesis should provide some insights to the readers into how the AdS/CFT correspondence works in a more explicit way and discuss some concepts which will be used in this thesis later.

Spectrum of operators   The precise field-operator mapping (2.42)

$$\left\langle e^{\int d^4 x \phi_0(\vec{x}) \mathcal{O}(\vec{x})} \right\rangle_{\text{CFT}} = \mathcal{Z}_{\text{string}} \left[\phi(\vec{x}, r) |_{r \to \infty} = \phi_0(\vec{x}) \right] , \tag{2.63}$$

can been found in detail in sections 3.5 and 5.6 of [14] and references therein, where it has been shown that, indeed, the spectrum of the operators described by the irreducible representations of the supergroup $\text{PSU}(2, 2|4)$ coincides on both sides of the correspondence. In the following, the mapping between BPS operator and BPS state on the field and string theory side of the correspondence will be described.

On the field theory side all local, gauge invariant operators can be constructed and classified as polynomials of the canonical fields X^i, λ_a, A_μ and the covariant derivative D_μ in (2.1). In the unitary representations of the superconformal algebra $\mathfrak{psu}(2, 2|4)$, these operators are characterized by the spin s, the scaling dimension Δ of the fields given by the eigenvalue of scaling transformation D

$$D : x^\mu \to \Lambda x^\mu , \qquad \phi(x) \to \Lambda^\Delta \phi(\Lambda x) , \tag{2.64}$$

and the quantum numbers denoting the representation of the $\mathfrak{su}(4)_R$. For a BPS operator, a certain bound described by a relation between the above quantum numbers has to be fulfilled, hence all BPS states may be characterized by s and Δ.

On the gravity side, fields propagate in $\text{AdS}_5 \times \text{S}^5$ background. The dimensions of operators corresponding to massive fields scale as $R/l_s \sim \lambda^{1/4}$, hence they vary with the coupling constant, and thus these fields cannot be considered as BPS states. Massless fields in 10-dimensional AdS have λ-independent scaling dimension and should correspond to BPS operators. Decomposing a massless field $\phi(\text{AdS})$ in a series on S^5, $\phi(\text{AdS})$ can be written as a sum over the basis Y_Δ of spherical harmonics on S^5

$$\phi(\text{AdS}) = \sum_{\Delta=0}^{\infty} \phi_\Delta(\text{AdS}_5) Y_\Delta(\text{S}^5) , \tag{2.65}$$

where Δ will later be identified with the conformal dimension of the dual operator while other quantum numbers are implicit in the above expression. Similar to the Kaluza-Klein reduction of fields on a circle, the field $\phi_\Delta(\text{AdS}_5)$ receives a mass contribution m. This mass contribution m is in a correspondence relation with the scaling dimension Δ depending on the spin s of the

field [12]. Some concrete realizations of the field-operator (mass-conformal dimension) mapping for the $\text{AdS}_{d+1}/\text{CFT}_d$ correspondence are listed in [14]:

$$
\begin{array}{ll}
\text{scalars} & R^2 m^2 = \Delta(\Delta - d)\,, \\
\text{spin } 1/2,\ 3/2 & R|m| = \Delta - d/2\,, \\
\text{spin } 2 & R^2 m^2 = 0\,, \quad \Delta = d\,, \\
p\text{-form} & R^2 m^2 = (\Delta - p)(\Delta + p - d)\,.
\end{array}
\tag{2.66}
$$

As an illustration, a concrete realization for the field-operator mapping for a scalar field of mass m in the Euclidean Poincaré patch of AdS_5

$$
\mathrm{d}s^2 = \frac{R^2}{z^2}\left(\mathrm{d}x_0^2 + \mathrm{d}x_1^2 + \mathrm{d}x_2^2 + \mathrm{d}x_3^2 + \mathrm{d}z^2\right)
\tag{2.67}
$$

will be presented. The metric (2.67) is obtained from the Euclidean version of (2.61) by a coordinate transformation $z = R^2/r$. The wave equation $(\Box_{\text{AdS}_5} + m^2)\phi_\Delta(\vec{x}, z) = 0$ has two independent solutions, which asymptotically behave like $\phi_0(\vec{x})z^{4-\Delta}$ and $\phi_1(\vec{x})z^\Delta$ near the boundary $z \to 0$, where

$$
\Delta = 2 + \sqrt{4 + R^2 m^2}\,.
\tag{2.68}
$$

These solutions distinguish from each other by their property of renormalizability at the boundary $z = 0$. The one proportional to $z^{4-\Delta}$ is not squared normalizable, i.e. $\int \mathrm{d}^5 x \sqrt{\det(G_{\text{AdS}_5})}|\phi_\Delta|^2$ diverges, thus it does not correspond to the bulk excitation and represents the coupling to an external source [85]. The normalizable mode proportional to z^Δ is identified with the vacuum expectation value of the dual operator on the field theory side, to which the non-normalizable mode couples. In general, the asymptotic behavior of the solution for scalar field propagating in the AdS space is

$$
\lim_{z \to 0} \phi_\Delta(\vec{x}, z) = \phi_0(\vec{x})z^{4-\Delta} + \langle \mathcal{O}_\phi \rangle z^\Delta.
\tag{2.69}
$$

At this point, it is important to mention that in AdS space-time the mass-squared of a field may be negative without causing any instability to the system. This peculiar property was found by Peter Breitenlohner and Daniel Z. Freedman [86–88] which essentially states that tachyons in AdS space-time only cause an instability if their mass-squared is lower than a negative bound determined by the dimensions and radius of the AdS. For scalars in AdS_{d+1} with radius R, this bound is

$$
m^2 = -\frac{d^2}{4R^2}\,.
\tag{2.70}
$$

In order to get a finite, non-vanishing value for the non-normalizable mode at the boundary which sources the dual operator, the boundary condition on the field on the right-hand side of (2.63) is changed to

$$
\phi_\Delta(\vec{x}, z \to \epsilon) = \lim_{\epsilon \to 0} \epsilon^{4-\Delta}\phi_0(\vec{x})\,,
\tag{2.71}
$$

The scalar field $\phi_\Delta(\vec{x}, z)$ is dimensionless, hence $\phi_0(\vec{x})$ should have dimensions $[\text{length}]^{\Delta-4}$. From this conclusion the left-hand side of (2.63) implies that the dual gauge invariant operator $\mathcal{O}(\vec{x})$ has dimension Δ as defined in (2.68) which explains the first relation in (2.66).

Correlation functions The equivalence in calculating some specific correlation functions using the methods whether on the field or string theory side are discussed in detail e. g. in chapter 3 of [13] or in chapter 6 of [14] (see also references given in these chapters). Here, we present the general structure of one-, two- and three-point functions in a conformal field theory, and sketch the main result in [89] which confirms the identical structure of the three-point functions which are obtained independently from both sides of the correspondence in the large N_c, λ limit for a restricted set of fields and their corresponding operators.

In general, the forms of the n-point correlation functions are strongly restricted by the conformal invariance [14]. For scalars of dimension Δ, the 1-point function is given by

$$\langle \mathcal{O}_\Delta(x) \rangle = \delta_{\Delta,0} \,, \tag{2.72}$$

which is in agreement with the requirement of translation invariance that this object must be independent of x, and by scaling invariance that an x-independent quantity can have dimension Δ only when $\Delta = 0$. The 2-point function is given by

$$\langle \mathcal{O}_{\Delta_1}(x_1)\mathcal{O}_{\Delta_2}(x_2) \rangle = \frac{\delta_{\Delta_1,\Delta_2}}{|x_1 - x_2|^{2\Delta_1}} \,, \tag{2.73}$$

which fulfills the requirement by Poincaré symmetry that this object only depends upon $(x_1 - x_2)^2$, by inversion symmetry that it must vanish unless $\Delta_1 = \Delta_2$, by scaling symmetry where the exponent $2\Delta_1$ is fixed, and by properly normalizing the operators that the 2-point function may be put in diagonal form with unit coefficients. The 3-point function is given by

$$\langle \mathcal{O}_{\Delta_1}(x_1)\mathcal{O}_{\Delta_2}(x_2)\mathcal{O}_{\Delta_3}(x_3) \rangle = \frac{c_{\Delta_1\Delta_2\Delta_3}(g_{\text{YM}}, N_c)}{|x_1 - x_2|^{\Delta-2\Delta_3}|x_2 - x_3|^{\Delta-2\Delta_1}|x_3 - x_1|^{\Delta-2\Delta_2}} \,, \tag{2.74}$$

where $\Delta = \Delta_1 + \Delta_2 + \Delta_3$. The coefficient $c_{\Delta_1\Delta_2\Delta_3}$ is independent of the x_i and in general depends on the coupling g_{YM}^2 and the number of colors N_c of the Yang-Mills theory. Expressions for n-point functions with $n > 3$ consist of many conformally invariant terms occurring in the correlators.

If the AdS/CFT correspondence holds, one will expect that similar expressions to (2.72−2.74) for operators of the superconformal $\mathcal{N} = 4\,\text{SU}(N_c)$ SYM have to be obtained independently either by using the generating functional for correlation functions on the left-hand side of (2.63) or by using the string partition function for the dual fields on the right-hand side of (2.63).

Technically, on the SYM side, results can be obtained only perturbatively for small g_{YM} but for arbitrary N_{c}, while on the AdS side, analytical calculations can be carried out only in the large N_{c}, λ limit. Comparison of the results which are in mutually exclusive regimes of validity often does not makes sense, but BPS operators and their dual states should overcome this obstacle. Indeed, it was shown explicitly in [89] that the three-point functions of the 1/2 BPS operators in $\mathcal{N} = 4$ $\mathrm{SU}(N_{\mathrm{c}})$ SYM at large N_{c} is identical to the three-point functions of the corresponding fields in supergravity at large N_{c} and λ. The fields considered in [89] belong to a restricted set of fields and are dual to chiral primary operators in the gauge theory.

In this case, on the SYM side, one has to look at the two-point functions to fix the normalization as in (2.73). For the three-point functions, only the zero order in the coupling is normalizable, hence the correlator is independent of the coupling. On the gravity side at large N_{c} and λ, the two- and three-point correlation functions are obtained by using the prescription (2.52). The explicit two-point function is needed for fixing the normalization as in (2.73), since it is in general not clear how a specific normalization in gauge theory transforms compared to a normalization in gravity theory. The authors of [89] found that independent from Δ_i the three-point correlation functions obtained by the methods from the field and gravity side take exactly the same form of (2.74) with the coefficients

$$\lim_{N_{\mathrm{c}},\lambda\to\infty} c_{\Delta_1,\Delta_2,\Delta_3}(g_s, N_{\mathrm{c}})\bigg|_{\mathrm{AdS}} = \lim_{N_{\mathrm{c}}\to\infty} c_{\Delta_1,\Delta_2,\Delta_3}(g_{\mathrm{YM}} \ll 1, N_{\mathrm{c}})\bigg|_{\mathrm{SYM}} . \quad (2.75)$$

This is clearly a non-trivial test of the field-operator mapping (2.63) .

Wilson loops The Wilson loop is a non-local gauge invariant operator. This quantity is defined as the trace of the path-ordered exponential of the gauge field which is transported along a close line $\mathcal{C}$. In field theory, the expectation value of a Wilson loop with closed contour $\mathcal{C}$ having the form of a rectangle with infinite temporal side T and finite spatial side L gives the static potential between the heavy quark and anti-quark separated by the distance L [90] . The potential is given by

$$V_{\mathrm{q\bar{q}}}(L) = - \lim_{T\to\infty} \frac{1}{T} \log \langle W(\mathcal{C}) \rangle . \quad (2.76)$$

In the context of AdS/CFT the expectation value of the Wilson loop

$$W(\mathcal{C}) = \mathrm{Tr} \left[\mathcal{P} \exp \left(i \oint_{\mathcal{C}} (A_\mu(\mathbf{x}(s))\dot{x}^\mu(s))\, ds \right) \right] \quad (2.77)$$

on field theory side corresponds to a minimal surface in AdS space ending on the loop $\mathcal{C}$ at the conformal boundary [91, 92]. In the above formula, s denotes the curve parameter, $\mathcal{P}$ the path-ordered operator and A_μ is the gauge field.

In this picture, the quark and anti-quark correspond to the two endpoints of a string attached to the conformal boundary and dragging in the interior of the AdS space. The expectation value of the Wilson loop is obtained by solving the Nambu-Goto action for the AdS_5 metric

$$\langle W(\mathcal{C})\rangle = e^{-S_{\mathrm{NG}}(\mathcal{C})}, \quad S_{\mathrm{NG}} = \frac{1}{2\pi\alpha'}\int d\tau d\sigma \sqrt{-\det_{\alpha,\beta}\left[\mathrm{G}_{\mathrm{MN}}\partial_\alpha \mathrm{X}^{\mathrm{M}}\partial_\beta \mathrm{X}^{\mathrm{N}}\right]}, \tag{2.78}$$

which minimizes the string world-sheet ending on $\mathcal{C}$. The coordinates τ and σ parameterize the world-sheet of the string, while $\alpha, \beta \in \{\tau, \sigma\}$. The result for $V_{\mathrm{q}\bar{\mathrm{q}}}(L)$ reads [91, 92]

$$V_{\mathrm{q}\bar{\mathrm{q}}}(L) = -\frac{4\sqrt{2}\pi^2 \sqrt{g_{\mathrm{YM}}^2 N_{\mathrm{c}}}}{\Gamma(1/4)^4 L}. \tag{2.79}$$

The $1/L$ dependence of the coulombic potential occurs as expected from conformal invariance. This result can be seen as a test for the AdS/CFT correspondence which states that in the large N_{c}, λ limit, classical supergravity on AdS geometry is dual to a conformal field theory with zero β function. Furthermore, the fractional $(g_{\mathrm{YM}}^2 N_{\mathrm{c}})^{1/2} = \lambda^{1/2}$ dependence in the leading order is a non-trivial fact of strong coupling which differs from weak coupling where the result usually depends on λ at the leading order. This also confirms the $1/\lambda^{1/2}$ expansion of the dual the field theory in the large N_{c}, λ limit mention in section 2.1.4.

2.2 Generalizations and extensions

The original AdS/CFT conjecture presented in section 2.1 describes a duality between type IIB superstring theory in $\mathrm{AdS}_5 \times \mathrm{S}^5$ and the superconformal $\mathcal{N} = 4\ \mathrm{SU}(N_{\mathrm{c}})$ SYM in four dimensions. On the SYM theory side, all fields are in the adjoint representation of the $\mathrm{SU}(N_{\mathrm{c}})$, thus there is no fundamental matter. Moreover, the absence of the temperature restricts the study from most physical phenomena in nature. In this section, methods for introducing temperature 2.2.1, fundamental matter 2.2.2 and background fields 2.2.3 – like electromagnetic fields – into the AdS/CFT correspondence will be presented.

We exclusively use the D3/D7 model in 2.2.2 and 2.2.3, however, in general the main idea is to deform the AdS metric by introducing additional objects like black holes and D-branes into the geometry. By doing so the global symmetry of the geometry will be changed, and the dual field theory will differ from the superconformal $\mathcal{N} = 4$ SYM theory. The presence of a black hole breaks the conformal and supersymmetric structure of the geometry and corresponds to introducing finite temperature on the field theory side. Additional D-branes in AdS space give rise to fundamental degrees of freedom, moreover, they also back-react on the AdS geometry.

So far the ultimate aim, the constructing of a geometry which is dual to QCD, is still out of reach, however, many results have been achieved which encourage further studies in this direction. In the subsequent sections, some basic steps going from the original AdS/CFT correspondence towards AdS/QCD will be discussed.

2.2.1 Field theories at finite temperature and AdS black holes

In this section we discuss some basic properties of field theory at finite temperature in equilibrium where all thermodynamic quantities can be determined from the grand canonical partition function. We then discuss the black hole thermodynamics and present the main result of [93] which states that introducing a black hole into the AdS geometry corresponds to introducing finite temperature in the dual field theory.

Field theory at finite temperature The grand canonical partition function $\mathcal{Z}$ defined as

$$\mathcal{Z}\left(V, T, \mu\right) \equiv \mathrm{Tr}\hat{\rho} = \mathrm{Tr}\left[e^{-\beta\mathcal{H}}\right] , \tag{2.80}$$

is a central quantity in field theory at finite temperature which completely determines the thermodynamics of the system. Here, $\hat{H}$ is the usual Hamiltonian and $\mathcal{H} = \hat{H} - \mu\hat{N}$ the generalized Hamiltonian of the system, $\beta = 1/(k_B T)$ where T is the temperature and the Boltzmann constant k_B is set to unity in the remaining of the thesis, $\hat{\rho}$ denotes the density matrix of the system, V the volume, μ the chemical potential and $\hat{N}$ the number operator of particles associated to the chemical potential μ. Note that the chemical potential μ measures the energy needed to add an additional particle to the thermal system, thus grand canonical ensemble with the generalized Hamitonian $\mathcal{H}$ may exchange energy with a heat bath and particles with a reservoir.

Thermodynamic quantities like pressure p, entropy S, number of particle N and total energy E can be determined by the grand canonical partition function as

$$p = T\frac{\partial \ln \mathcal{Z}}{\partial V}, \quad S = \frac{\partial (T \ln \mathcal{Z})}{\partial T}, \quad N = T\frac{\partial \ln \mathcal{Z}}{\partial \mu}, \quad E = T^2\frac{\partial \ln \mathcal{Z}}{\partial T},$$
$$-pV = E - TS - \mu N . \tag{2.81}$$

The combination $-pV$ is also the value of the potential function Ω in the grand canonical ensemble. Furthermore, the expectation value of any physical quantity $\langle \mathcal{O} \rangle$ is given by

$$\langle \mathcal{O} \rangle = \frac{\mathrm{Tr}\left[\hat{\rho}\mathcal{O}\right]}{\mathcal{Z}} . \tag{2.82}$$

The trace in the definition of the partition function leads to an interesting property following from the cyclicity of the trace, namely

$$
\begin{aligned}
\langle \mathcal{O}_1(t)\mathcal{O}_2(t')\rangle &= \frac{1}{\mathcal{Z}(\beta)}\mathrm{Tr}\left[e^{-\beta\mathcal{H}}\mathcal{O}_1(t)\mathcal{O}_2(t')\right] \\
&= \frac{1}{\mathcal{Z}(\beta)}\mathrm{Tr}\left[e^{-\beta\mathcal{H}}\mathcal{O}_2(t')e^{-\beta\mathcal{H}}\mathcal{O}_1(t)e^{\beta\mathcal{H}}\right] \\
&= \frac{1}{\mathcal{Z}(\beta)}\mathrm{Tr}\left[e^{-\beta\mathcal{H}}\mathcal{O}_2(t')\mathcal{O}_1(t+i\beta)\right] \\
&= \langle \mathcal{O}_2(t')\mathcal{O}_1(t+i\beta)\rangle .
\end{aligned}
\tag{2.83}
$$

Such a relation is known as the KMS (Kubo-Martin-Schwinger) relation which plays a central role in the imaginary time formalism of finite temperature field theory according to the periodicity of $i\beta$ in t, see e.g. [94]. Considering the partition function in the functional integral representation, observation can be made that the operator $e^{-\beta\mathcal{H}}$ acts like the Heisenberg time evolution operator in the imaginary time axis. Here, the trace in (2.80) can be replaced by a Euclidean functional integration over the eigenstates $|\phi_a\rangle$ of $e^{-\beta\mathcal{H}}$, and $\mathcal{Z}$ may be given by

$$
\mathcal{Z} = \mathrm{Tr}\left[e^{-\beta\mathcal{H}}\right] = \int \mathrm{d}\phi_a \langle \phi_a|e^{-\beta\mathcal{H}}|\phi_a\rangle .
\tag{2.84}
$$

In order to work in the Euclidean time, we carry out a Wick rotation $\tau = -it$. The trace also demands the (anti-)periodicity condition of $\mathcal{Z}$ with respect to $\tau \to \tau + \beta$. Compactifying the finite field theory on the time interval $t \in [0, t_\mathrm{f}]$ and after identifying $\beta \equiv it_\mathrm{f}$, i.e. the temperature is identified with the reciprocal of the imaginary time interval it_f, the partition function in the path integral representation takes the form

$$
\mathcal{Z} = \int \mathcal{D}\phi\, e^{-S_\mathrm{E}[\phi]} ,
\tag{2.85}
$$

where $S_\mathrm{E}[\phi] = \int_0^\beta \mathrm{d}\tau \int \mathrm{d}\vec{x}\mathcal{L}(\phi, \vec{x}, \tau)$ is the Euclidean action for the system over a finite Euclidean time interval $\tau \in [0, \beta]$. Thus, correlation functions of operators at finite temperature in the imaginary time formalism can be determined by

$$
\langle \mathcal{O}_1 \cdots \mathcal{O}_n \rangle = \frac{\int \mathcal{D}\phi\mathcal{O}_1 \cdots \mathcal{O}_n\, e^{-S_\mathrm{E}[\phi]}}{\mathcal{Z}} ,
\tag{2.86}
$$

The concrete boundary conditions for the field ϕ can be determine by the studying of thermal Green functions which describe the propagation the field ϕ from point $(\vec{x}, 0)$ to $(\vec{x}', \tau)$

$$
G(\vec{x}, \vec{x}'; 0, \tau) = \frac{\mathrm{Tr}\left[\hat{\rho}\mathrm{T}_\tau\{\phi(\vec{x}', \tau)\phi(\vec{x}, 0)\}\right]}{\mathcal{Z}} ,
\tag{2.87}
$$

where T_τ is the imaginary time-ordering operator, and we assume . Depending on whether ϕ is a bosonic field ϕ^B or a fermionic field ϕ^F, the time-ordering operator T_τ will act as

$$T_\tau\{\phi^B(\tau_1)\phi^B(\tau_2)\} = \phi^B(\tau_1)\phi^B(\tau_2)\theta(\tau_1 - \tau_2) + \phi^B(\tau_2)\phi^B(\tau_1)\theta(\tau_2 - \tau_1)\,,$$
$$T_\tau\{\phi^F(\tau_1)\phi^F(\tau_2)\} = \phi^F(\tau_1)\phi^F(\tau_2)\theta(\tau_1 - \tau_2) - \phi^F(\tau_2)\phi^F(\tau_1)\theta(\tau_2 - \tau_1)\,.$$
$$(2.88)$$

This difference leads to

$$G^B(\vec{x}, \vec{x}'; \tau, 0) = G^B(\vec{x}, \vec{x}'; \tau, \beta)\,, \quad G^F(\vec{x}, \vec{x}'; \tau, 0) = -G^F(\vec{x}, \vec{x}'; \tau, \beta)\,, \tag{2.89}$$

which imply periodic boundary conditions in time direction for bosonic fields and anti-periodic boundary conditions in time direction for fermionic fields

$$\phi^B(\vec{x}, 0) = \phi^B(\vec{x}, \beta)\,, \qquad \phi^F(\vec{x}, 0) = -\phi^F(\vec{x}, \beta)\,. \tag{2.90}$$

This difference in boundary conditions causes bosonic and fermionic fields to have different mode expansions which lead to *supersymmetry breaking*.

Black hole thermodynamics The thermodynamics of black holes is very similar to the thermodynamics of finite temperature field theories which is presented at the beginning of this section. In the Euclidean formalism $\tau = -it$, the partition function is given by

$$Z = \int \mathcal{D}[g, \phi] e^{-\mathcal{I}_E[g, \phi]}\,, \tag{2.91}$$

where $\mathcal{I}_E$ denotes the gravity Euclidean action depending on the metric g and some matter fields ϕ. For a general $(d + 1)$-dimensional space-time, the action reads

$$\mathcal{I}_E[g, \phi] = \frac{1}{16\pi G_N^{(d+1)}} \int_{\mathcal{M}} \mathrm{d}^{d+1}x \sqrt{g}\,\mathcal{R} + \frac{1}{8\pi G_N^{(d+1)}} \int_{\partial\mathcal{M}} \mathrm{d}^d x \sqrt{\gamma}\,\mathcal{K}\,, \tag{2.92}$$

where $G_N^{(d+1)}$ denotes the $(d + 1)$-dimensional gravitational Newton constant, g the determinant of the metric, $\mathcal{R}$ the Ricci scalar. The second term in the action is known as the Gibbons-Hawking term which is required so that upon variation with the metric fixed at the boundary, the action (2.92) yields Einstein equations, see e. g. [76]. This term is evaluated on the boundary of $\mathcal{M}$, where γ is the determinant of the metric on the boundary and $\mathcal{K}$ is the trace of the extrinsic curvature of the boundary. The extrinsic curvature of a hypersurface $\mathcal{K}_{ab}$ is given by the pull-back of the covariant derivative of the out-ward pointing normal unit vector n_ν, namely

$$\mathcal{K}_{ab} = \frac{\partial x^\mu}{\partial \xi^a} \frac{\partial x^\nu}{\partial \xi^b} \nabla_\mu n_\nu\,, \tag{2.93}$$

where greek indices run from $\{0, \cdots, d\}$ and latin indices from $\{0, \cdots, d-1\}$.

For the transition from a configuration (g_1, ϕ_1) at time τ_1 to a configuration (g_2, ϕ_2) at time τ_2, the amplitude is given by

$$\int \mathcal{D}[g, \phi] e^{-\mathcal{I}_E[g,\phi]} = \langle (g_2, \phi_2)\, \tau_2 |\, (g_1, \phi_1)\, \tau_1 \rangle = \langle (g_2, \phi_2) |e^{H(\tau_2 - \tau_1)}|\, (g_1, \phi_1) \rangle,$$
(2.94)

where in the last step the Schrödinger picture is used. Considering the situation where (g_1, ϕ_1) is identical with (g_2, ϕ_2), and after writing $\tau_1 - \tau_2 = \beta = 1/T$, the canonical thermodynamical ensemble takes the form

$$Z_{\text{can.}} = \sum_n e^{-\beta E_n},$$
(2.95)

where E_n denotes the eigenvalue corresponding to the eigenstate (g_n, ϕ_n) of the Hamiltonian. The probability of the system to be in the n-th state is then given by

$$p_n = \frac{1}{Z_{\text{can.}}} e^{-\beta E_n}.$$
(2.96)

In the semiclassical approximation, where only the most dominant contribution to the path integral, the extremal action $\mathcal{I}_E$, is considered, the path integral becomes

$$Z_{\text{can.}} = e^{-\mathcal{I}_E} \equiv e^{-\beta W_{\text{can.}}}.$$
(2.97)

$W_{\text{can.}} = E - TS$ denotes the canonical thermodynamic potential, where E is the energy, S the entropy and T the temperature of the system. Using (2.96) for constructing the average energy $\langle E \rangle$ and the entropy S, we obtain

$$\langle E \rangle = p_n E_n = -T^2 \frac{\partial \mathcal{I}_E}{\partial T}, \qquad S = -\sum_n p_n \log p_n = \frac{1}{T} \langle E \rangle - \mathcal{I}_E. \quad (2.98)$$

In general the temperature of the system, the Hawking temperature T_{H}, can be determined via the surface gravity κ evaluated at the event horizon r_{H} [95]. The surface gravity is defined by the time-like Killing vector χ, i.e. $\nabla_a \chi_b + \nabla_b \chi_a = 0$, and satisfies the relation

$$\kappa^2 = -\frac{1}{2} \left(\nabla_a \chi_b \right) \left(\nabla^a \chi^b \right).$$
(2.99)

The Hawking temperature is given by

$$T_{\text{H}} = \frac{\kappa}{2\pi} |_{r=r_{\text{H}}}.$$
(2.100)

The grand canonical partition function can be constructed if the charged black hole is considered. Its geometry is known as the Reissner-Nordström

metric. Since the black hole is charged, the action (2.92) is supplemented by a contribution from the Maxwell term

$$\mathcal{I}_M[g_{\text{RN}}, A] = -\frac{1}{16\pi G_{\text{N}}^{(d+1)}} \int_{\mathcal{M}} \mathrm{d}x^{d+1} \sqrt{g_{\text{RN}}} F_{\mu\nu} F^{\mu\nu} \,, \tag{2.101}$$

with a gauge potential $A = A_t \mathrm{d}t = (-\mu + Q/r^{d-2})\mathrm{d}t$ where Q is the charge, μ the chemical potential, t the time and r the radial coordinate of the Reissner-Nordström metric $g_{\text{RN}}^{\mu\nu}$. In the semiclassical limit, the extremal action obtained from (2.92) and (2.101) for the Reissner-Nordström metric gives rise to the grand canonical potential Ω, also known as the Gibbs potential, by equating

$$\begin{aligned} \mathcal{I}_{\text{grand}} &= \mathcal{I}_E[g_{\text{RN}}, \phi] + \mathcal{I}_M[g_{\text{RN}}, A] = \beta\Omega, \text{ where} \\ \Omega &= \langle E \rangle - TS - \mu Q \,. \end{aligned} \tag{2.102}$$

Comparing (2.102) to (2.81), the charge Q is the analogue of the particle number N. Similar to (2.98), the other standard thermodynamic relations for the grand canonical ensemble are

$$\begin{aligned} \langle E \rangle &= -T^2 \left(\frac{\partial \mathcal{I}_{\text{grand}}}{\partial T} \right) - \mu T \left(\frac{\partial \mathcal{I}_{\text{grand}}}{\partial \mu} \right) \,, \\ S &= -T \left(\frac{\partial \mathcal{I}_{\text{grand}}}{\partial T} \right) - \mathcal{I}_{\text{grand}} \,, \qquad Q = -T \left(\frac{\partial \mathcal{I}_{\text{grand}}}{\partial \mu} \right) \,. \end{aligned} \tag{2.103}$$

AdS Schwarzschild black hole   In the context of AdS/CFT correspondence, introducing finite temperature on the field theory side corresponds to adding black hole into the geometry of AdS [93]. Similar to the Minkowski space-time, AdS space-time supports black hole solutions such that the near horizon geometry is deformed, while asymptotically the geometry approaches the original metric. The thermodynamics of black holes in 4-dimensional Anti-de Sitter space were first studied in [96], where Hawking and Page show that at a critical temperature T_{HP} there is a first order transition - known as Hawking-Page transition - between two possible gravity solutions, the thermal AdS for $T < T_{\text{HP}}$ and the black hole AdS for $T > T_{\text{HP}}$.

   Analogous analysis was carried out in [93] for AdS_{d+1} space-time, where Witten found a Hawking-Page transition between two asymptotically AdS gravity solutions, namely the thermal and black hole AdS. These two solutions are interpreted to describe the confinement and deconfinement phase of the dual field theory, respectively. Here, the temperature is introduced by replacing the AdS_{d+1}-boundary $\mathbb{R}^d$ by $\mathcal{M}^{d-1} \times S^1$, where $\mathcal{M}$ is some spatial manifold and S^1 represents the periodic imaginary time with supersymmetry-breaking boundary conditions. For compact $\mathcal{M}$, e.g. S^{d-1}, the thermal AdS solution [93] is

$$\mathrm{d}s^2 = -f_{\text{th}}\mathrm{d}t^2 + f_{\text{th}}^{-1}\mathrm{d}r^2 + r^2\mathrm{d}\Omega_{d-1}^2 \,, \qquad f_{\text{th}}(r) = 1 + \frac{r^2}{R^2} \,, \tag{2.104}$$

with periodically identified Euclidean time coordinate $\tau \sim \tau + \beta$, where $\tau = -it$. The black hole AdS metric, also known as AdS Schwarzschild, is given by

$$ds^2 = -f_{\text{bh}}dt^2 + f_{\text{bh}}^{-1}dr^2 + r^2d\Omega_{d-1}^2 \,, \quad f_{\text{bh}}(r) = 1 + \frac{r^2}{R^2} - \frac{r_{\text{H}}^{d-2}}{r^{d-2}}\left(1 + \frac{r_{\text{H}}^2}{R^2}\right),$$
(2.105)

where r_{H} is the event horizon of the metric and $r_{\text{H}} \leqslant r < \infty$. Computing the Einstein-Hilbert action for the two solutions, it was found that the black hole AdS has smaller Euclidean action compared to that of the thermal AdS when $r_{\text{H}} > R$ and vice versa for $r_{\text{H}} < R$. Later we will see that the dual field temperature T is proportional to r_{H}, thus at low temperature, i.e. $r_{\text{H}} \ll R$, the field theory is dual to thermal AdS space-time, while at high temperature, i.e. $r_{\text{H}} \gg R$, the field theory is dual to black hole AdS. This is the generalized version of the Hawking-Page transition [96].

In general, we are interested in field theories living in non-compact space-times. This can be realized by taking the circumference of the S^{d-1} to be large compared to that of the S^1. In this limit the boundary of AdS_{d+1} can be seen as $\mathbb{R}^{d-1} \times S^1$. This flat space limit is essentially the same as the high temperature limit for conformal field theories [97]. Hence, for AdS black hole with horizon radius r_{H} much larger than the curvature radius R, the Schwarzschild $AdS_5 \times S^5$ geometry is given by

$$ds^2 = -fdt^2 + \frac{r^2}{R^2}\left(dx_1^2 + dx_2^2 + dx_3^2\right) + \frac{1}{f}dr^2 + R^2d\Omega_5^2 \,, \quad f \equiv \frac{r^2}{R^2}\left(1 - \frac{r_{\text{H}}^4}{r^4}\right).$$
(2.106)

The event horizon is located at $r = r_{\text{H}}$ where the geometry takes the form of three dimensional flat space in $\{x_1, x_2, x_3\}$-directions, hence this metric is sometimes called black three-brane. Calculating the minimal surface of the Wilson loop as described in (2.76) for the AdS Schwarzschild metric (2.106), the authors of [98] indeed found a deconfinement behavior which is expressed in the dissociation of quark and anti-quark as they are separated over a critical distance depending on the horizon radius r_{H}.

Hawking temperature and field theory temperature   It can be shown that the temperature of the dual field theory can be identified with the Hawking temperature of the AdS black hole geometry. In what follows a demonstration of this statement will be presented for the case of (2.106).

For the Schwarzschild solutions having the form of (2.105), we may choose the Killing vector to be $\chi = \chi^a\partial_a = \partial/\partial t$. Using (2.99) and (2.100), this choice of the Killing vector leads to

$$\kappa = \frac{1}{2}\frac{\partial f_{\text{bh}}(r)}{\partial r} \qquad \text{and} \qquad T_{\text{H}} = \frac{r_{\text{H}}^2 d + (d-2)R^2}{4\pi r_{\text{H}}R^2} \,.$$
(2.107)

For the large AdS_5 black hole (2.106), the Hawking temperature is

$$T_\text{H} = \frac{r_\text{H}}{\pi R^2}. \tag{2.108}$$

In what follows, we will see that the value for the Hawking temperature (2.108) can also be obtained by studying the behavior of the metric (2.106) close to the horizon r_H and taking into account the periodicity of the Euclidean time in the imaginary time formalism. Taylor expanding $f(r)$ near r_H, the interesting part containing g_tt and g_rr of the metric (2.106) takes the form

$$\mathrm{d}s'^2 = -\frac{4r_\text{H}}{R^2}\left(r - r_\text{H}\right)\mathrm{d}t^2 + \frac{R^2}{4r_\text{H}\left(r - r_\text{H}\right)}\mathrm{d}r^2. \tag{2.109}$$

After doing the coordinates transformation $r = r_\text{H} + \xi^2/r_\text{H}$ and Wick-rotating $t \to i\tau$, the expression above takes the form of the flat metric in polar coordinates

$$\mathrm{d}s'^2 = \frac{R^2}{r_\text{H}^2}\left(\mathrm{d}\xi^2 + \frac{4r_\text{H}^2}{R^4}\xi^2\mathrm{d}\tau^2\right). \tag{2.110}$$

Thus the Euclidean time τ is proportional to the angular coordinate $\theta = 2r_\text{H}\tau/R^2$ in this parameterization. In order to avoid conical singularity, i.e. the periodicity $\theta \to \theta + 2\pi$ has to be respected near $\xi = 0$, while demanding the periodicity $\tau \to \tau + \beta$, we find

$$\frac{1}{\beta} = \frac{r_\text{H}}{\pi R^2}. \tag{2.111}$$

From (2.108) and (2.111) the Hawking temperature T_H can be identified with the temperature $T = 1/\beta$ of the field theory living on the conformal boundary of the AdS Schwarzschild black hole.

The entropy On the gravity side, the Bekenstein-Hawking entropy as defined in (2.103) can be computed for a general $(d+1)$-dimensional black hole metric, and the result for the entropy is proportional to the area $\mathcal{A}_\text{H}$ of the horizon of the geometry, see for instance [76], namely

$$S_\text{bh} = \frac{\mathcal{A}_\text{H}}{4G_\text{N}^{(d+1)}}. \tag{2.112}$$

For the 5-dimensional AdS black hole from (2.106), the horizon is a three-sphere with $\mathcal{A}_\text{H} = 2\pi^2 r_\text{H}^3$, where r_H can be expressed in term of the Hawking temperature via (2.108). Using the parameter dictionary to write, we have for the AdS black hole (2.106)

$$S_\text{bh} = \pi^4 N_\text{c}^2 R^3 T_\text{H}^3. \tag{2.113}$$

This quantity is obtained on the gravity side, thus it is valid only in the large 't Hooft coupling limit $\lambda \gg 1$. The entropy S_{YM} of the $\mathrm{SU}(N_{\mathrm{c}})$ Yang-Mills field theory for a photon gas in ordinary three-sphere with radius r_{H} at temperature $T = T_{\mathrm{H}}$ can be obtained in the small 't Hooft coupling limit $\lambda \ll 1$, see e.g. [5], where one obtains

$$S_{\mathrm{YM}} = \frac{4}{3} S_{\mathrm{bh}} . \tag{2.114}$$

The results on the gauge and gravity side do not match. The reason for the difference is that they are obtained in different regime of λ. Nevertheless, it is expected that an exact calculation for arbitrary λ will show the course of the entropy depending on λ with two fixed points at very small and large λ.

2.2.2 Fundamental matter with D3/D7 model

The $\mathcal{N} = 4$ $\mathrm{SU}(N_{\mathrm{c}})$ **SYM** theory contains only fields in the adjoint representation of the gauge group $\mathrm{SU}(N_{\mathrm{c}})$. In order to study interactions not only among bosonic degrees of freedom, the original AdS/CFT needs to be extended by introducing fermionic degrees of freedom which are fields in the fundamental or anti-fundamental representation of the gauge group. This can be realized by adding N_{f} coincident flavor brane probes to the stack of N_{c} D3 color branes [99]. The flavor branes are referred to the name *probes* since their back-reaction on the embedding AdS geometry generated by the color branes is neglected in the $N_{\mathrm{f}} \ll N_{\mathrm{c}}$ limit.

The field theory living on the world-volume of the flavor branes is governed by the $\mathrm{U}(N_{\mathrm{f}})$ gauge group. Fields in fundamental representation of the $\mathrm{U}(N_{\mathrm{f}})$ are generated by strings with one endpoint on the N_{c} brane and the other endpoint on the N_{f} brane. Such strings carry one color index of the $\mathrm{SU}(N_{\mathrm{c}})$ and one flavor index of the $\mathrm{U}(N_{\mathrm{f}})$, and sometimes are referred to the name 'quarks' similar to QCD. Depending on the orientation of the strings, i.e. they end or start on the flavor branes, they represent matter in the fundamental or anti-fundamental representation of the gauge group $\mathrm{U}(N_{\mathrm{f}})$. The mass of one quark is proportional to the length l of the corresponding string stretching between the color N_{c} branes and the flavor N_{f} branes and is given by $m_{\mathrm{q}} = l/(2\pi\alpha')$. Strings starting and ending on the flavor branes carry one index in the fundamental and one index in the anti-fundamental representation of the $\mathrm{U}(N_{\mathrm{f}})$. These strings can be considered as objects in the adjoint representation of the gauge group $\mathrm{U}(N_{\mathrm{f}})$ and hence naturally describe mesonic degrees of freedom. In string theory these states describe fluctuations of the flavor branes in the background geometry. In AdS/CFT context, small oscillations of the branes are dual to mesons on the field theory side, for a review of mesons in gauge/gravity duality see e.g. [100].

The method for introducing fundamental matter using D3/D7 model is discussed in detail in [99, 101, 102]. The key result is that the D3/D7 model describes a BPS configuration which preserves $1/4$ of the supersymmetries of

type IIB superstring theory, and has an $SO(3, 1)$ symmetry on the world-volume of the D3-branes and $SO(4) \times SO(2)$ symmetry in the six-dimensional space transverse to the world-volume of the D3-branes. The dual field theory is the $(3+1)$-dimensional $\mathcal{N} = 4$ SYM theory coupled to the $\mathcal{N} = 2$ hypermultiplets arising from strings stretching between the D3- and the D7-branes. In the subsequent paragraphs we will follow the review [100] to sketch some main properties of this model which are relevant for this thesis.

The gravity picture of D3/D7 model   We consider the D3/D7-brane intersection in a $(9 + 1)$-dimensional flat space-time. A stack of N_c coincident D3-branes may be chosen to extend along the (0123)-directions, where 0 denotes the time direction. The N_c D3-branes generate the $AdS_5 \times S^5$ space. For a BPS configuration the stack of coincident N_f D7-branes is embedded along the (01234567)-directions which is illustrated in the table below.

	0	1	2	3	4	5	6	7	8	9
D3	X	X	X	X						
D7	X	X	X	X	X	X	X	X		

The N_f D7-branes should be seen as probes and do not deform the AdS geometry. In the directions transverse to the D3-branes, the presence of the D7-branes breaks the $SO(6)$ symmetry to $SO(4) \times SO(2)$. $SO(4)$ rotates the coordinates spanning the (4567) subspace and $SO(2)$ acts in the (89)-directions. If D3- and D7- branes have the different positions in the (89)-directions, the $SO(2)$ group is broken explicitly. In this case, the strings stretching between D3- and D7- branes can have non-zero length giving rise to massive quarks in the dual field theory. More details about the embedding of D7-branes in $AdS_5 \times S^5$ will be discussed later in this section. A schematic representation of the AdS/CFT duality with added flavor is displayed in figure 2.3.
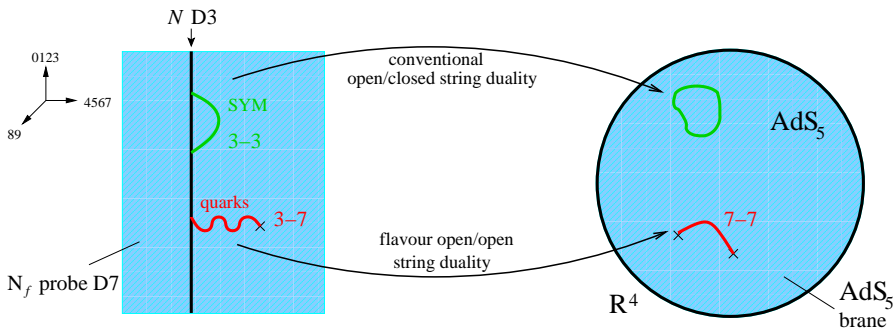

FIGURE 2.3:   Schematic representation of the AdS/CFT duality with added flavor. In addition to the original AdS/CFT duality, open string degrees of freedom representing quarks are mapped to open strings beginning and ending on the D7 probe, which asymptotically near the boundary wrap $AdS_5 \times S^3$ inside $AdS_5 \times S^5$, see equation (2.119). This figure is taken from [100].

The field theory picture of D3**/D**7 **model** The field content of the D3/D7-brane intersection consists of open strings which are attached to the D-branes. The massless modes of open strings with both ends on the N_c D3-branes, the 3-3 strings, give rise to the field content of the $\mathcal{N} = 4$ SYM theories with gauge group $\mathrm{SU}(N_c)$. In the presence of D7-branes, there are 3-7 and 7-3 string modes which give rise to the $\mathcal{N} = 2$ hypermultiplets in the (anti-)fundamental representation. There are also 7-7 string modes, but they decouple from the 3-3, 3-7 and 7-3 strings when large N_c limit is taken while keeping N_f fixed because the 8-dimensional 't Hooft coupling $\lambda^{(8)} = \lambda(2\pi\sqrt{\alpha'})^4 N_f/N_c$ vanishes in the low-energy $\alpha' \to 0$ and $N_f \ll N_c$ limit. Thus the field theory generated by the massless 7-7 strings decouples from the rest and the $\mathrm{U}(N_f)$ gauge group of the field theory on the world-volume of the D7-branes play the role of a global flavor group in the four-dimensional theory. The subgroup $\mathrm{U}(1)_B \in \mathrm{U}(N_f)$ describes the overall position of the stack of D7-branes in the transverse space. It is identified with the conservation of baryon number on the dual field theory side, thus fundamental fields in the hypermultiplet are charged under $\mathrm{U}(1)_B$.

The fields in the $\mathcal{N} = 2$ hypermultiplet are massless if the stack of N_f flavor branes and the stack of N_c color branes overlap in (89)-directions. The global symmetry $\mathrm{SO}(4) \times \mathrm{SO}(2)$ in the 6-dimensional space transverse to the D3-branes is translated to the $\mathrm{SU}(2)_\Phi \times \mathrm{SU}(2)_\mathcal{R} \times \mathrm{U}(1)_\mathcal{R}$ symmetry on the field theory side. If the $\mathrm{SO}(2) \simeq \mathrm{U}(1)_\mathcal{R}$ is broken explicitly by separating the flavor and color branes in the (89)-directions, the hypermultiplet becomes massive.

All the fields with the corresponding quantum numbers of the $\mathcal{N} = 2$ hypermultiplet for the D3-D7 model can be represented by the symmetry groups $\mathrm{SU}(2)_\Phi \times \mathrm{SU}(2)_\mathcal{R}$, $\mathrm{U}(N_f)$, $\mathrm{U}(1)_\mathcal{R}$ and $\mathrm{U}(1)_B$. For the fundamental fields in the hypermultiplet, the quark multiplet $q^m = (q, \bar{q}^\dagger)$ are in the $(0, \frac{1}{2})$ and $\mathbf{N_f}$ of the $\mathrm{SU}(2)_\Phi \times \mathrm{SU}(2)_\mathcal{R}$ and $\mathrm{U}(N_f)$, respectively. They have charge $+1$ under the $\mathrm{U}(1)_B$. Their supersymmetric partners, the squarks, $\psi_i = (\psi, \bar{\psi}^\dagger)$ are in the $(0, 0)$ and $\mathbf{N_f}$ of the $\mathrm{SU}(2)_\Phi \times \mathrm{SU}(2)_\mathcal{R}$ and $\mathrm{U}(N_f)$, respectively. They are charged ∓ 1 under $\mathrm{U}(1)_\mathcal{R}$ and $+1$ under $\mathrm{U}(1)_B$. For the other fields of the $\mathcal{N} = 2$ hypermultiplet with the corresponding quantum numbers, see [100].

Embedding D7**-branes in** AdS_5 It is difficult to construct the full dual gravity solution for the D3/D7 system due to the back-reaction of the D7-branes on the background geometry. Some pioneer works towards this direction can be found in [103, 104]. For simplicity, we consider the *probe limit* $N_f \ll N_c$, where the effect of back-reaction is of order N_f/N_c and thus can be neglected. On the field theory side, neglecting effects proportional to N_f/N_c is known as the *quenched approximation*, where diagrams with quark loops in perturbation theory are omitted. The N_c D3-branes generate an $\mathrm{AdS}_5 \times \mathrm{S}^5$ geometry. In the following, we will study how to construct a stable embedding of the D7-branes in the AdS background.

As discussed in section 2.1.3, the low-energy effective action of the Dp-

brane world-volume field theory is described by the Dirac-Born-Infeld and the Chern-Simons action, whose bosonic part is

$$S_{\mathrm{D7}} = -\tau_7 \int \mathrm{d}^8\xi \sqrt{-\det\left(\mathcal{P}[\mathrm{G}]_{\mathrm{ab}} + 2\pi\alpha'\mathrm{F}_{\mathrm{ab}}\right)} + \tau_7 \frac{(2\pi\alpha')^2}{2} \int \mathcal{P}[C_4] \wedge F \wedge F,$$
(2.115)

where $\tau_7 = [(2\pi)^7 g_\mathrm{s}\alpha'^4]^{-1}$ denotes the D7-brane tension from (2.22), G the background metric, C_4 the R-R 4-form and $F = \mathrm{d}A$ the field strength of the $\mathrm{U}(N_\mathrm{f})$ gauge field A^a living on the D7-brane.

For the simplest case here, we are only interested in the geometric embedding of the D7-branes without turning on the world-volume gauge field. Later in this thesis, non-vanishing gauge fields will be introduced and the embeddings of probe D-branes will be studied in a more general background geometry than $\mathrm{AdS}_5 \times \mathrm{S}^5$. We can write the AdS metric (2.67) in the form

$$\mathrm{d}s^2 = \frac{r^2}{R^2}(-\mathrm{d}x_0^2 + \mathrm{d}x_1^2 + \mathrm{d}x_2^2 + \mathrm{d}x_3^2) + \frac{R^2}{r^2}\left(\mathrm{d}\rho^2 + \rho^2\mathrm{d}\Omega_3^2 + \mathrm{d}w_5^2 + \mathrm{d}w_6^2\right),$$
(2.116)

with $\rho^2 = \sum_{i=1}^4 w_i^2$ and $r^2 = \sum_{i=1}^6 w_i^2$. Here, the coordinates $\{x_0, \cdots, x_3\}$ span the world-volume of the D3-branes, $\{x_0, \cdots, x_3, w_1, \cdots, w_4\}$ the world-volume of the D7-branes and $\{w_5, w_6\}$ denote the directions transverse to both D3- and D7-branes. The embedding should preserve the Lorentz symmetry $\mathrm{SO}(3,1)$ on the world-volume of the D3-branes and the rotational symmetry in the (4567)-directions, hence the embedding functions depend only on ρ. The action (2.115) for (2.116) gives

$$S_{\mathrm{D7}} = -\tau_7 \mathrm{Vol}(\mathrm{S}^3)\mathrm{Vol}(\mathbb{R}^{1,3})N_\mathrm{f} \int_0^\infty \mathrm{d}\rho \rho^3 \sqrt{1 + \left(\frac{\partial w_5}{\partial\rho}\right)^2 + \left(\frac{\partial w_6}{\partial\rho}\right)^2}.$$
(2.117)

The above action is minimized if w_5 and w_6 are constant, thus the D7-branes lie flat in the transverse (89)-directions. Going to polar coordinates in the (89)-directions, the embedding functions there can be written as

$$w_5(\rho) = L(\rho)\cos\Theta, \qquad w_6(\rho) = L(\rho)\sin\Theta.$$
(2.118)

Using the $\mathrm{SO}(2)$ symmetry to set $\Theta = 0$, the flat embedding configuration is described by $w_5 = L = \mathrm{const}$. The induced metric on the D7-brane world-volume is

$$\mathrm{d}s^2 = \frac{\rho^2 + L^2}{R^2}(-\mathrm{d}x_0^2 + \mathrm{d}x_1^2 + \mathrm{d}x_2^2 + \mathrm{d}x_3^2) + \frac{R^2}{\rho^2 + L^2}\mathrm{d}\rho^2 + \frac{R^2\rho^2}{\rho^2 + L^2}\mathrm{d}\Omega_3^2.$$
(2.119)

Hence, the minimum action configuration for the D7 brane probes with vanishing world-volume gauge fields embedded in $\mathrm{AdS}_5 \times \mathrm{S}^5$ corresponds to a configuration which asymptotically near the boundary $\rho \to \infty$ wraps an $\mathrm{AdS}_5 \times \mathrm{S}^3$ subspace of $\mathrm{AdS}_5 \times \mathrm{S}^5$. The radius of S^3 decreases along the way from the boundary to $\rho = 0$, where the radius of S^3 shrinks to zero.

This flat configuration will be deformed if the D7-branes are embedded in the AdS black hole metric, or if the gauge fields on the world volume are turned on. The just mentioned deformations can be observed in the next section 2.2.3, but in general, the equation of motion derived from (2.115) always has an asymptotic ($\rho \to \infty$) solution of the form

$$L\left(\rho\right) = l_{\mathrm{q}} + \frac{c}{\rho^2} + \cdots \tag{2.120}$$

for any metric which asymptotically reduces to AdS. The separation between the D3-branes and D7-branes l_{q} near the boundary corresponds to the length of the 3-7 strings and thus fixes the mass of the quarks $m_{\mathrm{q}} = l_{\mathrm{q}}/(2\pi\alpha')$. According to the AdS/CFT dictionary (2.69), the parameter c corresponds to the vacuum expectation value of an operator $\mathcal{O}_{\mathrm{m}}$ with the same symmetries as the mass. Since the dimension of $[L] = [\rho] = 1$, the dual operator with $\langle \mathcal{O}_{\mathrm{m}} \rangle \sim c$ must be of dimension three. The operator $\mathcal{O}_{\mathrm{m}}$ is identified with the supersymmetric version of quark bilinears with the schematic form

$$\mathcal{O}_{\mathrm{m}} \sim \psi\bar{\psi} + m_{\mathrm{q}} q^\dagger q + q^\dagger \Phi_3 q + \mathrm{h.\,c.}\,, \tag{2.121}$$

where q denotes the fundamental quark, ψ its supersymmetric partner and Φ_3 an adjoint scalar in the $\mathcal{N} = 2$ hypermultiplet [100]. Thus c corresponds to the quark condensate in the field theory.

2.2.3 D3/D7 model at finite density and finite temperature

Until now, the AdS/CFT has been extended by introducing the temperature and fundamental matter. To introduce finite density of fundamental matter and non-vanishing field strength on the dual field theory, the $\mathrm{U}(N_{\mathrm{f}})$ field theory on the world-volume of the D7-branes will be considered. The asymptotic form of the time-component of the gauge field gives rise to chemical potential and finite density of fundamental matter fields. The spatial components of the gauge fields parallel to the world-volume of the D3-branes give rise to electromagnetic fields of the dual SYM field theory. At the end of this section, phase transitions occurring at the embedding of D7 branes in AdS background will be considered when finite temperature and finite baryon density are introduced.

Chemical potential and finite density   Field theory on the world-volume of the N_{f} coincident D7-branes is described by the $\mathrm{U}(N_{\mathrm{f}})$ field theory. The group $\mathrm{U}(N_{\mathrm{f}})$ can be decomposed as $\mathrm{U}(1)_{\mathrm{B}} \times \mathrm{SU}(N_{\mathrm{f}})$, where the $\mathrm{U}(1)_{\mathrm{B}}$ is identified with the 'baryon number' of the dual SYM field theory. In QCD, the baryon

number is an approximate conserved quantum number. It is defined as the difference between the number of quarks and the number of anti-quarks in composite systems which are formed of quarks and anti-quarks.

The D7 world-volume abelian $U(1)$ gauge field $A_M = (A_\mu, A_m)$ with $\mu \in \{0, 1, 2, 3\}$ and $m \in \{4, 5, 6, 7\}$ is dual to the SYM $U(1)_B$ current J^μ, i.e. the field/operator dictionary (2.51) is extended by the equality

$$\left\langle e^{\int d^4 x A_\mu(\vec{x}) J^\mu(\vec{x})} \right\rangle_{\text{CFT}} = \mathcal{Z}_{\text{string}} \left[A_\mu(\vec{x}, r) |_{r \to \infty} = A_\mu(\vec{x}) \right] . \quad (2.122)$$

We work in the gauge where the transverse components A_m vanish. For non-vanishing time-component A_t, we can introduce a chemical potential μ_B associated to the baryon number symmetry. Generically, the chemical potential μ_B describes the amount of energy which is needed to introduce a charged particle into the system. The correspondence of A_t with the chemical potential μ_B on the field theory side can be deduced from the grand canonical partition function at finite temperature

$$\mathcal{Z}[\phi, \mu] = \text{Tr} \int \mathcal{D}\phi \, e^{-\int_0^\beta d\tau (H - \mu Q)} \quad (2.123)$$

and the fact that in field theory the charge Q is given by the spatial integral of the time-component of the current J^t, i.e. $Q = \int d^3 x J^t(x)$. Hence, the asymptotic value of the time-component A_t in the bulk, which couples to J^t at the boundary, is interpreted as the baryon chemical potential in the gauge theory, namely

$$\mu_B = \lim_{r \to \infty} A_t(r) . \quad (2.124)$$

The reason why we consider A_t only in the dependence of r-coordinate can be explained as follows. The presence of A_t on the world-volume of D7-branes should not change the global symmetries of the dual SYM field theory. Hence to preserve Lorentz invariance on the world-volume of the D3-branes, A_t should not depend on field theory coordinates $\vec{x} = (x_0, x_1, x_2, x_3)$. For simplicity, A_t is chosen not to depend on the coordinates of the S^3, and we just consider the case $A_t = A_t(r)$ where r is the radial coordinate of the AdS space. In this case, the only non-zero component of the field strength tensor is $F_{rt} = \partial_r A_t(r)$ which can be seen as the electric field on the D7-branes pointing in the radial direction of the AdS space. It is worth mentioning that generically the chemical potential is given by the difference of $A_t(r)$ at the horizon and the boundary of the geometry

$$\mu_B = \int_{r_H}^{r_{\text{boundary}}} dr F_{rt}(\vec{x}, r) = A_t(r_{\text{boundary}}) - A_t(r_H) . \quad (2.125)$$

Since the Killing vector corresponding to time translation becomes degenerate at the horizon, it is necessary impose the boundary condition $A_t(r_H) = 0$ in order to have a well-defined gauge field as a one-form at the horizon [105].

Solving the action (2.115) for the embedding of D7-branes in AdS space with non-zero $A_t(r)$, the solution for $A_t(r)$ near the boundary $r \to \infty$ has the generic form

$$\lim_{r \to \infty} A_t(r) = \mu_{\mathrm{B}} + \frac{d_t}{r^2} + \mathcal{O}\left(\frac{1}{r^4}\right) . \tag{2.126}$$

The quantity d_t is proportional the vacuum expectation value of the operator J^t dual to A_t. We call d_t the baryon number density, and using the AdS/CFT dictionary, $\langle J^t \rangle$ is obtained by

$$\langle J^t \rangle = \frac{\delta S_{\mathrm{DBI}}}{\delta A_t} . \tag{2.127}$$

World-volume gauge fields and the dual currents   The $\mathrm{U}(1)$ D7 world-volume gauge field A_μ is dual to the SYM $\mathrm{U}(1)_{\mathrm{B}}$ current J^μ. We saw in the last paragraph that non-zero A_t component gives rise to baryon chemical potential and baryon density on the SYM field theory. Turning on spatial components of the gauge field $A_x(\vec{x}, r)$, $A_y(\vec{x}, r)$ and $A_z(\vec{x}, r)$, non-zero elements of $F_{\mu\nu}$ at the boundary $r \to \infty$ represent the electromagnetic fields on the dual SYM field theory. The resulting vacuum expectation values for the currents J^x, J^y and J^z are given by

$$\langle J^x \rangle = \frac{\delta S_{\mathrm{DBI}}}{\delta A_x}, \qquad \langle J^y \rangle = \frac{\delta S_{\mathrm{DBI}}}{\delta A_y}, \qquad \langle J^z \rangle = \frac{\delta S_{\mathrm{DBI}}}{\delta A_z} . \tag{2.128}$$

Here, it is important to mention a technical detail when the above expressions are evaluated. Since the integration over the radial coordinate is from r_{H} to infinity, a straightforward calculation of (2.115) will lead to divergencies which need to be regularized. The prescription for removing such divergences is known as *holographic renormalization* of probe D-branes in AdS [106, 107], where appropriate counter terms have to be introduced. This prescription will be discussed in more detail later in section 4.2, where we make use of (2.128) to determine the electrical conductivity $\sigma_{ij} = \langle J^i \rangle / E_j$ of flavor fields propagating in SYM plasma in the presence of both electric and magnetic fields.

D3/D7 embeddings   In this paragraph the embedding of D7-branes in AdS space will be discussed when the temperature, finite baryon density and background gauge fields are turned on. In section 2.2.2, it was mentioned that the embedding of D7-branes in $\mathrm{AdS}_5 \times \mathrm{S}^5$ is flat in the (89)-directions transverse to the world-volume of the D7-branes, see (2.117). This flat configuration will be deformed if the D7-branes are embedded in Schwarzschild AdS metric (2.106), or if the world-volume gauge fields are turned on.

In the presence of a black hole, the deformation of the D7-branes will be described by the ansatz (2.118) where the solution $L(\rho)$ is a complicated
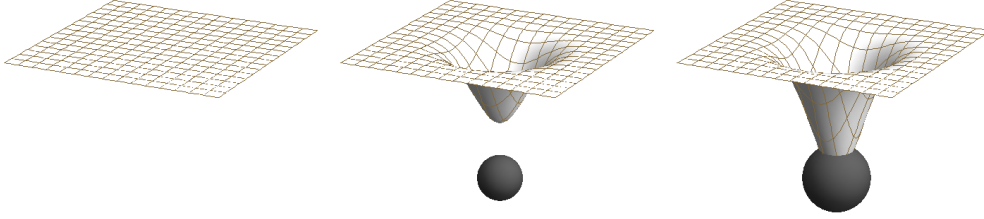
FIGURE 2.4:   Sketch of brane embeddings in the directions transverse to the D7-branes for different values of the temperature $T_H \sim r_H$ (relative to quark mass): on the left is the flat embedding at zero temperature; at the center is the Minkowski embedding for small temperature; and on the right is the black hole embedding for high temperature. This figure is taken from [80].

function of ρ and can be solved only numerically [108]. Near the boundary $\rho \to \infty$, $L(\rho)$ has the form

$$L(\rho) \sim m_q + \frac{c}{\rho^2} + \cdots , \qquad (2.129)$$

where m_q and c have the interpretation as the quark mass and the bilinear quark condensate, respectively. These values are taken as the boundary values for solving the second order differential equation of $L(\rho)$ using numerical methods. The result for $L(\rho)$ describes the deformation from the flat configuration and is sketched in figure 2.4. At zero-temperature, i.e. $r_H = 0$, we have flat configuration $L = $ const which is illustrated on the left picture in figure 2.4. As the temperature T_H increases, i.e. r_H becomes larger, the world-volume of the D7-branes get more and more attracted to the black hole along the radial coordinate ρ. A plausible explanation for this behavior is due to the effect of the attractive gravitational force between the black hole and the D7-branes. The larger the horizon r_H is, the larger is the mass of the black hole and the closer the D7-branes approach the horizon. If the D7-branes do not touch the black hole horizon, those embeddings are referred to the name *Minkowski embeddings*. In these cases the world-volume of the D7-branes ends at some finite ρ_f where the volume of the S^3 wrapping the S^5 shrinks to zero. For some critical value T_H^c relative to the quark mass m_q, the D7-branes end precisely on the horizon $r_H^c \sim T_H^c$. This embedding is called *critical embedding*. If the D7-branes end not only at one point on the horizon, we refer those embeddings to the name *black hole embeddings*, since the embedding exhibits a black hole horizon on the world-volume of the D7-branes.

The presence of magnetic and electric fields on the world-volume of the D7-branes influences the form of the embedding. In [109] the embedding of D7-branes in AdS space, i.e. the dual field theory is at zero temperature, is considered when a constant magnetic field strength B is turned on which is given e.g. by the gauge potential $A(\vec{x}, r) = Bx_2 \mathrm{d}x_3$ on the world-volume of the D3-branes and D7-branes. The presence of the magnetic field provides a

non-vanishing vacuum expectation value for the fermionic condensate $\tilde{c}$

$$L\left(\rho\right) \sim \tilde{m}_{\mathrm{q}} + \frac{\tilde{c}(B)}{\rho^2} + \cdots, \tag{2.130}$$

where ρ is defined as in (2.116), L as in (2.118) and the expression above is a series expansion of $L\left(\rho\right)$ near the boundary $\rho \to \infty$. The condensate $\tilde{c}(B)$ is finite even for zero bar quark mass $\tilde{m}_{\mathrm{q}} = 0$, hence it corresponds to a spontaneous chiral symmetry breaking which was first studied in [108] in a holographic context. In [110] the effects of external constant magnetic and electric fields on the embedding of an D7-branes have been extended to the AdS black hole geometry, i.e. finite dual SYM field theory. The so-called pure gauge ansätze in [110] are equivalent to the introduction of the one-form $\mathrm{U}(1)_{\mathrm{B}} \subset \mathrm{U}(N_{\mathrm{f}})$ world-volume gauge field

$$A(\vec{x}, r) = -Ex_0 \mathrm{d}x_1 \quad \text{and} \quad A(\vec{x}, r) = Bx_2 \mathrm{d}x_3. \tag{2.131}$$

These ansätze ensure that they are solutions to type IIB supergravity equations of motion [111] and that the electric field E and magnetic field B do not deform the AdS black hole background. It was found that the magnetic field B repels the D7-branes from the horizon. At a constant temperature $T_{\mathrm{H}} \sim r_{\mathrm{H}}$ there exists a critical strength of the magnetic field above which a black hole embedding is no longer possible. Considering the effect of the electric field on the embedding, it has been found that there is a singular region outside the black hole horizon where the DBI action becomes complex and ill-defined. The boundary of this singular region is often called as the singular shell which has an attracting effect on the D7-branes similar to the black hole horizon [110].

The influence of finite baryon number density on the embedding of N_{f} D7 flavor branes in the background of N_{c} black D3-branes is studied in [105]. It was mentioned at the beginning of this section that the baryon number density is introduced by the non-vanishing time-component of the $\mathrm{U}(1)_{\mathrm{B}} \subset \mathrm{U}(N_{\mathrm{f}})$ gauge field $A_t(r)$ on the world-volume of the D7-branes. At finite temperature and in the presence of finite baryon number density, only black hole embedding leads to a stable configuration [105]. This behavior can be explained as follows. For the one-form $A = A_t(r)\mathrm{d}t$ there is a non-vanishing field strength component $F_{rt} = \partial_r A_t(r)$ which can be seen as an electric field on the D7-brane world-volume pointing towards the radial direction r of the embedding geometry. The finite baryon density on the SYM field theory side is dual this the world-volume electric field which in D-branes language can be associated with fundamental strings dissolved into the D7-branes [73]. Hence the D-branes are not allowed to close off smoothly as the strings cannot simply terminate. These fundamental strings will extend all the way along the radial coordinate towards the horizon and pull the tip of the D7-branes down to meet the horizon [105]. For small temperatures or large quark mass, most part of the branes are very far from the horizon and the embedding looks like a Minskowski embedding with the difference that there is a thin long spike extending down to touch the horizon.

2.3   Summary

In this chapter we presented the original version of the AdS/CFT correspondence which had been conjectured by Maldacena [10] in 1997 and shortly after elaborated by Witten, Gubser et al. [11, 12]. We gave a brief description of the $\mathcal{N} = 4$ SYM theory, physics of D-branes, type IIB superstring theory at low energy, and provided arguments and tests for the correctness of the conjecture. We emphasized that utilizing the correspondence in the large N_c, large λ limits, physical processes in strongly coupled field theories can be analyzed by means of studying weakly coupled gravity duals. Some relevant generalizations and extensions of the correspondence for this thesis were discussed in 2.2, where we introduced finite temperature, fundamental matter, baryon charge density, baryon chemical potential and background gauge fields giving rise to electromagnetic fields to the correspondence. In particular, the D3/D7 model was discussed extensively which should be seen as a preparing step for the applications of gauge/gravity duality in the next chapters.

Quantum phase transitions in holographic superfluids

We start with applying the methods of the AdS/CFT correspondence on two different gravity setups which are related to phenomena of strongly coupled systems in *thermal equilibrium* such as quantum phase transitions and quantum critical points. We use the bottom-up approach in section 3.3 and the top-down approach in section 3.4 for the constructing of holographic superfluids at finite baryon and isospin chemical potential. We study the quantum phase transitions and look for a possible quantum critical point in our setups.

3.1 Introduction and motivation

Gauge/gravity duality, a generalized and extended version of the AdS/CFT correspondence [10–12] as discussed in section 2.2, maps a more general quantum field theory to a given background with the same global symmetries. It provides a novel method for studying strongly correlated systems at finite temperature and densities. In recent years, remarkable progress has been made towards application of gauge/gravity duality for describing strongly coupled condensed matter physics at low temperatures, see e.g. [19–22]. At low temperatures condensed matter shows many interesting properties including superconductivity and superfluidity. Some of the first applications of gauge/gravity duality towards the holographic description of superfluids and superconductors are described in [15, 17] and of (non-) Fermi liquids in [112]. Of special interest are the studies of quantum critical theories which arise at continuous phase transitions at zero temperature [24]. A phase transition at zero temperature is not driven by thermal fluctuations, but rather by quantum fluctuations. If the quantum phase transition is continuous, i.e. at least of second order, there is a quantum critical point. This quantum critical point influences the phase diagram also at non-zero temperature, see fig. 3.1 for a schematic picture of

the phase diagram near the quantum critical point. In this influenced region, the quantum critical region, the system may be described by a critical theory even at finite temperature [45–47]. There are speculations that quantum phase transitions might be important in describing high T_c-superconductors like cuprates, non-Fermi liquids or superconducting-insulator transitions in thin metallic films, see e.g. [19, 20] and references therein. Up to date, there is still a lack of a complete and satisfactory theoretical description for high T_c-superconductors, ultra-cold Fermi gases and non-Fermi liquids, and it is believed that a better understanding of the critical region may shed light on this branch of physics.
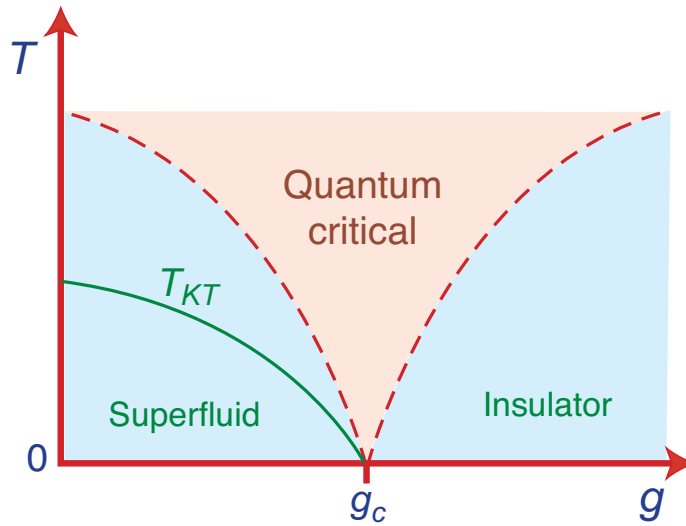

FIGURE 3.1: Typical phase diagram near a quantum critical point. The quantum critical point at zero temperature is triggered at some critical parameters $g = g_c$ which might be the chemical potential, the magnetic field, the chemical composition, etc. The superconducting and normal conducting phases are separated by a quantum critical region which may be described by a scale-invariant theory at finite temperature. The dashed lines denote the cross-overs, while the solid line denotes a possible Kosterlitz-Thouless phase transition at the temperature $T_{KT} > 0$. This figure is taken from [45].

Using the gauge/gravity duality it is possible to construct physical systems which show a phase transition from a normal to a superconducting phase, see e.g. the reviews [19–22]. Studying these systems, many properties of superconductors and superfluids can be recovered such as infinite direct current (DC) conductivities, mass gap for single-particle excitation and remnant of the Meisser-Ochsenfeld effect, see e.g. [15–18]. In general, the dual gravity solution for a superconducting state is a charged AdS black hole which develops hair. For black holes in asymptotically flat space, there is a no-hair theorem, see [113] for a review, which postulates that all black hole solutions of the Einstein-Maxwell equations in general relativity can be characterized by three classical parameters: mass, angular momentum and electric charge. This situation is changed if the embedding space-time is asymptotically AdS. AdS space-times are vacuum solutions of Einstein's field equations with negative

cosmological constant. The crucial difference to flat space-times is that an AdS space-time acts like a confining box such that charged particles cannot escape to infinity. This property allows AdS black holes to develop hair made of condensing charged particles [21, 114]. Depending on whether it is a scalar or vector hair, the dual field theory will be a s-wave or p-wave theory of superconductivity. Such a theory may describe superconductors or superfluids. In general, a superconducting condensate breaks an $U(1)$ symmetry spontaneously. If the underlying broken symmetry is a local symmetry, the system describes a superconductor, while for the case of a global symmetry the system describes a superfluid.

In this chapter we focus on the construction of holographic superfluids and study their phase diagrams. Of great interests are the quantum phase transitions and the possible existence of a quantum critical point in such systems. So far most of studied systems showing the transition to a holographic superfluid have only been considered with one control parameter, usually the ratio of the temperature to a chemical potential. In such systems the phase transition is at a finite temperature and thus these systems have no quantum phase transition, see e.g. [17, 48]. In this chapter we construct gravity systems which resemble a p-wave superfluid with continuous phase transitions at zero temperature and thus possess quantum critical points. That can be done by introducing a further chemical potential as a second control parameter. Varying this an additional parameter the phase transition temperature can be tuned to zero, so that studying quantum phase transition is possible. Studying the order of the phase transition at zero temperature by comparing the free energy of the normal and superconducting phase, it is possible to determine whether the system possesses a quantum critical point or not.

The main motivation for studying quantum phase transitions at finite baryon and isospin chemical potential using holographic methods is the following. First, studying physics at quantum criticality using gauge/gravity duality has obtained very promising results related to transport phenomena in strongly correlated systems, see again [19–22] and [47]. Moreover, gauge/ gravity duality seems to be the only known theory so far which is able to provide analytical results which are used to phenomenologically describe physical processes in this regime. Thus the recent developments encourage further studies using holographic methods to understand physical phenomena at quantum criticality. The second main motivation for the work presented in this chapter is that there are studies about quantum phase transitions at finite baryon and isospin chemical potential from QCD [49, 50], which can be used to compare with our results obtained from gravity models. For a clearer understanding what we could learn from our results combined with those from the works mentioned above, let us now briefly describe some for this chapter relevant results of [49, 50] in the next paragraph.

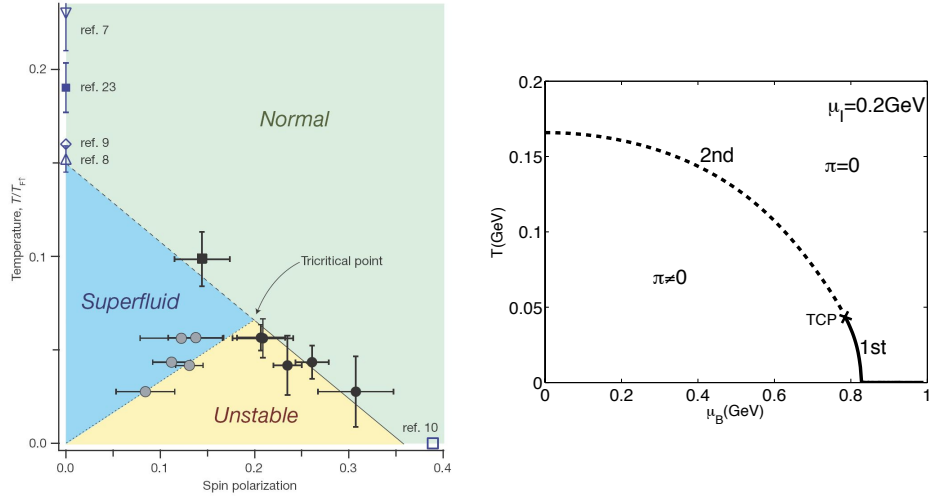Usually, systems with two chemical potentials are called imbalanced mix-

FIGURE 3.2:   Phase diagrams of real world systems: (a) Imbalanced Fermi mixture in the canonical ensemble [49]: The spin polarization is the thermodynamic conjugated variable to the ratio of the chemical potentials favoring the different spins. (b) QCD at finite baryon and isospin chemical potential [50]. In both phase diagrams we observe a superfluid phase at small temperature and small ratio of two chemical potentials. In addition in both diagrams the phase transition is second order for large temperature and becomes first order at low temperatures. Both diagrams show a first order quantum phase transition, thus in those systems there is no quantum critical point. The figures are taken from [49] and [50].

tures since two kinds of particles are present in imbalanced numbers. Examples are imbalanced Fermi mixtures where fermions with spin up and spin down are imbalanced [49], and QCD at finite baryon and isospin chemical potential where for instance up and down quarks are imbalanced [50] (see also [115]). Interestingly the phase diagrams of both these systems are very similar (see figure 3.2). In both systems there is a superfluid state at low temperatures and at certain ratios of the two chemical potentials. In addition also the order of the phase transition agrees in both examples: At low temperatures (also at zero temperature) the transition is first order while at higher temperatures the transition becomes second order. Thus, we want to address the question whether there is an universal structure which relates these two different systems? The answer we find in this chapter is no and will be explicated in subsection 3.4.4.

In the next section we will give a brief review how to construct superconductors and superfluids using holographic methods relying on [15, 17], and study quantum phase transitions in holographic superfluidity at finite baryon density and isospin density in an imbalanced mixture. We construct the phase diagrams via two different gravity models and compare these results among each other and with the results obtained from QCD [49, 50]. The materials presented in sections 3.3 and 3.4 are my own results which are obtained in collaboration with Johanna Erdmenger, Viviane Grass and Patrick Kerner [3].

3.2 Superfluidity and its holographic descriptions

This section serves as a very brief review on theories of superconductivity and superfluidity in condensed matter physics and a review how to construct holographic superfluids using gauge/gravity duality. For the latter, there are two approaches: (i) the bottom-up approach where the dual field theory is not specified; and (ii) the top-down approach where the dual field theory is explicitly known. We close this section by commenting on the two approaches. The content of subsection 3.2.1 closely follows the references [21, 116], and the content of subsection 3.2.2 closely follows the references [15, 17, 18, 114].

3.2.1 Superconductivity and superfluidity in condensed matter physics

Superconductivity was discovered by H. Kamerlingh Onnes in 1911, three years after he had liquefied helium [116]. It was observed that the electrical resistance of various metals disappears completely below some critical temperature T_c which is a characteristic of the conducting material. In 1933, Meissner and Ochsenfeld found that a magnetic field is not only excluded from a superconductor, but also expelled from an originally normal conducting sample as it is cooled through T_c. This phenomenon of *perfect diamagnetism* is known as the Meissner-Ochsenfeld effect. The existence of a reversible Meissner-Ochsenfeld effect implies that superconductivity will be destroyed by a critical magnetic field B_c which is related thermodynamically to the free energy difference between normal and superconducting states when the magnetic field is absent [116].

These two electrodynamic properties are well described by the London equations

$$\vec{E} = \frac{\partial}{\partial t}\left(\Lambda \vec{J}_s\right) , \qquad \vec{B} = -\nabla \times \left(\Lambda \vec{J}_s\right) , \qquad \Lambda = \frac{4\pi \lambda_L^2}{c^2} = \frac{m}{n_s e^2} , \quad (3.1)$$

which were first given by the London brothers in 1935. In the London equations, $\vec{E}$ is the electric field, $\vec{B}$ the magnetic field, $\vec{J}_s$ the supercurrent, m the electron mass, c the light velocity, e the electric charge, n_s the density of the superconducting electrons and Λ is a phenomenological parameter proportional to the magnetic penetration depth λ_L squared. The first London equation describes perfect conductivity, since any electric field accelerates the superconducting electrons rather than sustaining their velocity against resistance as in a normal conductor. The second London equation, when combined with the Maxwell equation $\nabla \times \vec{B} \sim \vec{J}_s$, leads to $\nabla^2 \vec{B} \sim \lambda_L^{-2} \vec{B}$. The solution $B(x) = e^{-x/\lambda_L}$ implies that a magnetic field is exponentially screened from the interior of a sample with penetration depth λ_L.

In 1950, the London theory had been generalized by the Ginzburg-Landau theory of superconductivity in terms of a second order phase transition [117]. At the time when the Ginzburg-Landau theory was presented, it was considered

as a purely phenomenological theory. As an order parameter for the super-conducting electrons Ginzburg and Landau introduced a complex pseudowave function ψ such that the local density of the superconducting electrons in the London equations is given by $n_s = |\psi(x)|^2$. It is a generalization of the London theory because one can derive the London equations from the Ginzburg-Landau theory and the Ginzburg-Landau theory is able to treat features which are beyond the scope of the London theory like spatial variation of n_s or nonlinear effects in field theory which can change n_s. Using a variational principle and working from an *assumed* expansion of the free energy near the phase transition as

$$F = F_\mathrm{n} + \alpha(T - T_c)|\psi|^2 + \frac{\beta}{2}|\psi|^4 + \frac{1}{2m}|(-i\hbar\nabla - \frac{e}{c}\vec{A})\psi|^2 + \cdots \quad (3.2)$$

where F_n is the free energy in the normal phase, α and β are some positive phenomenological coefficients, m the effective mass of electrons, e the effective charge, $\vec{A}$ the electromagnetic vector potential and the dots denotes terms of higher order in ψ or terms proportional to $\nabla\psi$, Ginzburg and Landau derived a differential equation for ψ

$$\alpha\left(T - T_\mathrm{c}\right)\psi + \beta|\psi(x)|^2\psi + \frac{1}{2m}\left(-i\hbar\nabla - \frac{e}{c}\vec{A}\right)^2\psi = 0\,. \quad (3.3)$$

Taking the gauge $\nabla\vec{A} = 0$ and noting $\Delta\vec{A} = -\frac{4\pi}{c}\vec{J_\mathrm{s}}$, the corresponding supercurrent is

$$\vec{J_\mathrm{s}} = \frac{e\hbar}{i2m}\left(\psi^*\nabla\psi - \psi\nabla\psi^*\right) - \frac{e^2}{mc}|\psi|^2\vec{A}\,. \quad (3.4)$$

Using Ginzburg-Landau theory, the behavior of the superconductor near the critical temperature T_c can be fully described by the magnetic penetration length λ_L and the coherence length ξ which are given by

$$\lambda_\mathrm{L}(T) = \sqrt{\frac{mc^2\beta}{4\pi e^2\alpha(T - T_\mathrm{c})}}\,, \qquad \xi(T) = \sqrt{\frac{\hbar^2}{2m\,\alpha(T - T_\mathrm{c})}}\,. \quad (3.5)$$

The ratio $\kappa = \lambda_\mathrm{L}/\xi$ is called the Ginzburg-Landau parameter and is used to distinguish type I and type II superconductors. In 1957 Abrikosov found that materials with $\kappa > 1/\sqrt{2}$ are not perfectly diamagnetic superconductors, i.e. the magnetic field is not completely expelled from the materials. These materials are called 'type II superconductors' to distinguish them from 'type I superconductors' which are perfect diamagnetic. For type II superconductors there is no discontinuous breakdown of superconductivity in a first order transition at a critical magnetic field B_c like in type I superconductors, but rather in a second order transition. We want to mention that we do not turn on the magnetic field and calculate the magnetic penetration depth λ_L and the

coherence length ξ in this thesis, however, interested readers may find models of holographic superconductors where the penetration depth and coherence length are found to be in perfect agreement with Ginzburg-Landau theory, see e.g. [118] for s-wave superconductors and [119] for p-wave superconductors.

In 1957, Bardeen, Cooper and Schrieffer presented a more complete description of superconductivity, the microscopic theory of superconductivity. This theory, known as BCS theory, provides a completely new insight on the theory of superconductivity. The main idea of the BCS theory is that electron-phonon interactions can cause pairs of electrons with opposite spin to bind and form a charged boson called a Cooper pair. Below a critical temperature T_c, there is a second order phase transition and these bosons condense. The DC conductivity becomes infinite signalizing effect of superconductivity. One main result of the BCS theory is the establishment of the existence of an energy gap between the ground state and the quasi-particle excitation of the system. This energy gap, also known as the mass gap, is the minimal energy required to break a pair and create two quasi-particle excitations. Such a gap has been affirmed experimentally and is typically related to the critical temperature as $\Delta E \approx 3.5 k_B T_c$ [116]. In 1959, Gor'kow showed that the Ginzburg-Landau theory is indeed a limiting form of the microscopic theory of BCS near the critical temperature. The effective charge e and mass m in (3.2) are identified with the charge and mass of the Cooper pair, i.e. two times the electrical charge and the mass of an electron. Near the phase transition temperature, ψ is directly proportional to the energy gap ΔE and, more physically, ψ can be thought of as a the wave function of the center-of-mass motion of the Cooper pairs. Today the Ginzburg-Landau theory is widely considered as a masterstroke of physical institution.

In 1986 and recently in 2008, new classes of high T_c superconductors were discovered, see [21] and references therein. They are called cuprates and iron pnictides. Although there is evidence that electron pairs still form in these high T_c materials, but the pairing mechanism is not well understood. Unlike BCS theory, it involves strong coupling, thus gauge/gravity duality might serve as an useful tool to study high T_c superconductors.

Superfluidity is the property of a liquid to flow without friction. The loss of viscosity in superfluids is the counterpart to the loss of electrical resistance in superconductors. Examples of superfluids are condensed Bose atoms, e.g. ^{4}He below $T_c = 2.17 K$, neutral BCS-paired Fermi atoms, e.g. ^{3}He liquid below $T_c = 1 mK$, or charged BCS-paired fermions like protons in neutron stars. Superfluid ^{4}He was discovered in 1938, superfluid ^{3}He in 1973 and recently superfluidity was observed in trapped atomic Bose-Einstein condensates and trapped paired Fermi-Dirac atoms. A unified description of superconductivity and superfluidity is possible in terms of symmetry breaking. There is always a condensate which breaks the symmetry spontaneously. The crucial difference between a theory describing superconductivity and and a theory describing superfluidity consists of whether this is a local or a global symmetry. In a

theory of superfluidity a global symmetry is spontaneously broken, thus the Goldstone boson survives. In a theory of superconductivity a local symmetry is spontaneously broken, hence the Goldstone boson is eaten up by the gauge field which couples to the charge belonging to the broken symmetry. This gauge field becomes massive. In a theory of superconductors with the broken local $U(1)$, the magnetic field, which can be seen as consisting of massive photons, can travel only for a short distance. This distance is called the magnetic penetration depth λ_L and just describes the before mentioned Meissner-Ochsenfeld effect.

Before going to construct holographic superfluids in the next subsection, let us come back to the Ginzburg-Landau theory in the simplest case [21], where the magnetic field is absent. The Ginzburg-Landau's assumption for the series expansion of the free energy near the critical temperature T_c (3.2) is

$$F = \alpha(T - T_c)|\psi|^2 + \frac{\beta}{2}|\psi|^4 + \cdots , \qquad (3.6)$$

where the dots denote gradient terms and higher powers of ψ and the free energy of the normal conducting state in (3.2) is set to be zero. We want to see how the spontaneous symmetry breaking arises as the temperature T approaches critical temperature T_c. Note, α and β are some positive phenomenological coefficients. For $T > T_c$ the minimum free energy is at $\psi = 0$. This corresponds to the ground state of the system where the superconducting condensate density $n_s = |\psi|^2$ is zero. For $T < T_c$, the minimum free energy is at a non-zero value of ψ and the condensate density[1] is

$$n_s = |\psi|^2 \approx \frac{\alpha}{\beta}|T - T_c| , \qquad (3.7)$$

where in the last step equation (3.3) was used. This is just like the Higgs mechanism in particle physics, and is associated with a spontaneous breaking of an $U(1)$ symmetry.

3.2.2 Holographic descriptions – bottom-up and top-down approach

Before dealing with the details of the construction of holographic superfluids, let us first discuss what the minimal ingredients necessary for the construction of holographic superconductors and superfluids are and how they can be realized using the dictionary of the gauge/gravity duality.

- First, we need a notion of temperature in the field theory. As discussed in detail in subsection 2.2.1, on the gravity side this can be realized by considering Schwarzschild AdS black hole geometry.

- Second, we need a condensate which is similar to the Cooper pairs in field theory. In the bulk, this is described by some field Ψ coupled to gravity. The field Ψ is charged under some $U(1)$ and should not have

---

[1]This relation explains the identity in the definition of the penetration length λ_L in (3.1) and (3.5)

a source, i.e. its boundary value is zero, such that the $U(1)$ is broken spontaneously if the condensate is formed. A non-zero condensate $\langle\Psi\rangle$ corresponds to a static non-zero field outside the black hole. A black hole geometry with a non-zero field in the bulk is often called 'hairy' black hole. In order to fulfill the requirements of being a dual geometry describing superconductors, the black hole geometry should not have 'hair' at high temperatures but will form 'hair' at low temperatures.

- Third, we need a gauge field charged under the $U(1)$, to which the field Ψ couples. Moreover, since we start with a scale-invariant conformal field theory, an additional quantity needs to be introduced to set a scale, otherwise all non-zero temperatures are equivalent and it would be not possible to study the phase diagram of the theory. The time-component of the $U(1)$ gauge field is an appropriate candidate because its boundary value is interpreted as the chemical potential in the dual field theory, see subsection 2.2.3, which can be used as a scale of the theory. There are two known methods how to introduce the $U(1)$ gauge field A on the gravity side which lead to the desired properties of superconductivity discussed above:

  - One possibility is considering the $U(1)$ Einstein-Yang-Mills theory with the gauge field A coupled to a charged scalar Ψ [15,16]. If there is no condensate, i.e. $\langle\Psi\rangle = 0$, the back-reaction of the gauge field on the Schwarzschild AdS black hole yields the Reissner-Nordström AdS black hole which is interpreted as the state dual to the normal conducting phase of the field theory. The main task now is to verify whether the Reissner-Nordström AdS background describes a stable configuration in the presence of 'hair', i.e. $\langle\Psi\rangle \neq 0$. If it does, that solution will be called 'hairy' black hole and interpreted as the state dual to the superconducting phase. This method is known as the *bottom-up* approach and will be discussed in detail in the next paragraph;

  - The second possibility is introducing $N_\mathrm{f} = 2$ flavor D-brane probes in the AdS Schwarzschild background [17,18]. The world-volume field theory is governed by the gauge group $U(2) = U(1)_\mathrm{B} \times SU(2)$. The $U(1)$ gauge field A can be seen as one component of the $SU(2)$ gauge field with this $U(1)$ being a diagonal subgroup of the $SU(2)$. The boundary value of the time-component A_t gives the chemical potential serving as a scale of the dual field theory. Switching on an further component of the $SU(2)$ gauge field, the authors of [17,18] show that a condensate is formed below some critical temperature which spontaneously breaks the diagonal subgroup $U(1)$ of $SU(2)$. Using the D3/D7 model, the dual field theory is explicitly known, thus this method is called the *top-down* approach and will be discussed in detail later in this subsection.

We end this paragraph with some comments about the U(1) symmetry which is spontaneously broken as the condensate is formed. In gauge/gravity duality, gauge symmetries in the bulk correspond to global symmetries in the dual field theory. In the holographic description, although the black hole hair breaks a local U(1) symmetry in the bulk, the dual description consists of a condensate breaking a global U(1), hence the dual field theory describes a superfluid rather than a superconductor. It was argued, however, that one can still view the dual theory as a superconductor in the limit that the U(1) symmetry is weakly gauge, i.e. the dual action would include terms like $|(i\hbar\nabla + e\vec{A}/c)\psi|^2$ with very small electric charge e [21]. Also most of condensed matter physics does not include dynamical photons, since their effects are usually small.

The bottom-up approach The first model for holographic superconductors was constructed by Hartnoll, Herzog and Horowitz [15]. This is a bottom-up approach for describing holographic superconductors, since the dual field theory is not explicitly known and some fields and parameters in the theory have to be introduced by hand. The superconducting condensate arises from the condensation of a charged scalar, thus this model describes holographic s-wave superconductors.

In [15] the authors present a gravity model where below a critical temperature a charged condensate consisting of pairs of charged quasiparticles can be formed. Signatures of superconductivity can be found like infinite DC conductivity and a gap in the frequency dependent conductivity. The model in [15] is $(2+1)$-dimensional which is motivated from physics of unconventional superconductors arranged in layers. In the frame of the AdS/CFT correspondence, a three-dimensional conformal field theory is dual to a M-theory on $AdS_4 \times S^7$ [120], thus in this model, the minimal holographic superconductor has a bulk description with

- an AdS_4 black hole metric fixing the field theory temperature T,

- a U(1) Maxwell field A with non-vanishing time-component which gives rise to a chemical potential in the field theory,

- and a scalar Ψ charged under the U(1) which forms the condensate if $T < T_c$ and breaks the U(1) spontaneously.

The U(1) symmetry breaking can be seen as follows. Under the U(1) Ψ and A transform as

$$A_\mu \to A_\mu + iq\partial_\mu\theta(\vec{x}, r)\,, \qquad \Psi \to e^{i\theta(\vec{x},r)}\Psi\,. \tag{3.8}$$

Once Ψ has a non-vanishing vacuum expectation value, the phase $\theta(\vec{x}, r)$ will be fixed and thus breaks the U(1) spontaneously. The choice of fields listed above is motivated by the discovery in [114] where Gubser shows that the coupling of the Abelian Higgs model to gravity plus a negative cosmological

constant leads to black holes which spontaneously break the gauge invariance via a charged scalar condensate outside their horizon. In other words the result in [114] is an example of stable AdS black holes with hair. The action for this model can be written as

$$S = \int \mathrm{d}^4x\sqrt{-g}\left(\mathcal{R} - 2\Lambda - \frac{1}{4}F_{ab}F^{ab} - |\nabla\Psi - iqA\Psi|^2 - m^2|\Psi|^2\right), \quad (3.9)$$

where $\mathcal{R}$ is the Ricci scalar, in AdS_4 the negative cosmological constant $\Lambda = -3/R^2$ with R being the AdS radius, $F_{ab} = \partial_a A_b - \partial_b A_a$ with $a, b \in \{0, 1, 2\}$, q the $\mathrm{U}(1)$ charge, m the mass of the charged scalar Ψ. The charge and the mass of the scalar field Ψ are just introduced by hand and should be considered as phenomenological parameters.

For simplicity and concreteness, in [15] the mass squared is chosen to be $m^2 = -2/R^2$. This value is above the Breitenlohner-Freedman bound (2.70) which is $-9/R^2$ in AdS_4 and hence does not induce an instability. In [15] the results are obtained in the limit where the Maxwell field and the scalar do not back-react the metric, therefore we can work with the planar Schwarzschild AdS black hole (2.106) in four dimensions

$$\mathrm{d}s^2 = -f(r)\mathrm{d}t^2 + \frac{r^2}{R^2}\left(\mathrm{d}x_1^2 + \mathrm{d}x_2^2\right) + \frac{\mathrm{d}r^2}{f(r)}, \quad f(r) = \frac{r^2}{R^2}\left(1 - \frac{r_{\mathrm{H}}^3}{r^3}\right). \quad (3.10)$$

The Hawking temperature (2.100) for the Schwarzschild AdS_4 black hole is $T_{\mathrm{H}} = 3r_{\mathrm{H}}/(4\pi R^2)$. Even in this limit of zero back-reaction, the author of [15] found signatures of superconductivity like infinite DC conductivity and a gap in the frequency dependent conductivity of the condensate.

A more precise treatment of the bottom-up approach is presented in [16], where the back-reactions of the scalar and the gauge field on the background metric are included. The ansatz for the metric preserving the $\mathrm{SO}(2)$ symmetry in the $(2 + 1)$-dimensional field theory is

$$\mathrm{d}s^2 = -h(r)e^{-\chi(r)}\mathrm{d}t^2 + \frac{r^2}{R^2}\left(\mathrm{d}x_1^2 + \mathrm{d}x_2^2\right) + \frac{\mathrm{d}r^2}{h(r)} \quad (3.11)$$

Taking the plane symmetric ansatz for the scalar and gauge field as

$$\Psi = \Psi(r), \qquad A_t = A_t(r), \quad (3.12)$$

the scalar, Maxwell and Einstein field equations coming from (3.9) reduce to a system of four coupled, non-linear, ordinary differential equations of $\Psi(r)$, $A_t(r)$, $h(r)$ and $\chi(r)$. We now discuss the boundary conditions of the fields at the horizon $r = r_{\mathrm{H}}$. The time component of the metric vanishes at the horizon, thus $h(r_{\mathrm{H}})$ vanishes. $A_t(r_{\mathrm{H}}) = 0$ must vanish in order for $g^{tt}A_tA_t$ to remain finite. Another argument from [21] for setting $A_t(r_{\mathrm{H}}) = 0$ is the following. For describing thermal properties of the black hole, the Euclidean solution will be

considered. The Wilson loop of A_μ around the Euclidean time circle is finite and gauge invariant. If A_t is nonzero at the horizon, the Wilson loop is nonzero around a vanishing circle which implies that the Maxwell field is singular. At the boundary we impose the following conditions. The metric should be asymptotically AdS_4, thus $\chi(r)$ vanishes at the boundary near $r \to \infty$. This also ensures that the Hawking temperature of the black hole can be identified with the field theory temperature. Also Ψ should be zero at the boundary, since Ψ is predetermined to break the $\text{U}(1)$ spontaneously and should not be sourced by anything.

In [16] the solution with the asymptotical behavior $\Psi = \Psi^{(2)}/r^2 + \mathcal{O}(r^{-3})$ leads to a stable hairy black hole solution, where $\Psi^{(2)}$ is proportional the value of superconducting condensate. The behavior of A_t near the boundary

$$A_t = \mu - \frac{n_\text{c}}{r} + \mathcal{O}\left(\frac{1}{r^2}\right) \tag{3.13}$$

determines the chemical potential μ and the charge density n_c. Solving the equations of motion coming from (3.9), the normal conducting phase, i.e. $\Psi = 0$, is given by the Reissner-Nordström AdS black hole,

$$\chi = \Psi = 0, \quad h = r^2 - \frac{1}{r}\left(r_\text{H}^3 + \frac{n_\text{c}^2}{4r_\text{H}}\right) + \frac{n_\text{c}^2}{4r^2}, \quad A_t = n_\text{c}\frac{r - r_\text{H}}{r r_\text{H}}, \tag{3.14}$$

where in the above solution the AdS radius R is set to be 1 which can be done using the symmetry of the equations of motion.

One crucial feature of such a model is that there exists a critical temperature where the Reissner-Nordström AdS black hole becomes unstable against perturbations of the scalar field Ψ. This instability occurs because the charge density acts an effective negative contribution to the mass term of the scalar field [114]. This argument can be clarified if we consider an electrically charged black hole. The effective mass of the scalar field Ψ is $m_\text{eff}^2 = m^2 + q^2 g^\text{tt} A_t^2$. The correction of the mass vanishes at the horizon. However, since g^tt is negative, there might be a region in the bulk where m_eff^2 goes below the Breitenlohner-Freedman bound and thus destabilizes the system.

Below a critical temperature T_c a condensate $\langle\Psi\rangle \sim \Psi^{(2)}$ can be formed. The non-vanishing Ψ makes it possible to stabilize the system. Thus the Reissner-Nordström AdS black hole solution undergoes a 'phase transition' to the so called hairy AdS black hole solution which is the dual description of the superconducting phase of superconductors. So far, there is no known hairy AdS black hole solution which can completely be given in an analytical form. Usually for $\Psi \neq 0$, we have to resort to numerics.

The top-down approach - A string theoretical realization   In the top-down approach [17, 18], a configuration of a probe of two flavor D7-branes embedded in the AdS black hole background is considered. Since the AdS black hole

background is generated by a stack of N_c coincident D3-branes, this approach can be seen as an application of the D3/D7 model. The dual field theory is the four-dimensional $\mathcal{N} = 4$ SYM theory coupled to the $\mathcal{N} = 2$ hypermultiplets which has been discussed in subsection 2.2.2. It is a top-down approach and describes a string theoretical realization of holographic superconductors/ superfluids, since in this gravity model all fields and parameters are explicitly determined by a low-energy limit of superstring theory. Also a string picture of the pairing mechanism can be provided. This model shows a second order phase transition to a phase in which a $U(1)$ subgroup of the $SU(2)$ symmetry is spontaneously broken by vector condensate, thus it gives a description for holographic p-wave superconductors/ superfluids.

In [17], the authors Ammon, Erdmenger, Kaminski and Kerner construct a holographic $(3 + 1)$-dimensional superfluid at finite isospin chemical potential μ_I using the D3/D7 setup. The isospin chemical potential μ_I is introduced as a source of the operator

$$J_t^3 \propto \bar{\psi}\tau^3\gamma_t\psi + \phi\tau^3\partial_t\phi = n_u - n_d \,, \tag{3.15}$$

where $n_{u/d}$ are the charge densities of the isospin fields, τ^i the usual Pauli and γ_μ the usual Dirac matrices, $\phi = (\phi_u, \phi_d)$ and $\psi = (\psi_u, \psi_d)$ represent the 'quarks' and 'squarks' duplet coming from the *two* $\mathcal{N} = 2$ supermultiplets denoted by *two* flavor indices u and d. Similar to the bottom-up approach, let us first list the minimal ingredients for realizing the holographic superfluid, namely

- an $AdS_5 \times S^5$ black hole metric fixing the field theory temperature T,

- an $SU(2)_I$ gauge field component $A_t = A_t^3\tau^3$ which gives rise to the isospin chemical potential $\mu_I = \lim_{r\to\infty} A_t^3(r)$ and explicitly breaks the symmetry group of two coincident D7-branes $U(2) \simeq U(1)_B \times SU(2)_I$ down to $U(1)_B \times U(1)_3$,

- and a further $SU(2)_I$ gauge field component $A_x = A_x^1\tau^1$ which gives rise to the condensate which breaks the $U(1)_3$ spontaneously.

The AdS black hole background in Minkowski signature can be written as

$$ds^2 = \frac{\varrho^2}{2R^2}\left(-\frac{f^2}{\tilde{f}}dt^2 + \tilde{f}d\vec{x}^2\right) + \left(\frac{R}{\varrho}\right)^2\left(d\varrho^2 + \varrho^2 d\Omega_5^2\right), \tag{3.16}$$

with $d\Omega_5^2$ the metric of the unit 5-sphere and

$$f(\varrho) = 1 - \frac{\varrho_H^4}{\varrho^4}, \quad \tilde{f}(\varrho) = 1 + \frac{\varrho_H^4}{\varrho^4}\,. \tag{3.17}$$

The AdS balck hole metric (2.106) can be recovered from the metric above by a coordinate transformation $\varrho^2 = r^2 + \sqrt{r^4 - r_H^4}$ and the identification
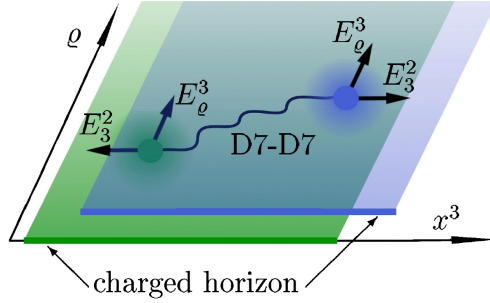
FIGURE 3.3: Sketch of the top-down approach with D3/D7 brane setup: Strings spanned from the horizon of the AdS black hole to the D7-branes (green and blue plane) induce a charge at the horizon. The D7-D7 strings are distributed along the AdS radial coordinate ϱ, since they have to balance the flavorelectric and gravitational, i.e. tension forces. Thus these D7-D7 strings distribute the charges along the AdS radial coordinate, leading to a stable configuration of reduced energy. This corresponds to a superconducting condensate given by the Cooper pairs. This figure is taken from [17]. Using the notations in this thesis, we identify $x \equiv x^3$ and $E_x^2 \equiv E_3^2$

$r_{\mathrm{H}} = \varrho_{\mathrm{H}}$. In this coordinate, the Hawking temperature (2.100) of the black hole (3.16) is given by $T_{\mathrm{H}} = \varrho_{\mathrm{H}}/(\pi R^2)$. The world-volume field theory on the two coincident D7-branes is a $\mathrm{SU}(2)_{\mathrm{I}}$ field theory. Taking the plane symmetric gauge ansatz to obtain an isotropic configuration in the field theory

$$A_t^3 = A_t^3(\varrho), \qquad A_x^1 = A_x^1(\varrho), \tag{3.18}$$

the non-vanishing components of the field strength tensor $F_{MN} = \sum_{a=1}^{3} F_{MN}^a \tau^a$ with

$$F_{MN}^a = \partial_M A_N^a - \partial_N A_M^a + \frac{\gamma}{\sqrt{\lambda}} f^{abc} A_M^b A_N^c, \tag{3.19}$$

and τ^a denoting the Pauli matrices, $\gamma/\sqrt{\lambda}$ the gauge coupling, f^{abc} an antisymmetric quantity in a, b, c with $f^{123} = 1$, are

$$F_{\varrho t}^3 = -F_{t\varrho}^3 = \partial_\varrho A_t^3, \quad F_{\varrho x}^1 = -F_{x\varrho}^1 = \partial_\varrho A_x^1, \quad F_{tx}^2 = -F_{xt}^2 = \frac{\gamma}{\sqrt{\lambda}} A_t^3 A_x^1. \tag{3.20}$$

Later we will explain that the first term in (3.20) is realized by D3-D7 strings, the second by D7-D7 strings and the last term describes an interaction between the D7-D7 and the D3-D7 strings which is the flavor-electric field $F_{tx}^2 = E_x^2$ pointing to the x-direction. This field stretches the D7-D7 strings in the x-direction. An illustration for this setup is shown in figure 3.3.

The action for embedding a probe of two flavor D7-branes in the AdS black hole background is given by the *non-Abelian* Dirac-Born-Infeld action which is a generalization of (2.115). For the case of $\mathcal{N}_{\mathrm{f}} = 2$ coincident D7-branes, the non-Abelian DBI action is given in [121]. In this subsection, we will not discuss in detail how to deal with the non-Abelian DBI action and postpone the

discussion to subsection 3.4.2 where an extension to [17] by adding a baryon chemical potential to the above setup is considered. The equations of motion arising from this action determine the profile of the D7-brane probes and of the gauge fields on these branes, i.e. shape of the brane embeddings as well as the configuration of the gauge fields A on these branes.

The string theory picture of the formation of the superfluid phase in [17] can be understood as follows. The field A_t^3 is generated by fundamental strings between the D7-branes and the horizon of the black hole [105, 122, 123]. These strings are D3-D7 strings. For non-zero A_t^3 the D7-branes will touch the horizon, i.e. black hole embedding, and these strings are localized at the horizon, since the tension of these strings would increase as they move to the boundary. By increasing the density of the D3-D7 strings, the total charge on the D7-branes at the horizon grows, and there is a critical density at which the setup becomes unstable [123]. Due to the repulsive force on their charged endpoints generated by the flavor-electric field pointing along the radial direction $E_\varrho^3 = F_{t\varrho}^3 = -\partial_\varrho A_t^3$, the strings would move towards the boundary. Turning on the A_x^1, the authors of [17] found that the system can be stabilized. The field A_x^1 is generated by the D7-D7 strings which are formed by the recombining processes of D3-D7 strings, thus A_x^1 carries isospin charge. There are two forces along the radial coordinates acting on the D7-D7 strings, the flavor-electric force E_ϱ^3 pushing the D7-D7 strings towards the boundary and the gravitational force pulling the D7-D7 strings towards the horizon. The stable position of the D7-D7 strings is determined by the equilibrium of these two forces. Thus in the presence of A_x^1, the isospin charges are not only at the horizon, but get distributed into the bulk, since the isospin-charged D7-D7 strings move away from the horizon towards the boundary. This distribution of isospin charge is crucial for stabilizing the system.

So far, without loss of generality, the field component of A_x^1 is chosen to be x. Similar to (3.21), this field is dual to the operator

$$J_x^1 \propto \bar{\psi}\tau^1\gamma_x\psi + \phi\tau^1\partial_x\phi = \bar{\psi}_u\gamma_x\psi_d + \bar{\psi}_d\gamma_x\psi_u + \text{bosons} . \tag{3.21}$$

A non-vanishing expectation value $\langle J_x^1 \rangle$ breaks both the $\mathrm{SO}(3)$ rotational symmetry and the $\mathrm{U}(1)_3$ flavor symmetry spontaneously. The rotational $\mathrm{SO}(3)$ is broken down to $\mathrm{SO}(2)$ which is generated by rotations around the x-axis. As argued in [17], since the back-reaction of the gauge fields on the metric is not considered, only the $\mathrm{U}(1)_3$ is the dynamical symmetry, and consequently only one Nambu-Goldstone boson associated to the spontaneous breaking of the $\mathrm{U}(1)_3$ could be found. The condensate $\langle J_x^1 \rangle$ is interpreted as the counterpart to the Cooper pairs of the BCS theory, the $\mathrm{U}(1)_3$ to $\mathrm{U}(1)_{\mathrm{em}}$ and the current J^3 to the electric current J_{em}.

Numerical results in [17] shows that below some critical valuel $T_{\mathrm{H}}/\mu_{\mathrm{I}}$ there is a stable solution with $\langle J_x^1 \rangle \neq 0$. This solution is interpreted as the gravity solution of the holographic superfluid at finite isospin chemical potential. It is

a model for a holographic p-wave superfluid, since on the gravity theory side there is a charged gauge field which condenses.

Gap in the frequency dependent conductivity and infinite DC conductivity   The frequency-dependent conductivity is obtained by considering the fluctuations about the stable gravity solution. In the bottom-up approach the fluctuations may be introduced by switching on the x-component of the Maxwell field, e.g. $\mathcal{A}_x(r, t) = e^{i\omega t} A_x(r)$ for computing the conductivity in the x-direction. Here, the harmonic time-dependent ansatz is used. In the top-down approach presented above, the fluctuations may be turned on in some other directions inside the $\mathrm{SU(2)_I}$, such that the general ansatz for the gauge field A on the branes can have the following form

$$A = A_t^3 \tau^3 \mathrm{d}t + A_x^1 \tau^1 \mathrm{d}x + \mathfrak{a}_\mu^j(\varrho, t)\tau^j \mathrm{d}x^\mu, \tag{3.22}$$

with $\mathfrak{a}_\mu^j(\varrho, t) = e^{i\omega t} a_\mu^j(\varrho)$. In linear response theory[2], the frequency-depenent conductivity can be computed using the Kubo formula,

$$\sigma(\omega) = \frac{\mathrm{i}}{\omega} G^{\mathrm{R}}(\omega, q = 0), \tag{3.23}$$

where G^{R} is the retarded Green's function of the corresponding current and q the momentum. Using the prescription in [81] for computing the Minkowski-space correlators in AdS/CFT correspondence, the retarded Green's function can be obtained via solving the equations of motion for $\mathcal{A}_x$ and $\mathfrak{a}_\mu^j$, respectively, while demanding incoming conditions at the horizon for those fluctuations. In general, the fluctuations have the following generic form near the boundary $r \to \infty$,

$$\mathcal{A}_x = \mathcal{A}_x^{(0)} + \frac{\mathcal{A}_x^{(1)}}{r} + \cdots. \tag{3.24}$$

Using the AdS/CFT dictionary, $\mathcal{A}_x^{(0)}$ corresponds to the electric field at the boundary $E_x = -\partial_t \mathcal{A}_x^{(0)}$, and the expectation value of the induced current is the first sub-leading term $J_x = \mathcal{A}_x^{(1)}$. Thus linear response theory gives

$$\sigma_{xx} = \frac{J_x}{E_x} = -\frac{\mathrm{i}}{\omega} \frac{\mathcal{A}_x^{(1)}}{\mathcal{A}_x^{(0)}}. \tag{3.25}$$

The same prescription can be applied for analyzing $\mathfrak{a}_\mu^j(\varrho, t)$, where for instance the current J_y^3 charged under the $\mathrm{U(1)_3}$ is the analog to the electric current which is transverse to the condensate in field theory coordinates. Plotting the real part of the conductivity, the authors of [15, 16] and [17, 18]

---

[2]Conductivity beyond linear response theory will be a subject in chapter 4.
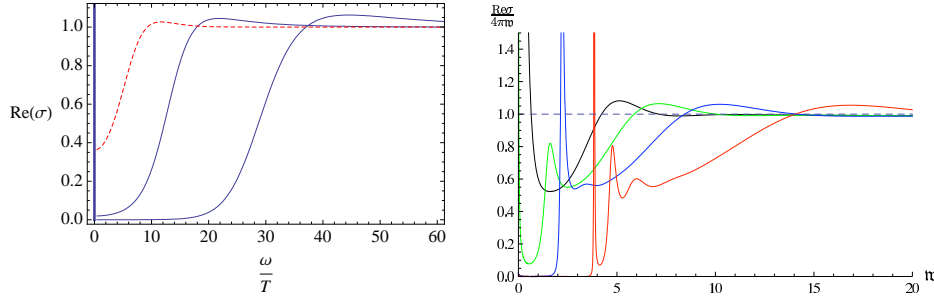
FIGURE 3.4:   Real part of the conductivity versus ω/T and $\mathfrak{w} = \omega/(2\pi T)$. Left figure: The dashed red line is the real part of the conductivity at $T = T_c$. The blue lines are the same conductivities at temperatures $T < T_c$. This figure is taken from [16]. Right figure: Real part of the conductivity at different temperatures: $T \approx 0.90T_c$ (black), $T \approx 0.66T_c$ (green), $T \approx 0.46T_c$ (blue), $T \approx 0.28T_c$ (red). This figure is taken from [17]. In both figures the formation of a gap is observed below the critical temperature. There is a delta peak at zero frequency which indicates infinite DC conductivity.

observe the formation of a gap in the real part of the conductivity as the temperature is lowered below the critical temperature, see figure 3.4. Using the Kramers-Kronig relation to connect the real and imaginary part of the complex conductivity, the authors of [15, 16] and [17, 18] found that there is a delta peak at $\omega = 0$ for all $T < T_c$, i.e. $\mathrm{Re}[\sigma(\omega)] \sim n_s \delta(\omega)$ with n_s denoting the density of the superconducting condensate. This peak corresponds to the infinite DC conductivity[3] which is another signature of superconductivity. Numerical results in [17] show that the condensate vanishes linearly at the critical temperature, $n_s \propto (1 - T/T_c)$ as T approaches T_c, which is in agreement with Ginzburg-Landau theory (3.7).

Some comments on the two approaches   One obvious advantage of the top-down approach compared to the bottom-up approach is that the dual field theory is known explicitly. In the case presented above it is the $\mathcal{N} = 4$ SYM theory coupled to two $\mathcal{N} = 2$ hypermultiplets. Since the field content of the dual field theory is known, it is possible to write down the corresponding Lagrangian [100], and therefore the condensate can be identified in terms of elementary fields (3.21). Using this model, results at strong coupling obtained from the gravity side can be compared with results at weak coupling obtained from the field theory side. Moreover, the top-down approach has a consistent string theory background. This approach implies, however, that for each

---

[3]There is an ambiguity that this peak might be seen as the Drude peak if the system is translation invariant and the charge carriers cannot lose energy as they are accelerated by the electric field. The objection of the Drude peak in [18] arises from the argument from [52, 54] saying that the adjoint degrees of freedom can transfer momentum at order N_c^2 while the fundamental degrees of freedom only at order N_c, thus the adjoint degrees of freedom effectively act as a heat sink into which the flavor fields can dissipate the energy, see also section 4.1 and 4.3.3 in chapter 4. In the bottom-up approach [16], where the backreaction is considered, there is a delta peak at $\omega = 0$ even when $T > T_c$. This peak in the normal conducting phase indeed corresponds to the Drude peak, but it differs in behavior by the peak at $\omega = 0$ when $T < T_c$.

dual field theory we need to construct a specific corresponding gravity setup. So far, there are only a few other holographic realizations of superfluids, e.g. [124–126], where dual fields theories can be identified explicitly, hence it is very hard to look for universal properties of holographic superconductors/ superfluids at strong coupling using only the results obtained from the top-down approach.

Using the bottom-up approach, fields are introduced by hands and the parameters occurring in such models are not fixed by any physical restrictions. This might be seen as a disadvantage compared to the top-down approach, but on the other hand this freedom in the bottom-up approach enables vast possibilities for extending and generalizing the model discussed above. As an example, instead of looking for hairy AdS black hole solutions using the Einstein-Maxwell theory coupled to a charged scalar for describing holographic s-wave superconductors, the setup can be easily changed in order to study p-wave superfluids by considering the $\mathrm{SU}(2)$ Einstein-Yang-Mills theory [48, 127]. Results obtained from the bottom-up approach have a kind of universality in the sense that they may be true for many different dual conformal field theories, since, in general, scanning through the values of the parameters in the gravity setup corresponds to scanning though different dual conformal field theories.

3.3 QPT in EYM theory at finite baryon and isospin chemical potential

In this section we use the botton-up approach to construct a gravity model for holographic superfluidity. In this model we can observe quantum phase transitions from a normal conducting to a superconducting phase of a holographic p-wave superfluid. Quantum phase transition occurs at zero temperature and can be accessed by varying physical parameters of the theory. In our case, the tuning physical parameter is the ratio between the baryon and the isospin chemical potential. Here, the main idea is to extend the discussed Einstein-Maxwell theory coupled to a charged scalar to an $\mathrm{U}(2) = \mathrm{U}(1)_\mathrm{B} \times \mathrm{SU}(2)_\mathrm{I}$ Einstein-Yang-Mills theory, where a baryon and an isospin chemical potential can be introduced via the AdS/CFT dictionary with the time-component of the $\mathrm{U}(1)_\mathrm{B}$ and $\mathrm{SU}(2)_\mathrm{I}$ gauge fields, respectively. The work presented in this section is an extension to the construction of holographic superfluids in the presence of only an isospin chemical potential [48, 127–129]. In the probe approximation [127], i.e. the gauge fields do not influence the metric, a second order phase transition to a state is found which spontaneously breaks an Abelian symmetry. This spontaneous breaking creates a superfluid. In [48], the back-reaction of the gauge field on the metric has been added to this scenario. By increasing the back-reaction, the critical temperature decreases. Beyond a critical strength of the back-reaction, the phase transition is first order. There is a maximal

value for the back-reaction beyond which the transition to the superfluid phase is not possible. The material in this section generalizes the results in [48] by including the baryon chemical potential which stems from my own work in collaboration with Johanna Erdmenger, Patrick Kerner and Viviane Grass [3].

3.3.1   U(2) **Einstein-Yang-Mills theory with back-reaction**

We consider the $\mathrm{U}(2)$ Einstein-Yang-Mills theory in $(4+1)$-dimensional asymptotically AdS space. The action is

$$
S = \int \mathrm{d}^5 x \sqrt{-g} \left[\frac{1}{2\kappa_5^2}(\mathcal{R} - \Lambda) - \frac{1}{4\hat{g}_{\mathrm{MW}}^2} \mathcal{F}_{\mu\nu}\mathcal{F}^{\mu\nu} - \frac{1}{4\hat{g}_{\mathrm{YM}}^2} F_{\mu\nu}^a F^{a\mu\nu} \right] , \quad (3.26)
$$

where κ_5 is the five-dimensional gravitational constant, $\Lambda = -12/R^2$ is the cosmological constant, with R being the AdS radius, $\hat{g}_{\mathrm{MW}}$ the Maxwell and $\hat{g}_{\mathrm{YM}}$ the Yang-Mills coupling. The $\mathrm{U}(2)$ gauge field is split into an $\mathrm{SU}(2)$ part with field strength tensor

$$
F_{\mu\nu}^a = \partial_\mu A_\nu^a - \partial_\nu A_\mu^a + \epsilon^{abc} A_\mu^b A_\nu^c , \quad (3.27)
$$

where ϵ^{abc} is the total antisymmetric tensor and $\epsilon^{123} = +1$, and into an $\mathrm{U}(1)$ part with field strength tensor

$$
\mathcal{F}_{\mu\nu} = \partial_\mu \mathcal{A}_\nu - \partial_\nu \mathcal{A}_\mu . \quad (3.28)
$$

Here, the a, b, c are tensor indices taking values in $\{1, 2, 3\}$ for the Pauli matrices, while μ, ν denote space-time indices for the world-volume coordinates of the D7-branes.

The Einstein and Yang-Mills equations derived from the above action are

$$
\begin{aligned}
\mathcal{R}_{\mu\nu} + \frac{4}{R^2} g_{\mu\nu} &= \kappa_5^2 \left(T_{\mu\nu} - \frac{1}{3} T_\rho^\rho g_{\mu\nu} \right) , \\
\nabla_\mu F^{a\mu\nu} &= -\epsilon^{abc} A_\mu^b F^{c\mu\nu} , \\
\nabla_\mu \mathcal{F}^{\mu\nu} &= 0 ,
\end{aligned} \quad (3.29)
$$

where the Yang-Mills energy-momentum tensor $T_{\mu\nu}$ is

$$
T_{\mu\nu} = \frac{1}{\hat{g}_{\mathrm{YM}}^2} \left[F_{\mu\rho}^a F_\nu^{a\rho} - \frac{1}{4} g_{\mu\nu} F_{\sigma\rho}^a F^{a\sigma\rho} \right] + \frac{1}{\hat{g}_{\mathrm{MW}}^2} \left[\mathcal{F}_{\mu\rho} \mathcal{F}_\nu^{\ \rho} - \frac{1}{4} g_{\mu\nu} \mathcal{F}_{\sigma\rho} \mathcal{F}^{\sigma\rho} \right] . \quad (3.30)
$$

Following [48], to construct charged black hole solutions with a vector hair we choose a gauge field ansatz

$$
\begin{aligned}
A &= \phi(r)\tau^3 \mathrm{d}t + w(r)\tau^1 \mathrm{d}x , \\
\mathcal{A} &= \psi(r)\mathrm{d}t .
\end{aligned} \quad (3.31)
$$

The motivation for this ansatz is as follows: In the field theory we introduce a baryon and isospin chemical potential by the the boundary values of the time components of the gauge fields, ϕ and ψ. This breaks the $U(2)$ symmetry down to a diagonal $U(1)$ which is generated by τ^3. We denote this $U(1)$ as $U(1)_3$. In order to study the transition to the superfluid state, we allow solutions with non-zero $\langle J_x^1 \rangle$ such that we include the dual gauge field $A_x^1 = w$ in the gauge field ansatz. Since we consider only isotropic and time-independent solutions in the field theory, the gauge fields exclusively depend on the radial coordinate r. With this ansatz the Yang-Mills energy-momentum tensor in (3.30) is diagonal. Solutions with $\langle J_x^1 \rangle \neq 0$ also break the spatial rotational symmetry $SO(3)$ down to $SO(2)$ [4] such that our metric ansatz will respect only $SO(2)$. Since the Yang-Mills energy-momentum tensor is diagonal, a diagonal metric is consistent. Following [48, 130], our metric ansatz is

$$\mathrm{d}s^2 = -N(r)\sigma(r)^2\mathrm{d}t^2 + \frac{1}{N(r)}\mathrm{d}r^2 + r^2 f(r)^{-4}\mathrm{d}x^2 + r^2 f(r)^2 \left(\mathrm{d}y^2 + \mathrm{d}z^2\right) ,$$

(3.32)

with $N(r) = -2m(r)/r^2 + r^2/R^2$.

Inserting our ansatz into the Einstein and Yang-Mills equations leads to six equations of motion for $m(r), \sigma(r), f(r), \phi(r), w(r), \psi(r)$ and one constraint equation from the rr component of the Einstein equations. The dynamical equations may be written as

$$m' = \frac{\alpha_{\mathrm{YM}}^2 r f^4 w^2 \phi^2}{6N\sigma^2} + \frac{r^3(\alpha_{\mathrm{YM}}^2 \phi'^2 + \alpha_{\mathrm{MW}}^2 \psi'^2)}{6\sigma^2} + N\left(\frac{r^3 f'^2}{f^2} + \frac{\alpha_{\mathrm{YM}}^2}{6}r f^4 w'^2\right) ,$$

$$\sigma' = \frac{\alpha_{\mathrm{YM}}^2 f^4 w^2 \phi^2}{3rN^2\sigma} + \sigma\left(\frac{2r f'^2}{f^2} + \frac{\alpha_{\mathrm{YM}}^2 f^4 w'^2}{3r}\right) ,$$

$$f'' = -\frac{\alpha_{\mathrm{YM}}^2 f^5 w^2 \phi^2}{3r^2 N^2\sigma^2} + \frac{\alpha_{\mathrm{YM}}^2 f^5 w'^2}{3r^2} - f'\left(\frac{3}{r} - \frac{f'}{f} + \frac{N'}{N} + \frac{\sigma'}{\sigma}\right) ,$$

$$\phi'' = \frac{f^4 w^2 \phi}{r^2 N} - \phi'\left(\frac{3}{r} - \frac{\sigma'}{\sigma}\right) ,$$

$$w'' = -\frac{w\phi^2}{N^2\sigma^2} - w'\left(\frac{1}{r} + \frac{4f'}{f} + \frac{N'}{N} + \frac{\sigma'}{\sigma}\right) ,$$

$$\psi'' = -\psi'\left(\frac{3}{r} - \frac{\sigma'}{\sigma}\right) .$$

(3.33)

The equations of motion are invariant under five scaling transformations (in-

---

[4]Note that the finite temperature and chemical potential already break the Lorentz group down to $SO(3)$.

variant quantities are not shown),

$$
\begin{aligned}
(I) \quad & \sigma \to \lambda\sigma, \quad \phi \to \lambda\phi, \quad \psi \to \lambda\psi, \\
(II) \quad & f \to \lambda f, \quad w \to \lambda^{-2}w, \\
(III) \quad & r \to \lambda r, \quad m \to \lambda^4 m, \quad w \to \lambda w, \quad \phi \to \lambda\phi, \quad \psi \to \lambda\psi, \\
(IV) \quad & r \to \lambda r, \quad m \to \lambda^2 m, \quad R \to \lambda R, \quad \phi \to \lambda^{-1}\phi, \quad \psi \to \lambda^{-1}\psi, \\
& \alpha_{\mathrm{YM}} \to \lambda\alpha_{\mathrm{YM}}, \quad \alpha_{\mathrm{MW}} \to \lambda\alpha_{\mathrm{MW}}, \\
(V) \quad & \psi \to \lambda\psi, \quad \alpha_{\mathrm{MW}} \to \lambda^{-1}\alpha_{\mathrm{MW}},
\end{aligned}
\tag{3.34}
$$

where in each case λ is some real positive number. As in [48] we use (I) and (II) to set the boundary values of both σ and f to one, so that the metric will be asymptotically AdS. Also we can use (III) to set the later to introduced horizon r_{H} to one, but we will keep it as a bookkeeping device. We use (IV) to set the AdS radius R to one. The relation (V) allows us to set $\alpha_{\mathrm{MW}} = 1$ by rescaling the baryon chemical potential, i.e. we can relate states with different baryon chemical potentials in different theories characterized by α_{MW} to each other.

A known solution of the equations of motion is the AdS Reissner-Nordström black hole,

$$
\begin{aligned}
& \phi(r) = \mu_{\mathrm{I}} - \frac{q_{\mathrm{I}}}{r^2}, \quad \psi = \mu_{\mathrm{B}} - \frac{q_{\mathrm{B}}}{r^2} \quad w(r) = 0, \quad \sigma(r) = f(r) = 1, \\
& N(r) = r^2 - \frac{2m_0}{r^2} + \frac{2(\alpha_{\mathrm{YM}}^2 q_{\mathrm{I}}^2 + \alpha_{\mathrm{MW}}^2 q_{\mathrm{B}}^2)}{3r^4} \\
& \quad \text{with} \quad q_i = \mu_i r_{\mathrm{H}}^2 \quad \text{and} \quad m_0 = \frac{r_{\mathrm{H}}^4}{2} + \frac{\alpha_{\mathrm{YM}}^2 q_{\mathrm{I}}^2 + \alpha_{\mathrm{MW}}^2 q_{\mathrm{B}}^2}{3r_{\mathrm{H}}^2}.
\end{aligned}
\tag{3.35}
$$

In order to obtain the solutions in the superfluid phase, i.e. $w(r) \not\equiv 0$, we have to resort to numerics. We will solve the equations of motion using a shooting method. We will vary the values of functions near the horizon until we find solutions with suitable values near the AdS boundary. We thus need the asymptotic forms of the solutions near the horizon $r = r_{\mathrm{H}}$ and near the boundary $r \to \infty$.

Near the horizon, we expand all fields in powers of $\epsilon_h = r/r_{\mathrm{H}} - 1 \ll 1$ with some constant coefficients. Three of these coefficients can be fixed as follows: We determine r_{H} by the condition $N(r_{\mathrm{H}}) = 0$ which gives $m(r_{\mathrm{H}}) = r_{\mathrm{H}}^4/2$. Additionally, the time components of the gauge fields must be zero to obtain well-defined one-forms (see for example [105]), i.e. $\phi(r_{\mathrm{H}}) = 0$ and $\psi(r_{\mathrm{H}}) = 0$. The equations of motion then impose relations among the other coefficients. A straightforward exercise shows that only five coefficients are independent,

$$
\left\{ \sigma_0^h, f_0^h, w_0^h, \phi_1^h, \psi_1^h \right\},
\tag{3.36}
$$

where the subscript denotes the order of ϵ_h. All other near-horizon coefficients are determined in terms of these five independent coefficients.

Near the boundary, we expand all fields in powers of $\epsilon_b = (r_H/r)^2 \ll 1$ with some constant coefficients. Again the equations of motion impose relations on these coefficients. There are seven independent coefficients

$$\left\{ m_0^b, \phi_0^b, \phi_1^b, \psi_0^b, \psi_1^b, w_1^b, f_2^b \right\} \,, \tag{3.37}$$

where here the subscript denotes the power of ϵ_b. All other near-boundary coefficients are determined in terms of these seven independent coefficients. We used the scaling symmetries (3.34) to set $\sigma_0^b = f_0^b = 1$. Our solutions will also have $w_0^b = 0$ since we do not want to source the operator J_x^1 in the dual field theory, i.e. the $U(1)_3$ symmetry will be spontaneously broken. In our shooting method we choose a value of $\phi_0^b = \mu_I$, the isospin chemical potential, and of $\psi_0^b = \mu_B$, the baryon chemical potential, and then vary the five independent near-horizon coefficients until we find a solution which produces the desired values at the boundary.

In the following it will be often convenient to work with dimensionless coefficients by scaling out factors of r_H. We thus define the dimensionless functions $\tilde{m}(r) = m(r)/r_H^4$, $\tilde{\phi}(r) = \phi(r)/r_H$, $\tilde{\psi}(r) = \psi(r)/r_H$ and $\tilde{w}(r) = w(r)/r_H$, while $f(r)$ and $\sigma(r)$ are already dimensionless.

3.3.2 Thermodynamics

In this section we extract thermodynamic information from our solutions. The gravity solutions describe thermal equilibrium in the boundary field theory. In order to extract thermodynamic quantities from the gravity solutions we can use well-known methods of black hole thermodynamics which have been discussed in section 2.2.1 previously.

The temperature T in the boundary field theory is identified with the Hawking temperature of the black hole (2.100). The Hawking temperature for our black hole solutions is given by

$$T = \frac{\kappa}{2\pi} = \frac{r_H \sigma_0^h}{\pi} \left(1 - \frac{\alpha_{\text{YM}}^2 \left(\phi_1^h \right)^2 + \alpha_{\text{MW}}^2 \left(\psi_1^h \right)^2}{12 \left(\sigma_0^h \right)^2} \right) \,, \tag{3.38}$$

where κ is the surface gravity of the black hole as defined in (2.99) and in the second equality we write T in terms of the near-horizon coefficients. In the following we will often convert from the black hole radius r_H to the temperature T by inverting the above equation.

The entropy S of the boundary field theory is identified with the Bekenstein-Hawking entropy of the black hole. For our ansatz we obtain

$$S = \frac{2\pi}{\kappa_5^2} A_h = \frac{2V\pi r_H^3}{\kappa_5^2} = \frac{2\pi^4 V T^3}{\kappa_5^2 \left(\sigma_0^h \right)^3} \left(1 - \frac{\alpha_{\text{YM}}^2 \left(\phi_1^h \right)^2 + \alpha_{\text{MW}}^2 \left(\psi_1^h \right)^2}{12 \left(\sigma_0^h \right)^2} \right)^{-3} \,,$$

$$(3.39)$$

where A_h is the area of the horizon and V the spatial volume of the Minkowski space.

The general statement of gauge/string duality which relates the field theory partition function to the string theory partition function may be used to calculate the thermodynamic potential of the boundary field theory, i.e. in our case the grand potential. In the gravity approximation, which we use in this chapter, the grand potential Ω is given as the temperature T times the on-shell bulk action in Euclidean signature. We thus analytically continue to Euclidean signature and compactify the time direction with period $1/T$. We denote the Euclidean action as I and its on-shell value as $I_{\text{on-shell}}$. Since our solutions are always static, we can integrate out the time direction which produces an overall factor of $1/T$. In order to simplify the expressions, we define $\tilde{I} = I/T$. From now on we refer to $\tilde{I}$ as the action. $\tilde{I}$ splits into three parts, a bulk term, a Gibbons-Hawking term and counterterms,

$$\tilde{I} = \tilde{I}_{\text{bulk}} + \tilde{I}_{GH} + \tilde{I}_{\text{ct}} . \qquad (3.40)$$

The counterterms are needed to cancel the divergences of the bulk action and Gibbons-Hawking term which appear on-shell. To regulate these divergencies we introduce a hypersurface at $r = r_{\text{bdy}}$ with some large but finite r_{bdy}. On the field theory side r_{bdy} corresponds to an UV cutoff. Ultimately we will remove the cutoff by taking $r_{\text{bdy}} \to \infty$. Using the equations of motion, we obtain $\tilde{I}_{\text{bulk}}^{\text{on-shell}}$ for our ansatz

$$\tilde{I}_{\text{bulk}}^{\text{on-shell}} = \frac{V}{\kappa_5^2} \frac{1}{2f^2} r N \sigma (r^2 f^2)' \bigg|_{r=r_{\text{bdy}}} . \qquad (3.41)$$

For our ansatz, the Euclidean Gibbons-Hawking term is

$$\tilde{I}_{\text{GH}}^{\text{on-shell}} = -\frac{1}{\kappa_5^2} \int \mathrm{d}^3 x \sqrt{\gamma} \, \nabla_\mu n^\mu = -\frac{V}{\kappa_5^2} N \sigma r^3 \left(\frac{N'}{2N} + \frac{\sigma'}{\sigma} + \frac{3}{r} \right) \bigg|_{r=r_{\text{bdy}}} , \qquad (3.42)$$

where γ is the induced metric on the $r = r_{\text{bdy}}$ hypersurface and $n_\mu \mathrm{d} x^\mu = 1/\sqrt{N(r)} \, \mathrm{d} r$ is the outward-pointing normal vector. The only divergence in the bulk action and Gibbons-Hawking term comes from the infinite volume of the asymptotically AdS space, hence, for our ansatz, the only nontrivial counterterm is

$$\tilde{I}_{\text{ct}}^{\text{on-shell}} = \frac{3}{\kappa_5^2} \int \mathrm{d}^3 x \sqrt{\gamma} = \frac{3V}{\kappa_5^2} r^3 \sqrt{N} \sigma \bigg|_{r=r_{\text{bdy}}} . \qquad (3.43)$$

Finally the grand potential Ω is given by

$$\Omega = \lim_{r_{\rm bdy} \to \infty} \tilde{I}_{\rm on\text{-}shell} \, . \tag{3.44}$$

The baryon chemical potential μ_B is simply given by the boundary value of $\mathcal{A}_t(r) = \psi(r)$, while the isospin chemical potential μ_I is given by the boundary value of $A_t^3(r) = \phi(r)$. The baryon charge density $\langle \mathcal{J}_t \rangle$ and isospin charge density $\langle J_t^3 \rangle$ of the dual field theory may be extracted from the on-shell action $\tilde{I}_{\rm on\text{-}shell}$ via the gauge/gravity dictionary (2.51),

$$\langle \mathcal{J}_t \rangle = \frac{1}{V} \lim_{r_{\rm bdy} \to \infty} \frac{\delta \tilde{I}_{\rm on\text{-}shell}}{\delta \mathcal{A}_t(r_{\rm bdy})} = -\frac{2\pi^3 \alpha_{\rm MW}^2 T^3}{\kappa_5^2 \left(\sigma_0^h\right)^3} \left(1 - \frac{\alpha_{\rm YM}^2 \left(\phi_1^h\right)^2 + \alpha_{\rm MW}^2 \left(\psi_1^h\right)^2}{12 \left(\sigma_0^h\right)^2}\right)^{-3} \tilde{\psi}_1^b \, ,$$

$$\langle J_t^3 \rangle = \frac{1}{V} \lim_{r_{\rm bdy} \to \infty} \frac{\delta \tilde{I}_{\rm on\text{-}shell}}{\delta A_t^3(r_{\rm bdy})} = -\frac{2\pi^3 \alpha_{\rm YM}^2 T^3}{\kappa_5^2 \left(\sigma_0^h\right)^3} \left(1 - \frac{\alpha_{\rm YM}^2 \left(\phi_1^h\right)^2 + \alpha_{\rm MW}^2 \left(\psi_1^h\right)^2}{12 \left(\sigma_0^h\right)^2}\right)^{-3} \tilde{\phi}_1^b \, . \tag{3.45}$$

Similarly, the current density $\langle J_x^1 \rangle$ is

$$\langle J_x^1 \rangle = \frac{1}{V} \lim_{r_{\rm bdy} \to \infty} \frac{\delta \tilde{I}_{\rm on\text{-}shell}}{\delta A_x^1(r_{\rm bdy})} = -\frac{2\pi^3 \alpha_{\rm YM}^2 T^3}{\kappa_5^2 \left(\sigma_0^h\right)^3} \left(1 - \frac{\alpha_{\rm YM}^2 \left(\phi_1^h\right)^2 + \alpha_{\rm MW}^2 \left(\psi_1^h\right)^2}{12 \left(\sigma_0^h\right)^2}\right)^{-3} \tilde{w}_1^b \, . \tag{3.46}$$

The expectation value of the energy-momentum-tensor of the dual field theory is [131, 132]

$$\langle T_{ij} \rangle = \lim_{r_{\rm bdy} \to \infty} \frac{2}{\sqrt{\gamma}} \frac{\delta \tilde{I}_{\rm on\text{-}shell}}{\delta \gamma^{ij}} = \lim_{r_{\rm bdy} \to \infty} \left[\frac{r^2}{\kappa_5^2} \left(-K_{ij} + K^l{}_l \gamma_{ij} - 3\gamma_{ij} \right) \right]_{r=r_{\rm bdy}} \, , \tag{3.47}$$

where $i, j, l \in \{t, x, y, z\}$ and $K_{ij} = 1/2 \sqrt{N(r)} \partial_r \gamma_{ij}$ is the extrinsic curvature. We find

$$\langle T_{tt} \rangle = \frac{3\pi^4 V T^4}{\kappa_5^2 \left(\sigma_0^h\right)^4} \left(1 - \frac{\alpha_{\rm YM}^2 \left(\phi_1^h\right)^2 + \alpha_{\rm MW}^2 \left(\psi_1^h\right)^2}{12 \left(\sigma_0^h\right)^2}\right)^{-4} \tilde{m}_0^b \, ,$$

$$\langle T_{xx} \rangle = \frac{\pi^4 V T^4}{\kappa_5^2 \left(\sigma_0^h\right)^4} \left(1 - \frac{\alpha_{\rm YM}^2 \left(\phi_1^h\right)^2 + \alpha_{\rm MW}^2 \left(\psi_1^h\right)^2}{12 \left(\sigma_0^h\right)^2}\right)^{-4} \left(\tilde{m}_0^b - 8f_2^b\right) \, ,$$

$$\langle T_{yy} \rangle = \langle T_{zz} \rangle = \frac{\pi^4 V T^4}{\kappa_5^2 \left(\sigma_0^h\right)^4} \left(1 - \frac{\alpha_{\rm YM}^2 \left(\phi_1^h\right)^2 + \alpha_{\rm MW}^2 \left(\psi_1^h\right)^2}{12 \left(\sigma_0^h\right)^2}\right)^{-4} \left(\tilde{m}_0^b + 4f_2^b\right) \, . \tag{3.48}$$

For $\psi \equiv 0$ we recover the results obtained in [48]. Notice that the energy-momentum tensor is still diagonal such that the momentum is zero even in the superfluid phase where the current $\langle J_x^1 \rangle$ is non-zero. This result is guaranteed by our ansatz for the gauge fields which implies a diagonal Yang-Mills energy-momentum tensor and a diagonal metric.

For $\tilde{m}_0^b = 1/2 + (\alpha_{\mathrm{YM}}^2 \tilde{\mu}_{\mathrm{I}}^2 + \alpha_{\mathrm{MW}}^2 \tilde{\mu}_{\mathrm{B}}^2)/3$, $\sigma_0^h = 1$, $\tilde{\phi}_1^h = 2\tilde{\mu}_{\mathrm{I}}$, $\tilde{\psi}_1^h = 2\tilde{\mu}_{\mathrm{B}}$, $f_2^b = 0$, $\tilde{\phi}_b^0 = \tilde{\mu}_{\mathrm{I}}$, and $\tilde{\psi}_b^0 = \tilde{\mu}_{\mathrm{B}}$ we recover the correct thermodynamics for the Reissner-Nordström black hole, which preserves the $\mathrm{SO}(3)$ rotational symmetry. For instance, we find that $\langle T_{xx} \rangle = \langle T_{yy} \rangle = \langle T_{zz} \rangle$ and $\Omega = -\langle T_{yy} \rangle$. For solutions with non-zero $\langle J_x^1 \rangle$ the $\mathrm{SO}(3)$ symmetry is spontaneously broken to $\mathrm{SO}(2)$ and we find $\langle T_{xx} \rangle \neq \langle T_{yy} \rangle = \langle T_{zz} \rangle$. However we also find $\Omega = -\langle T_{yy} \rangle$ by just using the equations of motion as in [48].

Since the energy-momentum tensor is traceless (in Lorentzian signature), the dual field theory is scale invariant and describes a conformal fluid. The only physical parameters in the dual field theory are thus the ratios μ_{B}/T, μ_{I}/T and $\mu_{\mathrm{B}}/\mu_{\mathrm{I}}$. Since only two of them are independent from each other, we choose μ_{I}/T and $\mu_{\mathrm{B}}/\mu_{\mathrm{I}}$ to determine the physical state of the boundary field theory in what follows.

3.3.3 Phase transition and phase diagram

We expect a phase transition from the normal phase to a superfluid phase with a non-zero condensate $\langle J_x^1 \rangle$ as the baryon and isospin chemical potential are varied. From [48] we know that this phase transition occurs at zero baryon chemical potential. In the following we study the phase transitions also at non-zero baryon chemical potential which are illustrated in fig. 3.5. The numerical results for the phase diagrams are displayed in fig. 3.6.

Let us first map out the phase diagram of the $\mathrm{U}(2)$ EYM theory at finite temperature, baryon and isospin chemical potential for different values of the coupling constant α_{YM}. We start our discussion for small α_{YM}. Our numerical results are shown in fig. 3.6 and are confirmed by an analytic calculation at $\alpha_{\mathrm{YM}} = 0$ presented in section 3.3.5. In the blue region the order parameter $\langle J_x^1 \rangle$ is non-zero and the system is in the superfluid phase while in the white region the order parameter $\langle J_x^1 \rangle$ is zero and the system is in the normal phase. We observe that the phase boundary moves monotonically to lower temperatures compared to the isospin chemical potential T/μ_{I} as we increase the baryon chemical compared to the isospin chemical potential $\mu_{\mathrm{B}}/\mu_{\mathrm{I}}$. The order of the phase transition does not depend on the baryon chemical potential and stays second order. At a critical value for the ratio of baryon to isospin chemical potential $(\mu_{\mathrm{B}}/\mu_{\mathrm{I}})_c$ we obtain a quantum critical point at zero temperature. In section 3.3.4 we determine this critical ratio analytically. Its value can be found in (3.54).

By increasing α_{YM} the area of the superfluid phase in the phase diagram decreases but the shape of the phase diagram stays the same until we reach
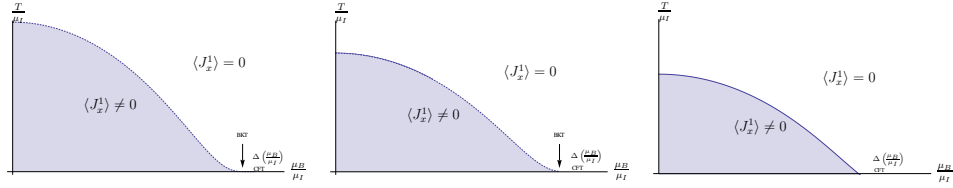
FIGURE 3.5: Sketch of the phase diagrams for the Einstein-Yang-Mills system for different strength of the back-reaction: In the white region the system is in the normal phase while in the blue region it is in the superfluid phase. The solid line marks a first oder phase transition and the dotted line a second order phase transition. In the normal phase at zero temperature the dual field theory contains an emergent one-dimensional CFT in the IR and the IR dimension of the operator depends on the ratio of the chemical potentials. For small back-reaction (a), the phase transition is second order for finite temperatures and we expect the quantum phase transition to be BKT-like. For intermediate back-reaction (b), there is a first order phase transition at large temperatures. At low temperatures the behavior is as for small back-reaction. For large back-reaction (c), the phase transition is always first order. Also the quantum phase transition is first order.
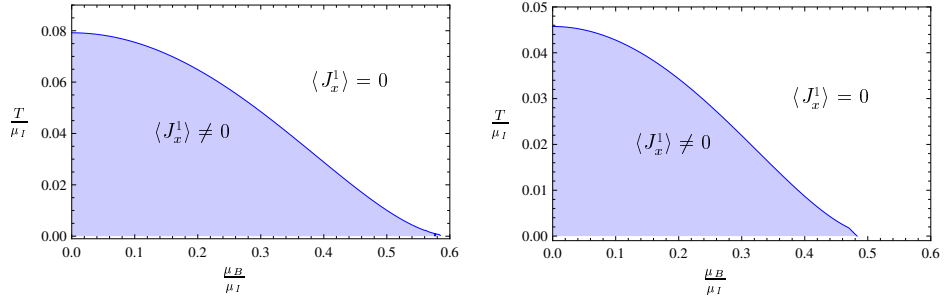

FIGURE 3.6: The phase diagram of the $U(2)$ Einstein Yang-Mills theory at finite temperature T, baryon μ_B and isospin chemical potential μ_I for $\alpha_{\mathrm{YM}} = 0.001$ (a) and $\alpha_{\mathrm{YM}} = 0.1$ (b): In the blue region the order parameter $\langle J_x^1 \rangle$ is non-zero and the system is in the superfluid phase while in the white region the order parameter $\langle J_x^1 \rangle$ is zero and the system is in the normal phase. The figures in 3.6 have been produced by Patrick Kerner [3].

a critical value for α_{YM}. Beyond the critical value $(\alpha_{\mathrm{YM}})_{c,1} = 0.365 \pm 0.001$ we know from [48] that the phase transition to the superfluid phase becomes first order at zero baryon chemical potential. If we now increase the baryon chemical potential, we find a critical point where the phase transition becomes second order again (for a sketch see figure 3.5 (b)). The phase transition at zero temperature is still continuous and therefore a quantum critical point. If we increase α_{YM}, the critical point describing the change of the phase transition from first to second order moves to larger values of the ratio of baryon to isospin chemical potential. We find a critical value of α_{YM} where the zero temperature phase transition becomes first order and the quantum critical point disappears. Its value is given by $(\alpha_{\mathrm{YM}})_{c,2} = 0.492 \pm 0.008$. For α_{YM} above this value the phase transition is always first order (for a sketch see figure 3.5 (c)).

3.3.4 Zero temperature solution and quantum critical point

In this section we consider the system exclusively at zero temperature. From the phase diagrams presented above we see that for large baryon compared to isospin chemical potential the system is in the normal state. Since the normal state is described by a Reissner-Nordström black hole, the zero temperature limit is an extremal Reissner-Nordström black hole. Zero temperature is given by fixing the isospin chemical potential,

$$\mu_{\mathrm{I}} = \frac{\sqrt{3r_{\mathrm{H}}^2 - \mu_{\mathrm{B}}^2 \alpha_{\mathrm{MW}}^2}}{\alpha_{\mathrm{YM}}} \,. \tag{3.49}$$

As usual this extremal black hole features an AdS_2 geometry in its near horizon region, i.e. in the IR. The full solution in the near-horizon region is given by

$$\mathrm{d}s^2 = -12\xi^2 \mathrm{d}t^2 + \frac{\mathrm{d}\xi^2}{12\xi^2} + r_{\mathrm{H}}^2 \mathrm{d}\vec{x}^2 \,,$$
$$\phi = \frac{2\sqrt{3r_{\mathrm{H}}^2 - \mu_{\mathrm{B}}^2 \alpha_{\mathrm{MW}}^2}}{\alpha_{\mathrm{YM}} r_{\mathrm{H}}} \xi \,, \quad \psi = \frac{2\mu_{\mathrm{B}}}{r_{\mathrm{H}}} \xi \,, \tag{3.50}$$

where $\xi = r - r_{\mathrm{H}}$. According to the AdS/CFT dictionary, the dual field theory contains a one-dimensional CFT in the IR. Let us now consider this theory as we decrease the baryon chemical potential. From our numerical solutions we expect a phase transition towards a superfluid phase with non-zero vev $\langle J_x^1 \rangle$. This phase transition should be triggered by an instability in the normal state. In order to obtain this instability we consider fluctuations of the gauge field $w(r)$ which is dual to the current J_x^1 about the extremal Reissner-Nordström background [133]. The equation of motion for this fluctuation is given by

$$w'' + \frac{2}{\xi} w' + \frac{3r_{\mathrm{H}}^2 - \mu_{\mathrm{B}}^2 \alpha_{\mathrm{MW}}^2}{36\alpha_{\mathrm{YM}}^2 r_{\mathrm{H}}^2 \xi^2} w = 0 \,, \tag{3.51}$$

where the prime denotes a derivative with respect to ξ. This equation is the equation of motion for a scalar field in AdS_2 with effective negative mass squared $m_{\mathrm{eff}}^2 = -\frac{3r_{\mathrm{H}}^2 - \mu_{\mathrm{B}}^2 \alpha_{\mathrm{MW}}^2}{36\alpha_{\mathrm{YM}}^2 r_{\mathrm{H}}^2}$. Thus according to the AdS/CFT dictionary, the IR dimension of the dual operator can be tuned by changing the baryon chemical potential. Hence, the fluctuation is stable until the mass is below the Breitenlohner-Freedman bound $m_{\mathrm{eff}}^2 = -1/4$.[5] In our case, the bound is given by

$$\frac{\sqrt{3r_{\mathrm{H}}^2 - \mu_{\mathrm{B}}^2 \alpha_{\mathrm{MW}}^2}}{6\alpha_{\mathrm{YM}} r_{\mathrm{H}}} \leq \frac{1}{2} \,. \tag{3.52}$$

From this equation we may determine the baryon chemical potential at which the bound is saturated,

$$\mu_{\mathrm{B}} = \frac{r_{\mathrm{H}} \sqrt{3 - 9\alpha_{\mathrm{YM}}^2}}{\alpha_{\mathrm{MW}}} \,. \tag{3.53}$$

---

[5]Note that at the boundary the geometry is AdS_5 where the Breitenlohner-Freedman bound is -4.

With equation (3.49), we may determine the ratio between the baryon and the isospin chemical potential at which the Breitenlohner-Freedman bound is saturated. This ratio determines the point at which the system becomes unstable,

$$\left(\frac{\mu_{\mathrm{B}}}{\mu_{\mathrm{I}}}\right)_c = \frac{\sqrt{1 - 3\alpha_{\mathrm{YM}}^2}}{\sqrt{3}\,\alpha_{\mathrm{MW}}}\,. \tag{3.54}$$

Thus the Reissner-Nordström black hole may be unstable if $\alpha_{\mathrm{YM}} < 1/\sqrt{3}$ and a quantum critical point may exist if in addition α_{MW} is non-zero. This confirms our intuition obtained from our numerical results that at a given ratio of the baryon to isospin chemical potential a phase transition to a superfluid phase occurs. Unfortunately this calculation only determines the value for the ratio of baryon to isospin chemical potential where the system becomes unstable and not the phase boundary in general. For a continuous phase transition the two values coincide while for a first order phase transition, the transition always occurs before the instability is reached. Thus only for $\alpha_{\mathrm{YM}} \leq (\alpha_{\mathrm{YM}})_{c,2}$ the phase boundary which is a quantum critical point and the critical value obtained here coincide. In [134] it is argued that the violation of the Breitenlohner-Freedman bound leads to a BKT-like transition.

Naively we may assume that the superfluid phase is non-degenerate at zero temperature and the entropy is zero. In the gravity dual this is translated to a zero horizon radius of the black hole. The solution with zero horizon radius differs from the zero temperature solutions described by the extremal limit of the AdS Reissner-Nordström black hole with finite horizon size. Similarly to [129, 135], we choose the following ansatz which is consistent with the numerical results near $r = 0$, namely

$$\phi \sim \phi_1(r)\,, \qquad \psi \sim \psi_1(r)\,, \qquad w \sim w_0 + \omega_1(r)\,, \qquad N \sim r^2 + N_1(r)\,,$$
$$m \sim m_1(r)\,, \qquad \sigma \sim \sigma_0 + \sigma_1(r)\,, \quad f \sim f_0 + f_1(r)\,, \tag{3.55}$$

such that all fields with index one go to zero at $r = 0$, e.g. $f_0 + f_1(r) \to f_0$ as $r \to 0$. Plugging the ansatz above in (3.33) and solving the equations of motion near the horizon $r = 0$, we obtain the following solutions in the asymptotic forms

$$\phi \sim \phi_0 \sqrt{\frac{\beta}{r}} e^{-\frac{\beta}{r}}\,, \qquad\qquad N \sim r^2 - \frac{\alpha_{\mathrm{YM}}^2 \beta^2 \phi_0^2}{3\sigma_0^2} \frac{e^{-\frac{2\beta}{r}}}{r^2}\,,$$

$$w \sim w_0 \left(1 - \frac{\phi_0^2}{4\sigma_0^2 \beta} \frac{e^{-\frac{2\beta}{r}}}{r}\right)\,, \qquad \psi = 0\,, \tag{3.56}$$

$$\sigma \sim \sigma_0 \left(1 + \frac{\alpha_{\mathrm{YM}}^2 \beta^2 \phi_0^2}{6\sigma_0^2} \frac{e^{-\frac{2\beta}{r}}}{r^4}\right)\,, \quad f \sim f_0 \left(1 - \frac{\alpha_{\mathrm{YM}}^2 \beta \phi_0^2}{12\sigma_0^2} \frac{e^{-\frac{2\beta}{r}}}{r^3}\right)\,,$$

with $\beta = f_0^2 w_0$. We can construct the full zero entropy solutions of the system by taking (3.56) as initial values near $r = 0$ and integrate (3.33) numerically to the boundary using the shooting method. The result from that will describe the gravity dual of the superfluid ground state of the theory.

It is important to notice that a zero entropy solution is only consistent with ψ being zero, i.e. no baryon chemical potential. Thus the domain walls we can construct from this asymptotics always have zero baryon chemical potential and coincide with the one found in [129]. At finite baryon chemical potential we expect a solution which interpolates between the domain wall solutions at zero baryon chemical potential and the extremal Reissner-Nordström solution in the normal phase. This solution should always contain a black hole with finite horizon radius and thus its entropy increases with the baryon chemical potential. By dimensional analysis we obtain $S \propto V \mu_{\mathrm{B}}^3$.

3.3.5 The semi-probe limit

In this section we study the EYM system taking just the back-reaction of the $\mathrm{U}(1)$ Maxwell field into account, i.e. $\alpha_{\mathrm{YM}} = 0$. We call this limit the semi-probe limit. From equation (3.54) we observe that there is the possibility of a quantum critical point at $\mu_{\mathrm{B}}/\mu_{\mathrm{I}} = 1/\sqrt{3}\,\alpha_{\mathrm{MW}}$ in this limit. In addition, the equations of motion (3.33) simplify significantly and we can obtain an analytical solution if we restrict ourselves to small baryon chemical potential μ_{B} and small condensate $\langle J_x^1 \rangle$. The equations of motion in the semi-probe limit read

$$
\begin{aligned}
m' &= \frac{\alpha_{\mathrm{MW}}^2 r^3 \psi'^2}{6}\,, & \psi'' &= -\frac{3}{r}\psi'\,, \\
w'' &= -\frac{w\phi^2}{N^2} - w'\left(\frac{1}{r} + \frac{N'}{N}\right)\,, & \phi'' &= \frac{w^2\phi}{r^2 N} - \phi'\left(\frac{3}{r}\right)\,,
\end{aligned}
\tag{3.57}
$$

since $\sigma = f = 1$ if the back-reaction of the $\mathrm{SU}(2)$ Yang-Mills field is neglected. The equation for m and ψ can be integrated directly,

$$
\begin{aligned}
m &= \frac{r_{\mathrm{H}}^4}{2} + \frac{\alpha_{\mathrm{MW}}^2 \mu_{\mathrm{B}}^2 r_{\mathrm{H}}^2}{3}\left(1 - \frac{r_{\mathrm{H}}^2}{r^2}\right)\,, \\
\psi &= \mu_{\mathrm{B}}\left(1 - \frac{r_{\mathrm{H}}^2}{r^2}\right)\,.
\end{aligned}
\tag{3.58}
$$

Thus we are left with the two equations of motion for the $\mathrm{SU}(2)$ gauge fields in the given Reissner-Nordström background. By solving these equations numerically we can map out the phase diagram for $\alpha_{\mathrm{YM}} = 0$ (see fig. 3.7). The phase diagram looks similar to the one where a small back-reaction of the $\mathrm{SU}(2)$ fields is included (see fig. 3.6).
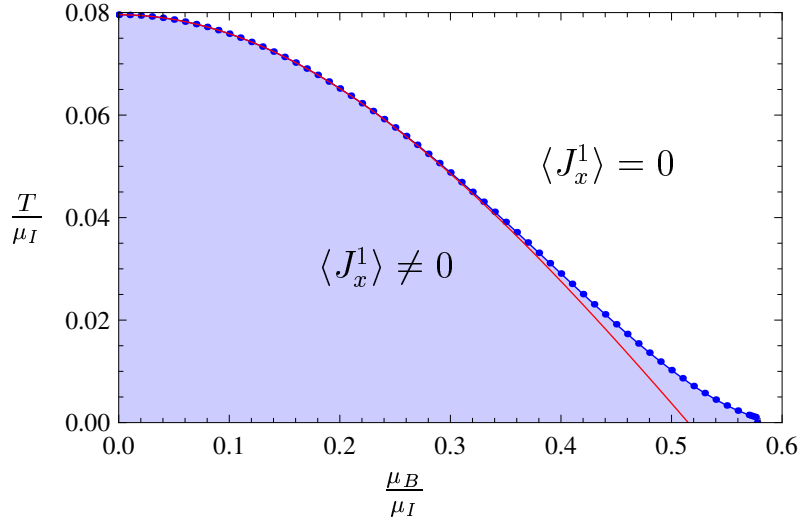
FIGURE 3.7: Phase diagram in the semi-probe limit: We compare the numerical data for the phase boundary (blue dots) with the analytic result (red line). We obtain a nice agreement for small baryon chemical potential where our approximation is valid.

The expansion In the limit of small μ_B and small $\langle J_x^1 \rangle$, we can solve the equations of motion for ϕ and w analytically. For the case $\mu_B = 0$, this has already been done in [136]. Similarly to [137], the solutions here are obtained as a double expansion in μ_B and $\langle J_x^1 \rangle$ which are chosen to be proportional to the expansion parameters δ and ϵ, respectively. More precisely, we choose $\delta \equiv \tilde{\mu}_B = \tilde{\psi}(\infty)$ and $\epsilon \equiv \tilde{w}_1^b \propto \langle J_x^1 \rangle$ from (3.46) where the tilde denotes dimensionless quantities which can be obtained by using (3.34) to set $R = r_H = 1$. We make the following ansatz for $\tilde{\phi}$ and $\tilde{w}$

$$
\begin{aligned}
\tilde{\phi}(r) = & \phi_{0,0}(r) + \delta^2 \, \phi_{2,0}(r) + \delta^4 \, \phi_{4,0}(r) + \mathcal{O}\left(\delta^6\right) \\
& + \epsilon^2 \left(\phi_{0,2}(r) + \delta^2 \, \phi_{2,2}(r) \right) + \mathcal{O}\left(\delta^4 \epsilon^2\right) \\
& + \epsilon^4 \, \phi_{0,4}(r) + \mathcal{O}\left(\delta^2 \epsilon^4\right) \\
& + \mathcal{O}\left(\epsilon^6\right) , \\
\tilde{w}(r) = & \epsilon \left(w_{0,1}(r) + \delta^2 \, w_{2,1}(r) + \delta^4 \, w_{4,1}(r) \right) + \mathcal{O}\left(\delta^6 \epsilon\right) \\
& + \epsilon^3 \left(w_{0,3}(r) + \delta^2 \, w_{2,3}(r) \right) + \mathcal{O}\left(\delta^4 \epsilon^3\right) \\
& + \epsilon^5 w_{0,5}(r) + \mathcal{O}\left(\delta^2 \epsilon^5\right) .
\end{aligned}
\tag{3.59}
$$

Inserting the ansatz (3.59) into (3.57), we can construct a solution order by order in δ and ϵ. The possible solutions are restricted by certain boundary conditions. At the horizon $r = 1$, we demand that $\tilde{\phi}$ vanishes while $\tilde{w}$ has to be regular. At the boundary, $\tilde{w}$ is fixed to the expectation value $\langle J_x^1 \rangle \propto \epsilon$ (3.46) while the isospin chemical potential $\tilde{\mu}_I$ associated to $\tilde{\phi}$ receives finite corrections in δ and ϵ.

The coefficient functions to lowest order,

$$\phi_{0,0}(r) = 4\left(1 - \frac{1}{r^2}\right),$$
$$w_{0,1}(r) = \frac{r^2}{(1+r^2)^2}$$

(3.60)

are already known from [138] while the coefficients in the pure ϵ expansion, that is with $\delta = 0$, were first computed in [136]. To order ϵ^4, they read

$$\phi_{0,2}(r) = \mu_{I0,2}\left(1 - \frac{1}{r^2}\right) + \frac{5 + 7r^2 - 9r^4 - 3r^6}{96r^2\left(1+r^2\right)^3},$$

$$w_{0,3}(r) = \frac{39 - 331r^2 - 819r^4 - 369r^6 + 156r^2(1+r^2)^3\ln(1+\frac{1}{r^2})}{20{,}160(1+r^2)^5},$$

$$\phi_{0,4}(r) = \mu_{I0,4}\left(1 - \frac{1}{r^2}\right) + \Phi_{0,4}(r),$$

$$\text{with } \mu_{I0,2} = \frac{71}{6{,}720} \quad \text{and} \quad \mu_{I0,4} = \frac{13\left(-4{,}015{,}679 + 5{,}147{,}520\ln(2)\right)}{75{,}866{,}112{,}000},$$

(3.61)

where $\Phi_{0,4}(r)$ is a complicated function of r which we do not write down explicitly here. The $\mu_{Im,n}$ are determined by the regular boundary condition of $\tilde{w}$ at the horizon $r = 1$ and describe corrections to the critical isospin chemical potential $\tilde{\mu}_{\mathrm{I}} = 4$ at $\delta^m\epsilon^n$ orders. The lowest order coefficient functions in the pure δ expansion read

$$\phi_{2,0}(r) = \mu_{I2,0}\left(1 - \frac{1}{r^2}\right), \quad \mu_{I2,0} = \frac{4}{9}\alpha_{\mathrm{MW}}^2\left(-17 + 24\ln(2)\right),$$

$$\phi_{4,0}(r) = \mu_{I4,0}\left(1 - \frac{1}{r^2}\right),$$

$$\mu_{I4,0} = \frac{2}{243}\alpha_{\mathrm{MW}}^2\Big[-5{,}495 + 192\ln(2)\left(61 + 12\ln(2)^2 - \ln(8)\right) + $$
$$+ 864\pi^2\ln(2) - 13{,}824\,\mathrm{Li}_3(1-i) - 13{,}824\,\mathrm{Li}_3(1+i) + 12\,\zeta(3)\Big].$$

(3.62)

For small baryon chemical potential $\tilde{\mu}_{\mathrm{B}} = \delta$, the critical isospin chemical potential for the phase transition will be corrected as

$$\tilde{\mu}_{\mathrm{I}}^c(\delta) = 4 + \mu_{I2,0}\delta^2 + \mu_{I4,0}\delta^4 + \mathcal{O}(\delta^6).$$

(3.63)

This determines the phase boundary between the superfluid and the normal phase. We compare this analytic result with our numerical results in fig. 3.7.

The lowest order coefficient functions in mixed orders read

$$\phi_{2,2}(r) = \mu_{I2,2}\left(1 - \frac{1}{r^2}\right) + \Phi_{2,2}(r)\,,$$

$$\mu_{I2,2} = \frac{(680{,}573 + 29{,}820\,\pi^2 - 404{,}232\ln(2) - 1{,}406{,}160\ln(2)^2)\,\alpha_{\mathrm{MW}}^2}{6{,}350{,}400}\,,$$

$$w_{2,1}(r) = \alpha_{\mathrm{MW}}^2\left(\frac{13 + r^2\,(7 + 6r^2 - 4\,\pi^2(1+r^2) + 24(1+r^2)\ln(2)^2)}{9(1+r^2)^3}\right.$$
$$+ \frac{4\,(3 - 20r^2 + 3r^4)\,\ln(r) - 48r^2\ln(r)^2 - 2\,(3+3r^4)\ln(1+r^2)}{9(1+r^2)^2}$$
$$- \frac{8r^2\,(-5 + \ln(64))\,\ln(1+r^2)}{9(1+r^2)^2}$$
$$\left.- \frac{8r^2\,\left(\mathrm{Li}_2(-r^2) + \mathrm{Li}_2(1-r^2) - 2\,\mathrm{Li}_2(\tfrac{1}{2}(1-r^2))\right)}{3(1+r^2)^2}\right)\,,$$

$$(3.64)$$

where $\Phi_{2,2}(r)$ is a complicated function of r which we do not display explicitly here.

The free energy Using the results from the last section, we compute the contribution to the free energy up to order $\delta^m\epsilon^n$ for $m + n \leqslant 4$ from the gauge field term in the on-shell action

$$S = -\frac{1}{4g_{\mathrm{YM}}^2}\int d^5x\sqrt{-g}F_{AB}^a F^{aAB}$$
$$= \frac{\beta\,\mathrm{Vol}_3 r_{\mathrm{H}}^4}{2g_{\mathrm{YM}}^2}\int_1^\infty dr\left(r^3(\partial_r\tilde\phi)^2 - r\tilde N(r)(\partial_r\tilde w)^2 + \frac{r}{\tilde N(r)}(\tilde\phi\tilde w)^2\right) \quad (3.65)$$
$$= \frac{\beta\,\mathrm{Vol}_3 r_{\mathrm{H}}^4}{2g_{\mathrm{YM}}^2}\left(r^3\tilde\phi\left(\partial_r\tilde\phi\right)|_{r\to\infty} - \int_1^\infty r\tilde N(r)\left(\partial_r\tilde w\right)^2\right)\,,$$

where Vol_3 is the spatial volume of the field theory and $\beta = 1/T$ is the inverse temperature. In the $\alpha_{\mathrm{YM}} \to 0$ limit, only $\psi(r)$ contributes to the back-reaction which is described by

$$\tilde N(r) = r^2 - \frac{1}{r^2} - \frac{2\,(r^2 - 1)}{3r^4}\alpha_{\mathrm{MW}}^2\delta^2\,, \qquad (3.66)$$

where the expansion parameter $\delta \equiv \tilde\mu_{\mathrm{B}}$ is chosen to be small.

For the background with vanishing condensate, i.e. $\omega(r) = 0$, and

$$\tilde\phi(r) = \frac{r^2 - 1}{r^2}\left(4 + \mu_{I0,2}\epsilon^2 + \mu_{I0,4}\epsilon^4 + \mu_{I2,0}\delta^2 + \mu_{I4,0}\delta^4 + \mu_{I2,2}\delta^2\epsilon^2\right)\,,$$

$$(3.67)$$

the on-shell action is

$$
\begin{aligned}
S_{\text{vac}} = \frac{\beta \, \text{Vol}_3 r_{\text{H}}^4}{g_{\text{YM}}^2} \Big[& 16 + 8\mu_{I0,2}\epsilon^2 + \left(\mu_{I0,2}^2 + 8\mu_{I0,4} \right) \epsilon^4 + 8\mu_{I2,0}\delta^2 \\
& + \left(\mu_{I2,0}^2 + 8\mu_{I4,0} \right) \delta^4 + 2 \left(\mu_{I0,2}\mu_{I2,0} + 4\mu_{I2,2} \right) \delta^2\epsilon^2 \\
& + \mathcal{O}\left(\delta^p \epsilon^q \right) \Big],
\end{aligned}
$$

(3.68)

for $p + q = 6$.

For the background where $w \neq 0$ has condensed, the on-shell action reads

$$
\begin{aligned}
S_{\text{sf}} = \frac{\beta \, \text{Vol}_3 r_{\text{H}}^4}{g_{\text{YM}}^2} \Big[& 16 + 8\mu_{I0,2}\epsilon^2 + \left(\mu_{I0,2}^2 + 8\mu_{I0,4} + \frac{71}{215{,}040} \right) \epsilon^4 + 8\mu_{I2,0}\delta^2 \\
& + \left(\mu_{I2,0}^2 + 8\mu_{I4,0} \right) \delta^4 + 2 \left(\mu_{I0,2}\mu_{I2,0} + 4\mu_{I2,2} \right) \delta^2\epsilon^2 \\
& + \mathcal{O}\left(\delta^p \epsilon^q \right) \Big].
\end{aligned}
$$

(3.69)

The difference in the values of the two on-shell actions is

$$
\beta \Delta P = S_{\text{vac}} - S_{\text{sf}} = \frac{\beta \text{Vol}_3 r_{\text{H}}^4}{4 g_{\text{YM}}^2} \left(-\frac{71}{53{,}760} \epsilon^4 + \mathcal{O}\left(\delta^p \epsilon^q \right) \right).
$$

(3.70)

This result is known from [136] which remains robust in our back-reacted background. The free energy in the grand canonical ensemble is minus the value of the on-shell action times the temperature, hence the quantity ΔP determines the difference in the free energy between the normal and superfluid phase. In this case, the free energy of the superfluid state is the smaller one because $\Delta P < 0$, and this implies the stability of the superfluid phase.

For small ϵ and small δ, we have $\epsilon^4 \sim (\tilde{\mu}_{\text{I}} - \tilde{\mu}_{\text{I}}^c(\delta))^2$. Using (III) in (3.34) to restore dimensions by taking $\lambda = r_{\text{H}} \sim T$ (3.38), the dimensionless $\tilde{\mu}_{\text{I}}$ will be replaced by $\frac{\mu_{\text{I}}}{r_{\text{H}}} \sim \frac{\mu_{\text{I}}}{T}$ and thus we have $\epsilon^2 \sim (T_c(\delta) - T)$. The cancelation of the term proportional to $\delta^2\epsilon^2$ in the free energy difference suggests that the phase transition stays second order with mean field exponents as we increase the baryon chemical potential which coincides with our numerical result.

3.4 QPT in D3/D7 model with finite baryon and isospin chemical potential

In this section we use the top-down approach to construct a gravity model for holographic p-wave superfluidity. This model might be seen as the string theory realization of the model studied in section 3.3, since both models have the same global symmetry. In particular, the $\text{U}(2) = \text{U}(1)_{\text{B}} \times \text{SU}(2)_{\text{I}}$ is realized

by embedding a probe of two coincident D7 flavor branes in the AdS black hole geometry. In this model we can also observe quantum phase transitions from a normal conducting to a superconducting phase. These transitions occur at a critical value of the ratio between the baryon and the isospin chemical potential. There are similarities in the phase diagram of the model discussed in this section and the one in section 3.3, however, there are also interesting differences. The main results of section 3.3 and 3.4 are summarized in the last subsection of 3.4 where comparisons of our phase diagrams to those obtained from QCD [49, 50] are made. The main content presented in this section stems from my own work in collaboration with Johanna Erdmenger, Patrick Kerner and Viviane Grass [3].

3.4.1 Background and brane configuration

In this section we investigate a string theory realization of the model studied above. We consider asymptotically $\mathrm{AdS}_5 \times \mathrm{S}^5$ spacetime which is the near-horizon geometry of a stack of D3-branes. The $\mathrm{AdS}_5 \times \mathrm{S}^5$ geometry is holographically dual to the $\mathcal{N} = 4$ Super Yang-Mills theory with gauge group $\mathrm{SU}(N_\mathrm{c})$. The dual description of a finite temperature field theory is an AdS black hole. We use the coordinates of [105] to write the AdS black hole background in Minkowski signature as

$$ds^2 = \frac{\varrho^2}{2R^2} \left(-\frac{f^2}{\tilde{f}} \mathrm{d}t^2 + \tilde{f} \mathrm{d}\vec{x}^2 \right) + \left(\frac{R}{\varrho} \right)^2 \left(\mathrm{d}\varrho^2 + \varrho^2 \mathrm{d}\Omega_5^2 \right) , \qquad (3.71)$$

with $\mathrm{d}\Omega_5^2$ the metric of the unit 5-sphere and

$$f(\varrho) = 1 - \frac{\varrho_H^4}{\varrho^4}, \quad \tilde{f}(\varrho) = 1 + \frac{\varrho_H^4}{\varrho^4} , \qquad (3.72)$$

where R is the AdS radius, with

$$R^4 = 4\pi g_s N_\mathrm{c} \, \alpha'^2 = 2\lambda \, \alpha'^2 . \qquad (3.73)$$

The AdS balck hole metric (2.106) can be recovered from the metric above by a coordinate transformation $\varrho^2 = r^2 + \sqrt{r^4 - r_\mathrm{H}^4}$ and the identification $r_\mathrm{H} = \varrho_\mathrm{H}$. The temperature of the black hole given by (3.71) may be determined by demanding regularity of the Euclidean section. It is given by

$$T = \frac{\varrho_H}{\pi R^2} . \qquad (3.74)$$

In the following we may use the dimensionless coordinate $\rho = \varrho/\varrho_H$, which covers the range from the event horizon at $\rho = 1$ to the boundary of the AdS space at $\rho \to \infty$.

To include fundamental matter, we embed N_f coinciding D7-branes into the ten-dimensional spacetime. These D7-branes host flavor gauge fields A_μ

with gauge group $U(N_f)$. This gauge field plays the same role as the gauge field in the Einstein-Yang-Mills systems. To write down the DBI action for the D7-branes, we introduce spherical coordinates $\{r, \Omega_3\}$ in the (4567)-directions and polar coordinates $\{L, \phi\}$ in the (89)-directions [105]. The angle between these two spaces is denoted by θ ($0 \leq \theta \leq \pi/2$). The six-dimensional space in the (456789)-directions is given by

$$
\begin{aligned}
\mathrm{d}\varrho^2 + \varrho^2 \mathrm{d}\Omega_5^2 &= \mathrm{d}r^2 + r^2 \mathrm{d}\Omega_3^2 + \mathrm{d}L^2 + L^2 \mathrm{d}\phi^2 \\
&= \mathrm{d}\varrho^2 + \varrho^2 \left(\mathrm{d}\theta^2 + \cos^2\theta \mathrm{d}\phi^2 + \sin^2\theta \mathrm{d}\Omega_3^2 \right) ,
\end{aligned}
\tag{3.75}
$$

where $r = \varrho \sin\theta$, $\varrho^2 = r^2 + L^2$ and $L = \varrho \cos\theta$.

Due to the $SO(4)$ rotational symmetry in the (4567)-directions, the embedding of the D7-branes only depends on the radial coordinate ρ. Defining $\chi = \cos\theta$, we parametrize the embedding by $\chi = \chi(\rho)$ and choose $\phi = 0$ using the $SO(2)$ symmetry in the (89)-direction. The induced metric G on the D7-brane probes is then

$$
ds^2 = \frac{\varrho^2}{2R^2} \left(-\frac{f^2}{\tilde{f}} \mathrm{d}t^2 + \tilde{f} \mathrm{d}\vec{x}^2 \right) + \frac{R^2}{\varrho^2} \frac{F_\chi + \varrho^2 (\partial_\varrho \chi)^2}{F_\chi} \mathrm{d}\varrho^2 + R^2 F_\chi \mathrm{d}\Omega_3^2 , \tag{3.76}
$$

where $F_\chi = (1 - \chi^2)$. The square root of the determinant of G is given by

$$
\sqrt{-G} = \frac{\sqrt{h_3}}{4} \varrho^3 f \tilde{f} F_\chi \sqrt{F_\chi + \varrho^2 (\partial_\varrho \chi)^2} , \tag{3.77}
$$

where h_3 is the determinant of the 3-sphere metric.

As in [123] we split the $U(2)$ gauge symmetry on the D7-brane into $U(1)_B \times SU(2)_I$ where the $U(1)_B$ describes the baryon charges and $SU(2)_I$ isospin charges. As before we may introduce an isospin chemical potential μ_I as well as a baryon chemical potential μ_B by introducing non-vanishing time component of the non-Abelian background fields. Here we choose the generators of the $SU(2)_I$ gauge group to be the Pauli matrices τ^i and the generator of the $U(1)_B$ gauge group to be $\tau^0 = \mathbb{1}_{2\times 2}$. This non-zero time-components of the gauge fields $A_t^0 = \mathcal{A}_t$ and A_t^3 break the $U(2)$ gauge symmetry down to $U(1)_3$ generated by the third Pauli matrix τ^3. In order to study the transition to the superfluid state we additionally allow the gauge field A_x^1 to be non-zero. To obtain an isotropic and time-independent configuration in the field theory, the gauge field A_x^1 only depends on ρ. This leads to a similar ansatz for the gauge field as in the Einstein-Yang-Mills theory,

$$
A = \left(\mathcal{A}_t(\varrho)\tau^0 + A_t^3(\varrho)\tau^3 \right) \mathrm{d}t + A_x^1(\varrho)\tau^1 \mathrm{d}x . \tag{3.78}
$$

With this ansatz, the field strength tensor on the branes has the following

non-zero components,

$$
\begin{aligned}
F^1_{\varrho x} &= -F^1_{x\varrho} = \partial_\varrho A^1_x \,, \\
F^2_{tx} &= -F^2_{xt} = \frac{\gamma}{\sqrt{\lambda}} A^3_t A^1_x \,, \\
F^3_{\varrho t} &= -F^3_{t\varrho} = \partial_\varrho A^3_t \,, \\
F^0_{\varrho t} &= -F^0_{t\varrho} = \partial_\varrho \mathcal{A}_t = \mathcal{F}_{\varrho t} = -\mathcal{F}_{t\varrho} \,.
\end{aligned}
\tag{3.79}
$$

3.4.2 Non-abelian DBI action and equations of motion

The action for embedding a probe of two flavor D7-branes in the AdS black hole background is given by the *non-Abelian* Dirac-Born-Infeld action which is a generalization of (2.115). For the case of $\mathcal{N}_\mathrm{f} = 2$ coincident D7-branes, the non-Abelian DBI action reads [121]

$$
S_{\mathrm{D7}} = -\tau_7 \,\mathrm{sTr} \int \mathrm{d}^8\xi \sqrt{\det Q} \left[\det\!\Big(\mathrm{P_{ab}}\big[\mathrm{E}_{\mu\nu} + \mathrm{E}_{\mu i}(\mathrm{Q}^{-1}-\delta)^{\mathrm{ij}} \mathrm{E}_{j\nu} \big] + 2\pi\alpha' \mathrm{F_{ab}} \Big) \right]^{\frac{1}{2}}
\tag{3.80}
$$

with sTr denoting the supersymmetric trace, $Q^i{}_j$ is defined as

$$
Q^i{}_j = \delta^i{}_j + i2\pi\alpha'[\Phi^i, \Phi^k] E_{kj}
\tag{3.81}
$$

and P_{ab} the pullback to the Dp-brane, where for a Dp-brane in d dimensions we have $\mu,\ \nu = 0,\dots,(d-1)$, $a,\ b = 0,\dots,p$, $i,\ j = (p+1),\dots,(d-1)$, $E_{\mu\nu} = g_{\mu\nu} + B_{\mu\nu}$. In our case we set $p = 7$, $d = 10$, $B \equiv 0$. The equations of motion arising from (3.80) determine the profile of the D7-brane probes and of the gauge fields on these branes, i.e. shape of the brane embeddings as well as the configuration of the gauge fields A on these branes.

Non-abelian DBI action In general it is not known how to solve the full non-abelian DBI action. The problem is that there is no general description how to deal with the supersymmetric trace (sTr) when F_{ab} is non-abelian. For instance for the case of $\mathrm{SU}(2)$, we have to deal with product of Pauli matrices occurring in the square root. The precise form of the non-abelian DBI action is known exactly only up to F^4 [139]. There are two possibilities how to deal with the non-abelian action, namely expanding the action to fourth order in the field strength F or using a prescription called symmetrized trace prescription [140] where we symmetrize the product of the generators of the gauge group first before taking the usual trace.

In [18], both of the above descriptions have been applied for the system of two coincident D7 flavor branes at finite isospin chemical potential in AdS black hole space. Expanding the non-abelian DBI action to fourth oder in the

field strength F, the DBI action takes the schematic form [18]

$$S_{\text{DBI}} = -\tau_7 \mathcal{N}_{\text{f}} \int d^8\xi \sqrt{-G} \left[1 + \mathcal{T}_2 \left(F^2 \right) + \mathcal{T}_4 \left(F^4 \right) + \mathcal{O} \left(F^6 \right) \right] , \quad (3.82)$$

where following non-vanishing results for the symmetrized traces are used

$$\text{Str} \left[\left(\tau^i \right)^2 \right] = \mathcal{N}_{\text{f}} , \qquad \text{Str} \left[\tau^i \tau^j \right] = \delta^{ij} \mathcal{N}_{\text{f}} ,$$

$$\text{Str} \left[\left(\tau^i \right)^4 \right] = \mathcal{N}_{\text{f}} , \qquad \text{Str} \left[\left(\tau^i \right)^2 \left(\tau^j \right)^2 \right] = \frac{\mathcal{N}_{\text{f}}}{3} , \qquad i \neq j . \quad (3.83)$$

Up to second order in F, the action (3.82) contains terms which also occur in the usual $\text{SU}(2)$ Yang-Mills action. Terms at fourth order in F can be found in the appendix of [18]. We do not use this prescription in this thesis, but another description called the *adapted symmetrized trace prescription* which is a simplification of the symmetrized trace prescription [140] and allows to solve the non-abelian action to all order of F. Here, we modified the symmetrized trace prescription by omitting the commutators of the generators τ^i and then setting $(\tau^i)^2 = \mathbb{1}_{2 \times 2}$. This prescription makes the calculation of the full DBI action feasible. One prize to pay for the adapted symmetrized trace prescription is that we have to 'assume'

$$\text{Str} \left[\left(\tau^{i_1} \right)^2 \right] = \text{Str} \left[\left(\tau^{i_1} \right)^2 \left(\tau^{i_2} \right)^2 \right] = \text{Str} \left[\left(\tau^{i_1} \right)^2 \cdots \left(\tau^{i_n} \right)^2 \right] = N_{\text{f}} , \quad (3.84)$$

which modifies our results. This prescription has been used in [17, 18] for the setup of two coincident D7-branes at finite isospin chemical potential embedded in AdS black hole. The authors of [18] find that evaluating the non-abelian DBI action using the adapted symmetrized trace prescription or the expansion to fourth order yields results which are phenomenologically equivalent, i.e. the structure of the phase transition from the normal to superconducting phase does not depend on the prescription used. In the following we will apply the adapted symmetrized trace prescription for our setup (3.78) which generalizes the result in [17] by including a finite baryon chemical potential.

Adapted symmetrized trace prescription for non-abelian DBI action   As described in [123] the non-abelian action (3.80) can be significantly simplified by using the spatial and gauge symmetries ansatz (3.78) present in the setup. The action becomes

$$S_{\text{DBI}} = -\tau_7 \int d^8\xi \, \text{sTr} \, \sqrt{|\det(G + 2\pi\alpha' F)|}$$

$$= -\tau_7 \int d^8\xi \, \sqrt{-G} \, \text{sTr} \left[1 + G^{tt} G^{\varrho\varrho} \left(\left(F^3_{\varrho t} \right)^2 \left(\tau^3 \right)^2 + 2 F^3_{\varrho t} \mathcal{F}_{\varrho t} \tau^3 \tau^0 \right) \right.$$

$$\left. + G^{tt} G^{\varrho\varrho} \left(\mathcal{F}_{\varrho t} \right)^2 \left(\tau^0 \right)^2 + G^{xx} G^{\varrho\varrho} \left(F^1_{\varrho x} \right)^2 \left(\tau^1 \right)^2 + G^{tt} G^{xx} \left(F^2_{tx} \right)^2 \left(\tau^2 \right)^2 \right]^{\frac{1}{2}} ,$$

$$ \tag{3.85} $$

where in the second line the determinant is calculated.

Due to the symmetric trace, all commutators between the matrices τ^i vanish (3.83). It is known that the symmetrized trace prescription in the DBI action is only valid up to fourth order in α' [140, 141]. However the corrections to the higher order terms are suppressed by N_{f}^{-1} [142] (see also [143]). As in [17, 18] we used two approaches to evaluate a non-Abelian DBI action similar to (3.85). Using adapted symmetrized trace prescription, i.e. modifying the symmetrized trace prescription [140] by omitting the commutators of the generators τ^i and then setting $(\tau^i)^2 = \mathbb{1}_{2\times2}$, the action becomes

$$ S_{\mathrm{DBI}} = -\frac{\tau_7}{4} \int \mathrm{d}^8\xi \; \varrho^3 f\tilde{f} F_\chi \left(\Upsilon_1(\rho, \chi, \tilde{A}) + \Upsilon_2(\rho, \chi, \tilde{A}) \right) , \tag{3.86} $$

with $F_\chi = (1 - \chi^2)$ and

$$ \Upsilon_i(\rho, \chi, \tilde{A}) = \left[F_\chi + \rho^2(\partial_\rho\chi)^2 - \frac{2\tilde{f}}{f^2} F_\chi \left(\partial_\rho \tilde{X}_i \right)^2 + \frac{2}{\tilde{f}} F_\chi \left(\partial_\rho \tilde{A}_x^1 \right)^2 \right. $$
$$ \left. - \frac{\gamma^2}{2\pi^2\rho^4 f^2} (F_\chi + \rho^2(\partial_\rho\chi)^2) \left((\tilde{X}_1 - \tilde{X}_2)\tilde{A}_x^1 \right)^2 \right]^{\frac{1}{2}} , \tag{3.87} $$

where the dimensionless quantities $\rho = \varrho/\varrho_H$ and $\tilde{A} = (2\pi\alpha')A/\varrho_H$ are used. The fields $X_1 = \mathcal{A}_t + A_t^3$ and $X_2 = \mathcal{A}_t - A_t^3$ are the gauge fields on the i-th brane. In [123] it is shown that the non-Abelian DBI action with $A_x^1 = 0$ decouples into two Abelian DBI actions in terms of these new gauge fields X_i. To obtain first order equations of motion for the gauge fields which are easier to solve numerically, we perform a Legendre transformation. Similarly to [105, 123] we calculate the electric displacement p_i and the magnetizing field p_x^1 which are given by the conjugate momenta of the gauge fields X_i and A_x^1,

$$ p_i = \frac{\delta S_{\mathrm{DBI}}}{\delta(\partial_\varrho X_i)}, \qquad p_x^1 = \frac{\delta S_{\mathrm{DBI}}}{\delta(\partial_\varrho A_x^1)} . \tag{3.88} $$

In contrast to [105, 122, 123, 144], the conjugate momenta are not constant any more but depend on the radial coordinate ϱ due to the non-Abelian term $A_t^3 A_x^1$ in the DBI action as in [17, 18]. For the dimensionless momenta $\tilde{p}_i$ and $\tilde{p}_x^1$ defined as

$$ \tilde{p} = \frac{p}{2\pi\alpha'\tau_7\varrho_H^3} , \tag{3.89} $$

we get

$$
\tilde{p}_i = \frac{\rho^3 \tilde{f}^2 F_\chi^2 \partial_\rho \tilde{X}_i}{2 f \Upsilon_i(\rho, \chi, \tilde{A})} \, ,
$$

$$
\tilde{p}_x^1 = -\frac{\rho^3 f F_\chi^2 \partial_\rho \tilde{A}_x^1}{2} \left(\frac{1}{\Upsilon_1(\rho, \chi, \tilde{A})} + \frac{1}{\Upsilon_2(\rho, \chi, \tilde{A})} \right) .
$$

(3.90)

Finally, the Legendre-transformed action is given by

$$
\begin{aligned}
\tilde{S}_{\mathrm{DBI}} &= S_{\mathrm{DBI}} - \int \mathrm{d}^8\xi \left[(\partial_\varrho X_i) \frac{\delta S_{\mathrm{DBI}}}{\delta (\partial_\varrho X_i)} + (\partial_\varrho A_x^1) \frac{\delta S_{\mathrm{DBI}}}{\delta (\partial_\varrho A_x^1)} \right] \\
&= -\frac{\tau_7}{4} \int \mathrm{d}^8\xi \, \varrho^3 f \tilde{f} F_\chi \sqrt{F_\chi + \rho^2 (\partial_\rho \chi)^2} \, V(\rho, \chi, \tilde{A}, \tilde{p}) \, ,
\end{aligned}
$$

(3.91)

with

$$
\begin{aligned}
V(\rho, \chi, \tilde{A}, \tilde{p}) &= \left(1 - \frac{\gamma^2}{2\pi^2 \rho^4 f^2} \left((\tilde{X}_1 - \tilde{X}_2) \tilde{A}_x^1 \right)^2 \right)^{\frac{1}{2}} \\
&\quad \times \left[\left(\sqrt{1 + \frac{8(\tilde{p}_1)^2}{\rho^6 \tilde{f}^3 F_\chi^3}} + \sqrt{1 + \frac{8(\tilde{p}_2)^2}{\rho^6 \tilde{f}^3 F_\chi^3}} \right)^2 - \frac{8(\tilde{p}_x^1)^2}{\rho^6 \tilde{f} f^2 F_\chi^3} \right]^{\frac{1}{2}} .
\end{aligned}
$$

(3.92)

This action agrees with the one for finite baryon and isospin chemical potential (see [123]) after $\tilde{p}_x^1 \to 0$ and with the one for the superconducting state at pure isospin chemical potential (see [17]) after $\tilde{p}_1 \to -\tilde{p}_2$ and $\tilde{p}_x^1 \to N_{\mathrm{f}} \tilde{p}_x^1$. The change in $\tilde{p}_x^1$ has to be done such that the definitions agree in both cases.

Then the first order equations of motion for the gauge fields and their conjugate momenta are

$$
\begin{aligned}
\partial_\rho \tilde{X}_i &= \frac{2 f \sqrt{F_\chi + \rho^2 (\partial_\rho \chi)^2}}{\rho^3 \tilde{f}^2 F_\chi^2} \tilde{p}_i W(\rho, \chi, \tilde{A}, \tilde{p}) U_i(\rho, \chi, \tilde{A}, \tilde{p}) \, , \\
\partial_\rho \tilde{A}_x^1 &= -\frac{2 \sqrt{F_\chi + \rho^2 (\partial_\rho \chi)^2}}{\rho^3 f F_\chi^2} \tilde{p}_x^1 W(\rho, \chi, \tilde{A}, \tilde{p}) \, , \\
\partial_\rho \tilde{p}_{1/2} &= \pm \frac{\tilde{f} F_\chi \sqrt{F_\chi + \rho^2 (\partial_\rho \chi)^2} \gamma^2}{8\pi^2 \rho f W(\rho, \chi, \tilde{A}, \tilde{p})} \left(\tilde{A}_x^1 \right)^2 (\tilde{X}_1 - \tilde{X}_2) \, , \\
\partial_\rho \tilde{p}_x^1 &= \frac{\tilde{f} F_\chi \sqrt{F_\chi + \rho^2 (\partial_\rho \chi)^2} \gamma^2}{8\pi^2 \rho f W(\rho, \chi, \tilde{A}, \tilde{p})} \left(\tilde{X}_1 - \tilde{X}_2 \right)^2 \tilde{A}_x^1 \, ,
\end{aligned}
$$

(3.93)

with

$$
U_i(\rho, \chi, \tilde{A}, \tilde{p}) = \frac{\sqrt{1 + \frac{8(\tilde{p}_1)^2}{\rho^6 \tilde{f}^3 F_\chi^3}} + \sqrt{1 + \frac{8(\tilde{p}_2)^2}{\rho^6 \tilde{f}^3 F_\chi^3}}}{\sqrt{1 + \frac{8(\tilde{p}_i)^2}{\rho^6 \tilde{f}^3 F_\chi^3}}} ,
$$

$$
W(\rho, \chi, \tilde{A}, \tilde{p}) = \sqrt{\frac{1 - \frac{\gamma^2}{2\pi^2 \rho^4 f^2}\left((\tilde{X}_1 - \tilde{X}_2)\tilde{A}_x^1\right)^2}{\left(\sqrt{1 + \frac{8(\tilde{p}_1)^2}{\rho^6 \tilde{f}^3 F_\chi^3}} + \sqrt{1 + \frac{8(\tilde{p}_2)^2}{\rho^6 \tilde{f}^3 F_\chi^3}}\right)^2 - \frac{8(\tilde{p}_x^1)^2}{\rho^6 \tilde{f} f^2 F_\chi^3}}} .
$$

$$(3.94)$$

For the embedding function χ we get the second order equation of motion

$$
\partial_\rho \left[\frac{\rho^5 f \tilde{f} F_\chi (\partial_\rho \chi) V}{\sqrt{F_\chi + \rho^2 (\partial_\rho \chi)^2}} \right] = -\frac{\rho^3 f \tilde{f} \chi}{\sqrt{F_\chi + \rho^2 (\partial_\rho \chi)^2}} \Bigg\{ \left[3F_\chi + 2\rho^2 (\partial_\rho \chi)^2\right] V
$$
$$
- \frac{24\left(F_\chi + \rho^2 (\partial_\rho \chi)^2\right)}{\rho^6 \tilde{f}^3 F_\chi^3} W \left[(\tilde{p}_1)^2 U_1 + (\tilde{p}_2)^2 U_2 - \frac{\tilde{f}^2}{f^2}(\tilde{p}_x^1)^2 \right] \Bigg\} .
$$

$$(3.95)$$

We solve the equations of motion numerically by integrating them from the horizon at $\rho = 1$ to the boundary $\rho = \infty$. The initial conditions may be determined by the asymptotic expansion of the gravity fields near the horizon

$$
\tilde{X}_i = \frac{b_i}{(1 - \chi_0^2)^{\frac{3}{2}} B_i}(\rho - 1)^2 + \mathcal{O}\left((\rho - 1)^3\right) ,
$$
$$
\tilde{A}_x^1 = a \qquad\qquad\qquad + \mathcal{O}\left((\rho - 1)^3\right) ,
$$
$$
\tilde{p}_{1/2} = b_{1/2} \pm \frac{\gamma^2 a^2}{32\pi^2}\left(\frac{b_1}{B_1} - \frac{b_2}{B_2}\right)(B_1 + B_2)(\rho - 1)^2 + \mathcal{O}\left((\rho - 1)^3\right) ,
$$
$$
\tilde{p}_x^1 = \qquad\qquad\qquad + \mathcal{O}\left((\rho - 1)^3\right) ,
$$
$$
\chi = \chi_0 \qquad\qquad -\frac{3\chi_0}{4B_1 B_2}(\rho - 1)^2 + \mathcal{O}\left((\rho - 1)^3\right) ,
$$

$$(3.96)$$

with

$$
B_i = \sqrt{1 + \frac{b_i^2}{(1 - \chi_0^2)^3}} .
$$

$$(3.97)$$

The terms in the asymptotic expansions are arranged according to their order in $(\rho - 1)$. There are four independent parameters $\{a, b_1, b_2, \chi_0\}$ which have to be determined. In order to obtain the field theory quantities we determine

the asymptotic expansion of the gravity fields near the AdS boundary

$$
\begin{aligned}
\tilde{X}_i &= \tilde{\mu}_i & -\frac{\tilde{d}_i}{\rho^2} && +\mathcal{O}\left(\rho^{-4}\right)\,, \\[4pt]
\tilde{A}_x^1 &= & +\frac{\tilde{d}_x^1}{2\rho^2} && +\mathcal{O}\left(\rho^{-4}\right)\,, \\[4pt]
\tilde{p}_i &= \tilde{d}_i & && +\mathcal{O}\left(\rho^{-4}\right)\,, \\[4pt]
\tilde{p}_x^1 &= \tilde{d}_x^1 & -\frac{\gamma^2 \tilde{d}_x^1 (\tilde{\mu}_1 - \tilde{\mu}_2)^2}{8\pi^2\rho^2} && +\mathcal{O}\left(\rho^{-4}\right)\,, \\[4pt]
\chi &= & \frac{m}{\rho} && +\frac{c}{\rho^3} + \mathcal{O}\left(\rho^{-4}\right)\,.
\end{aligned}
\tag{3.98}
$$

Note that the factor of two in $\tilde{A}_x^1$ is consistent with the earlier definitions in [18] since here we have a different definition of the conjugate momenta (factor N_f). In this asymptotic expansion we find seven independent parameters $\{\tilde{\mu}_i, \tilde{d}_i, \tilde{d}_x^1, m, c\}$. Using the transformation of the gauge field from $\tilde{X}_i$ to $\tilde{\mathcal{A}}_t$ and $\tilde{A}_t^3$, the independent parameters of the gauge fields X_i, $\{\tilde{\mu}_i, \tilde{d}_i\}$, may be translated into parameters of the asymptotic expansion of $\tilde{\mathcal{A}}_t$ and $\tilde{A}_t^3$,

$$
\begin{aligned}
\tilde{\mu}_\mathrm{B} &= \tilde{\mu}_t^0 = \frac{1}{2}(\tilde{\mu}_1 + \tilde{\mu}_2) & \tilde{d}_\mathrm{B} &= \tilde{d}_t^0 = \tilde{d}_1 + \tilde{d}_2\,, \\[4pt]
\tilde{\mu}_\mathrm{I} &= \tilde{\mu}_t^3 = \frac{1}{2}(\tilde{\mu}_1 - \tilde{\mu}_2) & \tilde{d}_\mathrm{I} &= \tilde{d}_t^3 = \tilde{d}_1 - \tilde{d}_2\,.
\end{aligned}
\tag{3.99}
$$

These parameters may be translated into field theory quantities according to the AdS/CFT dictionary (for details see [105]): μ_B is the baryon chemical potential, μ_I the isospin chemical potential,

$$
\tilde{\mu}_\mathrm{B} = \sqrt{\frac{2}{\lambda}}\frac{\mu_\mathrm{B}}{T}\,, \quad \tilde{\mu}_\mathrm{I} = \sqrt{\frac{2}{\lambda}}\frac{\mu_\mathrm{I}}{T}\,,
\tag{3.100}
$$

the parameters $\tilde{d}$ are related to the vev of the flavor current J by

$$
\tilde{d}_\mathrm{B} = \tilde{d}_t^0 = \frac{2^{\frac{5}{2}}\langle \mathcal{J}_t \rangle}{N_\mathrm{c}\sqrt{\lambda}T^3}\,, \quad \tilde{d}_\mathrm{I} = \tilde{d}_t^3 = \frac{2^{\frac{5}{2}}\langle J_t^3 \rangle}{N_\mathrm{c}\sqrt{\lambda}T^3}\,, \quad \tilde{d}_x^1 = \frac{2^{\frac{5}{2}}\langle J_x^1 \rangle}{N_\mathrm{c}\sqrt{\lambda}T^3}\,,
\tag{3.101}
$$

and m and c to the bare quark mass M_q and the quark condensate $\langle \bar{\psi}\psi \rangle$,

$$
m = \frac{2M_q}{\sqrt{\lambda}T}\,, \quad c = -\frac{8\langle \bar{\psi}\psi \rangle}{\sqrt{\lambda}N_\mathrm{f}N_\mathrm{c}T^3}\,,
\tag{3.102}
$$

respectively. There are three independent physical parameters, e.g. m, μ_B and μ_I in the grand canonical ensemble. The asymptotic expansion close to the horizon has four independent solutions. These parameters may be fixed by choosing the three independent physical parameters, i.e. the state in the field theory and by the constraint that $\tilde{A}_x^1$ goes to zero at the boundary, i.e. the $\mathrm{U}(1)_3$ symmetry is spontaneously broken. We use a standard shooting method to determine the parameters at the horizon.

3.4.3 Thermodynamics and phase diagram

In this section we study the contribution of the D7-branes to the thermodynamics. According to the AdS/CFT dictionary the partition function Z of the boundary field theory is given in terms of the Euclidean on-shell supergravity action $I_{\text{on-shell}}$,

$$Z = e^{-I_{\text{on-shell}}} . \tag{3.103}$$

Thus the thermodynamic potential, i.e. the grand potential in the grand canonical ensemble, is proportional to the Euclidean on-shell action

$$\Omega = -T \ln Z = T I_{\text{on-shell}} . \tag{3.104}$$

To calculate the contribution of the D7-branes to the grand potential, we have to determine the Euclidean version of the DBI-action (3.86) on-shell. For this purpose, we first perform a Wick rotation in the time direction. Next we renormalize the action by adding appropriate counterterms I_{ct} (see [106] for a review and [107] for probe D-branes). In our case the counterterms are the same as in [105, 123, 145],

$$I_{\text{ct}} = -\frac{\lambda N_{\text{c}} N_{\text{f}} V_3 T^3}{128} \left[\left(\rho_{\text{max}}^2 - m^2 \right)^2 - 4mc \right] , \tag{3.105}$$

where ρ_{max} is the UV-cutoff and V_3 the Minkowski space volume. Then the renormalized Euclidean on-shell action I_R may simply be written as

$$I_R = \frac{\lambda N_{\text{c}} N_{\text{f}} V_3 T^3}{32} \left(\frac{G(m,\tilde{\mu})}{N_{\text{f}}} - \frac{1}{4} \left[\left(\rho_{\text{min}}^2 - m^2 \right)^2 - 4mc \right] \right) , \tag{3.106}$$

where ρ_{min} determines the minimal value of the coordinate ρ on the D7-branes, i.e. $\rho_{\text{min}} = 1$ for black hole embeddings which we consider exclusively in this chapter and

$$G(m,\tilde{\mu}) = \int_{\rho_{\text{min}}}^{\infty} \mathrm{d}\rho \left[\rho^3 f \tilde{f} F_\chi \left(\Upsilon_1(\rho,\chi,\tilde{A}) + \Upsilon_2(\rho,\chi,\tilde{A}) \right) - N_{\text{f}} \left(\rho^3 - \rho m \right) \right] . \tag{3.107}$$

In the following we consider the dimensionless grand potential $\mathcal{W}_7$ defined as

$$\Omega_7 = T I_R = \frac{\lambda N_{\text{c}} N_{\text{f}} V_3 T^4}{32} \mathcal{W}_7 . \tag{3.108}$$

By considering the variation of the grand potential with resect to the gravity fields, it can be shown (see [18, section 5.3] for the pure isospin case) that the above definition of the grand potential is consistent and that the order parameter $\tilde{d}_x^1$ is not a thermodynamical variable.

Phase transition and phase diagram   We expect that a phase transition occurs between a normal fluid phase and a superfluid phase. At zero baryon chemical potential we know from [17, 18] that the phase transition from the normal phase to the superfluid phase is second order with mean field exponents. In this section we consider the phase transition at non-zero baryon chemical potentials.

First we map out the phase diagram of the given theory with zero quark mass $m = 0$. The phase diagram is shown in fig. 3.8. As we increase the baryon chemical potential the transition temperature to the superfluid phase first increases. For $\mu_B/\mu_I \gtrsim 0.4$ the transition temperature monotonically decreases to zero as the baryon chemical potential grows. We can show numerically that the phase transition is always second order. In the next subsection we will show numerically that the transition temperature is zero at $\mu_B/\mu_I \approx 1.23$, and hence we obtain a quantum critical point.
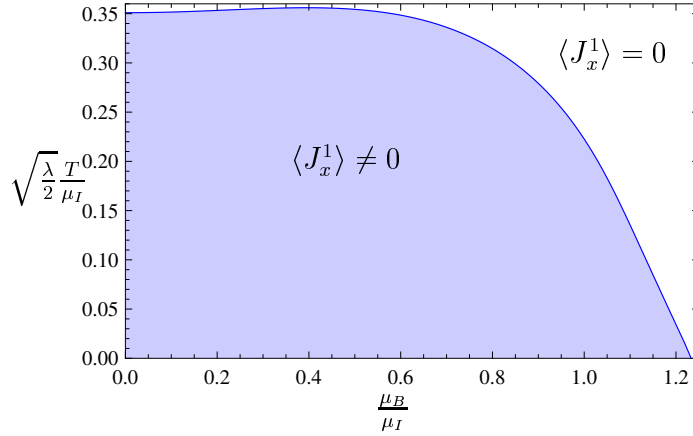
FIGURE 3.8:   The phase diagram for fundamental matter in thermal strongly-coupled $\mathcal{N} = 2$ SYM theory at zero quark mass with μ_I the isospin chemical potential, μ_B the baryon chemical potential, T the temperature and λ the 't Hooft coupling: In the blue region the order parameter $\langle J_x^1 \rangle$ is non-zero and the system is in the superfluid phase while in the white region the order parameter $\langle J_x^1 \rangle$ is zero and the system is in the normal phase. Figure by Patrick Kerner [3].

Zero temperature solutions and quantum critical point   In this paragraph we study the D3/D7-brane setup at zero temperature. The zero temperature limit is given by $\rho_h \to 0$, i.e. $f = \tilde{f} = 1$. The induced metric on the D7-branes may now be written in (L, r) coordinates (see equation (3.75))

$$\mathrm{d}s^2 = \frac{r^2 + L^2}{2R^2} \left(-\mathrm{d}t^2 + \mathrm{d}\vec{x}^2 \right) + \frac{R^2}{r^2 + L^2} \left(1 + (\partial_r L)^2 \right) \mathrm{d}r^2 + \frac{R^2 r^2}{r^2 + L^2} \mathrm{d}\Omega_3^2 .$$

(3.109)

The square root of the metric is now

$$\sqrt{-G} = \frac{\sqrt{h_3}}{4} r^3 \sqrt{1 + (\partial_r L)^2} ,$$

(3.110)

and using the adapted symmetrized trace prescription, the DBI action becomes

$$S_{\text{DBI}} = -\tau_7 \int d\xi^8 \frac{r^3}{4} \left[\Xi_1(\tilde{r}, \tilde{L}, \tilde{A}) + \Xi_2(\tilde{r}, \tilde{L}, \tilde{A}) \right], \tag{3.111}$$

with

$$\Xi_i(\tilde{r}, \tilde{L}, \tilde{A}) = \left[1 + (\partial_{\tilde{r}}\tilde{L})^2 - 2(\partial_{\tilde{r}}\tilde{X}_i)^2 + 2(\partial_{\tilde{r}}\tilde{A}_x^1)^2 \right.$$
$$\left. - \frac{\gamma^2}{2\pi^2(\tilde{r}^2 + \tilde{L}^2)^2}(1 + (\partial_{\tilde{r}}\tilde{L})^2)\left((\tilde{X}_1 - \tilde{X}_2)\tilde{A}_x^1\right)^2 \right]^{\frac{1}{2}}, \tag{3.112}$$

where the dimensionless quantities are now defined by

$$\tilde{r} = \frac{r}{R}, \quad \tilde{L} = \frac{L}{R}, \quad \tilde{A} = \frac{2\pi\alpha'}{R}A. \tag{3.113}$$

In the normal phase, i.e. $A_x^1 \equiv 0$, the equations of motion for the gauge fields X_i for the massless embedding $L = 0$,

$$\partial_{\tilde{r}}\tilde{X}_i = \frac{2\tilde{d}_i}{\sqrt{\tilde{r}^6 + 8\tilde{d}_i^2}} \tag{3.114}$$

can be solved analytically [122]. The solution expressed in terms of incomplete Beta functions is given by

$$\tilde{X}_i(\tilde{r}) = \frac{\tilde{d}_i^{\frac{1}{3}}}{6}B\left(\frac{\tilde{r}^6}{8\tilde{d}_i^2 + \tilde{r}^6}; \frac{1}{6}, \frac{1}{3}\right). \tag{3.115}$$

From the asymptotic form near the boundary, we can read off the chemical potential and the density (see equation (3.98)),

$$\tilde{X}_i = \frac{\tilde{d}_i^{\frac{1}{3}}2\sqrt{\pi}}{\sqrt{3}}\frac{\Gamma\left(\frac{7}{6}\right)}{\Gamma\left(\frac{2}{3}\right)} - \frac{\tilde{d}_i}{\tilde{r}^2} + \cdots. \tag{3.116}$$

In the normal fluid phase we may now consider fluctuations $Z_\pm = A_x^1 \pm iA_x^2$ (see [123, 146] for more details) and look for an instability which may lead to a phase transition. For the flat embedding $L = 0$, the equation of motion for the fluctuation $Z_\pm$ at zero momentum is given by

$$\frac{d^2\tilde{Z}_+(\tilde{r})}{d\tilde{r}^2} + \frac{F'(\tilde{r})}{F(\tilde{r})}\frac{d\tilde{Z}_+(\tilde{r})}{d\tilde{r}} + \frac{8}{\tilde{r}^4}\left(\tilde{\omega} + \frac{\gamma}{4\sqrt{2}\pi}\left(\tilde{X}_1 - \tilde{X}_2\right)\right)^2\tilde{Z}_+(\tilde{r}) = 0,$$

$$\frac{d^2\tilde{Z}_-(\tilde{r})}{d\tilde{r}^2} + \frac{F'(\tilde{r})}{F(\tilde{r})}\frac{d\tilde{Z}_-(\tilde{r})}{d\tilde{r}} + \frac{8}{\tilde{r}^4}\left(\tilde{\omega} - \frac{\gamma}{4\sqrt{2}\pi}\left(\tilde{X}_1 - \tilde{X}_2\right)\right)^2\tilde{Z}_-(\tilde{r}) = 0,$$

$$(3.117)$$

with $\tilde{\omega} = \sqrt{\frac{\lambda}{2}}\,\alpha'\omega$ coming from the ansatz $A_x^i(\tilde{r}, t) = A_x^i(\tilde{r})e^{-i\omega t}$. The analytical expression for $\tilde{X}_i(\tilde{r})$ is given in (3.115) and

$$F(\tilde{r}) = \tilde{r}^3 \left(\frac{1}{\sqrt{1 - 2\left(\partial_{\tilde{r}}\tilde{X}_1\right)^2}} + \frac{1}{\sqrt{1 - 2\left(\partial_{\tilde{r}}\tilde{X}_2\right)^2}} \right). \qquad (3.118)$$

The system is unstable if the imaginary part of the quasinormal frequency is positiveFor a massless embedding $L \equiv 0$, we find this instability at $\mu_{\mathrm{B}}/\mu_{\mathrm{I}} \approx 1.23$.

What is the origin of the instability? In the back-reacted Einstein-Yang-Mills theory we see that the instability of the extremal Reissner-Nordström black hole which triggers the phase transition to the superfluid phase can be related to the violation of the Breitenlohner-Freedman bound of the field A_x^1 in the near horizon geometry of the black hole. This near horizon geometry features an AdS_2 factor (see section 3.3.4). In this section we investigate the instability in the D3/D7 brane setup at zero temperature. In the following we show that in contrast to the back-reacted Einstein-Yang-Mills system, the instability in the brane setup cannot be related to the violation of the Breitenlohner-Freedman bound in the far IR, i.e. the fluctuation of the field A_x^1 does not become unstable in the far IR. In this system we expect that the instability occurs in the bulk.

Let us now consider a fluctuation A_x^1 about the solution in the normal phase given by equation (3.115) for zero quark mass, i.e. $L \equiv 0$. The equation of motion for this fluctuation is given by

$$(\tilde{A}_x^1)'' + \frac{F'(\tilde{r})}{F(\tilde{r})}(A_x^1)' + \frac{\gamma^2(\tilde{X}_1 - \tilde{X}_2)^2}{4\pi^2\tilde{r}^4}\tilde{A}_x^1 = 0. \qquad (3.119)$$

As in section 3.3.4 we consider the equation of motion in the far IR. Since there is no horizon at zero temperature in the brane setup, the expansion is around $\tilde{r} = 0$. The equation of motion becomes trivial $\partial_{\tilde{r}}^2\tilde{A}_x^1 = 0$ if we only expand to the first order only. Thus $\tilde{A}_x^1/r$ satisfies the equation of motion of a massless scalar in AdS_2. In contrast to the EYM setup, the mass cannot be tuned by changing a UV quantity and the Breitenlohner-Freedman bound can never be violated. Hence fluctuation is stable in the IR. We expect that the instability observed by the numerical study of the quasinormal modes above occurs in the bulk. Thus the origin of the instability in this brane setup is different compared to the one in the back-reacted Einstein-Yang-Mills system studied in section 3.3.4.

3.4.4 Summary and outlook

In section 3.3 and 3.4 we holographically study field theories which are expected to be similar to QCD models [49, 50] which have been mentioned in 3.1. Our field theories have a global $U(2)$ symmetry which can be split into $U(1) \times SU(2)$. This allows us to switch on two chemical potentials: one for the overall $U(1)$ and one for a diagonal $U(1)$ inside $SU(2)$. In analogy to QCD, the chemical potential for the overall $U(1)$ is the baryon chemical potential, while the one for the diagonal $U(1)$ inside $SU(2)$ is identified with the isospin chemical potential. From these two quantities we can construct two dimensionless control parameters: the ratio of the temperature to one chemical potential and the ratio of the two chemical potentials. Since we start with a conformal field theory which does not have a scale, the first parameter is needed to distinguish different finite temperatures. The phase transition from a normal to a superconducting phase might occur at some critical values of the first parameter, the ratio of the temperature to one chemical potential, which may be tuned to zero by the second control parameter. Thus it is possible to study systems containing quantum phase transitions.

The realization of the $U(2)$ gauge theory on the gravity side can be realized in two different ways. As a first model, we consider the $U(2)$ Einstein-Yang-Mills (EYM) theory in section 3.3 . In this model we allow the gauge fields to back-react on the geometry in order to get a coupling between the overall $U(1)$ gauge fields and the $SU(2)$ gauge fields. As a second model, we consider the D3/D7 brane setup with two coincident D7-brane probes which feature the $U(2)$ gauge theory in section 3.4 . In this model the interaction between the overall $U(1)$ and the $SU(2)$ gauge fields is obtained by the Dirac-Born-Infeld action.

Comparing the methods used in section 3.3 and 3.4, we can say that the simple bulk action of the Einstein-Yang-Mills theory has the great virtue of being universal in the sense that these results may be true for many different dual field theories independently of their dynamics. Unfortunately this simple construction does not allow to identify the dual field theory explicitly. However it has been shown in [17, 18, 138] that the Einstein-Yang-Mills system can be embedded into string theory by considering the D3/D7 brane setup (see e.g. [99, 100]). The dual field theory of the D3/D7 brane setup is known explicitly, namely the $\mathcal{N} = 4$ SYM theory coupled to $\mathcal{N} = 2$ hypermultiplets. In this setup we work in the probe approximation, i.e. we consider $N_c \gg 1$ D3-branes which generate the background metric $AdS_5 \times S^5$ and embed $N_f = 2$ D7-branes into the background space. The embedding of the D7-branes generates degrees of freedom which transform in the fundamental representation of the gauge group, the $\mathcal{N} = 2$ hypermultiplets, which we denote as quarks in analogy to QCD. Here we have $N_f = 2$ two quark flavors. Since the dual field theory is known explicitly, the identification of the two chemical potentials as corresponding to the $U(1)$ baryon and $SU(2)$ isospin symmetries is explicitly

realized. In both models mesonic bound states of the fundamental degrees of freedom may be formed, and the transition to the superfluid state is related to the condensation of vector mesons which spontaneously break an Abelian symmetry.

Comparing the underlying symmetry and symmetry breaking, in section 3.3 and 3.4 we start with two models having the same symmetries and find the same mechanism of breaking an Abelian symmetry in both the EYM and in the D3/D7 model. A non-zero vev of the time component of the gauge field A_t induces a chemical potential on the boundary theory. By fixing a gauge, we can choose the $\mathrm{SU}(2)$ gauge field in the direction of the third Pauli matrix to be non-zero, i.e. $A_t^3 \neq 0$. This breaks the $\mathrm{SU}(2)$ symmetry down to an Abelian symmetry which we call $\mathrm{U}(1)_3$. Beyond a critical value of the chemical potential, the systems become unstable against fluctuations of the gauge field pointing in some other direction inside the $\mathrm{SU}(2)$, for instance A_x^1 (see e.g. [127] for the Einstein-Yang-Mills system and [123] for the D3/D7 brane setup). This instability is cured by the condensation of this gauge field A_x^1 which then breaks the $\mathrm{U}(1)_3$ symmetry. In the boundary theory the non-trivial profile of the gauge field A_x^1 induces a vev of the current $\langle J_x^1 \rangle$, but no source. Thus the breaking of the $\mathrm{U}(1)_3$ symmetry is spontaneous and the order parameter for the transition to the superfluid phase is given by $\langle J_x^1 \rangle$. For the D3/D7 brane setup the explicit field content of J_x^1 is given in (3.21).

Comparisons between the EYM and the D3/D7 phase diagrams The phase diagrams for the two above mentioned models in the presence of only an isospin chemical potential can be found in [17, 48], where the phase transitions occur at finite critical values of T/μ_{I}. Compared to [17, 48], in section 3.3 and 3.4, we switch on an additional time component of the $\mathrm{U}(1)$ gauge field $\mathcal{A}_t$ in both models which induces the baryon chemical potential μ_{B}. Varying the two control parameters T/μ_{I} and $\mu_{\mathrm{B}}/\mu_{\mathrm{I}}$ we can map out the phase diagram of both systems at finite baryon and isospin chemical potential. We find interesting similarities and differences (see figures 3.5 and 3.8). In both cases the critical temperature where the phase transition occurs is finite at zero baryon chemical potential. By increasing the baryon chemical potential, we can tune the critical temperature to zero and we obtain a quantum phase transition. However it is interesting that the details of the phase diagram are very different for the two systems, although they are expected to be dual to very similar field theories. For instance, the local as well as global symmetries match. The differences in the phase diagram are: In the Einstein-Yang-Mills theory (see figure 3.6) the critical temperature is monotonically decreasing as we increase the baryon chemical potential, while in the D3/D7 brane setup (see figure 3.8) the critical temperature first increases as the baryon chemical potential is increased. In addition in the Einstein-Yang-Mills setup, the system exhibits first and second order phase transitions depending on the strength of the back-reaction (see figure 3.5 for a sketch), while in the D3/D7 brane setup we obtain only second

order phase transitions. Thus the question arises: What is the crucial difference between the systems which induces the different phase transitions?

From the construction there is one obvious difference. In the Einstein-Yang-Mills system, the $U(1)$ and $SU(2)$ gauge fields only couple indirectly via the metric. In the field theory this means that the coupling of the currents which are dual to the gauge fields only occurs due to gluon loops. In the D3/D7 brane setup these loops are neglected due to the probe approximation. In this case the field theory currents directly interact with each other. These interactions are induced by the non-linear terms of the DBI action. Due to this difference it is understandable that the phase transitions may be different. The different couplings of the gauge fields to each other may lead to different RG flows and therefore to different IR physics which lead to differences in the phase diagram.

In addition we find an interesting difference in the origin of the quantum critical point in the systems. In the Einstein-Yang-Mills setup we can pinpoint the origin of the instability to the violation of the Breitenlohner-Freedman bound in an IR AdS_2 region. This AdS_2 region shows up as the near horizon region of the extremal Reissner-Nordström black hole. According to the AdS/CFT dictionary, the dual field theory thus contains a one-dimensional CFT in the IR (see figure 3.5). It is also important that the IR dimension of the dual operator depends on the ratio of the chemical potentials, such that the dimension can be tuned to an unstable value. In [134] it is argued that the violation of the Breitenlohner-Freedman bound will lead to a BKT-like phase transition. A common feature for this kind of transition seems to be the turning point in the phase diagram, such that the critical temperature slowly goes to zero as the ratio of baryon to isospin chemical potential is increased. In contrast to this behavior, the critical temperature in the D3/D7 brane setup goes to zero linearly. In this second model we do not obtain a violation of the Breitenlohner-Freedman bound. Therefore we expect that the quantum phase transition is second order with mean field exponents.

Comparisons with the results obtained from QCD models   Comparing the phase diagrams obtained in our models (see figures 3.5 and 3.8) with the one obtained in imbalanced Fermi mixtures [49] and QCD at finite baryon and isospin chemical potential [50] (see figure 3.2), we see some similarities. In all cases the critical temperature is finite if the second control parameter, in our case the baryon chemical potential, is zero. By increasing the second control parameter we can tune the critical temperature to zero and we obtain a quantum phase transition. This seems to be a universal behavior for systems with two control parameters. However in imbalanced Fermi mixtures and QCD at finite baryon and isospin chemical potential shown in figure 3.2 the order of the phase transition is different from that in our models. In the models of figure 3.2, the phase transition is second order at large temperatures and becomes first order at low temperatures. On the other hand, in the holographic models this is different:

For large back-reaction the behavior in the Einstein-Yang-Mills system is completely opposite. The phase transition is first order at large temperatures and becomes continuous at small temperatures. Also for small back-reaction, we find a continuous quantum phase transition instead of a discontinuous one.

The difference in the order of the quantum phase transition may be related to the different behavior of the normal phase at zero temperature. For instance the BKT-like transition in the Einstein-Yang-Mills setup is possible since the theory is conformal in the IR and the IR dimension of the dual operator depend on $\mu_\mathrm{B}/\mu_\mathrm{I}$. In [134] a BKT-like transition has been discussed in conformal field theories. The transition may occur if two fixed points of the β-function annihilate. The Einstein-Yang-Mills setup is the only one which is conformal in the IR with tunable IR dimension of the dual operator, unlike both the models of figure 3.2 and the D3/D7 setup, such that a different order of the phase transition is plausible. In the D3/D7 probe brane setup we do not observe any change in the order of the phase transition which is always second order. Therefore, by comparing the different models, we conclude that the order of the phase transition is not universal and depends on the precise form of the interaction.

Outlook It would be interesting to study the origin of the discussed differences in the phase diagrams and the possible existence of the quantum critical point in our EYM and D3/D7 setups in more detail. For example a detailed analysis of how the order of the phase transition can be changed by varying the form of the interaction would be attractive. In addition the study of back-reaction effects in the D3/D7 model may lead to new behavior in the phase diagrams. Furthermore it is important to establish a full understanding of the instability mechanism in the D3/D7 brane setup and its difference to the violation of the Breitenlohner-Freedman bound found in the Einstein-Yang-Mills theory. This may lead to a characterization of the universality classes of quantum phase transitions.

Holographic flavor transport

Moving away from equilibrium, we study a gravity dual which allows to study *near-equilibrium* phenomena such as transport properties of charges like conductivity, energy and momentum loss of charge carriers moving through a conducting medium. The setup in this chapter can serve a model for describing quarks moving in the *near-equilibrium* quark-gluon plasma. Usually, in order to study transport phenomena, we need to disturb the system. Thus we bring the system to an out-of-equilibrium state and study its responses on external perturbations. In particular, using a method from gauge/gravity duality, we are able to study effects beyond linear response theory.

4.1   Introduction and motivation

In this chapter we use the D3/D7 model to describe electrical transport properties of flavor fields moving in a SYM plasma. The main content presented in sections 4.2 and 4.3 stems from my own work in collaboration with Martin Ammon and Andy O'Bannon [1] which is part of a larger program of studying transport phenomena in strongly-coupled systems using gauge/gravity duality. Methods within the gauge/gravity provide many solvable toy models for strongly-coupled systems which are useful to obtain qualitative and often quantitative insight into real physical systems. For instance, at finite temperature the scaling and supersymmetry are broken, thus the SYM plasma described by the black hole AdS might share common properties with the quark-gluon plasma (QGP) created at RHIC, thus the setup presented in this section might be seen as a toy model to describe quarks moving in a QGP.

Compared to holographic construction of the physical systems presented in chapter 3, here we also embed a probe of N_{f} flavor D7-branes in the AdS black hole background. However, we do not turn on the non-abelian $\mathrm{SU}(N_{\mathrm{f}})$ world-volume gauge fields, but only consider the abelian ones associated with the $\mathrm{U}(1)_{\mathrm{B}} \subset \mathrm{U}(N_{\mathrm{f}})$. As in chapter 3, the time component of the $\mathrm{U}(1)_{\mathrm{B}}$ gauge

field gives rise to a baryon chemical potential and a charge density. In order to study transport phenomena we need to *disturb* the system and study the response of the system on external sources. In our case we want to study the electrical conductivity of of charge carriers, i.e. the $U(1)_B$ flavor fields. For this purpose we will turn on an external electro-magnetic field. Obviously, this can be realized by switching on the additional spatial components of the $U(1)_B$ gauge field. The presence of the electro-magnetic field will drive the system to an out-of-equilibrium state, since the charge carriers will be accelerated and loss momentum and energy to the surrounding medium. This is a *first step* in this thesis to move from studying phenomena in equilibrium to phenomena in non-equilibrium physics. We will see later in this chapter that the non-equilibrium description presented below is valid only to a time interval of order (N_c/N_f) and describe an in-medium effect of the SYM plasma, i.e. we describe flavor fields losing momentum and energy to the plasma, but not the SYM plasma passing though the process of thermalization.

The subject in this chapter is motivated by the works in [52–54] and [51]. In [51] it was shown that scaling arguments lead to universal non-linearities in transport such as in conductivity if the system is near the quantum critical point. More precisely, the electric current at a quantum critical point in d spatial dimensions is characterized by the coherence length exponent ν, which determines how fast the coherence length diverges near the quantum critical point, and the dynamic scaling exponent z as

$$J(\omega, T, E) = E^{\frac{d-1+z}{1+z}} \mathcal{Y}\left(E/T^{1+1/z}, \omega/T\right) , \tag{4.1}$$

where ω denotes the frequency associated with the electric field E, T the temperature and $\mathcal{Y}$ some function which depends on the detail of the theory [147].

Investigating the origins of such non-linearities in transport is specially problematic since the system is necessarily driven far from equilirium. More-over, in the region near the quantum critical point, physical systems are usually strongly coupled. The methods developed within the AdS/CFT correspondence might be an appropriate approach to study non-linear transport properties at strong coupling. In this chapter, we do not consider systems with the presence of a quantum critical point as in [51]. In a simple gravity setup dual to a $\mathcal{N} = 4$ SYM theory at strong coupling coupled to $\mathcal{N} = 2$ hypermultiplets at finite temperature, we compute the electrical conductivity of charged carriers moving though an $\mathcal{N} = 4$ SYM plasma in the presence of the electro-magnetic field.

Typically in linear response theory, the conductivity tensor components are extracted from a low-frequency limit of the two point functions using a Kubo formula which is presented in (3.23). This method cannot be applied for studying non-linear effects in conductivity. In [52, 53] an alternative strategy was developed to study the electrical conductivity of charge carriers at all order

in E. This method uses the D3/D7 setup at finite temperature and baryon chemical potential to introduce flavor fields moving in a $\mathcal{N} = 4$ SYM plasma. Thus it can be seen as a model for describing quarks moving though a quark-gluon plasma produced at the Relativistic Heavy-Ion Collider (RHIC). In [52, 53] an electric field is turned on directly as an external source. Instead of calculating two-point functions for extracting the conductivity tensor, using the methods in [52, 53] it is sufficient to determine the one-point function corresponding to the expectation value of the induced current, since the conductivity tensor σ_{ij} measuring the electrical response of a conducting medium to externally applied fields is defined by

$$\langle J_i \rangle = \sigma_{ij} \, E_j \,, \tag{4.2}$$

where E are externally applied electric fields and $\langle J_i \rangle$ are the electrical currents induced in the medium.

Although the conductivity in the presence of an electric field is expected to be infinite for translation-invariant system because the charge carriers are accelerated forever, our probe limit $N_{\rm f} \ll N_{\rm c}$ effectively provides a mechanism for dissipation. To be more precise, the probe limit allows our system to mimic a dissipative system. As explained in more detail in refs. [52–54, 148], and as we will review in section 4.3, the charge carriers do indeed transfer energy and momentum to the $\mathcal{N} = 4$ plasma, but the *rates* at which they do so are of order $N_{\rm c}$. That means that only at times of order $N_{\rm c}$ will the charge carriers have transferred order $N_{\rm c}^2$ amounts of energy and momentum to the plasma, and hence the motion of the $\mathcal{N} = 4$ SYM plasma will no longer be negligible. For earlier times, we may treat the $\mathcal{N} = 4$ SYM plasma as a motionless reservoir into which the charge carriers may dump their energy and momentum, thus providing the charge carriers with an apparent mechanism for dissipation.

Using the results in [52, 53], the authors of ref. [54] study the momentum loss rates of massive flavor fields to the SYM theory plasma at the presence of a baryon number chemical potential and external electric and magnetic fields. In particular, they consider the case where the electric and magnetic field are *perpendicular* to each other [53]. In addition to [52, 53], the authors of [54] calculate the thermo-electric conductivity tensor α_{ij} which measures the thermal response

$$\langle Q_i \rangle = \alpha_{ij} \, E_j \,, \tag{4.3}$$

where $\langle Q_i \rangle$ are heat currents induced in the medium,

$$\langle Q_i \rangle = \langle T^t{}_i \rangle - \mu_{\rm B} \langle J_i \rangle \,, \tag{4.4}$$

and $\langle T^i{}_j \rangle$ are the components of the flavor fields stress-energy tensor, such that $\langle T^t{}_i \rangle$ are momentum densities and $\mu_{\rm B}$ is the baryon chemical potential. As first demonstrated in ref. [54], the rates at which the charge carriers lose energy and momentum can be computed holographically. To do so, the contribution that

the charge carriers make to the stress-energy tensor of the SYM theory have to be computed. The loss rates appear in two places. First, the holographic results for the energy and momentum densities exhibit divergences whose coefficients (using a suitable regulator) we can identify as the loss rates. Second, the loss rates appear explicitly as components of the holographic result for the stress-energy tensor, namely components whose upper index is the holographic (radial) coordinate [54, 149].

Our goal in this chapter is to generalize the results in [52–54] by considering *arbitrary orientations* between the constant electric and magnetic field, and compute the full conductivity tensor as well as the contribution to the stress-energy tensor associated with a number N_f of massive $\mathcal{N} = 2$ supersymmetric hypermultiplet fields propagating through an $\mathcal{N} = 4$ supersymmetric $\mathrm{SU}(N_\mathrm{c})$ Yang-Mills theory plasma at temperature T. For an arbitrary configuration of constant electric and magnetic fields, we may sum all the electric fields into a single vector, and similarly for the magnetic fields. The most general configuration is thus an electric field $\vec{E}$ pointing in some direction, which we will take to be $\hat{x}$, and a magnetic field $\vec{B}$ that may be decomposed into two components, one along $\hat{x}$, which we call B_x, and one perpendicular to it, along the $\hat{z}$ direction, which we call B_z. Stated simply, then, we will generalize the results of refs. [52–54] to include a magnetic field with non-zero $\hat{x}$ component, or equivalently a non-zero $\vec{E} \cdot \vec{B} \sim F \wedge F$.

In what follows we will give a list of arguments why we want to generalize the results of refs. [52–54] and what we achieve by introducing a non-zero $\vec{E} \cdot \vec{B}$. With perpendicular electric and magnetic fields E and B_z, we expect a current $\langle J^x \rangle$ parallel to the electric field (because it pushes the charges) and a Hall current $\langle J^y \rangle$ orthogonal to both the electric and magnetic field. With non-zero B_x, we expect a current $\langle J^z \rangle$, and hence we can compute a transport coefficient σ_{xz} which is new to [52–54]. More generally, we can compute the entire conductivity tensor and determine its dependence on B_x.

Many previous gauge/gravity calculations of conductivities were in $(3+1)$-dimensional AdS space, so that the boundary CFT was $(2+1)$-dimensional [150–153], which precludes the existence of $\vec{E} \cdot \vec{B}$. Another drawback of the systems studied in refs. [150–153] was translation invariance, which implies momentum conservation. The system thus has no way to dissipate momentum, so the DC transport behavior was singular. For example, the DC conductivity at finite density is infinite, because the charge carriers in the presence of an external electric field but without frictional forces accelerate forever.

Additionally, in a Lorentz-invariant system, we can build two Lorentz-invariant quantities from $\vec{E}$ and $\vec{B}$, namely $|\vec{E}|^2 - |\vec{B}|^2$ and $\vec{E} \cdot \vec{B}$. When $\vec{E} \cdot \vec{B} = 0$, and $|\vec{B}| > |\vec{E}|$, we can boost to a frame where the electric field is zero, which immediately tells us that all the physics must be in equilibrium. For example, as reviewed in ref. [151], the form of the Hall conductivity is fixed by Lorentz invariance to be $\langle J^t \rangle / B_z$. When $\vec{E} \cdot \vec{B}$ is non-zero we can no longer

boost to a frame in which the electric field is zero, hence the physics cannot be purely equilibrium. As in ref. [54], we will study observers in the field theory who 'see' no loss rates. The simplest example is an observer who moves along with the charges: in that frame, the charges are at rest, so obviously such an observer should not see the charges lose energy and momentum. As mentioned in ref. [54], we can also find a second observer who sees no loss rates, but only when $\vec{E} \cdot \vec{B} = 0$. When $\vec{E} \cdot \vec{B} \neq 0$, the observer measures a current with non-zero divergence $J^2 (\vec{E} \cdot \vec{B})$, where $J^2 = \langle J_\mu \rangle \langle J^\mu \rangle$. The identity of this observer was left as an open question in ref. [54]. Here we find that this observer's four-vector is in fact the magnetic field as measured by the moving charges. Much like the holographic result for the stress-energy tensor, the loss rate $J^2 (\vec{E} \cdot \vec{B})$ appears as the coefficient of a (suitably regulated) divergence in the current itself. Notice also that, given the $\vec{E} \cdot \vec{B}$ anomaly in this current, if we were to study transport of the charge associated with this current we should find a special kinetic coefficient [154, 155] whose form is fixed by the anomaly coefficient (in our case, J^2) and thermodynamics (the equation of state), as explained in ref. [156].

This chapter is organized as follows. In section 4.2 we present a solution for the worldvolume fields of probe D7-branes in the AdS-Schwarzschild background, representing a finite baryon density of flavor degrees of freedom in the presence of external electric and magnetic fields. In section 4.2.4 we use our gravity solution to compute the conductivity tensor associated with transport of baryon number charge. In section 4.3 we compute the contribution that the flavor degrees of freedom make to the stress-energy tensor, study divergences in the components of the stress-energy tensor and their relation to energy and momentum loss rates, and then discuss two reference frames in which the divergences are absent. We conclude with some suggestions for future research in section 4.4. We collect some technical results in an appendix A.

4.2 Conductivity and transport coefficients

This section generalizes the results obtained in [52, 53] by introducing an additional component of the magnetic field B_x to the configuration discussed in [52, 53] where only E_x and B_z are present. As mentioned in 4.1, by turning on B_x, we allow arbitrary orientations between the electric and magnetic fied. We compute a new transport coefficient σ_{xz} and determine dependence of the whole conductivity tensor on B_x. In section 4.2.1 we review the method and the key results presented in [52]. In the following sections we compute the conductivity tensor and compare our results with those in [52, 53]. The content of 4.2.2 to 4.2.5 mainly stems from my own work in collaboration with Martin Ammon and Andy O'Bannon [1].

4.2.1   Metallic AdS/CFT and beyond linear response theory

In this section we review the main idea and the key results presented in [52]. The authors of [52] show that instead of calculating two-point functions for extracting the conductivity tensor using the Kubo formula 3.23 as in linear response, using methods developed in the frame of gauge/gravity duality, it is sufficient to determine the one-point function corresponding to the expectation value of the induced electric current. The conductivity tensor to all order of the electrical field is then obtained by the Ohm's law 4.2. Using the D3/D7 model, see section 2.2, $U(1)_B$ charge carriers and external electro-magnetic fields can be introduced. The static configuration is obtained by minimizing the abelian DBI action 2.115. It was found via a method called holographic renormalization [107, 131, 132], which is needed for removing the divergence of the DBI action due to integration over the infinite volume of AdS space, that the expectation value of the induced current corresponds to the constants of motion arising from the regularized DBI action, see the appendix of [52]. Thus with the explicit expressions for the current, the conductivity tensor can be extracted straightforwardly from the Ohm's law 4.2.

In what follows we will sketch some basic steps to obtained the conductivity tensor in [52]. The calculation in detail is postponed to the subsequent parts of this section where besides E_x we also turn on B_z and B_x. The authors [52] embed N_f flavor D7-branes in the background of N_c color D3-branes which is $AdS_5 \times S^5$ space. We want to study field theory at finite temperature, thus we replace AdS space by black hole AdS. The induced D7-branes metric can be generically given by

$$\mathrm{d}s_{D_7}^2 = g_{uu}\,\mathrm{d}u^2 + g_{tt}\,\mathrm{d}t^2 + g_{xx}\,\mathrm{d}\vec{x}^2 + g_{ss}\mathrm{d}\Omega_3^2\,, \tag{4.5}$$

where we use u to denote the radial coordinate of AdS space and $g_{ss}\mathrm{d}\Omega_3^2 = \cos^2\theta(u)\mathrm{d}\Omega_3^2$ the metric of the three-sphere part of the S^5 and the black hole horizon is at $g_{tt}(u_H) = 0$. As described in (2.126) and (2.128), the charge density and electric current $\langle J_x \rangle$ can be introduced by the following ansatz for the $U(1)_B \subset U(N_f)$ gauge field

$$A_t = A_t(u), \qquad A_x = -E_x t + h(u)\,, \tag{4.6}$$

where $h(u)$ is some function of u. After solving the DBI action and identifying the charge density d_t and x-component of the current with

$$d_t = \langle J^t \rangle = \frac{\delta S_{\mathrm{DBI}}}{\delta A_t}\,, \qquad \langle J^x \rangle = \frac{\delta S_{\mathrm{DBI}}}{\delta A_x}\,, \tag{4.7}$$

the authors of [52] find the following generic form for the conductivity

$$\sigma_{xx} \sim \sqrt{c_1 f(E_x)\cos^6\theta(u_*) + c_2 f^{-2}(E_x)d_t^2}\,, \tag{4.8}$$

where c_1, c_2 are some constant, $f(E_x)$ some non-linear function of E_x and u_* denotes the special position along the radial coordinate whose meaning will

become clear later in section 4.2.4. The $\theta(u_*)$ describes the mass m of the flavor field with $m \to \infty$ as $\cos\theta(u)$ approaches zero and $m \to 0$ as $\cos\theta(u)$ approaches one. From (4.8) we can see that the conductivity depends on E_x. Moreover, there are two types of charge carriers contributing to the conductivity. One type represented by the d_t-term comes from the charge carriers which are introduced explicitly. The other type comes from charge carriers thermally produced in charge-neutral pairs [52]. This effect is interpreted as pair production at strong coupling.

4.2.2 Setup with arbitrary background fields

In this section we present a solution of supergravity, plus probe D7-branes, describing massive hypermultiplets propagating through an $\mathcal{N} = 4$ SYM plasma with finite $\mathrm{U}(1)_\mathrm{B}$ density and in the presence of external electric and magnetic fields. Compared to the last section, we introduce a magnetic field component B_z as in [53]. Moreover, we also turn on the B_x component in order to construct the most general configuration where the constant electric and magnetic fields can point to any arbitrary direction.

The supergravity solution includes a ten-dimensional metric with a $(4 + 1)$-dimensional AdS-Schwarzschild factor and an S^5 factor. We will use an AdS-Schwarzschild metric of the form

$$\mathrm{d}s^2_{\mathrm{AdS}_5} = g_{uu}\,\mathrm{d}u^2 + g_{tt}\,\mathrm{d}t^2 + g_{xx}\,\mathrm{d}\vec{x}^2\,, \tag{4.9}$$

where u is the AdS radial coordinate. When we need an explicit metric, we will use

$$\mathrm{d}s^2_{\mathrm{AdS}5} = \frac{\mathrm{d}u^2}{u^2} - \frac{1}{u^2}\frac{(1 - u^4/u_\mathrm{H}^4)^2}{1 + u^4/u_\mathrm{H}^4}\,\mathrm{d}t^2 + \frac{1}{u^2}(1 + u^4/u_\mathrm{H}^4)\,\mathrm{d}\vec{x}^2\,. \tag{4.10}$$

The boundary is at $u = 0$ and the horizon is at $u = u_\mathrm{H}$ with $u_\mathrm{H}^{-1} = \frac{\pi}{\sqrt{2}}T$. Here we are using units in which the radius of AdS is equal to one. In these units, we convert from string theory to SYM theory quantities using $\alpha'^{-2} = \lambda$. We will use an S^5 metric of the form

$$\mathrm{d}s^2_{\mathrm{S}^5} = \mathrm{d}\theta^2 + \sin^2\theta\,\mathrm{d}s^2_{\mathrm{S}^1} + \cos^2\theta\,\mathrm{d}s^2_{\mathrm{S}^3}\,, \tag{4.11}$$

where θ is an angle between zero and $\pi/2$ and $\mathrm{d}s^2_{\mathrm{S}^1}$ and $\mathrm{d}s^2_{\mathrm{S}^3}$ are metrics for a unit-radius circle and 3-sphere, respectively. The supergravity solution also includes N_c units of five-form flux through the S^5, but the five-form will be irrelevant in what follows, so we omit it.

We next introduce N_f coincident probe D7-branes. As we will be interested only in the $\mathrm{U}(1)$ part of the $\mathrm{U}(N_\mathrm{f})$ worldvolume gauge field, the relevant part of their action will be the Dirac-Born-Infeld (DBI) term,

$$S_{\mathrm{D7}} = -N_\mathrm{f}\tau_7\int d^8\zeta\sqrt{-\det\left[g_{ab} + (2\pi\alpha')F_{ab}\right]}\,. \tag{4.12}$$

Here τ_7 is the D7-brane tension, ζ^a are the worldvolume coordinates, g_{ab} is the induced worldvolume metric, and F_{ab} is the U(1) worldvolume field strength. The D7-branes will be extended along all of the AdS_5 directions, as well as the S^3 directions inside the S^5.

Ansatz for the gauge fields Our ansatz for the worldvolume fields will include the worldvolume scalar $\theta(u)$. The D7-brane induced metric is then identical to the background metric, except for the radial component, which is $g_{uu} = \frac{1}{u^2} + \theta'(u)^2$, where prime denotes differentiation with respect to u. Starting now, the notation g_{uu} will include the θ'^2 term. We will discuss $\theta(u)$'s equation of motion, boundary conditions, and holographic dual operator later in this section.

The U(N_f) gauge invariance of the coincident D7-branes is dual to the U(N_f) symmetry of the mass-degenerate flavor fields in the SYM theory. We identify the U(1) subgroup as baryon number, U(1)$_\mathrm{B}$. The D7-brane world-volume Abelian gauge field A_μ is dual to the SYM U(1)$_\mathrm{B}$ current J^μ, so to introduce a finite U(1)$_\mathrm{B}$ density in the SYM theory, we must introduce the worldvolume gauge field $A_t(u)$.

To introduce electric and magnetic fields, and the resulting currents $\langle J^x \rangle$, $\langle J^y \rangle$, and $\langle J^z \rangle$, we also include in our ansatz the gauge field components

$$A_x(t,u) = -E_x t + f_x(u)\,, \quad A_y(x,u) = B_z\, x + f_y(u)\,, \quad A_z(y,u) = B_x\, y + f_z(u)\,.$$

$$(4.13)$$

In each case, the leading term is a non-normalizable mode that introduces an external field into the SYM theory. Choosing a gauge in which $A_u = 0$, we can write the non-zero elements of F_{ab}:

$$\begin{aligned} F_{tx} &= -E_x\,, & F_{xy} &= B_z\,, & F_{yz} &= B_x\,, \\ F_{ut} &= A_t'\,, & F_{ux} &= A_x'\,, & F_{uy} &= A_y'\,, & F_{uz} &= A_z'\,. \end{aligned}$$

$$(4.14)$$

We will now write the action for our ansatz. Let us first define some notation. The fields in our ansatz depend only on u, so in eq. (4.12) we can immediately perform the integration over the SYM theory directions (t, x, y, z) and over the S^3 directions. Starting now we will divide both sides of eq. (4.12) by the volume of $\mathbb{R}^{3,1}$, so S_D7 will actually denote an action density. L will denote the Lagrangian density, $S_\mathrm{D7} \equiv -\int du\, L$. Using $\tau_7 = \frac{\alpha'^{-4} g_s^{-1}}{(2\pi)^7} = \frac{\lambda N_\mathrm{c}}{2^5 \pi^6}$, we will also define the constant

$$\mathcal{N} \equiv N_\mathrm{f} \tau_7 V_{\mathrm{S}^3} = \frac{\lambda}{(2\pi)^4} N_\mathrm{f} N_\mathrm{c}\,, \tag{4.15}$$

where $V_{\mathrm{S}^3} = 2\pi^2$ is the volume of a unit-radius S^3. Lastly, a tilde over a quantity denotes a factor of $(2\pi\alpha')$, for example, $\tilde{F}_{ab} \equiv (2\pi\alpha') F_{ab}$.

The action and the equations of motion Plugging our ansatz into the action eq. (4.12), we have

$$S_{\text{D7}} = -\mathcal{N} \int du \, \cos^3 \theta \, \sqrt{g_{uu}|g_{tt}|g_{xx}^3 - g_{xx}A_2 - A_4} \,, \qquad (4.16)$$

where A_2 and A_4 contain terms with two or four factors of $\tilde{F}_{ab}$, respectively,

$$A_2 = g_{uu}g_{xx}\tilde{E}_x^2 + g_{tt}g_{uu}(\tilde{B}_x^2 + \tilde{B}_z^2) + g_{xx}^2 \tilde{A}_t'^2 + g_{tt}g_{xx}\left(\tilde{A}_x'^2 + \tilde{A}_y'^2 + \tilde{A}_z'^2\right) \,,$$

$$A_4 = g_{xx}\tilde{E}^2 \left(\tilde{A}_y'^2 + \tilde{A}_z'^2\right) + g_{xx}\tilde{A}_t'^2 \left(\tilde{B}_x^2 + \tilde{B}_z^2\right) + g_{uu}\tilde{E}^2\tilde{B}_z^2 + g_{tt}\tilde{B}_z^2\tilde{A}_z'^2$$
$$+ g_{tt}\tilde{B}_x^2\tilde{A}_x'^2 + 2g_{tt}\tilde{B}_x\tilde{B}_z\tilde{A}_x'\tilde{A}_z' - 2g_{xx}\tilde{E}_x\tilde{B}_z\tilde{A}_t'\tilde{A}_y'.$$

$$(4.17)$$

The action only depends on the u derivatives of A_t, A_x, A_y, and A_z, so the system has four constants of motion. As shown in refs. [52,53], we can identify these as the components of the $\text{U}(1)_{\text{B}}$ current density in the SYM theory[1],

$$\langle J^\mu \rangle = \frac{\delta L}{\delta A_\mu'}. \qquad (4.18)$$

Our ansatz thus allows for a non-zero $\text{U}(1)_{\text{B}}$ density $\langle J^t \rangle$ as well as $\text{U}(1)_{\text{B}}$ currents $\langle J^x \rangle$, $\langle J^y \rangle$, and $\langle J^z \rangle$. Given these constants of motion, we can solve algebraically for the derivatives of the gauge field (the field strength components):

$$A_t'(u) = -\frac{\sqrt{g_{uu}|g_{tt}|}}{g_{xx}^2 + \tilde{B}_x^2} \frac{\langle J^t \rangle \xi - B_z a_1}{\sqrt{\xi\chi - \frac{a_1^2}{g_{xx}^2 + \tilde{B}_x^2} + \frac{a_2^2}{|g_{tt}|g_{xx} - \tilde{E}_x^2}}} \,, \qquad (4.19a)$$

$$A_x'(u) = \sqrt{\frac{g_{uu}}{|g_{tt}|}} \frac{1}{g_{xx}} \frac{\langle J^x \rangle \xi - B_x a_2}{\sqrt{\xi\chi - \frac{a_1^2}{g_{xx}^2 + \tilde{B}_x^2} + \frac{a_2^2}{|g_{tt}|g_{xx} - \tilde{E}_x^2}}} \,, \qquad (4.19b)$$

---

[1]As in refs. [52,53], the D7-brane action diverges due to integration all the way to the AdS$_5$ boundary at $u = 0$, and thus requires renormalization. The recipe for the "holographic renormalization" of the D7-brane action appears in refs. [52,53,107,157]. We first introduce a cutoff at $u = \epsilon$ and then add a counterterm action S_{CT} to cancel the divergences as $\epsilon \to 0$. The precise expression for $\langle J^\mu \rangle$ is

$$\langle J^\mu \rangle = \lim_{\epsilon \to 0} \left(\frac{1}{\epsilon^4} \frac{1}{\sqrt{-\gamma}} \frac{\delta S_{reg}}{\delta A_\mu(\epsilon)} \right) \,,$$

where γ is the determinant of the induced metric on the $u = \epsilon$ hypersurface and S_{reg} denotes the regulated action: $S_{reg} = S_{\text{D7}} + S_{CT}$. In the $B_x = 0$ case, the counterterms appearing in S_{CT} were computed in ref. [53]. A straightforward analysis reveals that no new counterterms are necessary with non-zero B_x and that, as in ref. [53], the counterterms do not contribute to $\langle J^\mu \rangle$. Eq. (4.18) then follows for on-shell A_μ. For more details, see the appendix of ref. [53]

$$A'_y(u) = \sqrt{\frac{g_{uu}}{|g_{tt}|}} \frac{1}{g_{xx}} \frac{\langle J^y \rangle \xi + E_x a_1}{\sqrt{\xi\chi - \frac{a_1^2}{g_{xx}^2 + \tilde{B}_x^2} + \frac{a_2^2}{|g_{tt}|g_{xx} - \tilde{E}_x^2}}} \,, \tag{4.19c}$$

$$A'_z(u) = \frac{\sqrt{g_{uu}|g_{tt}|}}{|g_{tt}|g_{xx} - \tilde{E}_x^2} \frac{\langle J^z \rangle \xi - B_z a_2}{\sqrt{\xi\chi - \frac{a_1^2}{g_{xx}^2 + \tilde{B}_x^2} + \frac{a_2^2}{|g_{tt}|g_{xx} - \tilde{E}_x^2}}} \,, \tag{4.19d}$$

where we have defined

$$\xi = |g_{tt}|g_{xx}^3 - g_{xx}^2 \tilde{E}_x^2 + |g_{tt}|g_{xx}\left(\tilde{B}_x^2 + \tilde{B}_z^2\right) - \tilde{E}_x^2 \tilde{B}_x^2 \,, \tag{4.20a}$$

$$\begin{aligned}\chi =\ & |g_{tt}|g_{xx}^2 \mathcal{N}^2 (2\pi\alpha')^4 \cos^6\theta - (2\pi\alpha')^2(\langle J^x \rangle^2 + \langle J^y \rangle^2) \\ & + (2\pi\alpha')^2 \left(\frac{|g_{tt}|g_{xx}}{g_{xx}^2 + \tilde{B}_x^2}\langle J^t \rangle^2 - \frac{|g_{tt}|g_{xx}}{|g_{tt}|g_{xx} - \tilde{E}_x^2}\langle J^z \rangle^2\right) \,,\end{aligned} \tag{4.20b}$$

$$a_1 = (2\pi\alpha')^2 \left(|g_{tt}|g_{xx}B_z\langle J^t \rangle + \left(g_{xx}^2 + \tilde{B}_x^2\right) E_x\langle J^y \rangle\right) \,, \tag{4.20c}$$

$$a_2 = (2\pi\alpha')^2 \left(\left(|g_{tt}|g_{xx} - \tilde{E}_x^2\right) B_x\langle J^x \rangle + |g_{tt}|g_{xx}B_z\langle J^z \rangle\right) \,. \tag{4.20d}$$

Notice that ξ is the value of $-\det\left(g_{\mathrm{ab}} + (2\pi\alpha')F_{\mathrm{ab}}\right)$ in the (t, x, y, z) subspace. It has a form characteristic of the $(3 + 1)$-dimensional Born-Infeld Lagrangian, $(-g - \frac{1}{2}g\tilde{F}^2 - \frac{1}{4}(\tilde{F} \wedge \tilde{F})^2)$.

4.2.3 Mass of the hypermultitplet and the embedding

The embedding function $\theta(u)$ determines the mass of the flavor fields. Its equation of motion can be obtained in two different ways. We can find its Euler-Lagrange equation of motion from the original D7-brane action, eq. (4.16), and then plug into that equation of motion the solutions for the field strengths in eq. (4.19). Equivalently, we can plug the solutions for the field strengths into the D7-brane action, eq. (4.16), to obtain an effective action for $\theta(u)$, perform a Legendre transform, and then find the Euler-Lagrange equation of motion. Plugging the solutions in eq. (4.19) into S_{D7}, we find

$$S_{\mathrm{D7}} = -\mathcal{N}^2(2\pi\alpha')^2 \int du\, \cos^6\theta\, g_{xx}\sqrt{g_{uu}|g_{tt}|}\frac{\xi}{\sqrt{\xi\chi - \frac{a_1^2}{g_{xx}^2 + \tilde{B}_x^2} + \frac{a_2^2}{|g_{tt}|g_{xx} - \tilde{E}_x^2}}} \cdot \tag{4.21}$$

The Legendre-transformed on-shell action, $\hat{S}_{\mathrm{D7}}$, is then

$$
\hat{S}_{\mathrm{D7}} = S_{\mathrm{D7}} - \int du \left(A_t' \frac{\delta S_{\mathrm{D7}}}{\delta A_t'} + A_x' \frac{\delta S_{\mathrm{D7}}}{\delta A_x'} + A_y' \frac{\delta S_{\mathrm{D7}}}{\delta A_y'} + A_z' \frac{\delta S_{\mathrm{D7}}}{\delta A_z'} \right)
$$
$$
= -\frac{1}{(2\pi\alpha')^2} \int du \, g_{xx}^{-1} \sqrt{\frac{g_{uu}}{|g_{tt}|}} \sqrt{\xi\chi - \frac{a_1^2}{g_{xx}^2 + \tilde{B}_x^2} + \frac{a_2^2}{|g_{tt}|g_{xx} - \tilde{E}_x^2}}. \tag{4.22}
$$

To complete our solution, we must specify boundary conditions for the worldvolume fields, namely $\theta(u)$ and the gauge fields.

The boundary conditions for the gauge fields were discussed in refs. [54, 105]. For $A_t(u)$, the geometry imposes a boundary condition upon us: the Killing vector corresponding to time translations becomes degenerate at the horizon, hence for the gauge field to remain well-defined as a one-form, we must impose $A_t(u_{\mathrm{H}}) = 0$. What about the other components of the gauge field? The key point is that the calculation of the next section implicitly fixes the values of these components at the horizon. In the next section we will demand that the on-shell action remains real for all u. For given values of E_x, B_x, B_z and $\langle J^t \rangle$, that only happens for particular values of $\langle J^x \rangle$, $\langle J^y \rangle$ and $\langle J^z \rangle$. For those values of $\langle J^x \rangle$, $\langle J^y \rangle$, and $\langle J^z \rangle$, the solutions for A_x, A_y and A_z are fixed by our solutions above, and hence we can then (working backwards) infer their values at the horizon. In other words, we will implicitly be choosing the values of A_x, A_y, and A_z at the horizon to produce exactly the values of $\langle J^x \rangle$, $\langle J^y \rangle$ and $\langle J^z \rangle$ such that the action remains real for all u. Unfortunately, our solution for $A_x(t, u)$ diverges at the horizon. The conductivity tensor does not depend on the values of the gauge fields at the horizon, so it is "safe" from the divergence. The stress-energy tensor does depend on the values at the horizon, but as explained in ref. [54], these divergences (suitably regulated) have a sensible interpretation in the field theory as rates of energy and momentum loss, as we will discuss in section 4.3.

We now turn to the boundary conditions on $\theta(u)$. The field $\theta(u)$ is holographically dual to an operator that is given by taking $\frac{\partial}{\partial m}$ of the SYM Lagrangian. We will denote the operator as $\mathcal{O}_m$. The operator $\mathcal{O}_m$ is the $\mathcal{N} = 2$ supersymmetric completion of the hypermultiplet fermions' mass operator, and includes several terms. The exact operator appears in ref. [105]. For our purposes, just thinking of $\mathcal{O}_m$ as the hypermultiplet mass operator will be sufficient. For a given solution $\theta(u)$, we can obtain the corresponding values of m and $\langle \mathcal{O}_m \rangle$ via a near-boundary asymptotic expansion (where the powers of u follow simply from the equation of motion),

$$
\theta(u) = \theta_1 u + \theta_3 u^3 + O\left(u^5\right). \tag{4.23}
$$

As shown in refs. [107, 157], we identify the mass as $m = \frac{\theta_1}{2\pi\alpha'}$ and the expectation value as $\langle \mathcal{O}_m \rangle \propto -2\theta_1 + \frac{1}{3}\theta_3^3$.

When $A_t(u)$ is zero, we have two topologically distinct ways to embed the D7-brane in the AdS-Schwarzschild background. The first type of embedding

is a "Minkowski embedding," in which the worldvolume S^3 shrinks as we move along the D7-brane away from $u = 0$ and eventually collapses to a point at some $u = u'$ outside the horizon, $u' < u_H$. We then have the boundary conditions $\theta(u') = \frac{\pi}{2}$, such that $\cos \theta(u') = 0$ and the S^3 has zero volume, and $\theta'(u') = \infty$, so that the D7-brane does not develop a conical singularity when the S^3 collapses to zero volume [157]. The D7-brane then does not extend past u', but rather appears to end abruptly at u'.

The second type of embedding is a "black hole" embedding, in which the S^3 shrinks but does not collapse, and the D7-brane intersects the horizon. We can then choose the value of $\theta(u)$ at the horizon, $\theta(u_H) \in [0, \frac{\pi}{2})$, while for the derivative we must have $\theta'(u_H) = 0$ for the embedding to be static.

When $A_t(u)$ is zero, a discontinuous (first order) transition between the two types of embeddings occurs as a function of m/T. The transition has been studied in great detail [108, 145, 157–162]. Roughly speaking, large values of m/T (above a critical value) correspond to Minkowski embeddings while small values of m/T correspond to black hole embeddings.

As argued in ref. [105], however, when $A_t(u)$ is non-zero, only black hole embeddings are allowed, for a simple physical reason. With non-zero $A_t(u)$, the D7-brane has a worldvolume electric field pointing in the u direction, F_{tu}. What source produces the electric field? The simplest possible source is a density $\langle J^t \rangle$ of strings ending on the D7-brane. A straightforward analysis then shows that the force the strings exert on the D7-brane is greater than the tension of the D7-brane [105]. We thus expect the strings to pull the D7-brane into the black hole, producing a D7-brane black hole embedding with electric field lines in the u direction.

As shown numerically in ref. [105], we then have a one-to-one map between values of $\theta(u_H)$ (the free parameter in the bulk) and $m = \frac{1}{2\pi\alpha'}\theta_1$ (the free parameter near the boundary). In what follows we will not solve numerically for $\theta(u)$, however, we know the solution for $\theta(u)$ in two limits. The first limit is $m = 0$, which corresponds to the trivial solution $\theta(u) = 0$ and hence has $\theta(u_H) = 0$. The second limit is $m \to \infty$, where $\theta(u_H) \to \frac{\pi}{2}$.

4.2.4 Conductivity tensor

From eq. (4.20a), we see that ξ is negative at the horizon but positive at the boundary, thus ξ must change sign at some value of u, which we will call u_*. We can straightforwardly calculate u_* from the equation[2] $\xi(u_*) = 0$,

$$\frac{u_*^4}{u_H^4} = G - \sqrt{G^2 - 1}\,, \tag{4.24}$$

with

$$G \equiv e^2 - b_z^2 - b_x^2 + \sqrt{(e^2 - b_z^2)^2 + (b_x^2 + 1)(b_x^2 + 1 + 2(e^2 + b_z^2))}\,, \tag{4.25}$$

---

[2]We actually find four solutions for u_*^4/u_H^4. The one we present is the only one for which u_*^4/u_H^4 takes physical values, between 0 and 1.

where we have introduced the dimensionless quantities

$$
e \equiv \pi \alpha' u_{\mathrm{H}}^2 \, E_x = \frac{E_x}{\frac{\pi}{2}\sqrt{\lambda}T^2} \,, \quad b_z \equiv \pi \alpha' u_{\mathrm{H}}^2 \, B_z = \frac{B_z}{\frac{\pi}{2}\sqrt{\lambda}T^2} \,,
$$
$$
b_x \equiv \pi \alpha' u_{\mathrm{H}}^2 \, B_x = \frac{B_x}{\frac{\pi}{2}\sqrt{\lambda}T^2} \,.
$$

(4.26)

Later we will need g_{xx}^2 evaluated at u_* in order to translate our result for the conductivity tensor into SYM theory quantities. Using eq. (4.24), we find

$$
g_{xx}^2(u)|_{u=u_*} = \frac{\pi^4 T^4}{2}(1 + G) \equiv \pi^4 T^4 \mathcal{F}(e, b_x, b_z) \,,
$$

(4.27)

where in the last step we removed a factor of $\pi^4 T^4$ and defined the rest to be $\mathcal{F}(e, b_x, b_z)$, which will appear in our result for the conductivity tensor. A useful limit is $e = 0$, where $G = 1$ and hence $\mathcal{F} = 1$.

Following refs. [52, 53], we now focus on the on-shell action, eq. (4.21), and in particular we focus on the square root in the denominator of eq. (4.21), which we reproduce here for convenience,

$$
\sqrt{\xi \chi - \frac{a_1^2}{g_{xx}^2 + \tilde{B}_x^2} + \frac{a_2^2}{|g_{tt}|g_{xx} - \tilde{E}_x^2}} \,,
$$

and which also appears in the solutions for the field strengths $A'_\mu(u)$ for $\mu = t, x, y, z$, eq. (4.19), as well as the Legendre-transform of the on-shell action, eq. (4.22). We will argue that the four functions ξ, χ, a_1 and a_2, must all vanish at u_* in order for the above square root, and hence the on-shell action, to remain real for all u.

When $\xi = 0$ the a_2^2 term is negative, because the equation $\xi(u_*) = 0$ itself tells us that $\left(|g_{tt}|g_{xx} - \tilde{E}_x^2\right) = -\frac{|g_{tt}|g_{xx}\tilde{B}_z^2}{\left(g_{xx}^2 + \tilde{B}_x^2\right)} < 0$ at u_*. To avoid an imaginary action at u_* we must have $a_1(u_*) = a_2(u_*) = 0$.

Arguing why χ has to vanish at u_* is more subtle. χ has the same behavior as ξ: it is positive at the boundary and negative at the horizon, so it must have a zero at some u value, which we will call u_χ. If u_* and u_χ are not the same, so that ξ and χ have distinct zeroes, then the product $\xi\chi$ will be negative on the interval between u_* and u_χ. The crucial question then is whether the a_2^2 term is positive or negative on that interval. If it is positive (and sufficiently large) it could keep the action real. The sign of the a_2^2-term is determined by $\left(|g_{tt}|g_{xx} - \tilde{E}_x^2\right)$, which (like ξ and χ) is positive at the boundary and negative at the horizon, and hence must have have a zero at some value of u that we will call $u_{E_x^2}$. We showed above that $\left(|g_{tt}|g_{xx} - \tilde{E}_x^2\right)$ is negative at u_*, so the zero must obey $u_{E^2} < u_*$ (it is closer to the boundary than u_*). Now suppose χ changes sign at $u_\chi > u_*$. As we just showed, the a_2^2 term is negative there,

so the on-shell action would be imaginary on the interval (u_*, u_χ), hence we demand $u_\chi \leqslant u_*$. We want to exclude the possibility that $u_\chi < u_*$. We know that $u_{E_x^2}$ is also less than u_*, so we must compare u_χ and $u_{E_x^2}$. If $u_\chi < u_{E_x^2}$, then the on-shell action is imaginary on the interval $(u_{E_x^2}, u_*)$, and if $u_\chi > u_{E_x^2}$, the action is imaginary on the interval (u_χ, u_*). In order for the on-shell action to remain real for all u, then, we demand that $u_\chi = u_*$.

The upshot is that we obtain four equations, $\xi(u_*) = \chi(u_*) = a_1(u_*) = a_2(u_*) = 0$, for four unknows, u_*, $\langle J^x \rangle$, $\langle J^y \rangle$, and $\langle J^z \rangle$. The equation $\xi(u_*) = 0$ gives us u_*, as we explained above. We will now solve for the currents $\langle J^x \rangle$, $\langle J^y \rangle$, and $\langle J^z \rangle$.

The equation $a_1(u_*) = 0$ gives us $\langle J^y \rangle$, while the equation $a_2(u_*) = 0$ gives us $\langle J^z \rangle$. We then plug the results for $\langle J^y \rangle$ and $\langle J^z \rangle$ into $\chi(u_*) = 0$ to find $\langle J^x \rangle$. The result for the current in each case includes an overall factor of E, so invoking Ohm's law $\langle J^i \rangle = \sigma_{ix} E$, we identify the components of the conductivity tensor:

$$
\sigma_{xx} = \frac{g_{xx}^2 + \tilde{B}_x^2}{g_{xx}\left(g_{xx}^2 + \tilde{B}_x^2 + \tilde{B}_z^2\right)}
$$
$$
\times \sqrt{\mathcal{N}^2(2\pi\alpha')^4 g_{xx}\left(g_{xx}^2 + \tilde{B}_x^2 + \tilde{B}_z^2\right)\cos^6\theta(u_*) + (2\pi\alpha')^2\langle J^t \rangle^2}
$$

(4.28a)

$$
\sigma_{xy} = \frac{(2\pi\alpha')\tilde{B}_z\langle J^t \rangle}{g_{xx}^2 + \tilde{B}_x^2 + \tilde{B}_z^2}
$$

(4.28b)

$$
\sigma_{xz} = \frac{\tilde{B}_x \tilde{B}_z}{g_{xx}^2 + \tilde{B}_x^2}\,\sigma_{xx}
$$

(4.28c)

where all functions of u are evaluated at u_*. In analogy with eq. (4.26), we define

$$
\rho \equiv \pi\alpha' u_{\mathrm{H}}^2 \langle J^t \rangle = \frac{\langle J^t \rangle}{\frac{\pi}{2}\sqrt{\lambda}T^2}.
$$

(4.29)

We then use the result for $g_{xx}^2(u_*)$ in eq. (4.27) to write the components of the conductivity tensor in terms of SYM theory quantities

$$
\sigma_{xx} = \sqrt{\frac{N_{\mathrm{f}}^2 N_{\mathrm{c}}^2 T^2}{16\pi^2}\frac{(\mathcal{F} + b_x^2)^2}{\sqrt{\mathcal{F}}(\mathcal{F} + b_x^2 + b_z^2)}\cos^6\theta(u_*) + \frac{\rho^2(\mathcal{F} + b_x^2)^2}{\mathcal{F}(\mathcal{F} + b_x^2 + b_z^2)^2}}
$$

(4.30a)

$$\sigma_{xy} = \frac{\rho\, b_z}{\mathcal{F} + b_x^2 + b_z^2} \tag{4.30b}$$

$$\sigma_{xz} = \frac{b_x\, b_z}{\mathcal{F} + b_x^2}\, \sigma_{xx}\,. \tag{4.30c}$$

As in refs. [52, 53], the result for σ_{xx} includes two terms adding in quadrature. As discussed in refs. [52–54], these two terms have different physical interpretations. The system has two types of charge carriers. First we have the density of charge carriers we introduced explicitly in $\langle J^t \rangle$, whose contribution appears as the second term under the square root in σ_{xx}. Even when $\langle J^t \rangle = 0$ we find a non-zero σ_{xx} and hence a non-zero current, however, so the system must have some other source of charge carriers.

The other type of charge carriers come from pair production in the electric field. Their contribution appears as the term in σ_{xx} with the $\cos^6 \theta(u_*)$ factor. We have two pieces of evidence that suggests the $\cos^6 \theta(u_*)$ term represents pair production. First is the behavior of the pair-production term as a function of the mass m. When $m \to \infty$, so that the pair production should be suppressed, we indeed have $\cos^6 \theta(u_*) \to 0$, while when $m \to 0$, so that the pair production should be maximal, we have $\cos^6 \theta(u_*) \to 1$. Second, as shown in ref. [54] for the case with $B_x = 0$, when the density $\langle J^t \rangle = 0$ the flavor fields have zero momentum in the $\hat{x}$ direction, which is consistent with pair production: the oppositely-charged particles in each pair move in opposite directions, producing a finite $\langle J^x \rangle$ but zero net momentum. For our case, with $B_x \neq 0$, we see that $\sigma_{xz} \propto \sigma_{xx}$, so both types of charge carriers contribute to $\langle J^z \rangle$, too. Using our results for the stress-energy tensor in section 4.3, in particular for $\langle T^t_{\ x} \rangle$ and $\langle T^t_{\ z} \rangle$, we can show that when $\langle J^t \rangle = 0$, the flavor fields have zero momentum in the $\hat{x}$ and $\hat{z}$ directions, so we again find a nicely consistent picture.

4.2.5 Drag force and the Drude model

In this section we will check our results in some limits. As a mild check, we set $B_x = 0$, which reproduces the result of ref. [53], in which $\vec{E}$ and $\vec{B}$ were perpendicular. In the large mass limit, i.e. we take the mass of the flavor field to infinity, our results are reduced to known results from electrodynamics, the Drude model, and the drag force obtained by an independent method using the gauge/gravity dualilty. In the following paragraphs, let us first review what the Drude model is and how we can use AdS/CFT to describe the drag force acting on charged particles moving in a plasma.

Drude model Consider a density $\langle J^t \rangle$ of massive quasi-particles propagating through an isotropic, homogeneous, dissipative neutral medium. In the rest

frame of the medium we introduce an electric field $\vec{E}$ in the $\hat{x}$ direction, and a magnetic field $\vec{B}$ with a component B_z in the $\hat{z}$ direction and a component B_x in the $\hat{x}$ direction. The force on a quasi-particle is then

$$\frac{\mathrm{d}\vec{p}}{\mathrm{d}t} = \vec{E} + \vec{v} \times \vec{B} - \mu_{\mathrm{D}}\vec{p}, \tag{4.31}$$

where our quasi-particle has charge $+1$ and μ_{D} is a drag coefficient. We replace the momentum with the velocity using $\vec{p} = M\vec{v}$ for quasi-particle mass M. We then replace the velocity with the induced current using $\vec{v} = \langle \vec{J} \rangle / \langle J^t \rangle$. Imposing the steady-state condition $d\vec{p}/dt = 0$ and solving for $\langle \vec{J} \rangle$ yields

$$\sigma_{xx} = \sigma_0 \frac{(B_x/\mu_{\mathrm{D}}HM)^2 + 1}{|\vec{B}|^2/(\mu_{\mathrm{D}}M)^2 + 1}, \qquad \sigma_{xy} = \sigma_0 \frac{(B_z/\mu_{\mathrm{D}}M)}{|\vec{B}|^2/(\mu_{\mathrm{D}}M)^2 + 1},$$

$$\sigma_{xz} = \sigma_0 \frac{(B_x/\mu M)(B_z/\mu_{\mathrm{D}}M)}{|\vec{B}|^2/(\mu_{\mathrm{D}}M)^2 + 1}, \tag{4.32}$$

where $\sigma_0 = \langle J^t \rangle / \mu_{\mathrm{D}}M$ is the conductivity when $\vec{B} = 0$.

The drag force in AdS/CFT In this paragraph we comment on the drag force acting on a moving heavy particle like a quark in a thermal medium described by the AdS black hole metric [37, 39]. The below derivation of drag force follows closely the description in [39]. Assuming a constant velocity of the quark moving though a quark-gluon plasma, it is of interest to find out how much force is needed to maintain the constant motion. The force is needed to maintain the constant motion is called drag force. Using the methods in AdS/CFT, a quark is described by a single string with one end located on the flavor D-branes. Working in the restframe of the plasma described by the AdS-Schwarzschild metric, the motion of the string along the x_3 field coordinate can be described by

$$x_3(r, t) = vt + \zeta(r), \tag{4.33}$$

where $\xi(r)$ describes the trajectory of the dual string along the radial coordinate. Recall the metric for AdS-Black hole

$$\mathrm{d}s^2 = -f\mathrm{d}t^2 + \frac{r^2}{R^2}(\mathrm{d}x_1^2 + \mathrm{d}x_2^2 + \mathrm{d}x_3^2) + \frac{1}{f}\mathrm{d}r^2 + R^2\mathrm{d}\Omega_5^2, \quad f \equiv \frac{r^2}{R^2}\left(1 - \frac{r_{\mathrm{H}}^4}{r^4}\right), \tag{4.34}$$

and taking the usual parameterization $t = \tau$, $r = \sigma$ while all other coordinates are independent of τ and σ, the Nambu-Goto action (2.78) reads

$$S = \frac{1}{2\pi\alpha'}\int \mathrm{d}\tau\mathrm{d}r \sqrt{1 + \frac{r^2 f}{R^2}\xi'^2 - \frac{r^2}{R^2 f}v^2} \tag{4.35}$$

$$= \frac{1}{2\pi\alpha'}\int \mathrm{d}\tau\mathrm{d}r \sqrt{1 + \frac{n}{H}\zeta'^2 - \frac{v^2}{n}} \quad ; \ H \equiv \frac{R^4}{r^4}, \quad n \equiv f\sqrt{H}.$$

A conserved quantity $\pi_\zeta = \frac{\partial \mathcal{L}}{\partial \zeta'}$ can be obtained from the above equation since the Lagrangian does not depend on ζ, and from this relation we get

$$\zeta'^2 = \pi_\zeta^2 \frac{H^2}{n^2} \frac{n - v^2}{n - \pi_\zeta^2 H} \tag{4.36}$$

$\zeta(r)$ describes the string shape dangling from the boundary at infinity to the horizon at r_{H}, so ζ'^2 has to be non-negative in this interval[3]. Since n takes the values in [0,1), $(n - v^2)$ will switch its sign at some radial position for $v > 0$. To avoid a negative left hand side of the above equation, $n - \pi_\zeta^2 H$ has to change its sign at the same radial position as its numerator. Hence, this condition leads to

$$\pi_\zeta^2 = \frac{v^2}{1 - v^2} \frac{r_{\mathrm{H}}^4}{R^4} \ . \tag{4.37}$$

Plugging π_ζ into (4.36), we get

$$\zeta' = v \frac{r_{\mathrm{H}}^2 R^2}{r^4 - r_{\mathrm{H}}^4} \tag{4.38}$$

which after integrating ζ' gives the dragging string shape trailing out behind the quark, arcing downwards into the horizon. This string exerts a drag force on the external quark which will be determined next.

The equations of motion for the Nambu-Goto action may be expressed as

$$\frac{\partial \mathcal{P}_\mu^\tau}{\partial \tau} + \frac{\partial \mathcal{P}_\mu^\sigma}{\partial \sigma} = 0 \ ; \qquad \mathcal{P}_\mu^\kappa \equiv \frac{\partial \mathcal{L}}{\partial(\frac{\partial X^\mu}{\partial \kappa})} \ . \tag{4.39}$$

$\mathcal{P}_\mu^\tau$ and $\mathcal{P}_\mu^\sigma$ are the current densities in the τ and σ directions of the p_μ component of the spacetime momentum. The drag force is then described by the time derivative of the momentum $\frac{dp_{x_3}}{dt}$ where

$$p_{x_3}(\tau) = \int \mathcal{P}_{x_3}^\tau(\tau, \sigma) d\sigma \ . \tag{4.40}$$

The momentum p_{x_3} above is computed by integrating the flux $\mathcal{P}_{x_3}$ over a constant τ-path on the string world-sheet and since the $\mathcal{P}_{x_3}^\sigma$ is parallel to any constant τ-path it does not contribute to the flux. From another point of view p_{x_3} can be seen as the conserved charge obtain by integrating the zeroth component $\mathcal{P}_{x_3}^\tau$ of the current over space.
Using (4.39) the drag force is

$$\frac{dp_{x_3}}{dt} = \int \frac{\partial \mathcal{P}_{x_3}^\tau}{\partial \tau} d\sigma = -\int \frac{\partial \mathcal{P}_{x_3}^\sigma}{\partial \sigma} d\sigma = -\mathcal{P}_{x_3}^\sigma \ . \tag{4.41}$$

---

[3]For zero velocity $\zeta'(r)$ vanishes giving the usual straight string hanging from the boundary down to the horizon.

We have calculated $\mathcal{P}^{\sigma}_{x_3} = \frac{\partial \mathcal{L}}{\partial x_3'} = \frac{\partial \mathcal{L}}{\partial \zeta'} = \pi_\zeta$ before in (4.38), using this result the final expression for the drag force reads

$$\frac{\mathrm{d}p_{x_3}}{\mathrm{d}t} = -\frac{1}{2\pi\alpha'}\frac{v}{\sqrt{1-v^2}}\frac{r_{\mathrm{H}}^2}{R^2} = -\frac{\pi\sqrt{\lambda}\,T_{\mathrm{H}}^2}{2}\frac{v}{\sqrt{1-v^2}}. \tag{4.42}$$

There is a world-sheet momentum $\mathcal{P}^{\sigma}_{x_3}$ flowing into the horizon. In order to maintain the constant motion, a force acting on the quark has to be added which depends on the velocity of the quark and the temperature of the medium[4]

Later in the next paragraphs we will show that a constant electric field on the probe brane would provide precisely such a force so that the quark will approach an equilibrium value v at which the rate of momentum loss to the plasma is balanced by the driving force exerted by the electric field. This was proposed to be another[5] back-to-back jet solution with external forcing in which quark and antiquark move apart at constant velocity after dissociation.

Comparing our results to the drag force and the Drude model Following refs. [52, 53], we can also take a limit of large mass, when we take m to be much larger than any other scale in the problem, which includes not only T but also the scale of thermal corrections to the energy of a heavy quark, $\frac{1}{2}\sqrt{\lambda}T$ [37]. We will call this the '$m \to \infty$' limit. This limit reduces our results to known results from the Drude model in electrodynamics and the drag force described above. As explained in section 4.2, in the large mass limit, $\cos\theta(u_*) \to 0$. In this limit, we expect the charge carriers to behave as classical quasi-particles experiencing a drag force due to the $\mathcal{N} = 4$ SYM plasma and a Lorentz force due to the external electric and magnetic fields. Our answer for the conductivity should then reduce to the Drude form.

To show that our answer reduces to the Drude result, eq. (4.32), when $m \to \infty$, we need to know what $\mu_{\mathrm{D}}M$ is for our charge carriers, that is, we must compute the drag force on the charge carriers, following refs. [52, 53]. We begin by rewriting the force law eq. (4.31), in the steady state $d\vec{p}/dt = 0$, as

$$\begin{aligned}
\mu_{\mathrm{D}}|\vec{p}| &= \sqrt{E^2 + |\vec{v}\times\vec{B}|^2 + 2\vec{E}\cdot(\vec{v}\times\vec{B})} \\
&= \sqrt{E_x^2 + v_y^2(B_x^2 + B_z^2) + (v_zB_x - v_xB_z)^2 + 2E_xv_yB_z} .
\end{aligned} \tag{4.43}$$

As $m \to \infty$, pair creation will be suppressed and only the charge carriers in $\langle J^t \rangle$ will contribute to $\langle \vec{J} \rangle$, hence we may write $\langle \vec{J} \rangle = \langle J^t \rangle \vec{v}$, where we drop the $\cos\theta(u_*)$ terms in $\langle J^x \rangle$ and $\langle J^z \rangle$, as these vanish in our $m \to \infty$ limit.

---

[4]For a string with both endpoints on the probe brane there is no drag force [38] acting on its endpoints, which can be interpreted as that a color singlet state does not interact with the thermal medium.

[5]The other 'solution' is the trivial one where the dissociation process occurs near the boundary transverse to the plasma where the quarks can escape the medium without suffering significant loss of energy.

Notice that all components of the conductivity tensor are then proportional to $\langle J^t \rangle$, so from our answer for the conductivity tensor we find the components of $\vec{v} = \langle \vec{J} \rangle / \langle J^t \rangle$ as functions of E, B_x and B_z. What is more instructive, however, is to use the original equations $\xi(u_*) = \chi(u_*) = a_1(u_*) = a_2(u_*) = 0$ to write $\vec{v}$ in terms of $g_{xx}(u_*)$ and $g_{tt}(u_*)$. For example, the speed of the heavy charge carriers is

$$|\vec{v}| = \sqrt{\left. \frac{|g_{tt}|}{g_{xx}} \right|_{u_*}} \,, \tag{4.44}$$

which is the local speed of light at u_*. The drag force is

$$\mu_D |\vec{p}| = \frac{1}{2\pi\alpha'} \sqrt{|g_{tt}(u_*)| g_{xx}(u_*)} \,, \tag{4.45}$$

which is simply the Nambu-Goto Lagrangian (density) for a string extended in the $\hat{x}$ direction, sitting at fixed radial position u_*. Following refs. [37, 39, 52, 53], if we employ the relativistic relation $|\vec{p}| = \gamma M v$ with $\gamma = \frac{1}{\sqrt{1-v^2}}$ and M the quasi-particle mass, then we find

$$\mu_D M = \frac{1}{2\pi\alpha'} \sqrt{g_{xx}(u_*)^2 - |g_{tt}(u_*)| g_{xx}(u_*)} = \frac{\pi}{2} \sqrt{\lambda} T^2 \,. \tag{4.46}$$

The result for the drag force

$$\mu_D |\vec{p}| = \mu_D M \gamma v = \frac{\pi \sqrt{\lambda} T^2}{2} \frac{v}{\sqrt{1-v^2}} \tag{4.47}$$

is identical to the zero-density result of refs. [37, 39] which is given in (4.42)[6] and the finite density results of refs. [52, 53], but now with non-zero B_x. That we recover the same answer is not surprising in the probe limit $N_f \ll N_c$. In the probe limit, the flavor excitations are too dilute to experience a significant number of collisions with one another. Most of their energy loss comes from their interactions with the $\mathcal{N} = 4$ SYM plasma, rather than with other flavor excitations, hence the drag force is independent of $\langle J^t \rangle$.

We can now compare to the Drude form eq. (4.32). We take $m \to \infty$, so that $\cos\theta(u_*) \to 0$ in the conductivity tensor. We also 'linearize' in the electric field, that is, we consider the regime of linear response, where the currents are linear in E and hence the conductivity is constant in E. (Recall that the Drude form relies on Maxwell's equations, which are linear.) In practical terms, that means setting $E = 0$ in our result for the conductivity. That means we take $\mathcal{F}(e = 0, b_x, b_z) = 1$ as explained above. Lastly, using our identification of $\mu_D M$ in eq. (4.46), we can write

$$\rho = \frac{\langle J^t \rangle}{\frac{\pi}{2} \sqrt{\lambda} T^2} = \frac{\langle J^t \rangle}{\mu M} \,, \tag{4.48}$$

---

[6] The difference of an overall sign between (4.47) and (4.42) can be 'corrected' if the reference frame of (4.42) is boosted in $-x_3$ direction.

and similarly for b_x and b_z (recall eq. (4.26)). We immediately find that our result for the conductivity tensor (4.30) is identical to the Drude form shown in (4.32).

Effects of B_x   Given that the novelty of our result is the presence of B_x, we can take limits that highlight the effects of B_x. For example, we can show that, generically, B_x enhances the process of pair production. We first linearize in the electric field again, so $\mathcal{F} = 1$, and then isolate the pair-production term by taking zero density ($\langle J^t \rangle = 0$, hence $\rho = 0$). The result for σ_{xx} is then

$$\sigma_{xx} = \frac{N_{\mathrm{f}} N_{\mathrm{c}} T}{4\pi} \frac{1 + b_x^2}{\sqrt{1 + b_x^2 + b_z^2}} \cos^3 \theta(u_*). \tag{4.49}$$

If we further consider $b_x \gg b_z$, then we see that σ_{xx} has a $\sqrt{1 + b_x^2}$ factor. Clearly, increasing B_x increases the contribution to $\langle J^x \rangle$ from pair production. Conversely, if we suppress the pair production by taking $m \to \infty$, so that $\cos^6 \theta(u_*) \to 0$, while keeping $\langle J^t \rangle$ finite, then σ_{xx} reduces to

$$\sigma_{xx} = \rho \, \frac{1 + b_x^2}{1 + b_x^2 + b_z^2} \, , \tag{4.50}$$

(which is of course the Drude result from eq. (4.32)) so that now taking $b_x \gg b_z$ we find that $\sigma_{xx} \to \rho$. Increasing B_x does not enhance the contribution to $\langle J^x \rangle$ coming from the net density $\langle J^t \rangle$ of charge carriers. (By contrast, the limit $b_z \gg b_x$ clearly suppresses both contributions to the current.)

4.3   The stress-energy tensor of flavor fields

In this section we use our holographic setup to compute the contribution that the flavor fields make to the expectation value of the stress-energy tensor of the field theory. We will call this contribution $\langle T^\mu_\nu \rangle$. We also identify certain divergences in the stress-energy tensor which are related to the rates of energy and momentum loss of the charge carriers (the flavor fields). We also discuss two special quantities that are free from these IR divergences. This section is a direct extension of the results of ref. [54] to include non-zero B_x.

4.3.1   Electric polarization and magnetization

Many contributions to the stress-energy tensor come simply from the electric polarization and the magnetization of the medium, as we will now review. Even in an equilibrium system, background electric and magnetic fields produce non-vanishing momentum currents due to polarization effects, so that we expect a contribution to $\langle T_{\mu\nu} \rangle$ of the form

$$\langle T^\mu_\nu \rangle_{\mathrm{pol}} = M^\mu_\sigma \, F^\sigma_\nu. \tag{4.51}$$

where $M^{\mu\nu}$ is the polarization tensor,

$$M^{\mu\sigma} = -\frac{\delta\Omega}{\delta F_{\mu\sigma}}, \tag{4.52}$$

with Ω the free energy density (and where we take the variation with other variables held fixed). The components of $M^{\mu\sigma}$ with one t index and one spatial index are electric polarizations while components with two spatial indices are magnetizations. The full energy-momentum tensor $\langle T^\mu_{\ \nu}\rangle$ then divides into two pieces:

$$\langle T^\mu_{\ \nu}\rangle = \langle T^\mu_{\ \nu}\rangle_{\text{fluid}} + \langle T^\mu_{\ \nu}\rangle_{\text{pol}}, \tag{4.53}$$

where, for example, $\langle T^t_{\ i}\rangle_{\text{fluid}}$ corresponds to the genuine momentum current due to the flow in the medium. Both $\langle T^\mu_{\ \nu}\rangle$ and $\langle T^\mu_{\ \nu}\rangle_{\text{fluid}}$ obey the same (non-) conservation equation,

$$\partial^\mu \langle T_{\mu\nu}\rangle = F_{\nu\rho}\langle J^\rho\rangle, \tag{4.54}$$

but only $\langle T^\mu_{\ \nu}\rangle_{\text{fluid}}$ represents observable quantities that can couple to external probes of the system (and hence is the appropriate object to use when studying transport).

In gauge-gravity duality, we identify $\Omega = -S_{\text{D7}}$, where here S_{D7} is the D7-brane action evaluated on a particular solution for the worldvolume fields, so that

$$M^{\mu\nu} = \frac{\delta S_{\text{D7}}}{\delta F_{\mu\nu}}. \tag{4.55}$$

As an explicit example, consider for example the calculation of M^{tx}. We start with eq. (4.12), evaluated on a particular solution. The on-shell action S_{D7} will have explicit E dependence, as well as implicit dependence through the solutions for $\theta(u)$ and the worldvolume gauge fields. We thus employ the chain rule[7],

$$\frac{dS_{\text{D7}}}{dE} = -\int du \left[\frac{\partial L}{\partial E} + \frac{\partial\theta}{\partial E}\frac{\partial L}{\partial\theta} + \frac{\partial\theta'}{\partial E}\frac{\partial L}{\partial\theta'} + \sum_{\mu=t,x,y,z} \frac{\partial A'_\mu}{\partial E}\frac{\partial L}{\partial A'_\mu} \right]. \tag{4.56}$$

We then use the fact that partial derivatives commute to write $\frac{\partial}{\partial E}\frac{\partial}{\partial u} = \frac{\partial}{\partial u}\frac{\partial}{\partial E}$, and integrate by parts to find

$$\begin{aligned}
\frac{dS_{\text{D7}}}{dE} = & -\int du \left[\frac{\partial L}{\partial E} + \left(\frac{\partial L}{\partial\theta} - \frac{\partial}{\partial u}\frac{\partial L}{\partial\theta'} \right)\frac{\partial\theta}{\partial E} - \sum_{\mu=t,x,y,z} \frac{\partial A_\mu}{\partial E}\frac{\partial}{\partial u}\frac{\partial L}{\partial A'_\mu} \right] \\
& - \frac{\partial\theta}{\partial E}\frac{\partial L}{\partial\theta'}\bigg|_0^{u_{\text{H}}} - \sum_{\mu=t,x,y,z} \frac{\partial A_\mu}{\partial E}\frac{\partial L}{\partial A'_\mu}\bigg|_0^{u_{\text{H}}}.
\end{aligned} \tag{4.57}$$

---

[7]We are using arguments similar to those in refs. [145, 163, 164].

Of the terms under the integral, the term in parentheses and the terms in the sum over μ vanish due to the equations of motion. That leaves the $\frac{\partial L}{\partial E}$ term under the integral, and the boundary terms. The main point is that the only contribution to the polarization from the bulk of AdS_5 comes from $\frac{\partial L}{\partial E}$. Similar statements apply for the magnetizations, for example, for M^{xy} the only bulk term comes from $\frac{\partial L}{\partial B_z}$.

In fact, we find that all six components of the polarization tensor are non-zero. All three electric polarizations, M^{ti} with $i = x, y, z$, are non-zero, despite the fact that our solution describes an electric field only in the $\hat{x}$ direction. In other words, if, for example, we introduce an electric field in the $\hat{y}$ direction, E_y, take the variation of S_{D7} with respect to E_y, and then set $E_y = 0$, we find a non-zero answer. Similarly, all three components of the magnetization are non-zero although our solution only includes B_x and B_z. In all cases the only bulk contribution is from a $\frac{\partial L}{\partial F_{\mu\nu}}$ term, evaluated on our solution (where only E_x, B_x and B_z are non-zero). We present explicit expressions for the derivatives $\frac{\partial L}{\partial F_{\mu\nu}}$ in the appendix. We will shortly see the derivatives $\frac{\partial L}{\partial F_{\mu\nu}}$ appearing in the stress-energy tensor. Most of these arise from the expected contribution to $\langle T_{\mu\nu} \rangle$ from $\langle T^\mu_{\ \nu} \rangle_{\mathrm{pol}}$.

4.3.2 Stress-energy tensor

We now come to the calculation of the stress-energy tensor. As explained in ref. [54], we may invoke the Hamiltonian form of the AdS/CFT correspondence [12], which allows us to equate conserved charges in the boundary field theory and the bulk gravity theory. For example, if p_i denotes the momentum associated with the flavor fields in the SYM theory, with $i = x, y, z$, then in the Hamiltonian framework we identify the conserved charges

$$p_i = \int \mathrm{d}t \, \mathrm{d}\vec{x} \, \langle T^t_{\ i} \rangle = \int \mathrm{d}t \, \mathrm{d}\vec{x} \, \mathrm{d}u \, d^3\alpha \, \sqrt{-g_{\mathrm{D7}}} \, U^t_{\ i}. \tag{4.58}$$

The α are coordinates on the S^3 wrapped by the D7-branes, g_{D7} is the determinant of the induced metric on the D7-branes, and $U^t_{\ i}$ is the D7-branes' momentum density. If the energy-momentum tensors are independent of the four spacetime coordinates, then the integrals over $dt \, d\vec{x}$ will only produce a factor of the spacetime volume, so that we can equate the momentum densities directly:

$$\langle T^t_{\ i} \rangle = \int \mathrm{d}u \, d^3\alpha \, \sqrt{-g_{\mathrm{D7}}} \, U^t_{\ i}. \tag{4.59}$$

To compute the stress-energy tensor of the flavor fields, then, we must compute the stress-energy tensor of the D7-branes, $\Theta^a_{\ b}$, defined as

$$\Theta^a_{\ b} \equiv \int \mathrm{d}u \, \mathrm{d}^3\alpha \, \sqrt{-g_{\mathrm{D7}}} \, U^a_{\ b}. \tag{4.60}$$

When the indices a and b are in SYM theory directions, we can identify $\langle T^a_{\ b} \rangle = \Theta^a_{\ b}$. The indices a and b can also be in the u or S^3 directions, however, in which case the SYM theory interpretation is more difficult. Following ref. [54], we will be able to provide a field theory interpretation for some, but not all, components.

We can compute $\Theta^a_{\ b}$ in two different ways. One way is to compute the variation of the D7-brane action, S_{D7}, with respect to the background metric. The other way is to use a Noether procedure, since the momenta are the generators of translation symmetries. We have used both methods and have found perfect agreement. The calculation by variation of the action is longer and more difficult than the Noether procedure, however, so we will not present it. The result of the Noether procedure is

$$\Theta^a_{\ b} = -\int du \left(L\, \delta^a_{\ b} + 2F_{cb} \frac{\delta L}{\delta F_{ac}} - \partial_b \theta \frac{\delta L}{\delta \partial_a \theta} \right) , \qquad (4.61)$$

where we have performed the trivial integration over the S^3.

We expect the last term in eq. (4.61) to contribute to $T^u_{\ u}$, given our ansatz $\theta(u)$. We find, however, that the last term in eq. (4.61) also contributes to the $T^\mu_{\ u}$ components with $\mu = t, x, y, z$. In other words, suppose we allow θ to depend on t, x, y, z. We then find that, taking the derivatives $\frac{\delta L}{\delta \partial_\mu \theta}$, with $\mu = t, x, y, z$, and then setting $\partial_\mu \theta = 0$ produces a non-zero result. This is very similar to what we saw for the polarization tensor above, where all six components were non-zero even though our solution has only E, B_x and B_z non-zero. We write explicit expressions for the derivatives $\frac{\delta L}{\delta \partial_\mu \theta}$ in the appendix.

We will now present all the components of the stress-energy tensor.

In the S^3 directions the only components are on the diagonal, and all are simply $-\int du\, L = S_{D7}$. The nontrivial components are in the (u, t, x, y, z) subspace. For notational simplicity, we will identify current components, $\langle J^\mu \rangle$, whenever possible, and we will not write $\int du$, which appears for every component. Primes denote $\frac{\partial}{\partial u}$.

The components with upper index t are

$$\Theta^t_{\ t} = -L - F_{xt}\frac{\delta L}{\delta F_{tx}} - F_{ut}\frac{\delta L}{\delta F_{tu}} = -L + E_x \frac{\partial L}{\partial E_x} + \langle J^t \rangle A'_t ,$$

$$\Theta^t_{\ x} = -F_{ux}\frac{\delta L}{\delta F_{tu}} - F_{yx}\frac{\delta L}{\delta F_{ty}} = \langle J^t \rangle A'_x - \frac{\partial L}{\partial E_y} B_z ,$$

$$\Theta^t_{\ y} = -F_{xy}\frac{\delta L}{\delta F_{tx}} - F_{zy}\frac{\delta L}{\delta F_{tz}} - F_{uy}\frac{\delta L}{\delta F_{tu}} = B_z \frac{\partial L}{\partial E_x} - B_x \frac{\partial L}{\partial E_z} + \langle J^t \rangle A'_y ,$$

$$\Theta^t_{\ z} = -F_{yz}\frac{\delta L}{\delta F_{ty}} - F_{uz}\frac{\delta L}{\delta F_{tu}} = B_x \frac{\partial L}{\partial E_y} + \langle J^t \rangle A'_z .$$

The components with upper index x are

$$\Theta^x_{\;t} = -F_{ut}\frac{\delta L}{\delta F_{xu}} = \langle J^x\rangle A'_t\,,$$

$$\Theta^x_{\;x} = -L - \frac{F_{tx}\delta L}{\delta F_{xt}} - \frac{F_{yx}\delta L}{\delta F_{xy}} - \frac{F_{ux}\delta L}{\delta F_{xu}} = -L + \frac{E_x\partial L}{\partial E_x} + \frac{B_z\partial L}{\partial B_z} + \langle J^x\rangle A'_x\,,$$

$$\Theta^x_{\;y} = -F_{zy}\frac{\delta L}{\delta F_{xz}} - F_{uy}\frac{\delta L}{\delta F_{xu}} = -B_x\frac{\partial L}{\partial B_y} + \langle J^x\rangle A'_y\,,$$

$$\Theta^x_{\;z} = -F_{yz}\frac{\delta L}{\delta F_{xy}} - F_{uz}\frac{\delta L}{\delta F_{xu}} = -B_x\frac{\partial L}{\partial B_z} + \langle J^x\rangle A'_z\,.$$

The components with upper index y are

$$\Theta^y_{\;t} = -F_{xt}\frac{\delta L}{\delta F_{yx}} - F_{ut}\frac{\delta L}{\delta F_{yu}} = E_x\frac{\partial L}{\partial B_z} + \langle J^y\rangle A'_t\,,$$

$$\Theta^y_{\;x} = -F_{ux}\frac{\delta L}{\delta F_{yu}} - F_{tx}\frac{\delta L}{\delta F_{yt}} = E_x\frac{\partial L}{\partial E_y} + \langle J^y\rangle A'_x\,,$$

$$\Theta^y_{\;y} = -L - \frac{F_{xy}\delta L}{\delta F_{yx}} - \frac{F_{zy}\delta L}{\delta F_{yz}} - \frac{F_{uy}\delta L}{\delta F_{yu}} = -L + \frac{B_z\partial L}{\partial B_z} + \frac{B_x\partial L}{\partial B_x} + \langle J^y\rangle A'_y\,,$$

$$\Theta^y_{\;z} = -F_{uz}\frac{\delta L}{\delta F_{yu}} = \langle J^y\rangle A'_z\,.$$

The components with upper index z are

$$\Theta^z_{\;t} = -F_{xt}\frac{\delta L}{\delta F_{zx}} - F_{ut}\frac{\delta L}{\delta F_{zu}} = -E_x\frac{\partial L}{\partial B_y} + \langle J^z\rangle A'_t\,,$$

$$\Theta^z_{\;x} = -F_{ux}\frac{\delta L}{\delta F_{zu}} - F_{tx}\frac{\delta L}{\delta F_{zt}} - F_{yx}\frac{\delta L}{\delta F_{zy}} = E_x\frac{\partial L}{\partial E_z} - B_z\frac{\partial L}{\partial B_x} + \langle J^z\rangle A'_x\,,$$

$$\Theta^z_{\;y} = -F_{xy}\frac{\delta L}{\delta F_{zx}} - F_{uy}\frac{\delta L}{\delta F_{zu}} = -B_z\frac{\partial L}{\partial B_y} + \langle J^z\rangle A'_y\,,$$

$$\Theta^z_{\;z} = -L - F_{yz}\frac{\delta L}{\delta F_{zy}} - F_{uz}\frac{\delta L}{\delta F_{zu}} = -L + B_x\frac{\partial L}{\partial B_x} + \langle J^z\rangle A'_z\,.$$

The components with upper index u are

$$\Theta^u_{\;t} = -F_{xt}\frac{\delta L}{\delta F_{ux}} = -\langle J^x\rangle E_x\,,$$

$$\Theta^u_{\;x} = -F_{tx}\frac{\delta L}{\delta F_{ut}} - F_{yx}\frac{\delta L}{\delta F_{uy}} = \langle J^t\rangle E_x + \langle J^y\rangle B_z\,,$$

$$\Theta^u_{\;y} = -F_{xy}\frac{\delta L}{\delta F_{ux}} - F_{zy}\frac{\delta L}{\delta F_{uz}} = -\langle J^x\rangle B_z + \langle J^z\rangle B_x\,,$$

$$\Theta^u_{\;z} = -F_{yz}\frac{\delta L}{\delta F_{uy}} = -\langle J^y\rangle B_x\,.$$

(4.62)

The components with lower index u are

$$\Theta^t{}_u = -A'_x \frac{\partial L}{\partial E_x} - A'_y \frac{\partial L}{\partial E_y} - A'_z \frac{\partial L}{\partial E_z} + \theta' \frac{\delta L}{\delta \partial_t \theta},$$

$$\Theta^x{}_u = A'_t \frac{\partial L}{\partial E_x} + A'_y \frac{\partial L}{\partial B_z} - A'_z \frac{\partial L}{\partial B_y} + \theta' \frac{\delta L}{\delta \partial_x \theta},$$

$$\Theta^y{}_u = A'_t \frac{\partial L}{\partial E_y} - A'_x \frac{\partial L}{\partial B_z} + A'_z \frac{\partial L}{\partial B_x} + \theta' \frac{\delta L}{\delta \partial_y \theta},$$

$$\Theta^z{}_u = A'_t \frac{\partial L}{\partial E_z} + A'_x \frac{\partial L}{\partial B_y} - A'_y \frac{\partial L}{\partial B_x} + \theta' \frac{\delta L}{\delta \partial_z \theta},$$

$$\Theta^u{}_u = -L - \sum_{\mu=t,x,y,z} F_{\mu u} \frac{\delta L}{\delta F_{u\mu}} + \theta' \frac{\delta L}{\delta \theta'} = -L + \sum_{\mu=t,x,y,z} \langle J^\mu \rangle A'_\mu + \theta' \frac{\delta L}{\delta \theta'}.$$

All quantities on the right-hand sides are evaluated on-shell.

We would like to convert the components of $\Theta^a{}_b$ to field theory quantities. In most cases, whether we can do so depends on whether we can perform the u integration. Sometimes this is easy. For example, we know that $\int du\, L = -S_{\mathrm{D7}} = \Omega$, and $\int du\, A'_t(u) = -\mu_{\mathrm{B}}$, where μ_{B} is the $\mathrm{U}(1)_{\mathrm{B}}$ chemical potential. In some cases we can translate to SYM theory quantities without doing the u integrals. For instance, terms with the derivatives $\frac{\partial L}{\partial F_{\mu\nu}}$ multiplying the u-independent quantities E_x, B_x, or B_z we can interpret as contributions from the polarization tensor, as explained above. On the other hand, we have not found a field theory interpretation for the components $\Theta^\mu{}_u$ with $\mu = t, x, y, z$ because the u integration is non-trivial. For many components, converting to SYM theory quantities requires integrating A'_x, A'_y, or A'_z, for which the field theory meaning is not immediately clear.

As discussed in ref. [54] (following ref. [149]), the components $\Theta^u{}_\mu$, with $\mu = t, x, y, z$, do have a clear interpretation in the SYM theory: they are proportional to rates of energy or momentum loss. To explain this, we return to the field theory side of the correspondence. Recall that in the presence of background electric and magnetic fields, the (non-)conservation law for the stress-energy tensor was

$$\partial^\mu \langle T_{\mu\nu} \rangle = F_{\nu\rho} \langle J^\rho \rangle. \tag{4.63}$$

For our spatially homogeneous solution, all the spatial derivatives on the left-hand side will vanish, leaving only the time derivatives. With our background fields and current, we thus have

$$\begin{aligned}
\partial_t \langle T^t{}_t \rangle &= -E_x \langle J^x \rangle, \\
\partial_t \langle T^t{}_x \rangle &= E_x \langle J^t \rangle + B_z \langle J^y \rangle, \\
\partial_t \langle T^t{}_y \rangle &= -B_z \langle J^x \rangle + B_x \langle J^z \rangle, \\
\partial_t \langle T^t{}_z \rangle &= -B_x \langle J^y \rangle.
\end{aligned} \tag{4.64}$$

Our system also has a net density of charge carriers in an external electric field. The electric field is thus doing net work on the system. The charge carriers (the flavor degrees of freedom) will transfer energy and momentum to the $\mathcal{N} = 4$ SYM plasma, so that, over time, the $\mathcal{N} = 4$ SYM plasma will heat up, and begin to move. Eq. (4.64) tells us the rates at which the energy and momentum of the flavor degrees of freedom are changing.

4.3.3 Energy and momentum loss rates

The energy and momentum loss rates on the right-hand-side of eq. (4.64) are identical to the components of the stress-energy tensor with upper index u and lower index $\mu = t, x, y, z$, the $\Theta^u{}_\mu$, up to a constant factor (4.62). In the expressions above for the $\Theta^u{}_\mu$, the constant factor comes from the integration over u (suppressed for notational clarity), which produces a factor $\int_0^{u_H} du = u_H = \frac{\sqrt{2}}{\pi T}$. The holographic calculation thus encodes the energy and momentum loss rates in the components of the stress-energy tensor with upper index u, as previously discussed in refs. [54, 149].

As an important aside, notice that our system has translation invariance, which implies momentum conservation. In other words, the system appears to have no mechanism for dissipation of momentum. Why then do we find a finite Ohmic conductivity, σ_{xx}? The answer comes from the probe limit, $N_f \ll N_c$. The very dilute flavor degrees of freedom will indeed transfer energy and momentum to the far more numerous $\mathcal{N} = 4$ SYM degrees of freedom, but the rates at which they do so are of order $N_f N_c$, as we can see from eq. (4.64). The rates go as factors of the $\langle J^\mu \rangle$ components times the external fields E, B_x and B_z. The $\langle J^\mu \rangle$ that we study are order $N_f N_c$, while the external fields are order one in the large N_c counting. We may thus conclude that only after a time on the order of N_c will the flavor degrees of freedom have transferred an order N_c^2 amount of energy and momentum to the $\mathcal{N} = 4$ SYM plasma. For earlier times, we may safely ignore the motion of the plasma, that is, the plasma will act as a reservoir into which the flavor fields may "dump" energy and momentum. For those early times, then, the probe limit allows the system to mimic a dissipative system, and hence we find our finite Ohmic conductivity. At late times (on the order of N_c), however, we could no longer ignore the motion of the plasma (and hence we would need to do a new calculation of the conductivity and stress-energy tensors).

Back on the supergravity side of the correspondence, the loss rates in eq. (4.64) also appear as divergences in the corresponding components of the D7-brane's stress-energy tensor, as explained in ref. [54]. Specifically, the energy and momentum densities $\Theta^t{}_\mu$ exhibit divergences coming from the $u = u_H$ endpoint of the u integration (which was suppressed for notational clarity above). Such divergences are familiar from the dragging string solution of refs. [37, 39], which represented a field theory process in which a single heavy charge carrier lost energy and momentum to the SYM plasma. We are

thus not too surprised to see similar divergences here, where we have a density of charge carriers.

The divergences in $\Theta^t{}_\mu$ appear to come from two sources. One is a divergence in our solution for $A'_x(u)$. If we Taylor expand our solution for $A'_x(u)$ in powers of $|g_{tt}|$, we find

$$A'_x(u) = -E_x \sqrt{\frac{g_{uu}}{|g_{tt}|}} + O\left(\sqrt{|g_{tt}|}\right), \tag{4.65}$$

so that $\int du\, A'_x(u)$, which appears in $\Theta^t{}_x$, produces a divergence at the $u = u_{\mathrm{H}}$ endpoint. In contrast, the other field strengths, $A'_t(u)$, $A'_y(u)$, and $A'_z(u)$, all vanish at the horizon (the leading term in their expansions in $\sqrt{|g_{tt}|}$) and hence these produce no divergences at $u = u_{\mathrm{H}}$.

The second source of divergences is from the derivatives $\frac{\partial L}{\partial E_i}$ with $i = x, y, z$. These are the bulk contributions to the electric polarizations, as explained above. Performing a Taylor expansion in $|g_{tt}|$ for these, we find

$$\frac{\partial L}{\partial E_i} = \langle J^i \rangle \sqrt{\frac{g_{uu}}{|g_{tt}|}} + O\left(\sqrt{|g_{tt}|}\right). \tag{4.66}$$

In the $\Theta^t{}_\mu$, these appear multiplied by E, B_x and B_z, so that the integral over u produces a divergence at $u = u_{\mathrm{H}}$. We note in passing that $\frac{\partial L}{\partial B_x}$, $\frac{\partial L}{\partial B_y}$, and $\frac{\partial L}{\partial B_z}$ have no such divergences (for each, the leading term is $\sqrt{|g_{tt}|}$).

Following ref. [54], we can relate the *coefficients* of the divergent terms with the loss rates in eq. (4.64) as follows. On the SYM theory side, the divergences comes from the infra-red (IR): the charges have been losing energy and momentum at constant rates for infinite *time*. To regulate the divergence, then, we want to consider charges moving for some finite time Δt. We can then identify the divergences in the $\Theta^t{}_\mu$ as the constant rates times Δt: $\partial_t \langle T^t{}_\mu \rangle \Delta t$. On the supergravity side, we should only include those parts of the spacetime that had time to communicate with the boundary in the time Δt. In particular, we would like the boundary to communicate with the horizon. We thus define Δt as the time required for a light ray to travel from the boundary to the horizon,

$$\Delta t = \int_0^{u_{\mathrm{H}} - \epsilon} du \sqrt{\frac{g_{uu}}{|g_{tt}|}}, \tag{4.67}$$

where we have introduced a regulator to make Δt finite: we integrate not to the horizon u_{H} but to some $u_{\mathrm{H}} - \epsilon$. As $\epsilon \to 0$, Δt diverges as $\frac{1}{\epsilon}$. Clearly the divergences in the $\Theta^t{}_\mu$ are of the form in eq. (4.67). We thus plug eqs. (4.65) and (4.66) into our expressions for the $\Theta^t{}_\mu$ above, and using eq. (4.67), we immediately reproduce the right-hand side of eq. (4.64). The holographic calculation thus encodes the energy and momentum loss rates in the coefficients of the $u = u_{\mathrm{H}}$ divergences of the $\Theta^t{}_\mu$, as discussed previously in ref. [54].

4.3.4 IR safe quantities

As also discussed in ref. [54], we can find observers who will not see the charges lose any energy or momentum. These observers will thus see no divergences; the energy and momenta they measure will be "IR-safe." We will identify two such observers, who we will call observer 1 and observer 2.

Observer 1 moves along with the charges. In that observer's reference frame, the charges are at rest (and the surrounding plasma is moving past), so obviously observer 1 will not see the charges lose energy or momentum. Observer 1 should thus see no divergences. More formally, observer 1 will have a four-velocity proportional to the charge current, $v_1^\mu \propto \langle J^\mu \rangle$. Notice that v_1^μ is thus covariantly constant, $\partial_\mu v_1^\nu = 0$. The mass-energy four-vector associated with observer 1 is then proportional to

$$I_1^\mu = \langle T^\mu_\nu \rangle \, v_1^\nu \propto \langle T^\mu_\nu \rangle \, \langle J^\nu \rangle,$$

and using $\partial_\mu \langle T^\mu_\nu \rangle = F_{\nu\alpha} \langle J^\alpha \rangle$, we can easily show that $\partial_\mu I_1^\mu = F_{\alpha\beta} \langle J^\alpha \rangle \langle J^\beta \rangle = 0$, so I_1^μ is a conserved current. Furthermore, I_1^μ is free of divergences, that is, if we write the t component explicitly,

$$I_1^t = \langle T^t_t \rangle \langle J^t \rangle + \langle T^t_x \rangle \langle J^x \rangle + \langle T^t_y \rangle \langle J^y \rangle + \langle T^t_z \rangle \langle J^z \rangle, \tag{4.68}$$

and insert our expressions for the $\langle T^t_\mu \rangle$ from our Θ^t_μ, we find that all the divergences (of the form $\sqrt{g_{uu}/|g_{tt}|}$) cancel exactly.

Observer 2 has four-velocity $v_2^\mu \propto \epsilon^{\mu\alpha\beta\gamma} F_{\alpha\beta} \langle J_\gamma \rangle$. Notice that v_2^μ is again covariantly constant, $\partial_\mu v_2^\nu = 0$, because the currents and external fields are constant. Notice also that observer 2 is moving orthogonally to observer 1, that is, their four-velocities are orthogonal: $v_1^\mu v_{2\,\mu} \propto \langle J_\mu \rangle \epsilon^{\mu\alpha\beta\gamma} F_{\alpha\beta} \langle J_\gamma \rangle = 0$. In fact, in the language of section 4.2 of ref. [165], v_2^μ is (proportional to) the magnetic field as measured by observer 1. The mass-energy four-vector of observer 2 is

$$I_2^\mu = \langle T^\mu_\nu \rangle \, v_2^\nu \propto \langle T^\mu_\nu \rangle \, \epsilon^{\nu\alpha\beta\gamma} F_{\alpha\beta} \langle J_\gamma \rangle, \tag{4.69}$$

and again using $\partial_\mu \langle T^\mu_\nu \rangle = F_{\nu\alpha} \langle J^\alpha \rangle$, we can show that $\partial_\mu I_2^\mu \propto (F \wedge F) J^2$, where $J^2 = J^\mu J_\mu$, so I_2^μ is only a conserved current when $F \wedge F \propto \vec{E} \cdot \vec{B} = 0$. In other words, when $\vec{E} \cdot \vec{B}$ is non-zero we should have $\partial_t I_2^t \propto (F \wedge F) J^2$, so that, as we saw for the stress-energy tensor, we should find a divergence in I_2^t whose coefficient is the loss rate, $(F \wedge F) J^2$. Indeed, a straightforward calculation shows that I_2^t includes the usual $\sqrt{g_{uu}/|g_{tt}|}$ divergence, with coefficient $(F \wedge F) J^2$. Observer 2 only sees an "IR-safe" conserved current I_2^μ when $\vec{E} \cdot \vec{B} = 0$.

4.4 Summary and outlook

Using the holographic setup described in section 4.2, we computed the conductivity tensor, and the contribution to the stress-energy tensor, of $\mathcal{N} = 2$

supersymmetric flavor fields propagating through a strongly-coupled $\mathcal{N} = 4$ SYM theory plasma at temperature T. We included a finite $\mathrm{U}(1)_{\mathrm{B}}$ density $\langle J^t \rangle$ and considered the most general configuration of constant external fields, namely an electric field E and a magnetic field with a component B_z perpendicular to E and a component B_x parallel to E. We also discussed divergences in the flavor fields' contribution to the stress-energy tensor, and discussed some "IR-safe" quantities that are free from these divergences.

Outlook We suggest three obvious directions for future research. The first would be a direct extension of our work, while the latter two would be tangentially related.

First, as mentioned in the introduction, we could study transport of the charge associated with the current I_2^μ discussed in section 4.3. In particular, the authors of ref. [156] (following the results of refs. [154, 155]) showed that associated with any current with an $\vec{E} \cdot \vec{B}$ anomaly is a special transport coefficient whose form is fixed by the anomaly coefficient and the equation of state. Our I_2^μ is appears to be such an anomalous current, hence the kinetic coefficient associated with transport of I_2^μ charge should take the form determined in ref. [156].

Second, we could introduce a thermal gradient into the holographic setup and compute the thermal conductivity and the thermo-electric transport coefficients (called α_{ij} in the introduction) associated with the flavor fields. A further extension would be to work with two coincident D7-branes, and hence two flavors in the SYM theory, and to compute the thermal conductivity and thermo-electric transport coefficients associated with isospin charge. As demonstrated in refs. [17, 18, 138], a sufficiently large isospin chemical potential triggers a phase transition to a superconducting (more accurately, superfluid) phase, so a holographic study of thermo-electric transport may be relevant for high-T_c superconductors, which exhibit unusually large thermo-electric response even outside the superconducting phase.

Third, we could compute the full conductivity tensor of $\mathcal{N} = 4$ SYM theory itself (without flavor), which remains to be done. To date, only the longitudinal conductivity, which we called σ_{xx}, has been computed. To compute σ_{xy} and σ_{xz} for $\mathcal{N} = 4$ SYM theory holographically would require new supergravity solutions, however. In particular, a non-zero Hall current requires a non-zero density and a non-zero magnetic field, hence we would first need to find a supergravity solution describing a dyonic black hole. Such a solution exists for $(3 + 1)$-dimensional AdS, but not yet for $(4 + 1)$-dimensional AdS.

Toy model for holographic thermalization

In general, the process of thermalization is described by an initially *far-from-equilibrium* state evolving to *equilibrium*. Within gauge/gravity duality the holographic thermalization may be described by considering time-dependent configurations on the gravity side, for instance a gravitational collapse of a matter configuration in Anti-de Sitter space leading to the formation of a black hole horizon. As a further step towards studying strongly coupled system *far-from-equilibrium*, in this chapter we consider a time-dependent process in the bulk of AdS space which is relevant for the formulation of holographic thermalization of strongly coupled field theory.

5.1 Motivation and introduction

AdS/CFT correspondence states that strongly coupled quantum field theory in d dimensions at finite temperature in thermal equilibrium can be described in terms of supergravity in a $(d+1)$-dimensional background AdS_{d+1} of AdS black hole geometry [93]. This prescription has been proven to be particularly useful for describing properties of the strongly coupled quark-gluon plasma (QGP) created at RHIC. For describing the process of thermalization of QGP, it is essential to consider the relaxation from an initial non-equilibrium state to a final state in thermal equilibrium. Within gauge/gravity duality, this is expected to be modeled by time-dependent AdS geometries which evolve to form AdS black holes.

Usually, describing time-dependent geometries is a difficult task and often requires heavy use of numerics. One approach is to study the collision of gravitational shock waves in AdS space [55–59, 62–64, 66]. Different aspects of heavy ion collisions have been studied in shock wave collision models, such as early time dynamics [55, 56, 63, 64], entropy production and critical

conditions on thermalization [57–62, 65]. More recently, the initial value problem for the non-linear Einstein equations has been solved numerically for planar gravitational shock waves [66]. Despite the success of this approach, information other than the one-point function of the stress tensor remains very difficult to obtain due to the complexity of the metric resulting from the collision.

An alternative approach is to consider a collapsing matter distribution in AdS space. It is natural to assume that in order to model far from equilibrium processes in quantum field theories and the relaxation into equilibrium, the supergravity picture should describe the dynamical process of black hole formation from some initially regular spacetime. A mathematically clearly arranged setup is e. g. given by an infinitesimally thin but massive shell which collapses to form a stable black hole as a final state. So far, the collapsing shell scenario has been considered in the quasi-static approximation where the shell is considered to move adiabatically [40, 41, 67, 68], which simplifies the calculations significantly. In these approaches, a collapsing thin shell geometry is probed by a scalar field or a graviton field. The dual boundary two-point correlator is calculated as a function of the radial position of the shell and thus describes the thermalization process.

A slightly different avenue in this context has been followed by [42–44]. The authors of [44] demonstrate analytically that a weak scalar perturbation collapses to form a black hole. The authors of [42, 43] investigate the gravitational collapse of energy injected into AdS space and the formation of an event horizon by considering the evolution of locally anisotropic metric perturbations initially located near the AdS boundary. At a late stage, the numerical results match with the analytical solutions based on an asymptotic expansion [166, 167]. An interesting link between the thin shell and perturbative approaches described above has recently been established in [168–170]. The evolutions of entanglement entropy in $d = 2$ and $d = 3$ have been studied in a Vaidya metric describing a collapsing shell in the formation of a black hole. In [170] the equal-time two-point function, Wilson loop and entanglement entropy are explored in various dimensions.

The content of this chapter closely relies on [2] where we start a program in view of studying gravitational collapse of a thin matter shell beyond the quasi-static approximation considered [41]. Looking for a method of evaluating two-point functions for time-dependent gravity duals, we consider a simple toy model for a time-dependent geometry. This model consists of a mirror moving in the bulk of the AdS space. We impose Dirichlet boundary conditions at the position of the mirror and calculate the two-point function of a scalar field in this geometry. In the special case of the mirror moving with constant velocity, scaling symmetry of AdS space is preserved. We compute the two point function based on the eigenmode decomposition and find that the singularities of the two-point correlator are related to the physics of bouncing light ray between the moving mirror and the AdS boundary, see figs. 5.1 and 5.2. Thus

the singularity structure of the correlator is determined by a geometric optics picture. Our results generalize the static mirror case considered in [69] to the time-dependent case.

We explore the geometric optics limit in more detail with a WKB analysis, which enables us to reduce a general PDE to an ODE. This approach leads to a *procedure* for calculating the two-point correlator for general trajectories of the mirror along the radial direction of the AdS space (5.52). The final formula for the correlator is expressed as a Mellin transform involving the ratio of incoming and outgoing waves for each component in the eigenmode decomposition. We test our procedure using two sample trajectories of the mirror. In the first case of a mirror moving with constant velocity, we reproduce the geometric optics limit of the two-point correlator found previously using scaling variables. In the second case where a 'mirror' moves along a spacelike geodesic, we find the singularities of the correlator are consistent with the bulk-cone singularities conjecture [171], which states that the two-point correlator becomes singular when the two boundary points are connected by a bulk null geodesic. The application of this conjecture to a collapsing shell model establishes a connection between a distinct signature for the boundary observables and horizon formation in the bulk.

This chapter is organized as follows. In section 5.2 we solve the eigenmodes of the scalar wave equation in the presence of a mirror moving with constant velocity. In section 5.3, we derive an explicit formula for the time-dependent, spatially integrated two-point correlator in terms of the eigenmodes. It takes the form of a Mellin transform. We test this formula by considering its vacuum limit, where the mirror is absent. In section 5.4, based on a WKB analysis we establish a more general prescription for the two-point function which allows for an arbitrary mirror trajectory. We test the prescription by reproducing the geometric optics limit of the correlator obtained previously. In section 5.4.2 we test our correlator prescription for a mirror moving along a spacelike geodesic and find results which are consistent with the bulk cone singularities conjecture [171]. Some details of the computation are moved to the appendices.

The content presented in the following sections has been obtained in a collaboration with Johanna Erdmenger and Shu Lin [2].

5.2 Moving mirror in AdS_{d+1}

In this section, we calculate the scalar two-point function for a special trajectory of the mirror which preserves scaling symmetry. We work with the AdS_{d+1} metric in the Poincaré patch

$$\mathrm{d}s^2 = \frac{R^2}{z^2}\left(-\mathrm{d}t^2 + \mathrm{d}\vec{x}^2 + \mathrm{d}z^2\right)\,, \tag{5.1}$$

and start with the standard scalar wave equation

$$\frac{1}{\sqrt{-g}}\partial_\mu(\sqrt{-g}g^{\mu\nu}\partial_\nu)\phi = 0\,. \tag{5.2}$$

The usual way of solving the equation of motion is to consider a specific Fourier component $\phi(t, z) = e^{i\omega t}\phi(\omega, z)$ to reduce the PDE to an ODE. In other words, the equation of motion is simplified by focusing on an eigenfunction of the operator ∂_t. We know from quantum mechanics that this is possible, since the operator ∂_t commutes with the Lagrangian operator

$$\mathcal{L} \equiv \frac{1}{\sqrt{-g}}\partial_\mu(\sqrt{-g}g^{\mu\nu}\partial_\nu) = \frac{z^2}{R^2}(-\partial_t^2 + \nabla^2 + \partial_z^2) - \frac{(d-1)z}{R^2}\partial_z\,. \tag{5.3}$$

An alternative explanation for the commutation of ∂_t and $\mathcal{L}$ comes from the fact that time translation symmetry is an isometry of AdS_{d+1}. In the presence of a moving mirror along the radial coordinate, the time translation symmetry will be broken by the Dirichlet boundary condition on the mirror.

Defining $\bar{t} = \frac{t}{R}$, $\bar{x} = \frac{x}{R}$, $\bar{z} = \frac{z}{R}$, we can write $\mathcal{L}$ in terms of dimensionless coordinates $\bar{t}$, $\bar{x}$ and $\bar{z}$. In the following the bar will be suppressed and we should keep in mind that physical quantities are measured in units of the AdS radius R. Although the time translation symmetry is broken, scaling symmetry can be preserved for some special mirror trajectories. The scaling symmetry is generated by the operator

$$\mathcal{L}_x = x^\mu\partial_\mu = t\,\partial_t + \vec{x}\,\vec{\nabla} + z\partial_z\,. \tag{5.4}$$

We can verify explicitly that $[\mathcal{L}, \mathcal{L}_x] = 0$. For simplicity, we focus on solutions which depend on $(t,\, z)$ only. Solving the eigenvalue equation, we obtain

$$\mathcal{L}_x\phi = \lambda\phi \Rightarrow \phi = v^{\lambda/2}f(u)\,, \tag{5.5}$$

with $v = tz$, $u = \frac{t}{z}$ and f being an arbitrary function of u. An obvious choice of the mirror trajectory that preserves the scaling symmetry is $t/z = u_0$, i.e. a mirror moving with constant velocity $1/u_0$. The general solution to (5.3) is given by

$$\begin{aligned}
f(u) = &A\,u^{-\lambda/2}\,(u-1)^{\lambda+\frac{1-d}{2}}\,F\left(\frac{1-d}{2}, \frac{1+d}{2}; \lambda+\frac{3-d}{2}; \frac{1-u}{2}\right)\\
&+ B\,u^{-\lambda/2}\,(u+1)^{\lambda+\frac{1-d}{2}}\,F\left(\frac{1-d}{2}, \frac{1+d}{2}; -\lambda+\frac{1+d}{2}; \frac{1-u}{2}\right).
\end{aligned} \tag{5.6}$$

The solution $\phi(u, v) = v^{\frac{\lambda}{2}}f(u)$ is analogous to the solution in momentum representation, $\phi(t, z) = e^{i\omega t}\phi(\omega, z)$. Here, $\phi(u, v)$ describes the common

eigenfunction of the Lagrangian $\mathcal{L}$ and the scaling operator $\mathcal{L}_x$. We can view λ as playing the role of the frequency ω. Writing the solution in the more familiar coordinates (t, z), we have

$$\phi(t, z) = A\, z^{\frac{d-1}{2}} (t - z)^{\lambda + \frac{1-d}{2}} F\left(\frac{1-d}{2}, \frac{1+d}{2}; \lambda + \frac{3-d}{2}; \frac{1 - t/z}{2}\right)$$
$$+ B\, z^{\frac{d-1}{2}} (t + z)^{\lambda + \frac{1-d}{2}} F\left(\frac{1-d}{2}, \frac{1+d}{2}; -\lambda + \frac{1+d}{2}; \frac{1 - t/z}{2}\right). \tag{5.7}$$

Near the boundary at $z = 0$, we find that the scalar field given by (5.7) behaves as

$$\phi(t, z) \sim t^\lambda + \cdots + z^d t^{\lambda - d} + \cdots \tag{5.8}$$

The two exponents correspond to non-normalizable and normalizable modes in AdS, respectively. In the flat limit $z \to \infty$, i.e. in the deep interior of AdS, (5.7) becomes

$$\phi(t, z) \sim z^{\frac{d-1}{2}} \left(a(\lambda)\, (t + z)^{\lambda + \frac{1-d}{2}} + b(\lambda)\, (t - z)^{\lambda + \frac{1-d}{2}} \right), \tag{5.9}$$

with $a(\lambda)$ and $b(\lambda)$ two λ-dependent constants. Obviously, $(t + z)^{\lambda + \frac{1-d}{2}}$ and $(t - z)^{\lambda + \frac{1-d}{2}}$ in (5.9) correspond to outgoing and incoming waves. Comparing (5.9) to the flat limit of ingoing and outcoming contributions to the scalar wave in momentum representation,

$$\phi(t, z) = z^{\frac{d}{2}} e^{i\omega t} H^{(1)}_{\frac{d}{2}}(\omega z) \propto z^{\frac{d-1}{2}} e^{i\omega(t+z)},$$
$$\phi(t, z) = z^{\frac{d}{2}} e^{i\omega t} H^{(2)}_{\frac{d}{2}}(\omega z) \propto z^{\frac{d-1}{2}} e^{i\omega(t-z)}, \tag{5.10}$$

we conclude that λ should take the value $\lambda = \frac{d-1}{2} + i\Lambda$ with Λ an arbitrary real number. We now rewrite λ as $\lambda = \lambda' - \frac{1-d}{2}$, such that λ' is purely imaginary. In terms of λ', (5.7) becomes

$$\phi(t, z) = A z^{\frac{d-1}{2}} (t - z)^{\lambda'} F\left(\frac{1-d}{2}, \frac{1+d}{2}; \lambda' + 1; \frac{1 - t/z}{2}\right)$$
$$+ B z^{\frac{d-1}{2}} (t + z)^{\lambda'} F\left(\frac{1-d}{2}, \frac{1+d}{2}; -\lambda' + 1; \frac{1 - t/z}{2}\right). \tag{5.11}$$

For simplicity, we drop the prime on λ in the subsequent.
The Dirichlet boundary condition at $u = t/z = u_0$ fixes the ratio of A and B,

$$\frac{A}{B} \left(\frac{u_0 - 1}{u_0 + 1}\right)^\lambda F\left(\frac{1-d}{2}, \frac{1+d}{2}; \lambda + 1; \frac{1 - u_0}{2}\right) =$$
$$- F\left(\frac{1-d}{2}, \frac{1+d}{2}; 1 - \lambda; \frac{1 - u_0}{2}\right). \tag{5.12}$$

5.3 The two-point correlator

In this section, we will use the solution of the scalar in the bulk to compute the correlation functions of the dual operator in the boundary field theory. We are interested in computing the correlation functions in coordinate space. We perform the "Fourier space" analysis for the transformation to λ space in general d dimensions instead of setting $d = 4$.

5.3.1 Derivation of the correlator

We will follow [12] for the computation of the two point correlator[1]. The two point correlator of the operator dual to a massless scalar in AdS_{d+1} is given by

$$G(x, x') = \langle O(x)O(x') \rangle = \frac{\delta^2 S}{\delta\phi^0(x)\delta\phi^0(x')}, \qquad (5.13)$$

where S is the action of the scalar field. Using a regulator near the boundary $z = \epsilon$, the resultant action reads[2]

$$
\begin{aligned}
S_\epsilon &= \frac{1}{2} \int \mathrm{d}z\mathrm{d}t\mathrm{d}^{d-1}x \sqrt{-g}g^{\mu\nu}\partial_\mu\phi\partial_\nu\phi \\
&= \frac{1}{2} \int \mathrm{d}t\mathrm{d}^{d-1}x \frac{1}{z^{d-1}}\phi\partial_z\phi|_\epsilon^{z_m(t)} - \frac{1}{2} \int \mathrm{d}z\mathrm{d}t\mathrm{d}^{d-1}x\phi\partial_\mu(\sqrt{-g}g^{\mu\nu}\partial_\nu\phi) .
\end{aligned}
\qquad (5.14)
$$

The second term vanishes by the bulk equation of motion. Furthermore, by the Dirichlet boundary condition ϕ vanishes at the locus of the mirror $z_m(t)$ and we are left with

$$S_\epsilon = -\frac{1}{2} \int \mathrm{d}t\,\mathrm{d}^{d-1}x\phi(t, z)\frac{\partial_z\phi(t, z)}{z^{d-1}}|_{z=\epsilon} . \qquad (5.15)$$

Note that our scalar wave in the bulk has no dependence on spatial x. The vertex that couples the source $\phi(t, x)$, the boundary value of $\phi(t, x, z)$, with the operator $O(t, x)$ simplifies to

$$\int \mathrm{d}t\,\mathrm{d}^{d-1}x\phi(t, x)O(t, x) = \int \mathrm{d}t\phi(t) \int \mathrm{d}^{d-1}xO(t, x) . \qquad (5.16)$$

The functional derivative of the action with respect to $\phi(t)$ gives

$$\langle \int \mathrm{d}^{d-1}xO(t, x) \int \mathrm{d}^{d-1}x'O(t', x') \rangle = -\lim_{z\to 0} \frac{\delta\partial_z\phi(t, z)}{z^{d-1}\delta\phi(t', z)}\text{Vol}, \quad (5.17)$$

---

[1]Note a subtlety involved in this procedure is elaborated in [172], but this does not affect our result for the massless scalar.

[2]We will suppress the overall normalization from the SUGRA action in this thesis.

with Vol $= \int d^{d-1}x$ being the spatial volume, since we assume a spatially infinite mirror that does not break translational invariance in spatial dimensions. The causal nature of (5.17) will be specified in each explicit example later and discussed in section 4.

Expanding (5.11) near $z = 0$, the solution to (5.2) takes the form

$$\phi_\lambda(t, z) = K(d, \lambda, A, B)\, t^{\lambda + \frac{d-1}{2}} + \cdots + L(d, \lambda, A, B)\, t^{\lambda - \frac{d+1}{2}} z^d + \cdots , \quad (5.18)$$

with

$$K(d, \lambda, A, B) = \left(\frac{1}{2}\right)^{\frac{-1+d}{2}} \frac{\Gamma(d)}{\Gamma(\frac{1+d}{2})} \left[\frac{\Gamma(1+\lambda)}{\Gamma(\frac{1+d}{2} + \lambda)} A + \frac{\Gamma(1-\lambda)}{\Gamma(\frac{1+d}{2} - \lambda)} B\right],$$

$$L(d, \lambda, A, B) = \left(\frac{1}{2}\right)^{\frac{-1-d}{2}} \frac{\Gamma(-d)}{\Gamma(\frac{1-d}{2})} \left[\frac{\Gamma(1+\lambda)}{\Gamma(\frac{1-d}{2} + \lambda)} A + \frac{\Gamma(1-\lambda)}{\Gamma(\frac{1-d}{2} - \lambda)} B\right],$$

$$(5.19)$$

and the $\cdots$ denote terms of the form $W(d, \lambda)z^{d'}$ with integer $d' \neq d$. We do not write down $W(d, \lambda)z^{d'}$ explicitly, since they do not contribute to the two-point correlation functions (5.17). Using the eigenfunction (5.6) as a basis set, we can express an arbitrary wave $\phi(t, z)$ as a superposition of $\phi_\lambda(t, z)$, namely

$$\phi(t, z) = \int \phi_\lambda(t, z) g(\lambda) \mathrm{d}\lambda = \int \phi_\lambda^0(t) g(\lambda) \mathrm{d}\lambda + \cdots + z^d \int \phi_\lambda^d(t) g(\lambda) \mathrm{d}\lambda + \cdots$$

$$\equiv \phi^0(t) \cdots + z^d\, \phi^d(t) + \cdots .$$

$$(5.20)$$

Here $g(\lambda)$ describes the weighting function for the component $\phi_\lambda(t, z)$ with eigenvalue λ. In the following we will look for an explicit expression for the weighting function $g(\lambda)$, then using that result we will be able to write $\phi^d(t)$ as a functional of $\phi^0(t)$. This is the crucial step to determine the two point-correlator coming from inserting (5.20) in (5.17), giving

$$\langle \int \mathrm{d}^{d-1}x\, O(t, x) O(t', 0)\rangle = -d \frac{\delta\phi^d(t)}{\delta\phi^0(t')}, \quad (5.21)$$

where contact terms from $\cdots$ in (5.20) are excluded.

At the moment we do not care about the causal nature of the correlator (5.21), but later we will discuss it in subsection 5.3.2. The relevant explicit decomposition of $\phi^0(t)$ and $\phi^d(t)$ defined in (5.20) are obtained from (5.18) as

$$\phi^0(t) = \int_{-i\infty}^{+i\infty} K(d, \lambda, A, B)\, t^{\lambda + \frac{d-1}{2}}\, g(\lambda)\, \mathrm{d}\lambda, \quad (5.22\text{a})$$

$$\phi^d(t) = \int_{-i\infty}^{+i\infty} L(d, \lambda, A, B)\, t^{\lambda - \frac{d+1}{2}}\, g(\lambda)\, \mathrm{d}\lambda. \quad (5.22\text{b})$$

Defining $\bar{\phi}^0(t) = \phi^0(\frac{1}{t})$, we identify (5.22a) as the inverse Mellin transform. This observation allows us to invert (5.22a) using the Mellin transform and obtain $g(\lambda)$ via the relation

$$K(d, \lambda, A, B)\, g(\lambda) = \frac{1}{2\pi i} \int_0^\infty \bar{\phi}^0(t) t^{\lambda + \frac{d-3}{2}}\, \mathrm{d}t = \frac{1}{2\pi i} \int_0^\infty \phi^0(t') t'^{-\lambda - \frac{d+1}{2}}\, \mathrm{d}t', \tag{5.23}$$

where in the intermediate step, a change of variable $t = 1/t'$ is used. Plugging (5.23) to (5.22b), we obtain

$$\phi^d(t) = \frac{1}{2\pi i} \int_{-i\infty}^{+i\infty} \frac{L(d, \lambda, A, B)}{K(d, \lambda, A, B)} t^\lambda \int_0^\infty t'^{-\lambda} (tt')^{-\frac{d+1}{2}} \phi^0(t')\, \mathrm{d}t' \mathrm{d}\lambda. \tag{5.24}$$

Using (5.21), we end up with the correlator in the integral representation

$$\langle \int \mathrm{d}^{d-1} x\, O(t, x) O(t', 0) \rangle = -\frac{d}{2\pi i} \int_{-i\infty}^{+i\infty} \frac{L(d, \lambda, A, B)}{K(d, \lambda, A, B)} \times \frac{t^\lambda t'^{-\lambda}}{(tt')^{\frac{d+1}{2}}} \mathrm{d}\lambda, \tag{5.25}$$

with $K(d, \lambda, A, B)$ and $L(d, \lambda, A, B)$ defined in (5.19) and A, B satisfying (5.12).

Before we proceed to the evaluation of this expression, let's make some comments on the correlator (5.25) :

- As is common in Minkowski signature, the correlator obtained from (5.25) will depend on the specific wave we use in the bulk. In the mirror geometry, the causal structure of the correlator is in general complicated. In a certain limit, it should reduce to the retarded ($B = 0$) or advanced ($A = 0$) correlator. We will see later that the limiting correlator does agree with those obtained in momentum space representation;

- We have derived the correlator for $u_0 > 1$, which is defined for $t, t' > 0$. Actually most formulae are equally true for $u_0 < -1$, corresponding to $t, t' < 0$. We will however, focus on the case $u_0 > 1$ for definiteness in what follows;

- Our moving mirror does not introduce any dissipation to the background, the correlator should therefore be real;

- The correlator should be finite. We note the possible divergent factor $\frac{\Gamma(-d)}{\Gamma(\frac{1-d}{2})}$ when $d = 2, 4, 6 \cdots$. This potential pole should be cancelled out by the λ-integral.[3]

---

[3] In those dimensions, the scalar wave contains a logarithmically divergent term near the boundary, which is encoded in the definition of the Hypergeometric function.

5.3.2 Different limits of the correlator

Before evaluating the integral (5.25), let us look at the limit $B = 0$ and $A = 0$. These correspond to the incoming and outgoing waves, respectively. We should expect (5.25) to give retarded and advanced correlators from experience in the momentum space representation. We show in the following that this is also true in the λ representation, which will serve as a nontrivial check of our prescription. For definiteness, we choose $t, t' > 0$. At $B = 0$, the λ dependent part of the integrand simplifies to $\frac{\Gamma(\lambda + \frac{1+d}{2})}{\Gamma(\lambda + \frac{1-d}{2})} \left(\frac{t}{t'}\right)^{\lambda}$. The poles in the complex λ plane are at $\lambda = -n - \frac{1+d}{2}$ with integer $n \geq 0$. The integral is only nonvanishing when the integration contour is closed counter-clockwise, i.e. when $t > t'$. Summing over residues, we obtain for the correlator defined in (5.21)

$$\frac{\delta \phi^d(t)}{\delta \phi^0(t')} = \theta(t - t') \frac{2^d}{(t - t')^{d+1}} \frac{\Gamma(\frac{1+d}{2})}{\Gamma(\frac{1-d}{2}) \Gamma(d)} \, . \tag{5.26}$$

For $A = 0$, the situation is quite similar. The λ-dependent integrand simplifies to $\frac{\Gamma(\frac{1+d}{2} - \lambda)}{\Gamma(\frac{1-d}{2} - \lambda)} \left(\frac{t}{t'}\right)^{\lambda}$, with the poles located at $\lambda = n + \frac{1+d}{2}$ with integer $n \geq 0$. Physically we require $d \geq 1$, and as a result the integral is only nonvanishing when the integration contour is closed clockwise, i.e. when $t < t'$. Summing over the residues, we obtain

$$\frac{\delta \phi^d(t)}{\delta \phi^0(t')} = \theta(t' - t) \frac{2^d}{(t' - t)^{d+1}} \frac{\Gamma(\frac{1+d}{2})}{\Gamma(\frac{1-d}{2}) \Gamma(d)} \tag{5.27}$$

for the correlator. Let us now compare this result with the standard momentum and frequency representation, in which the incoming wave is given by

$$\phi_{in} = \begin{cases} z^{d/2} H^{(2)}_{\frac{d}{2}}(\omega z) & \omega > 0 \\ z^{d/2} H^{(1)}_{\frac{d}{2}}(-\omega z) & \omega < 0, \end{cases} \tag{5.28}$$

which gives rise to

$$\frac{\delta \phi^d(\omega)}{\delta \phi^0(\omega)} = \begin{cases} -e^{\frac{i\pi d}{2}} \frac{\Gamma(1 - \frac{d}{2})}{\Gamma(1 + \frac{d}{2})} \left(\frac{\omega}{2}\right)^d & \omega > 0 \\ -e^{\frac{-i\pi d}{2}} \frac{\Gamma(1 - \frac{d}{2})}{\Gamma(1 + \frac{d}{2})} \left(\frac{-\omega}{2}\right)^d & \omega < 0 \, . \end{cases} \tag{5.29}$$

Fourier transforming the above back to coordinate space, we obtain

$$\frac{\delta \phi^d(t)}{\delta \phi^0(t')} = -\theta(t - t') \frac{\Gamma(d + 1)}{(t - t')^{d+1}} \frac{\Gamma(1 - \frac{d}{2})}{\Gamma(1 + \frac{d}{2})} \frac{\cos\left(\pi(d + \frac{1}{2})\right)}{2^d \, \pi} \, . \tag{5.30}$$

After writing the cos-term as a product of two Γ-functions and using some relations between the Γ-functions, it can be shown that (5.30) and (5.26)

are indeed identical, demonstrating the equivalence of using the λ or the ω representation.

Keen readers may have noticed that our correlator vanishes for odd d. This is true in the domain of time we are interested in, i.e. for $t \neq t'$. In appendix B.2, we present explicit examples of spatially integrated correlators for $d = 3$ and 4 starting with a general formula for unintegrated correlators in CFT[4]. These examples clearly display the subtle difference between the calculation in odd and even dimensions.

A similar analysis shows that the advanced correlator obtained from the momentum representation also agrees with (5.27). This boosts our confidence in the λ representation of the correlator, and we will extract the time-dependent correlator in the moving mirror background using this representation.

We focus on the UV part of the correlator following the work in [69]. Specifically, these authors of [69] show that the UV part of the correlator, i.e. the part obtained by considering only frequencies with $|\omega| \gg 1$, has an equivalent description in terms of geometric optics in AdS. Moreover, they found that the singularities of the correlator correspond to the time when the light ray bouncing between the AdS boundary and the mirror hits the boundary. This is a special case of the bulk-cone singularities conjecture presented in [171]. The latter, originally formulated in global AdS space, states that the singularities occur when the two boundary points are connected by a bulk null geodesic, i.e. by a light ray trajectory. In the Poincaré patch, the light ray will not return to the boundary without being reflected at the mirror. It should be stressed that while the authors of [69] use a static mirror in AdS which introduces an explicit scale to the boundary CFT, our mirror moves in such a way that scale invariance of the boundary CFT is still preserved. Therefore, the UV limit of our case amounts to summing over all residues in the complex λ plane, with $|\lambda| \gg 1$. As we will see, the geometric picture is robust in our moving mirror geometry.

The UV part of the correlator is evaluated in appendix B.1 . As explained there in detail, the causal nature of the correlator is related to the chosen integration contour of λ. In particular, in the UV limit, which amounts in

---

[4]At $t = t'$, there is a non-analyticity resulting from the lightcone non-analyticity of the unintegrated correlators.
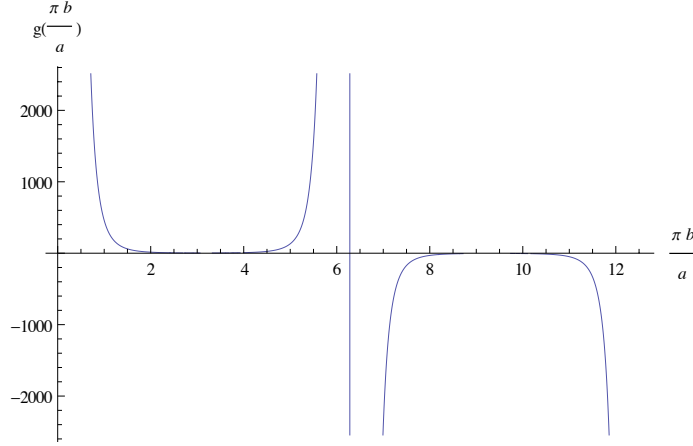
FIGURE 5.1: The correlator contribution $g\left(\frac{\pi b}{a}\right)$ as defined in (5.31) versus $\frac{\pi b}{a}$ at $d = 4$. $g\left(\frac{\pi b}{a}\right)$ has a period of 4π. In every odd interval $(2n\pi, (2n + 1)\pi)$, the correlator is positive, while in every even interval $((2n + 1)\pi, (2n + 2)\pi)$, the correlator flips sign

particular to using the relations (B.3), the retarded correlator is given by

$$
\left\langle \mathrm{d}^{d-1}xO(t,x)O(t',0)\right\rangle_R = -\theta(t - t') \sum_{+,-}(tt')^{\frac{-d-1}{2}} d\left(\frac{2}{a}\right)^d
$$
$$
\times \frac{1 - e^{\mp i\pi d}}{a} \frac{\Gamma(-d)\Gamma(\frac{1+d}{2})}{\Gamma(\frac{1-d}{2})\Gamma(d)} e^{\pm\frac{i\pi(d-1)}{2}(\frac{b}{a}-c)}
$$
$$
\times \left[\frac{d!}{(-c)^{d+1}(\pm i2\pi)} - \sum_{r=0}^{\infty} \frac{B_{d+r+1}(\frac{d-1}{4})c^r(\pm i2\pi)^{d+r}}{r!(d + r + 1)}\right]
$$
$$
\equiv -\theta(t - t')\frac{d}{a^{d+1}}(tt')^{\frac{-d-1}{2}}g\left(\frac{\pi b}{a}\right),
$$

$$(5.31)$$

with $a = \ln\frac{u_0+1}{u_0-1}$ and $b = \ln\frac{t}{t'}$. $B_n(x)$ are the Bernoulli polynomials and

$$
e^{i2\pi c} = e^{\frac{i2\pi b}{a}}, \quad |c| < \frac{1}{2}. \tag{5.32}
$$

Note that the square bracket is only a function of c, which according to (5.32) is a periodic function with period 1. As $c \to 0$, the first term in the square bracket is singular while the second term is regular. The correlator diverges when $b/a = n$, with $n \in \mathbb{N}$. Another interesting observation is that for odd dimensions ($d = 1, 3, \cdots$), the correlator vanishes identically due to the d-dependent prefactor, which is a remnant of the behavior of the vacuum correlator.
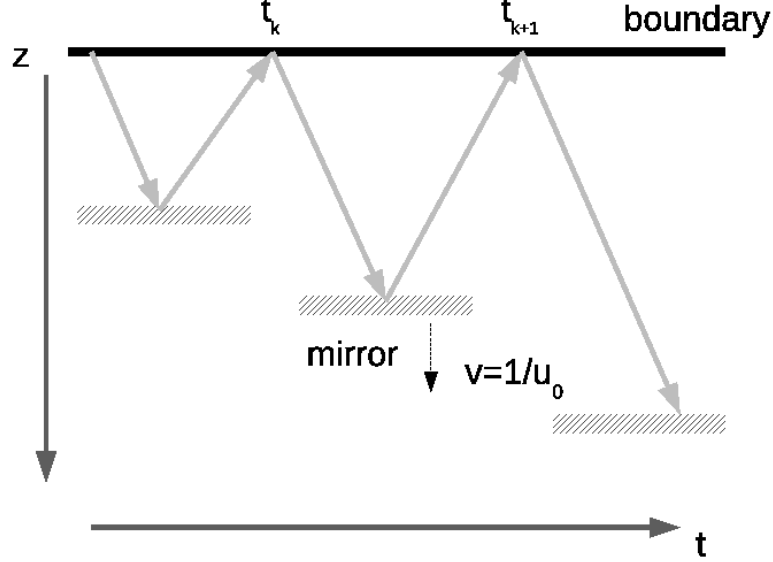
FIGURE 5.2: A schematic picture of a moving mirror in the AdS background, and the trajectory of a bouncing light ray. The correlator we obtain displays a singularity structure in agreement with this geometric optics picture.

The periodic divergence of the correlator in the moving mirror geometry is consistent with the expectation from the geometric optics limit proposed in [69]: Suppose the mirror starts moving with velocity $1/u_0$ at $t = 0$ from the AdS boundary. If at t_k the light ray reaches the boundary, it is easy to see that the next time the light ray hits the boundary will be at $t_{k+1} = \frac{u_0+1}{u_0-1}t_k$, thus $\ln \frac{t_{k+1}}{t_k} = \ln \frac{u_0+1}{u_0-1}$, which amounts to $b = a$. Indeed at $b/a = n$ when b is an integer multiple of a, we observe singularities in the correlator. A plot of the correlator is included in Fig.5.1. The structure of the correlator deserves some explanations: The function $g\left(\frac{\pi b}{a}\right)$ has a period of 4π, which is due to the oscillatory factor $e^{\pm \frac{i\pi(d-1)}{2}(\frac{b}{a}-c)} = e^{\pm \frac{i\pi(d-1)}{2}n}$. The period of the singularities in the correlator is 2π because there are two singularities in one period of $g\left(\frac{\pi b}{a}\right)$. From (5.31), one might expect the period to be π, however half of the singularities vanish as we sum over the plus and minus contributions in (5.31). This is an artifact of choosing the retarded correlator. The Feynman correlator e.g. will pick either a plus or a minus sign, displaying the other half of the singularities explicitly. We have also included a view of a bouncing light ray in the presence of the moving mirror in Fig. 5.2. This figure shows schematically that the time separation of the singularities increases with time as the mirror moves further and further away from the boundary.

5.4 Moving mirror in the limit of geometric optics

As we have derived in the previous section, the two point correlator in the UV limit contains singularities when the times are related by a geometric optics path. In this section, we make this connection more precise. In particular, we develop a prescription for calculating the two-point function for general trajectories of the mirror. As a test of our prescription, we reproduce the result of the two-point function obtained in the previous section.

5.4.1 The WKB approximation and the limit of geometric optics

The geometric optics limit can be described by a WKB solution for the scalar wave in the AdS background. Let us write the scalar wave as $\phi = A e^{i\theta/\epsilon}$, with A and θ being the amplitude and the phase of the wave. The essence of the WKB approximation is that the phase θ varies much faster than the amplitude A. We plug $\phi = A e^{i\theta/\epsilon}$ to the equation of motion $\Box\phi = 0$ and perform a series expansion in ϵ. The equation of motion for A and θ are given by the leading order and next-to-leading order terms[5]

$$-\dot{\theta}^2 + \theta'^2 = 0\,, \tag{5.33}$$

$$-2\dot{A}\dot{\theta} + 2A'\theta' + (-\ddot{\theta} + \theta'')A - \frac{d-1}{z}A\theta' = 0\,, \tag{5.34}$$

where the dot and prime denote derivatives with respect to t and z, respectively. The first equation can be solved for $\theta = \theta_\pm(t \pm z)$. They will be used to eliminate the bracket in the second equation. The latter is solved by $A = z^{\frac{d-1}{2}} A_\pm(t \pm z)$. The positive and negative sign solutions have obvious identifications as outgoing and incoming waves. They form two linearly independent solutions to the EoM. Therefore, we split the solution of $\Box\phi = 0$ into

$$\phi(t,z) = z^{\frac{d-1}{2}} \left(A_+(t+z) e^{\frac{i\theta_+(t+z)}{\epsilon}} + A_-(t-z) e^{\frac{i\theta_-(t-z)}{\epsilon}} \right)$$

$$\equiv z^{\frac{d-1}{2}} \left(F_+(t+z) + F_-(t-z) \right)\,. \tag{5.35}$$

The WKB solution breaks down near the singularities of the original equation of motion $\Box\phi = 0$. In the case of the AdS background, the only singularity is the AdS boundary $z = 0$. Near the AdS boundary, a general scalar wave can be written as a superposition of eigenmodes,

$$\phi(t,z) = \int \left[g_-(\lambda) z^{\frac{d-1}{2}} (t-z)^\lambda F\left(\frac{1-d}{2}, \frac{1+d}{2}; \lambda+1; \frac{1-t/z}{2} \right) \right.$$

$$\left. + g_+(\lambda) z^{\frac{d-1}{2}} (t+z)^\lambda F\left(\frac{1-d}{2}, \frac{1+d}{2}; -\lambda+1; \frac{1-t/z}{2} \right) \right] d\lambda\,.$$

---

[5]We focus only on spatially homogeneous solutions and discard derivatives with respect to $\vec{x}$.

$$(5.36)$$

where $g_\pm(\lambda)$ are the weighting functions for the incoming and outgoing components with eigenvalue λ, respectively. In the UV limit $|\lambda| \to \infty$, (5.36) can be nicely matched with the WKB solution. Since $\lim_{\gamma \to \infty} F(\alpha, \beta; \gamma; z) = 1$, equation (5.36) simplifies to

$$\phi(t, z) = z^{\frac{d-1}{2}} \int \left[g_-(\lambda)(t - z)^\lambda + g_+(\lambda)(t + z)^\lambda \right] d\lambda \,, \qquad (5.37)$$

and we identify

$$F_+(t + z) = \int g_+(\lambda)(t + z)^\lambda d\lambda \,, \qquad (5.38)$$

$$F_-(t - z) = \int g_-(\lambda)(t - z)^\lambda d\lambda \,, \qquad (5.39)$$

with F_+ and F_- defined in (5.35).

We now aim for an expression for the correlator in a more general time-dependent situation, where the mirror follows a general, not necessarily scale invariant trajectory. Before proceeding to the derivation of such an expression, let us take a moment to look at the setting of the problem. Since we are interested in a time-dependent scalar wave in the bulk, which amounts to solving a 2D PDE (in the absence of $\vec{x}$ dependence), we need to specify both boundary conditions and initial conditions in order to have a unique solution. The boundary conditions are provided by the source at the AdS boundary and the Dirichlet boundary condition at the mirror. There is no further initial condition.

The mirror with trajectory $z = t/u_0$ is special in the sense that it allows us to study the "steady wave" (analogous to a planar wave in the AdS background), which does not require an initial condition. This particular trajectory does not couple the eigenmodes with different λ and allows us to determine a ratio $\frac{g_+(\lambda)}{g_-(\lambda)}$ for every λ. In terms of the boundary field theory, the missing initial condition is encoded in the state on which the operator $O(t, x)$ acts.

In non-equilibrium field theory, the correlator should be studied using the in-in contour [173, 174], which is composed of one forward and one backward contour in the complex time plane. This was formulated holographically in real-time gauge/gravity duality by Skenderis and van Rees [175–177]. The state should be prepared by inserting sources in the Euclidean segments of the in-in contour. One of the essential points of [175–177] is that the bulk solution should be completely fixed by matching the Lorentzian segments to the Euclidean ones. The matching effectively provides the initial condition. Our mirror can be viewed as an effective source which creates the state. Despite the ambiguity related to the missing initial condition as described below (5.39), we will see that taking the UV limit as before actually allows us to obtain the wave solution without specifying an initial condition. In the UV limit $|\lambda| \to \infty$, the

solution in the bulk only depends on $t \pm z$, as defined in (5.35), thus reducing the PDE to an ODE.

To solve the wave equation, we start with the Dirichlet boundary condition on the trajectory of the mirror which implies that the wave vanishes there,

$$\int \left[g_-(\lambda)\,(t - z_m(t))^\lambda + g_+(\lambda)(t + z_m(t))^\lambda \right] \mathrm{d}\lambda = 0 \,. \tag{5.40}$$

Here and below, we suppress the integration bounds, with the understanding that the λ integral runs always from $-i\infty$ to $+i\infty$, while the t integral runs from 0 to ∞. This is to be combined with the asymptotic behavior near $z = 0$ similar to (5.18), where the unique weighting function $g(\lambda)$ in (5.20) is replaced by the more general weighting functions $g_\pm(\lambda)$ as described in (5.36),

$$\phi^0(t) = \left(\frac{1}{2}\right)^{\frac{d-1}{2}} \frac{\Gamma(d)}{\Gamma(\frac{1+d}{2})} \int \left(K_+(\lambda)\,g_-(\lambda) + K_-(\lambda)\,g_+(\lambda) \right) t^{\lambda + \frac{d-1}{2}} \,\mathrm{d}\lambda \,, \tag{5.41}$$

with

$$K_+(\lambda) = \frac{\Gamma(1 + \lambda)}{\Gamma(\frac{1+d}{2} + \lambda)} \,, \quad K_-(\lambda) = \frac{\Gamma(1 - \lambda)}{\Gamma(\frac{1+d}{2} - \lambda)} \,. \tag{5.42}$$

For the sake of clarity, we introduce a shorthand notation $\tilde{\phi}(\lambda)$ defined as

$$\tilde{\phi}(\lambda) \equiv K_+(\lambda)g_-(\lambda) + K_-(\lambda)g_+(\lambda) \,, \tag{5.43}$$

hence equation (5.41) can be written as

$$\phi^0(t) = \left(\frac{1}{2}\right)^{\frac{d-1}{2}} \frac{\Gamma(d)}{\Gamma(\frac{1+d}{2})} \int \tilde{\phi}(\lambda)\, t^{\lambda + \frac{d-1}{2}} \,\mathrm{d}\lambda. \tag{5.44}$$

Next we will use equations (5.40) and the definition in (5.43) to write $g_\pm(\lambda)$ in terms of $\tilde{\phi}(\lambda)$. Later we will use the Mellin transform of (5.44) to express $g_\pm(\lambda)$ as functions $\phi^0(t)$. Then using these results, we can determine the coefficient function $\phi^d(t)$ as an expression of $\phi^0(t)$ and compute the two-point correlation functions. First using (5.43) for rewriting (5.40), we obtain two relations

$$\int \left(K_+(t + z_m)^\lambda - K_-(t - z_m)^\lambda \right) \frac{g_-}{K_-}\mathrm{d}\lambda = \int \frac{\tilde{\phi}(\lambda)}{K_-}(t + z_m)^\lambda \mathrm{d}\lambda \,,$$

$$\int \left(K_-(t - z_m)^\lambda - K_+(t + z_m)^\lambda \right) \frac{g_+}{K_+}\mathrm{d}\lambda = \int \frac{\tilde{\phi}(\lambda)}{K_+}(t - z_m)^\lambda \mathrm{d}\lambda \,. \tag{5.45}$$

Defining $\mathcal{D}_F(\lambda, t)$ as the inverse of the time-dependent part on the LHS of (5.45) with respect to integration over t, i.e.

$$K_+(\lambda')(t + z_m(t))^{\lambda'} - K_-(\lambda')(t - z_m(t))^{\lambda'} \equiv F(\lambda', t),$$

$$\int \mathrm{d}t\, \mathcal{D}_F(\lambda, t) F(\lambda', t) = \frac{1}{i}\delta\left(\frac{\lambda - \lambda'}{i}\right). \qquad (5.46)$$

The insertion of the i's is to remind us that λ and λ' are purely imaginary. The solutions for (5.45) can be formally written as

$$\frac{g_-(\lambda)}{K_-(\lambda)} = \int \mathrm{d}t \mathrm{d}\lambda'\, \mathcal{D}_F(\lambda, t) \frac{\tilde{\phi}(\lambda')}{K_-(\lambda')}(t + z_m)^{\lambda'},$$

$$\frac{g_+(\lambda)}{K_+(\lambda)} = -\int \mathrm{d}t \mathrm{d}\lambda'\, \mathcal{D}_F(\lambda, t) \frac{\tilde{\phi}(\lambda')}{K_+(\lambda')}(t - z_m)^{\lambda'}, \qquad (5.47)$$

respectively. The next step is to determine the near boundary coefficient function $\phi^d(t)$ in terms of $\phi^0(t)$. Similarly to (5.41), $\phi^d(t)$ is given by

$$\phi^d(t) = \left(\frac{1}{2}\right)^{\frac{-1-d}{2}} \frac{\Gamma(-d)}{\Gamma(\frac{1-d}{2})} \int \left(L_+(\lambda)\, g_-(\lambda) + L_-(\lambda)\, g_+(\lambda)\right) t^{\lambda - \frac{d+1}{2}} \mathrm{d}\lambda, \qquad (5.48)$$

with

$$L_+(\lambda) = \frac{\Gamma(1+\lambda)}{\Gamma(\frac{1-d}{2}+\lambda)}, \quad L_-(\lambda) = \frac{\Gamma(1-\lambda)}{\Gamma(\frac{1-d}{2}-\lambda)}. \qquad (5.49)$$

After using the Mellin transform of (5.44)

$$\tilde{\phi}(\lambda') = \frac{1}{2\pi i} \frac{\Gamma(\frac{1+d}{2})}{\Gamma(d)} \left(\frac{1}{2}\right)^{\frac{-d+1}{2}} \int \mathrm{d}t'\phi^0(t') t'^{-\lambda' - \frac{d+1}{2}} \qquad (5.50)$$

to replace $\tilde{\phi}(\lambda')$ by $\phi^0(t')$ in (5.47) and then inserting (5.47) into (5.48), we obtain

$$\phi^d(t) = \frac{2^d}{2\pi i} \frac{\Gamma(-d)\Gamma(\frac{1+d}{2})}{\Gamma(\frac{1-d}{2})\Gamma(d)} \int \mathrm{d}\lambda \mathrm{d}\lambda' \mathrm{d}t'' \mathcal{A}(\lambda, \lambda', t'', z_m(t'')) \int \mathrm{d}t'\phi^0(t') \frac{t^\lambda t'^{-\lambda'}}{(tt')^{\frac{d+1}{2}}},$$

$$\mathcal{A} \equiv \mathcal{D}_F(\lambda, t'') \left(L_+(\lambda)K_-(\lambda)\frac{(t'' + z_m)^{\lambda'}}{K_-(\lambda')} - L_-(\lambda)K_+(\lambda)\frac{(t'' - z_m)^{\lambda'}}{K_+(\lambda')}\right). \qquad (5.51)$$

Using (5.21), we end up with the correlator in the integral representation,

$$\left\langle \int d^{d-1}x O(t, x) O(t', 0) \right\rangle = \frac{-2^d d}{2\pi i} \frac{\Gamma(-d)\Gamma(\frac{1+d}{2})}{\Gamma(\frac{1-d}{2})\Gamma(d)} \int \mathrm{d}\lambda \mathrm{d}\lambda' \mathrm{d}t'' \mathcal{A} \frac{t^\lambda t'^{-\lambda'}}{(tt')^{\frac{d+1}{2}}}.$$

$$\text{(5.52)}$$

This is our main result. The main difference between (5.52) and (5.25) are the integrations over λ' and t'' in (5.52) which encode the motion of the mirror for non-constant velocity. In the following we will see that (5.52) and (5.25) indeed give the same results if the mirror moves with constant velocity along the radial coordinate. For this purpose, we apply the result (5.52) to the case of a mirror moving with constant velocity $t/z_m = u_0$. Then $F(\lambda, t)$ and its inverse $\mathcal{D}_F(\lambda, t)$ defined in (5.46) are given by

$$F(\lambda, t) = \left(K_+(\lambda) \left(1 + \frac{1}{u_0} \right)^\lambda - K_-(\lambda) \left(1 - \frac{1}{u_0} \right)^\lambda \right) t^\lambda, \quad \text{(5.53)}$$

$$\mathcal{D}_F(\lambda, t) = \frac{1}{2\pi i} \frac{t^{-\lambda - 1}}{K_+(\lambda)(1 + \frac{1}{u_0})^\lambda - K_-(\lambda)(1 - \frac{1}{u_0})^\lambda}. \quad \text{(5.54)}$$

Plugging the above expression to (5.52), we see the integrals of t'' and λ' are trivial. The final integral of λ is identical to (5.25) up to setting the hypergeometric function to 1, which is precisely the UV limit which we used in appendix B.1 for the evaluation of the correlator. As a result, we are bound to reproduce (5.31).

5.4.2 The correlator for mirror's spacelike geodesics

In this section, we will illustrate the procedure for obtaining the correlator in the presence of a mirror moving with non-constant velocity. We will see that the results are again consistent with expectations from geometric optics. The procedure derived in the previous subsection works for any trajectory of the mirror, but in practice this is hard to deal with for complicated trajectories, since it involves the inversion of the integral operator in order to obtain $\mathcal{D}_F(\lambda, t)$ from $F(\lambda, t)$. In principle, this is possible to calculate by applying the Fredholm theory [178]. However, this can be extremely complicated. We aim at finding some special trajectories which can lead to significant simplifications of the inversion procedure. We will see that it is possible at least in the UV limit.

Suppose we propose the trajectory with $t - z_m = \frac{1}{t + z_m}$, or equivalently $z_m = \sqrt{t^2 - 1}$, defined for $t > 1$. This is a spacelike trajectory, thus cannot be associated with a physical mirror. We should understand it as providing a boundary condition in the bulk. Since this is a spacelike trajectory, any light emitted from the boundary into the bulk after $t = 1$ will not catch the 'mirror' and no reflection is expected. Therefore, we should not see any singularities in the two point correlator according to the geometric optics picture. We will confirm this by explicitly computing the correlator in the UV limit.

Note that $F(\lambda, t) = K_+(\lambda)(t + z_m)^\lambda - K_-(\lambda)(t - z_m)^\lambda$ as defined in (5.46) and $K_+(\lambda) = K_-(-\lambda)$. With the proposed trajectory, we have

$$F(\lambda, t) = K_+(\lambda)(t + z_m)^\lambda - K_+(-\lambda)(t + z_m)^{-\lambda} = -F(-\lambda, t). \quad \text{(5.55)}$$

In the limit $\lambda \to \infty$, $K_+(\lambda) = \frac{\Gamma(\lambda+1)}{\Gamma(\lambda+\frac{1+d}{2})} \sim \lambda^{\frac{1-d}{2}}$, where the argument is fixed by $|\arg(\lambda)| < \pi$. Writing $\lambda = i\Lambda$, we have the explicit expression for $F(\lambda, t)$

$$
\begin{aligned}
F(\lambda, t) &= \mathrm{sgn}(\Lambda) \, |\Lambda|^{\frac{1-d}{2}} \, 2i \, \sin\left(|\Lambda| \tilde{t} + \frac{\pi(1-d)}{4}\right) \\
&= \mathrm{sgn}(\Lambda) |\Lambda|^{\frac{1-d}{2}} \, 2i \, \cos\left(|\Lambda| \tilde{t} - \frac{\pi(1+d)}{4}\right),
\end{aligned}
\tag{5.56}
$$

with $\tilde{t} = \ln(t + z_m)$. To solve for $\int \mathrm{d}t \mathcal{D}_F(\lambda', t) F(\lambda, t) = \frac{1}{i} \delta(\frac{\lambda - \lambda'}{i})$, we look at the UV limit of the orthogonality relation of Bessel functions

$$
\int_0^\infty x J_\nu(\xi x) J_\nu(\xi' x) \mathrm{d}x = \frac{\delta(\xi - \xi')}{\xi}
$$

$$
\Rightarrow \frac{2}{\pi} \int_0^\infty \cos(\xi x - \frac{\pi\nu}{2} - \frac{\pi}{4}) \cos(\xi' x - \frac{\pi\nu}{2} - \frac{\pi}{4}) \mathrm{d}x = \delta(\xi - \xi').
\tag{5.57}
$$

For this case we are able to identify the kernel defined in (5.47) explicitly. The expression above implies that $\mathcal{D}_F(\lambda, t) = \frac{\mathrm{sgn}(\Lambda)}{|\Lambda|^{\frac{1-d}{2}} 2i} \cos\left(|\Lambda| \tilde{t} - \frac{\pi(1+d)}{4}\right) \frac{2}{\pi i} \frac{1 + z_m'}{t + z_m}$. This formula is only defined on the imaginary axis, but has a natural and useful extension in the complex plane,

$$
\mathcal{D}_F(\lambda, t) = -\frac{1}{2\pi i} \left(e^{\lambda \tilde{t}} \frac{1}{K_-(\lambda)} - e^{-\lambda \tilde{t}} \frac{1}{K_+(\lambda)}\right) \frac{1 + z_m'}{t + z_m}.
\tag{5.58}
$$

To further simplify (5.51), we define

$$
\bar{F}(\lambda, t) = K_+(\lambda)(t + z_m)^\lambda + K_-(\lambda)(t - z_m)^\lambda,
\tag{5.59}
$$

and express $(t \pm z_m)^\lambda$ in terms of $F(\lambda, t)$ and $\bar{F}(\lambda, t)$,

$$
\frac{(t \pm z_m)^\lambda}{K_\mp(\lambda)} = \frac{\pm F(\lambda, t) + \bar{F}(\lambda, t)}{2K_+(\lambda) K_-(\lambda)}.
\tag{5.60}
$$

Inserting (5.60) into (5.51), we obtain

$$
\begin{aligned}
\frac{\delta\phi^d(t)}{\delta\phi^0(t')} ={}& \frac{2^{d-1}}{2\pi i} \frac{\Gamma(-d)\Gamma(\frac{1+d}{2})}{\Gamma(\frac{1-d}{2})\Gamma(d)} \int \mathrm{d}t'' \mathrm{d}\lambda \mathrm{d}\lambda' \frac{t^{\lambda - \frac{1+d}{2}} t'^{-\lambda' - \frac{1+d}{2}}}{K_-(\lambda') K_+(\lambda')} \\
&\times \left[P(\lambda) \mathcal{D}_F(\lambda, t'') F(\lambda', t'') + Q(\lambda) \mathcal{D}_F(\lambda, t'') \bar{F}(\lambda', t'')\right],
\end{aligned}
\tag{5.61}
$$

with $P(\lambda) = L_+(\lambda) K_-(\lambda) + L_-(\lambda) K_+(\lambda)$ and $Q(\lambda) = L_+(\lambda) K_-(\lambda) - L_-(\lambda) K_+(\lambda)$. Using the definition of $\mathcal{D}_F$, the $P(\lambda)$ term can be simplified to

$$
\begin{aligned}
& \frac{2^{d-1}}{2\pi i} \frac{\Gamma(-d)\Gamma(\frac{1+d}{2})}{\Gamma(\frac{1-d}{2})\Gamma(d)} \int \left(\frac{L_+(\lambda)}{K_+(\lambda)} + \frac{L_-(\lambda)}{K_-(\lambda)}\right) \left(\frac{t}{t'}\right)^{\lambda - \frac{1+d}{2}} \mathrm{d}\lambda \\
&= 2^{d-1} \frac{\Gamma(\frac{1+d}{2})}{\Gamma(\frac{1-d}{2})\Gamma(d)} \left(\theta(t - t') \frac{1}{(t - t')^{d+1}} + \theta(t' - t) \frac{1}{(t' - t)^{d+1}}\right).
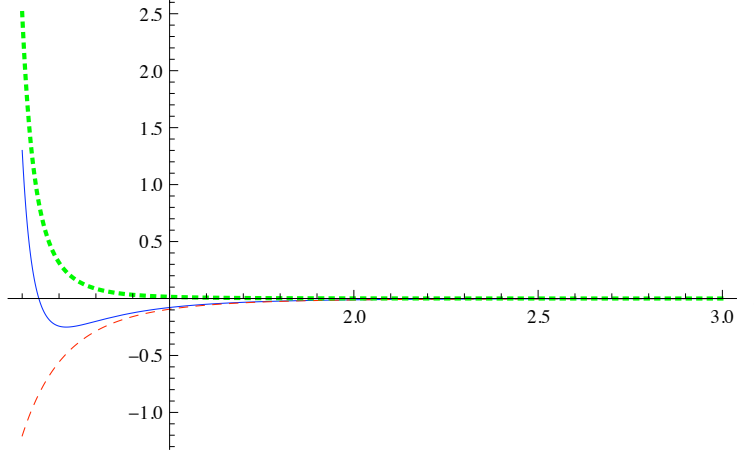\end{aligned}
$$

FIGURE 5.3: The correlator (5.63) as a function of t for $t' = 2$ at $d = 4$. The green dotted and red dashed lines represent the first and second terms in the square bracket, respectively. The blue solid line is their sum.

This is just the average of the retarded and advanced correlators in the vacuum. We will not include this piece since we are only interested in a state (trajectory) dependent contribution to the correlator, which is given by the $Q(\lambda)$ term in (5.61). Let us rewrite (5.61) without the $P(\lambda)$-term in the explicit form

$$
\frac{\delta\phi^d(t)}{\delta\phi^0(t')} = \frac{-2^{d-1}}{(2\pi i)^2} \frac{\Gamma(-d)\Gamma(\frac{1+d}{2})}{\Gamma(\frac{1-d}{2})\Gamma(d)} \int d\tilde{t} d\lambda d\lambda' \frac{t^{\lambda - \frac{1+d}{2}} t'^{-\lambda' - \frac{1+d}{2}}}{K_+(\lambda')K_-(\lambda')} \left(\frac{e^{\lambda\tilde{t}}}{K_-(\lambda)} - \frac{e^{-\lambda\tilde{t}}}{K_+(\lambda)} \right)
$$

$$
\times \left(e^{\lambda'\tilde{t}} K_+(\lambda') + e^{-\lambda'\tilde{t}} K_-(\lambda') \right) \left[L_+(\lambda)K_-(\lambda) - K_+(\lambda)L_-(\lambda) \right],
$$
(5.62)

with $K_\pm$, $L_\pm$ given by (5.42), (5.49). We perform this integral in appendix B.3, with the result

$$
\left\langle \int d^{d-1}x \, TO(t,x)O(t',0) \right\rangle = \frac{d \, 2^{d-1}}{\Gamma(d)} \frac{\Gamma(\frac{1+d}{2})}{\Gamma(\frac{1-d}{2})} \left[-\frac{1}{(tt'-1)^{1+d}} + \right.
$$

$$
\left. \frac{\Gamma(\frac{1+d}{2})}{2\Gamma(\frac{1-d}{2})\Gamma(1+d)} F\left(1+d, \frac{3+d}{2}, 2+d; \frac{t'-t}{(t'-1)\,t}\right) \frac{1}{(tt'-t)^{1+d}} \right]
$$
(5.63)

for the correlator defined in (5.21). This result is displayed in fig. 5.3. Note that we have specified the correlator as a time-ordered one. This is because we focused on only one segment in the in-in contour. The causal nature follows from the principle of the real-time gauge/gravity duality [175–177].

We see that the d-dependence of the correlator is qualitatively similar to the constantly moving mirror case. It is again finite for even dimensions and

zero for odd dimensions, a reminiscent of vacuum correlator. Turning to the singularities of the correlator, we see that the first term has singularities at $t = t' = 1$. The hypergeometric function in the second term can be expressed in terms of elementary functions, but this is not necessary for our purposes. Singularities appear when the argument $\frac{t'-t}{(t'-1)t}$ becomes 0, 1 or ∞, corresponding to $t = t'$, $t = 1$ or $t' = 1$ respectively. The singularity at $t = t'$ is just the usual lightcone one. The singularities at $t = 1$ and $t' = 1$ are closely related to the starting time of the mirror. No other singularity is found in the correlator, consistent with the geometric optics expectation. This example provides a further nontrivial check for our approach.

We note that the relatively simple procedure leading to the two-point correlator is related to the $SO(1,1)$ symmetry preserved by the 'mirror' trajectory $t^2 - z^2 = 1$. We expect that a method for solving the wave equation exists which is similar to that of Section 2, introducing variables which make the symmetry manifest. It will be interesting to see whether the two-point correlator following from such a method agrees with the result given by the general prescription, away from the singularities.

5.5   Summary and outlook

To summarize, we have solved the time-dependent problem of a spatially homogeneous scalar wave equation in AdS space in the presence of a radially moving mirror. First we considered a mirror with constant velocity which preserves scaling symmetry. We used the complete set of solutions to obtain the spatially integrated time-dependent two-point function for the CFT state defined by the moving mirror geometry. We found the result to be consistent with a geometric optics picture, in agreement with the bulk-cone singularities conjecture of [171].

Moreover, we have determined the precise relation between the geometric optics limit and the WKB approximation to the scalar wave solution. The established connection allows us to solve the scalar wave equation beyond scaling symmetry. As the main results of this work, we have established a formula for the two-point function corresponding to a moving mirror geometry with arbitrary trajectory, valid in the UV limit. We have tested this formula by reproducing the two-point function in the case of a mirror moving with constant velocity obtained before. We performed a further nontrivial check by considering a spacelike trajectory of the 'mirror' (which is not reached by the light ray in this case). We found that the singularities of the result are again consistent with a geometric optics picture.

Outlook   Let us compare our results for two-point functions of a massless scalar field with light-like separation to previous discussions of space-like separation, for instance those of [168, 179, 180]. There it was pointed out that

for large masses, or alternatively for large conformal dimension, the correlator is dominated by the contribution of the space-like geodesic joining the two points. Our result is that the pole structure of the correlator is determined by the geometric optics limit, i.e. by the trajectory of a light ray, is an analogous statement for the light-like case valid also for the massless case corresponding to small conformal dimension. We expect that our proposed study of correlators in thermalization geometries along the lines developed in this thesis will also allow for a further study of the role of geodesics for correlators in these geometries.

Moreover, our analysis provides essential technical tools for the study of two-point function in time-dependent geometries. These tools may now serve as a starting point for studying the behaviour of two-point functions during thermalization in strongly coupled field theories. A possible generalization of our results is to apply our prescription to the boost-invariant background of [166]. The idea is again to match the bulk WKB solution to a near-boundary solution, which is expressed as a superposition of the eigenmodes in pure AdS background. Due to the additional proper time τ appearing in the boost invariant metric, both the WKB solution and the eigenmode set consistent with scaling symmetry will take a different form from the one discussed in this thesis. This will give rise to a proper time dependent correlator with rapidity and transverse space coordinates integrated out, instead of a time dependent spatially integrated correlator. A direct application to [166] with infalling boundary conditions of the wave imposed on the horizon will allow us to obtain the quasi-normal modes beyond the adiabatic approximation used in [181].

Conclusions and outlook

We have presented some applications of the gauge/gravity duality towards studying field theory systems at strong coupling. The systems studied in this thesis might be used as models for describing condensed matter physics near the quantum critical point and the physics of quark-gluon plasma which has been recently created at RHIC. Moreover, we follow the line of considering different gravity setups whose dual descriptions show interesting phenomena in thermal equilibrium, slightly out-of-equilibrium and far-from-equilibrium.

In particular, starting with looking at phenomena of strongly coupled systems in thermal equilibrium, in chapter 3 we study quantum phase transitions in holographic superfluidity at finite baryon density and isospin density in an imbalanced mixture. We apply two approaches, namely a bottom-up approach in section 3.3 using an $U(2)$ Einstein-Yang-Mills theory with back-reaction and a top-down approach in section 3.4 using a D3/D7 model setup. The results obtained in chapter 3 are discussed in detail in section 3.4.4. Here, we summarize some of the main results. Studying the phase diagrams, in both approaches we observe quantum phase transitions from a normal to a superfluid phase and indications for the existence of quantum critical points. The quantum phase transition, however, is different in the two systems. In the D3/D7 brane setup we always find a second order phase transition. In the Einstein-Yang-Mills theory, depending on the strength of the back-reaction, we obtain a continuous or first order transition. While in the D3/D7 model setup, the phase diagram and the position of the QCP can be determined only via a numerical method, in the Einstein-Yang-Mills setup we can relate the position of the QCP with the instability due to the violation of the Breitenlohner-Freedman bound and found a critical ratio of the baryon and isospin chemical

$$\left(\frac{\mu_{\mathrm{B}}}{\mu_{\mathrm{I}}}\right)_c = \frac{\sqrt{1 - 3\alpha_{\mathrm{YM}}^2}}{\sqrt{3}\,\alpha_{\mathrm{MW}}}\,. \tag{6.1}$$

at the QCP. In the semi-probe limit, where only the back-reaction of the $U(1)$

Maxwell field is taken into account, i.e. $\alpha_{\mathrm{YM}} = 0$ and $\alpha_{\mathrm{MW}} \neq 0$, we are able to solve the equations of motion analytically at small baryon chemical potential and reproduce the phase diagram in this regime, see fig. 3.7. Comparing our results with those obtained from QCD in [49, 50], we find many interesting similarities, but also differences concerning the order of phase transitions whose origin has not been resolved completely.

Taking a first step away from studying dual field theories in thermal equilibrium, we use another D3/D7 model setup to describe properties of flavor transport in a $\mathcal{N} = 4$ SYM plasma. Motivated by the work in [51] where an universal non-linear behavior near the quantum critical point has been found, such as in conductivity. In chapter 4 we use a holographic method introduced [52] to compute the conductivity tensor of flavor fields beyond linear response. Thereby, we generalize the results in [53, 54] by including an additional component of the magnetic field, just extending the case of *perpendicular* orientation between the magnetic and electric field studied in [53, 54] to the case of *arbitrary* orientations. We calculate the energy and momentum loss rates of the flavor fields to the SYM plasma. The results obtained in this part of the thesis have been summarized in section 4.4. As the main results in this chapter, we compute the *full* conductivity tensor with the new transport coefficient σ_{xz} which could not be obtained with the setups in [52, 53]. Computing the energy and momentum loss rates as in [54], we find a covariant form of a current with an $\vec{E} \cdot \vec{B}$ anomaly

$$I_2^\mu = \langle T^\mu_\nu \rangle \, v_2^\nu \propto \langle T^\mu_\nu \rangle \, \epsilon^{\nu\alpha\beta\gamma} \, F_{\alpha\beta} \, \langle J_\gamma \rangle \,, \tag{6.2}$$

whose corresponding kinetic coefficient is of relevance to a new transport coefficient in hydrodynamics which has been only recently discovered in the context of gauge/gravity duality [156].

Following the line of using gauge/gravity duality for studying phenomena of strongly coupled systems in a thermal equilibrium towards an out-of-equilibrium state, in chapter 5, we derive a prescription for computing two-point correlation functions of scalar fields in a time-dependent background geometry which is modeled by a mirror moving in the bulk of AdS space. By studying this model we want to make a further step towards a holographic description of thermalization. The reason for that is that thermalization corresponds to time-dependent backgrounds which evolve to form black hole horizon giving notion of temperature. For mirror trajectories preserving the scaling symmetry of the AdS space we obtain time-dependent two-point correlators whose singularity structure is related to the physics of bouncing light ray between the moving mirror and the AdS boundary. Such a relation is known so far only to the time-independent case, i.e. static mirror [69]. For arbitrary trajectories of the mirror along the radial direction of the AdS space, we use a WKB analysis and obtain a general prescription for calculating the two-point correlator (5.52).

Outlook Modeling the process of thermalization of strongly coupled medium like quark-gluon plasma is extremely complicated, even using gauge/gravity methods, because early stages of the thermalization require the understanding far-from-equilibrium physics. Another reason is the time-dependence of the process. Our toy model of mirror moving in the bulk of AdS is very far away from a realistic model for holographic thermalization. One big disadvantage of our model is the absence of any notation for the temperature. This is because we work in AdS space and not, for example, in AdS black hole geometries.

Our analysis, however, provides essential technical tools for the study of two-point functions in time-dependent geometries. These tools may serve as a starting point for studying the behavior of two-point functions in a more complex time-dependent backgrounds which are more suitable to describe the process of thermalization in strongly coupled field theories. For instance, the two-point function obtained for a moving mirror in AdS space can be generalized to the case of a gravitational collapsing geometry [40, 41]. The time-dependent geometry is then described by a collapsing spherical shell where inside the shell the geometry is AdS and outside the shell the geometry is AdS black hole. Using the Israel junction conditions [182], the matching of the coordinates inside and outside the shell gives the equation of motion of the collapsing shell. A direct generalization of our work in chapter 5 would be replacement of the mirror trajectory by a collapsing shell trajectory. This will involve solving the wave equation in a thermal AdS background outside the collapsing shell, and the Dirichlet boundary condition used here has to be replaced by a matching condition of a scalar outside and inside the shell.

Many other possible direct extensions of our work have been mentioned earlier in the concluding sections called 'Summary and outlook' at the end of each chapter, e.g. in sections 3.4.4, 4.4 and 5.5. Here, we would like to mention one further possible extension of the work which is relevant to both subjects presented in chapter 3 and 4.

One of the motivation for studying the conductivity of flavor fields in a SYM plasma as presented in chapter 4 comes from the results of the work in [51], where it was shown that scaling arguments lead to universal non-linearities in transport such as in conductivity if the system is near the quantum critical point. In chapter 4 we study the transport of flavor fields moving in a $\mathcal{N} = 4$ SYM plasma, which is dual a D3/D7 brane setup described in section 4.2.2. This setup does not possess a quantum critical point in the phase diagram. In chapter 3, however, we find two gravity setups which show continuous quantum phase transitions which indicate the existence of a quantum critical point in these systems. Thus the next logical step is studying conductivity with the U(2) Einstein-Yang-Mills theory in section 3.3 or with the D3/D7 model setup in section 3.4. In both setups, there are already notations for charge densities. For studying conductivity we need to turn on additional spatial components of the Maxwell fields which give rise to the electromagnetic fields. Analytical

results for the conductivity in the $U(2)$ Einstein-Yang-Mills setup seem quite promising, since the position of the quantum critical point can be determined analytically.

Acknowledgments

First of all, I want to express my gratitude to Johanna Erdmenger for her tremendous efforts in supervising my work during the last three years. I am very thankful for her patience, constant willingness to help, intensive care, great support and encouragement. Also I have benefited a lot from her ability for creating a very stimulating and solidary atmosphere in our work group.

Furthermore, I would like to thank Dieter Lüst for providing excellent working conditions in his groups at the Max-Planck-Institut für Physik (Werner-Heisenberg-Institut) and at the Ludwig- Maximilians- Universität in Munich. I also thank him for working through this thesis as an interested second referee.

Moreover, I would like to thank my external supervisor Michael Haack for his constant interest on the progress of my work. I would like to thank Rosita Jurgeleit and Monika Goldammer for their administrative assistance and I want to thank Thomas Hahn for his great computer support.

I thank Martin Ammon, Johanna Erdmenger, Viviane Grass, Patrick Kerner, Shu Lin and Andy O'Bannon for the fruitful collaboration.

I would like to thank the International Max Planck Research School for providing various seminars and promoting interchanges among the Ph. D. students. In particular, I would like to thank Frank Steffen und Otmar Biebel for their great efforts in organizing many interesting colloquia at many pleasant places.

I also thank my fellows Saeid Aminian, Martin Ammon, Veselin Filev, Jan Germer, Viviane Grass, Constantin Greubel, Sebastian Halter, Daniel Härtl, Johannes Held, Stephan Höhne, Matthias Kaminski, Patrick Kerner, Phillip Kostka, Shu Lin, René Meyer, Steffen Müller, Dao Thi Nhung, Le Duc Ninh, Andy O'Bannon, Felix Rust, Jonathan Schock, Katja Seidel, Martin Spinrath, Migael Strydom and Hansjörg Zeller for sharing many pleasant moments during the last few years.

I am indebted to Johanna Erdmenger, Jan Germer, Constantin Greubel, Patrick Kerner, Migael Strydom and Hansjörg Zeller for many comments on the manuscript.

Finally, I want to thank Na, Sophie, my parents and family for their constant care, support and encouragement at any time.

Flavor transport

A.1 Derivatives of the on-shell action

In this appendix we write explicit expressions for derivatives of the on-shell action with respect to various fields, as mentioned in section 4.3.

For notational simplicity, we first define a function

$$d(u) = g_{uu}|g_{tt}|g_{xx}^3 - g_{xx}A_2 - A_4, \tag{A.1}$$

where A_2 and A_4 were defined in eqs. (4.17), which we repeat here for completeness:

$$A_2 = g_{uu}g_{xx}\tilde{E}^2 + g_{tt}g_{uu}(\tilde{B}_x^2 + \tilde{B}_z^2) + g_{xx}^2\tilde{A}_t'^2 + g_{tt}g_{xx}\left(\tilde{A}_x'^2 + \tilde{A}_y'^2 + \tilde{A}_z'^2\right),$$

$$A_4 = g_{xx}\tilde{E}^2\left(\tilde{A}_y'^2 + \tilde{A}_z'^2\right) + g_{xx}\tilde{A}_t'^2\left(\tilde{B}_x^2 + \tilde{B}_z^2\right) + g_{uu}\tilde{E}^2\tilde{B}_x^2 + g_{tt}\tilde{B}_z^2\tilde{A}_z'^2$$
$$+ g_{tt}\tilde{B}_x^2\tilde{A}_x'^2 + 2g_{tt}\tilde{B}_x\tilde{B}_z\tilde{A}_x'\tilde{A}_z' - 2g_{xx}\tilde{E}\tilde{B}_z\tilde{A}_t'\tilde{A}_y'. \tag{A.2}$$

Recall from section 4.2 that in our notation g_{uu} represents the uu component of the induced D7-brane metric: $g_{uu} = \frac{1}{u^2} + \theta'(u)^2$.

The derivatives $\frac{\partial L}{\partial F_{\mu\nu}}$, evaluated on our solution, are

$$\frac{\partial L}{\partial E_x} = \frac{\mathcal{N}\cos^3\theta}{\sqrt{d(u)}}\left[g_{xx}\tilde{B}_z\tilde{A}_t'\tilde{A}_y' - \tilde{E}\left(g_{uu}\left(g_{xx}^2 + \tilde{B}_x^2\right) + g_{xx}\left(\tilde{A}_y'^2 + \tilde{A}_z'^2\right)\right)\right],$$

$$\frac{\partial L}{\partial E_y} = \frac{\mathcal{N}\cos^3\theta}{\sqrt{d(u)}}\left[\left(\tilde{E}\tilde{A}_x'\tilde{A}_y' + \tilde{B}_x\tilde{A}_t'\tilde{A}_z' - \tilde{B}_z\tilde{A}_t'\tilde{A}_x'\right)g_{xx}\right],$$

$$\frac{\partial L}{\partial E_z} = \frac{\mathcal{N}\cos^3\theta}{\sqrt{d(u)}}\left[g_{xx}\tilde{E}\tilde{A}_x'\tilde{A}_z' - g_{xx}\tilde{B}_x\tilde{A}_t'\tilde{A}_y' - g_{uu}\tilde{E}\tilde{B}_x\tilde{B}_z\right],$$

$$\frac{\partial L}{\partial B_x} = \frac{\mathcal{N}\cos^3\theta}{\sqrt{d(u)}}\left[\tilde{B}_x\left(g_{uu}|g_{tt}|g_{xx} + |g_{tt}|\tilde{A}_x'^2 - g_{xx}\tilde{A}_t'^2 - g_{uu}\tilde{E}^2\right)\right.$$
$$\left.+|g_{tt}|\tilde{B}_z\tilde{A}_x'\tilde{A}_z'\right],$$

$$\frac{\partial L}{\partial B_y} = \frac{\mathcal{N}\cos^3\theta}{\sqrt{d(u)}}\left[|g_{tt}|\tilde{B}_x\tilde{A}_x'\tilde{A}_y' + |g_{tt}|\tilde{B}_z\tilde{A}_y'\tilde{A}_z' - g_{xx}\tilde{E}\tilde{A}_t'\tilde{A}_z'\right], \quad \text{(A.3)}$$

$$\frac{\partial L}{\partial B_z} = \frac{\mathcal{N}\cos^3\theta}{\sqrt{d(u)}}\left[\tilde{B}_z\left(g_{uu}|g_{tt}|g_{xx} + |g_{tt}|\tilde{A}_z'^2 - g_{xx}\tilde{A}_t'^2\right)\right.$$
$$\left.+|g_{tt}|\tilde{B}_x\tilde{A}_x'\tilde{A}_z' + g_{xx}\tilde{E}\tilde{A}_t'\tilde{A}_y'\right].$$

The variations with respect to the $\partial_\mu\theta$ (with $\mu = t, x, y, z$), evaluated on our solution, are

$$\frac{\delta L}{\delta\partial_t\theta} = -\frac{\mathcal{N}\cos^3\theta}{\sqrt{d(u)}}\left[\tilde{B}_x\tilde{B}_z\tilde{A}_z' + \tilde{A}_x'\left(g_{xx}^2 + \tilde{B}_x^2\right)\right]\tilde{E}\,\theta',$$

$$\frac{\delta L}{\delta\partial_x\theta} = -\frac{\mathcal{N}\cos^3\theta}{\sqrt{d(u)}}\left[|g_{tt}|g_{xx}\tilde{B}_z\tilde{A}_y' - \tilde{E}\tilde{A}_t'\left(g_{xx}^2 + \tilde{B}_x^2\right)\right]\theta',$$

$$\frac{\delta L}{\delta\partial_y\theta} = -\frac{\mathcal{N}\cos^3\theta}{\sqrt{d(u)}}\left[\tilde{B}_x\tilde{A}_z'\left(|g_{tt}|g_{xx} - \tilde{E}^2\right) - |g_{tt}|g_{xx}\tilde{B}_z\tilde{A}_x'\right]\theta',$$

$$\frac{\delta L}{\delta\partial_z\theta} = +\frac{\mathcal{N}\cos^3\theta}{\sqrt{d(u)}}\left[\tilde{E}\tilde{B}_z\tilde{A}_t' + \tilde{A}_y'\left(|g_{tt}|g_{xx} - \tilde{E}^2\right)\right]\tilde{B}_x\,\theta'.$$

Toy model for holographic thermalization

B.1   The UV limit of (5.25)

The core of the correlator (5.25) is the following integral

$$\frac{1}{2\pi i}\int d\lambda \left(\frac{\Gamma(\lambda+1)A}{\Gamma(\lambda+\frac{1-d}{2})}+\frac{\Gamma(1-\lambda)B}{\Gamma(\frac{1-d}{2}-\lambda)}\right)\left(\frac{\Gamma(\lambda+1)A}{\Gamma(\lambda+\frac{1+d}{2})}+\frac{\Gamma(1-\lambda)B}{\Gamma(\frac{1+d}{2}-\lambda)}\right)^{-1}\left(\frac{t}{t'}\right)^{\lambda}.$$

(B.1)

For definiteness, from (5.12) we take

$$A = (u_0+1)^{\lambda}F(\frac{1-d}{2},\frac{1+d}{2};-\lambda+1;\frac{1-u_0}{2}),$$ (B.2)

$$B = -(u_0-1)^{\lambda}F(\frac{1-d}{2},\frac{1+d}{2};\lambda+1;\frac{1-u_0}{2}).$$

First of all, we note that the integrand (denoted as $F(\lambda,t,t')$) has the property: $F(\lambda^*,t,t') = F^*(\lambda,t,t')$. Combined with the fact that the integration path is the imaginary axis, we see the integral is manifestly real, which is consistent with the reality condition of the correlator. We will use the residue theorem to evaluate (B.1). The UV part of the correlator is given by the contribution from poles with large $|\lambda|$. For this, we do an asymptotic expansion of the integrand. The following properties of Γ-functions and Hypergeometric functions are useful [183]:

$$\frac{\Gamma(\lambda+\alpha)}{\Gamma(\lambda+\beta)} \sim \lambda^{\alpha-\beta}; \quad \frac{\Gamma(-\lambda+\alpha)}{\Gamma(-\lambda+\beta)} \sim \frac{\sin\pi(\lambda-\beta)}{\sin\pi(\lambda-\alpha)}\lambda^{\alpha-\beta};$$

$$\lim_{\gamma\to\infty} F(\alpha,\beta;\gamma;z) = 1.$$

(B.3)

A branch cut at the negative real axis is needed, with the argument of λ fixed by $|arg\, z| < \pi$. Using the above asymptotic behavior, we obtain the integrand $\sim \lambda^d (\frac{t}{t'})^\lambda$ as $\lambda \to \infty$. If $t > t'$, we close the contour counter-clockwise and the integral receives contribution from poles in the left half complex plane, while if $t < t'$, we close the contour clockwise then the integral receives contribution from poles in the right half complex plane.

The possible poles in the whole complex plane are poles of the Gamma function, Hypergeometric function and roots of

$$\frac{\Gamma(\lambda + 1)}{\Gamma(\lambda + \frac{1+d}{2})} A + \frac{\Gamma(-\lambda + 1)}{\Gamma(-\lambda + \frac{1+d}{2})} B = 0 \,. \tag{B.4}$$

Note that $F(\alpha, \beta; \gamma, z)$ as a function of γ has the same singularities as $\Gamma(\gamma)$ [183], we can show that all the poles of the Gamma function and Hypergeometric function are removable. Thus we are only left with roots of (B.4). Due to the non-algebraic nature of (B.4), finding analytic expression of all the roots is not possible. However, we can deduce a general property of the roots: (B.4) can be equivalently written as

$$\frac{\Gamma(\lambda + 1)}{\Gamma(\lambda + \frac{1+d}{2})} \left(\frac{u_0 + 1}{u_0 - 1} \right)^{\frac{\lambda}{2}} F(\frac{1-d}{2}, \frac{1+d}{2}; -\lambda + 1; \frac{1 - u_0}{2}) =$$

$$\frac{\Gamma(-\lambda + 1)}{\Gamma(-\lambda + \frac{1+d}{2})} \left(\frac{u_0 + 1}{u_0 - 1} \right)^{\frac{-\lambda}{2}} F(\frac{1-d}{2}, \frac{1+d}{2}; \lambda + 1; \frac{1 - u_0}{2}),$$

or $R(\lambda) = R(-\lambda)$ with

$$R(\lambda) = \frac{\Gamma(\lambda + 1)}{\Gamma(\lambda + \frac{1+d}{2})} \left(\frac{u_0 + 1}{u_0 - 1} \right)^{\frac{\lambda}{2}} F(\frac{1-d}{2}, \frac{1+d}{2}; -\lambda + 1; \frac{1 - u_0}{2}) \,. \tag{B.5}$$

We note that $R(\lambda^*) = R^*(\lambda)$. It is easy to show that if λ is a root of (B.4), $-\lambda, \lambda^*, -\lambda^*$ are also roots. We plot the left hand side of (B.4) in the complex λ plane, and find the zeros lie nearly equally spaced on the imaginary axis. Therefore, we conclude that the roots must be purely imaginary. Now let us determine the asymptotic form of the roots. In the limit $\lambda \to \infty \, (\Lambda \to \infty)$, (B.4) has the following asymptotic expression

$$\lambda^{\frac{1-d}{2}} \left[(u_0 + 1)^\lambda - (u_0 - 1)^\lambda e^{\pm i\pi \frac{d-1}{2}} \right], \tag{B.6}$$

and the root is given by

$$\lambda = \pm i\pi \frac{\frac{d-1}{2} + 2k}{\ln \frac{u_0 + 1}{u_0 - 1}} \,, \tag{B.7}$$

with integer $k \geq 0$. Our approximate roots indeed are consistent with numerical plots in the sense that they are symmetric with respect to the real axis and equally spaced. Furthermore we expect (B.7) to be more accurate when $\ln \frac{u_0+1}{u_0-1} \to 0$, i.e. $u_0 \to \infty$. As the mirror moves more and more slowly, essentially all modes are effectively UV.

The poles lie precisely along the integration contour of λ. In order to obtain a well defined result, we have to deform the contour to circumvent the poles. The ambiguity associated with the detour corresponds to the different causal natures of the resulting correlator[1]. In practice, it is easy to calculate the advanced correlator, for which we shift the integration of λ slightly to the left. Then all the UV poles lie to the right of the contour. The integration contour has to be closed counter-clockwise, which requires $t' > t$. In this way, we can avoid the branch cut on the negative real axis. The residue at each root is obtained with asymptotic expressions as

$$\left(\frac{\Gamma(\lambda+1)A}{\Gamma(\lambda+\frac{1-d}{2})} + \frac{\Gamma(1-\lambda)B}{\Gamma(\frac{1-d}{2}-\lambda)} \right) \frac{d}{d\lambda} \left[\frac{\Gamma(\lambda+1)A}{\Gamma(\lambda+\frac{1+d}{2})} + \frac{\Gamma(1-\lambda)B}{\Gamma(\frac{1+d}{2}-\lambda)} \right] \left(\frac{t}{t'} \right)^\lambda \to \lambda^d \left(\frac{t}{t'} \right)^\lambda \frac{1-e^{\mp i\pi d}}{\ln \frac{u_0+1}{u_0-1}}.$$
$$(B.8)$$

We are happy to see the emergence of the factor $(1-e^{\mp i\pi d})$, which will precisely cancel the pole from $\frac{\Gamma(-d)}{\Gamma(\frac{1-d}{2})}$. Denote $a = \ln \frac{u_0+1}{u_0-1}$ and $b = \ln \frac{t}{t'}$. The correlator is given by the sum of residues

$$\left\langle \int d^{d-1}x\, O(t,x)O(t',0) \right\rangle_A = -d\theta(t'-t) \sum_{k=0}^{\infty} 2^d \lambda^d e^{b\lambda} \frac{1-e^{\mp i\pi d}}{a(tt')^{\frac{d+1}{2}}} \frac{\Gamma(-d)\Gamma(\frac{1+d}{2})}{\Gamma(\frac{1-d}{2})\Gamma(d)}$$
$$(B.9)$$

evaluated at $\lambda = \pm i\pi \frac{\frac{d-1}{2}+2k}{a}$. The subscript 'A' stands for the advanced correlator. We find that the sum over k can be expressed in terms of the Lerch transcendent function $\Phi(z,s,\alpha)$

$$\left\langle \int d^{d-1}x\, O(t,x)O(t',0) \right\rangle_A = -d \sum_{+,-} \frac{\theta(t'-t)}{(tt')^{\frac{d+1}{2}}} e^{\pm \frac{i(d-1)\pi b}{2a}} \left(\frac{\pm 2i\pi}{a} \right)^d \frac{1-e^{\mp i\pi d}}{a}$$
$$\times \frac{\Gamma(-d)\Gamma(\frac{1+d}{2})}{\Gamma(\frac{1-d}{2})\Gamma(d)} 2^d \Phi\left(e^{\pm \frac{2i\pi b}{a}}, -d, \frac{d-1}{4} \right).$$

---

[1]The ambiguity is familiar in the standard calculation of the vacuum correlator. It can be fixed by a prescription of the integration contour of the frequency

As $d \rightarrow$ integer, this reduces to

$$
\langle \int d^{d-1} x O(t, x) O(t', 0) \rangle_A = -d \sum_{+,-} \theta(t'-t)(tt')^{\frac{-d-1}{2}} \left(\frac{2}{a}\right)^d \frac{1 - e^{\mp i\pi d}}{a}
$$

$$
\times \frac{\Gamma(-d)\Gamma(\frac{1+d}{2})}{\Gamma(\frac{1-d}{2})\Gamma(d)} e^{\pm \frac{i\pi(d-1)}{2}(\frac{b}{a}-c)}
$$

$$
\times \left[\frac{d!}{(-c)^{d+1}(\pm i 2\pi)} - \sum_{r=0}^{\infty} \frac{B_{d+r+1}(\frac{d-1}{4}) c^r (\pm i 2\pi)^{d+r}}{r!(d+r+1)} \right],
$$

(B.10)

where the $B_n(x)$ are the Bernoulli polynomials [184]. The constant c is defined as $e^{i 2\pi c} = e^{\frac{i 2\pi b}{a}}$ with $|c| < \frac{1}{2}$. To obtain the retarded correlator, we note a useful property of the integrand: $F(\lambda, t, t') = F(-\lambda, t', t)$. This leads to the following relation between retarded and advanced correlators,

$$
\langle \int d^{d-1} x O(t, x) O(t', 0) \rangle_A = \langle \int d^{d-1} x O(t', x) O(t, 0) \rangle_R .
$$

(B.11)

B.2 Spatially integrated correlator in $d = 3$ and $d = 4$

We begin with the unintegrated correlator with conformal dimension d. The retarded correlator is given by [185]

$$
G^R(t, \vec{x}) = -i \frac{\Gamma(d+1)}{\pi^{d/2}\Gamma(\frac{d}{2})} \theta(t) \left(\frac{1}{(-(t-i\epsilon)^2 + \vec{x}^2)^d} - \frac{1}{(-(t+i\epsilon)^2 + \vec{x}^2)^d} \right) .
$$

(B.12)

We note the retarded correlator only has support at $t = r = |\vec{x}|$. Integrated with $\int d^{d-1} x$ for $d = 3$, we obtain

$$
\int d^2 x G^R(t, \vec{x}) = \frac{6i}{\pi} \left(\frac{1}{(-(t-i\epsilon)^2 + r^2)^2} - \frac{1}{(-(t+i\epsilon)^2 + r^2)^2} \right) \Big|_{r=0}^{\infty} .
$$

(B.13)

In the limit $\epsilon \rightarrow 0$, this vanishes identically.

For $d = 4$, we have, apart from rational function of t and r, also the logarithmic function, which makes the $i\epsilon$ prescription relevant

$$
\int d^3 x G^R(t, \vec{x}) = -\frac{3}{\pi} \left(\frac{\ln(r - (t - i\epsilon))}{(t - i\epsilon)^5} - \frac{\ln(r - (t + i\epsilon))}{(t + i\epsilon)^5} \right) \Big|_{r=0}^{\infty} + \cdots
$$

(B.14)

The terms in $\cdots$ drop out as the limit $\epsilon \to 0$ is taken. The logarithmic terms give rise to a finite contribution

$$\int d^3 x G^R(t, \vec{x}) = -\theta(t)\frac{6}{t^5} \, . \tag{B.15}$$

This agrees with $-d\frac{\delta \phi^d(t)}{\delta \phi^0(t')}$ when (5.26) is used in $d = 4$ dimension.

B.3 Evaluation of equation (5.62)

The core part of (5.62) is given by

$$\int d\tilde{t} d\lambda d\lambda' \left(\frac{\Gamma(\lambda+1)\Gamma(-\lambda+1)}{\Gamma(\lambda+\frac{1-d}{2})\Gamma(\frac{1+d}{2}-\lambda)} - \frac{\Gamma(\lambda+1)\Gamma(-\lambda+1)}{\Gamma(\lambda+\frac{1+d}{2})\Gamma(\frac{1-d}{2}-\lambda)} \right)$$

$$\times \frac{\Gamma(\lambda'+\frac{1+d}{2})\Gamma(-\lambda'+\frac{1+d}{2})}{\Gamma(\lambda'+1)\Gamma(-\lambda'+1)} \times \left(e^{\lambda\tilde{t}}\frac{\Gamma(-\lambda+\frac{1+d}{2})}{\Gamma(-\lambda+1)} - e^{-\lambda\tilde{t}}\frac{\Gamma(\lambda+\frac{1+d}{2})}{\Gamma(\lambda+1)} \right)$$

$$\times \left(e^{\lambda'\tilde{t}}\frac{\Gamma(\lambda'+1)}{\Gamma(\lambda'+\frac{1+d}{2})} + e^{-\lambda'\tilde{t}}\frac{\Gamma(-\lambda'+1)}{\Gamma(-\lambda'+\frac{1+d}{2})} \right) t^\lambda t'^{-\lambda'} \, . \tag{B.16}$$

Note that $\tilde{t} = \ln(t + \sqrt{t^2 - 1}) \geq 0$. We introduce an upper cutoff T to regularize the $\tilde{t}$ integral. With $\tilde{t}$ integrated out, (B.16) takes the following form

$$\int d\lambda d\lambda' \left(\frac{\Gamma(\lambda+1)\Gamma(-\lambda+1)}{\Gamma(\lambda+\frac{1-d}{2})\Gamma(\frac{1+d}{2}-\lambda)} - \frac{\Gamma(\lambda+1)\Gamma(-\lambda+1)}{\Gamma(\lambda+\frac{1+d}{2})\Gamma(\frac{1-d}{2}-\lambda)} \right)$$

$$\times \frac{\Gamma(\lambda'+\frac{1+d}{2})\Gamma(-\lambda'+\frac{1+d}{2})}{\Gamma(\lambda'+1)\Gamma(-\lambda'+1)} t^\lambda t'^{-\lambda'}$$

$$\times \left[\frac{\Gamma(\frac{1+d}{2}-\lambda)\Gamma(\lambda'+1)}{\Gamma(1-\lambda)\Gamma(\lambda'+\frac{1+d}{2})} \frac{e^{(\lambda+\lambda')T}-1}{\lambda+\lambda'} + \frac{\Gamma(\frac{1+d}{2}-\lambda)\Gamma(1-\lambda')}{\Gamma(-\lambda+1)\Gamma(-\lambda'+\frac{1+d}{2})} \frac{e^{(\lambda-\lambda')T}-1}{\lambda-\lambda'} \right.$$

$$\left. - \frac{\Gamma(\lambda+\frac{1+d}{2})\Gamma(\lambda'+1)}{\Gamma(\lambda+1)\Gamma(\lambda'+\frac{1+d}{2})} \frac{e^{(-\lambda+\lambda')T}-1}{-\lambda+\lambda'} - \frac{\Gamma(\lambda+\frac{1+d}{2})\Gamma(1-\lambda')}{\Gamma(\lambda+1)\Gamma(\frac{1+d}{2}-\lambda')} \frac{e^{(-\lambda-\lambda')T}-1}{-\lambda-\lambda'} \right] \, . \tag{B.17}$$

We now use the residue theorem to evaluate the integrals of λ and λ'. Note that the appearance of $\frac{e^{(\pm\lambda\pm\lambda')T}-1}{\pm\lambda\pm\lambda'}$ does not introduce any new poles as they have finite limits when $\pm\lambda \pm \lambda' \to 0$. We begin with the integral of λ'. It is helpful to keep in mind that $t, t' > 1$ since the "mirror" does not leave the boundary until $t = 1$. Completing the λ' integral, we find only the first and third terms in the bracket contribute and the dependence on the cutoff T drops out naturally.

We obtain the result

$$
2\pi i \int d\lambda \left(\frac{\Gamma(\lambda+1)\Gamma(-\lambda+1)}{\Gamma(\lambda+\frac{1-d}{2})\Gamma(-\lambda+\frac{1+d}{2})} - \frac{\Gamma(\lambda+1)\Gamma(-\lambda+1)}{\Gamma(\lambda+\frac{1+d}{2})\Gamma(-\lambda+\frac{1-d}{2})} \right) t^\lambda
$$
$$
\times \sum_{n=0}^{\infty} \frac{(-1)^n}{n!\,\Gamma(1-n-\frac{1+d}{2})} \left[\frac{-t'^{-n-\frac{1+d}{2}}}{\lambda+n+\frac{1+d}{2}} \frac{\Gamma(\frac{1+d}{2}-\lambda)}{\Gamma(1-\lambda)} + \frac{t'^{-n-\frac{1+d}{2}}}{n-\lambda+\frac{1+d}{2}} \frac{\Gamma(\lambda+\frac{1+d}{2})}{\Gamma(\lambda+1)} \right].
$$

(B.18)

We again perform the contour integral. This time it is much simpler: As $t > 1$, only the poles in the left half plane contribute. Considering the first term in the sum, we find that poles at $\lambda + 1 = -m$ for $m \in \{0, 1, 2 \cdots\}$ and $\lambda + n + \frac{1+d}{2} = 0$ are relevant. The contribution from the first set of poles is proportional to

$$
\sum_{m=0}^{\infty} \frac{(-1)^m t^{-m-1}}{m!\,(m+1-n-\frac{1+d}{2})} \left[\frac{1}{\Gamma(\frac{1-d}{2}-m-1)} - \frac{\Gamma(m+1+\frac{1+d}{2})}{\Gamma(m+1+\frac{1-d}{2})\Gamma(\frac{1+d}{2}-m-1)} \right]
$$
$$
= \left[\frac{\sin(\frac{\pi(3+d)}{2})\Gamma(\frac{3+d}{2})}{\pi} - \frac{1}{\Gamma(\frac{-1-d}{2})} \right] F\left(\frac{3+d}{2}, -n+\frac{1-d}{2}; -n+\frac{3-d}{2}, \frac{1}{t} \right) \frac{1}{t(n+\frac{d-1}{2})}.
$$

(B.19)

We note that the d-dependent prefactor vanishes identically by the properties of the Gamma function. The pole at $\lambda + n + \frac{1+d}{2} = 0$ gives the contribution

$$
\sum_{n=0}^{\infty} -\frac{(-1)^n}{n!} \left(\frac{1}{\Gamma(-n-d)} - \frac{\Gamma(1+d+n)}{\Gamma(1+n)\Gamma(-n)} \right) (tt')^{-n-\frac{1+d}{2}} = -\frac{1}{\Gamma(-d)} \frac{(tt')^{\frac{1+d}{2}}}{(tt'-1)^{1+d}},
$$

(B.20)

where $\frac{1}{\Gamma(-d)}$ cancels the overall divergent factor $\Gamma(-d)$ to yield a finite numerical coefficient. Next we consider the second term in the sum of (B.18), the relevant poles are at $\lambda + \frac{1+d}{2} = -m$, with the contributions

$$
\sum_{n,m=0}^{\infty} \frac{(-1)^{m+n}}{m!n!} \frac{\Gamma(m+\frac{1+d}{2}+1)}{\Gamma(-n-\frac{1+d}{2}+1)\Gamma(-m-d)\Gamma(m+1+d)} \frac{t^{-m-\frac{1+d}{2}} t'^{-n-\frac{1+d}{2}}}{m+n+1+d}
$$
$$
= \sum_{n,m=0}^{\infty} \frac{(-1)^{m+n}}{m!n!} \frac{\sin\pi(n+\frac{d-1}{2})\Gamma(n+\frac{1+d}{2})}{\pi} \frac{\sin\pi(m+d)\Gamma(m+\frac{1+d}{2}+1)}{\pi}
$$
$$
\times \frac{t'^{-n} t^{-m}}{m+n+1+d} (tt')^{-\frac{1+d}{2}}
$$
$$
= \sum_{n,m=0}^{\infty} \frac{\sin\pi\frac{d-1}{2}\sin\pi d}{\pi^2} \frac{\Gamma(\frac{1+d}{2})\Gamma(\frac{3+d}{2})}{1+d} \frac{(\frac{1+d}{2})_n(\frac{3+d}{2})_m(1+d)_{m+n}}{(2+d)_{m+n}m!n!} (tt')^{-\frac{1+d}{2}},
$$

where $(\alpha)_m = \frac{\Gamma(\alpha+m)}{\Gamma(\alpha)}$ is the Pochhammer symbol. The double sum can be expressed in terms of Appell function, which again can be converted to a Hypergeometric function

$$\frac{\sin\pi\frac{d-1}{2}\sin\pi d}{\pi^2}\frac{\Gamma(\frac{1+d}{2})\Gamma(\frac{3+d}{2})}{1+d}F_1\left(1+d,\frac{3+d}{2},\frac{1+d}{2},2+d,\frac{1}{t},\frac{1}{t'}\right)(tt')^{-\frac{1+d}{2}}$$

$$=\frac{\sin\pi\frac{d-1}{2}\sin\pi d}{\pi^2}\frac{\Gamma(\frac{1+d}{2})\Gamma(\frac{3+d}{2})}{1+d}\left(1-\frac{1}{t'}\right)^{-1-d}$$

$$\times F\left(1+d,\frac{3+d}{2},2+d;\frac{t'-t}{(t'-1)\,t}\right)(tt')^{-\frac{1+d}{2}}.$$

Writting sin-functions as product of two Γ-functions, collecting all nonvanishing terms and inserting the overall factor, we end up with the following result

$$\frac{\delta\phi^d(t)}{\delta\phi^0(t')}=-\frac{\Gamma(\frac{1+d}{2})2^{d-1}}{\Gamma(\frac{1-d}{2})\Gamma(d)}\left[-\frac{1}{(tt'-1)^{1+d}}\right.$$

$$\left.+\frac{\Gamma(\frac{1+d}{2})}{2\Gamma(\frac{1-d}{2})\Gamma(1+d)}F\left(1+d,\frac{3+d}{2},2+d;\frac{t'-t}{(t'-1)\,t}\right)\frac{1}{(tt'-t)^{1+d}}\right].$$

$$(B.21)$$

Bibliography

[1] M. Ammon, T. H. Ngo, and A. O'Bannon, *Holographic Flavor Transport in Arbitrary Constant Background Fields*, JHEP **10** (2009) 027, arXiv:0908.2625.

[2] J. Erdmenger, S. Lin, and T. H. Ngo, *A moving mirror in AdS space as a toy model for holographic thermalization*, JHEP **04** (2011) 035, arXiv:1101.5505.

[3] J. Erdmenger, V. Grass, P. Kerner, and T. H. Ngo, *Holographic Superfluidity in Imbalanced Mixtures*, arXiv:1103.4145.

[4] **DONUT** Collaboration, K. Kodama *et al.*, *Observation of tau-neutrino interactions*, Phys. Lett. **B504** (2001) 218–224, arXiv:hep-ex/0012035.

[5] B. Zwiebach, *A First Course in String Theory*. Cambridge University Press, second edition ed., 2009.

[6] J. Polchinski, *String Theory*, vol. I+II. Cambridge University Press, paperback ed., 2005.

[7] L. A. Anchordoqui, H. Goldberg, X. Huang, D. Lust, and T. R. Taylor, *Stringy origin of Tevatron Wjj anomaly*, arXiv:1104.2302.

[8] D. Lust, S. Stieberger, and T. R. Taylor, *The LHC String Hunter's Companion*, Nucl. Phys. **B808** (2009) 1–52, arXiv:0807.3333.

[9] K. Becker, M. Becker, and J. H. Schwarz, *String Theory and M-Theory*. Cambridge University Press, 2007.

[10] J. M. Maldacena, *The large N limit of superconformal field theories and supergravity*, Adv. Theor. Math. Phys. **2** (1998) 231–252, arXiv:hep-th/9711200.

[11] S. S. Gubser, I. R. Klebanov, and A. M. Polyakov, *Gauge theory correlators from non-critical string theory*, Phys. Lett. **B428** (1998) 105–114, arXiv:hep-th/9802109.

[12] E. Witten, *Anti-de Sitter space and holography*, Adv. Theor. Math. Phys. **2** (1998) 253–291, arXiv:hep-th/9802150.

[13] O. Aharony, S. S. Gubser, J. M. Maldacena, H. Ooguri, and Y. Oz, *Large N field theories, string theory and gravity*, Phys. Rept. **323** (2000) 183–386, arXiv:hep-th/9905111.

[14] E. D'Hoker and D. Z. Freedman, *Supersymmetric gauge theories and the AdS/CFT correspondence*, arXiv:hep-th/0201253.

[15] S. A. Hartnoll, C. P. Herzog, and G. T. Horowitz, *Building a Holographic Superconductor*, Phys. Rev. Lett. **101** (2008) 031601, arXiv:0803.3295.

[16] S. A. Hartnoll, C. P. Herzog, and G. T. Horowitz, *Holographic Superconductors*, JHEP **12** (2008) 015, arXiv:0810.1563.

[17] M. Ammon, J. Erdmenger, M. Kaminski, and P. Kerner, *Superconductivity from gauge/gravity duality with flavor*, Phys. Lett. **B680** (2009) 516–520, arXiv:0810.2316.

[18] M. Ammon, J. Erdmenger, M. Kaminski, and P. Kerner, *Flavor Superconductivity from Gauge/Gravity Duality*, JHEP **10** (2009) 067, arXiv:0903.1864.

[19] S. A. Hartnoll, *Lectures on holographic methods for condensed matter physics*, Class. Quant. Grav. **26** (2009) 224002, arXiv:0903.3246.

[20] C. P. Herzog, *Lectures on Holographic Superfluidity and Superconductivity*, J. Phys. **A42** (2009) 343001, arXiv:0904.1975.

[21] G. T. Horowitz, *Introduction to Holographic Superconductors*, arXiv:1002.1722.

[22] J. McGreevy, *Holographic duality with a view toward many-body physics*, Adv. High Energy Phys. **2010** (2010) 723105, arXiv:0909.0518.

[23] M. Kaminski, *Flavor Superconductivity and Superfluidity*, arXiv:1002.4886.

[24] S. Sachdev, *Quantum Phase Transitions*. Cambridge University Press, paperback ed., 2001.

[25] K. Jensen, A. Karch, and E. G. Thompson, *A Holographic Quantum Critical Point at Finite Magnetic Field and Finite Density*, JHEP **05** (2010) 015, arXiv:1002.2447.

[26] N. Evans, K. Jensen, and K.-Y. Kim, *Non Mean-Field Quantum Critical Points from Holography*, Phys. Rev. **D82** (2010) 105012, arXiv:1008.1889.

[27] K. Jensen, *More Holographic Berezinskii-Kosterlitz-Thouless Transitions*, Phys. Rev. **D82** (2010) 046005, arXiv:1006.3066.

[28] E. D'Hoker and P. Kraus, *Magnetic Field Induced Quantum Criticality via new Asymptotically AdS_5 Solutions*, Class. Quant. Grav. **27** (2010) 215022, arXiv:1006.2573.

[29] **BRAHMS** Collaboration, I. Arsene *et al.*, *Quark Gluon Plasma an Color Glass Condensate at RHIC? The perspective from the BRAHMS experiment*, Nucl. Phys. **A757** (2005) 1–27, arXiv:nucl-ex/0410020.

[30] **PHENIX** Collaboration, K. Adcox *et al.*, *Formation of dense partonic matter in relativistic nucleus nucleus collisions at RHIC: Experimental evaluation by the PHENIX collaboration*, Nucl. Phys. **A757** (2005) 184–283, arXiv:nucl-ex/0410003.

[31] B. B. Back *et al.*, *The PHOBOS perspective on discoveries at RHIC*, Nucl. Phys. **A757** (2005) 28–101, arXiv:nucl-ex/0410022.

[32] G. Policastro, D. T. Son, and A. O. Starinets, *The shear viscosity of strongly coupled N = 4 supersymmetric Yang-Mills plasma*, Phys. Rev. Lett. **87** (2001) 081601, arXiv:hep-th/0104066.

[33] P. Kovtun, D. T. Son, and A. O. Starinets, *Viscosity in strongly interacting quantum field theories from black hole physics*, Phys. Rev. Lett. **94** (2005) 111601, arXiv:hep-th/0405231.

[34] J. Casalderrey-Solana, H. Liu, D. Mateos, K. Rajagopal, and U. A. Wiedemann, *Gauge/String Duality, Hot QCD and Heavy Ion Collisions*, arXiv:1101.0618.

[35] H. Liu, K. Rajagopal, and U. A. Wiedemann, *Calculating the jet quenching parameter from AdS/CFT*, Phys. Rev. Lett. **97** (2006) 182301, arXiv:hep-ph/0605178.

[36] H. Liu, K. Rajagopal, and U. A. Wiedemann, *Wilson loops in heavy ion collisions and their calculation in AdS/CFT*, JHEP **03** (2007) 066, arXiv:hep-ph/0612168.

[37] C. P. Herzog, A. Karch, P. Kovtun, C. Kozcaz, and L. G. Yaffe, *Energy loss of a heavy quark moving through N = 4 supersymmetric Yang-Mills plasma*, JHEP **07** (2006) 013, arXiv:hep-th/0605158.

[38] S. D. Avramis and K. Sfetsos, *Supergravity and the jet quenching parameter in the presence of R-charge densities*, JHEP **01** (2007) 065, arXiv:hep-th/0606190.

[39] S. S. Gubser, *Drag force in AdS/CFT*, Phys. Rev. **D74** (2006) 126005, arXiv:hep-th/0605182.

[40] S. B. Giddings and A. Nudelman, *Gravitational collapse and its boundary description in AdS*, JHEP **02** (2002) 003, arXiv:hep-th/0112099.

[41] S. Lin and E. Shuryak, *Toward the AdS/CFT Gravity Dual for High Energy Collisions. 3.Gravitationally Collapsing Shell and Quasiequilibrium*, Phys. Rev. **D78** (2008) 125018, arXiv:0808.0910.

[42] P. M. Chesler and L. G. Yaffe, *Horizon formation and far-from-equilibrium isotropization in supersymmetric Yang-Mills plasma*, Phys. Rev. Lett. **102** (2009) 211601, arXiv:0812.2053.

[43] P. M. Chesler and L. G. Yaffe, *Boost invariant flow, black hole formation, and far-from- equilibrium dynamics in N = 4 supersymmetric Yang-Mills theory*, Phys. Rev. **D82** (2010) 026006, arXiv:0906.4426.

[44] S. Bhattacharyya and S. Minwalla, *Weak Field Black Hole Formation in Asymptotically AdS Spacetimes*, JHEP **09** (2009) 034, arXiv:0904.0464.

[45] S. Sachdev, *Quantum magnetism and criticality*, Nature Physics **4** (Mar., 2008) 173–185, arXiv:0711.3015.

[46] S. Sachdev, *Where is the quantum critical point in the cuprate superconductors?*, arXiv:0907.0008.

[47] S. Sachdev, *Condensed matter and AdS/CFT*, arXiv:1002.2947.

[48] M. Ammon, J. Erdmenger, V. Grass, P. Kerner, and A. O'Bannon, *On Holographic p-wave Superfluids with Back-reaction*, Phys. Lett. **B686** (2010) 192–198, arXiv:0912.3515.

[49] Y. Shin, C. Schunck, A. Schirotzek, and W. Ketterle, *Phase diagram of a two-component Fermi gas with resonant interactions*, Nature **451** (2008), no. 4, 689–693.

[50] L.-y. He, M. Jin, and P.-f. Zhuang, *Pion superfluidity and meson properties at finite isospin density*, Phys. Rev. **D71** (2005) 116001, arXiv:hep-ph/0503272.

[51] A. G. Green and S. L. Sondhi, *Nonlinear Quantum Critical Transport and the Schwinger Mechanism for a Superfluid-Mott-Insulator Transition of Bosons*, Phys. Rev. Lett. **95** (Dec, 2005) 267001.

[52] A. Karch and A. O'Bannon, *Metallic AdS/CFT*, JHEP **09** (2007) 024, arXiv:0705.3870.

[53] A. O'Bannon, *Hall Conductivity of Flavor Fields from AdS/CFT*, Phys. Rev. **D76** (2007) 086007, arXiv:0708.1994.

[54] A. Karch, A. O'Bannon, and E. Thompson, *The Stress-Energy Tensor of Flavor Fields from AdS/CFT*, arXiv:0812.3629.

[55] D. Grumiller and P. Romatschke, *On the collision of two shock waves in AdS5*, JHEP **08** (2008) 027, arXiv:0803.3226.

[56] J. L. Albacete, Y. V. Kovchegov, and A. Taliotis, *Modeling Heavy Ion Collisions in AdS/CFT*, JHEP **07** (2008) 100, arXiv:0805.2927.

[57] S. S. Gubser, S. S. Pufu, and A. Yarom, *Entropy production in collisions of gravitational shock waves and of heavy ions*, Phys. Rev. **D78** (2008) 066014, arXiv:0805.1551.

[58] S. Lin and E. Shuryak, *Grazing Collisions of Gravitational Shock Waves and Entropy Production in Heavy Ion Collision*, Phys. Rev. **D79** (2009) 124015, arXiv:0902.1508.

[59] Y. V. Kovchegov and S. Lin, *Toward Thermalization in Heavy Ion Collisions at Strong Coupling*, JHEP **03** (2010) 057, arXiv:0911.4707.

[60] I. Y. Aref'eva, A. A. Bagrov, and L. V. Joukovskaya, *Critical Trapped Surfaces Formation in the Collision of Ultrarelativistic Charges in (A)dS*, JHEP **03** (2010) 002, arXiv:0909.1294.

[61] I. Y. Aref'eva, A. A. Bagrov, and E. A. Guseva, *Critical Formation of Trapped Surfaces in the Collision of Non-expanding Gravitational Shock Waves in de Sitter Space- Time*, JHEP **12** (2009) 009, arXiv:0905.1087.

[62] S. Lin and E. Shuryak, *On the critical condition in gravitational shock wave collision and heavy ion collisions*, Phys. Rev. **D83** (2011) 045025, arXiv:1011.1918.

[63] A. Taliotis, *Heavy Ion Collisions with Transverse Dynamics from Evolving AdS Geometries*, JHEP **09** (2010) 102, arXiv:1004.3500.

[64] A. Taliotis, *Evolving Geometries in General Relativity*, arXiv:1007.1452.

[65] A. Duenas-Vidal and M. A. Vazquez-Mozo, *Colliding AdS gravitational shock waves in various dimensions and holography*, JHEP **07** (2010) 021, arXiv:1004.2609.

[66] P. M. Chesler and L. G. Yaffe, *Holography and colliding gravitational shock waves in asymptotically AdS5 spacetime*, Phys. Rev. Lett. **106** (2011) 021601, arXiv:1011.3562.

[67] U. H. Danielsson, E. Keski-Vakkuri, and M. Kruczenski, *Spherically collapsing matter in AdS, holography, and shellons*, Nucl. Phys. **B563** (1999) 279–292, arXiv:hep-th/9905227.

[68] U. H. Danielsson, E. Keski-Vakkuri, and M. Kruczenski, *Black hole formation in AdS and thermalization on the boundary*, JHEP **02** (2000) 039, arXiv:hep-th/9912209.

[69] I. Amado and C. Hoyos-Badajoz, *AdS black holes as reflecting cavities*, JHEP **09** (2008) 118, arXiv:0807.2337.

[70] J. Wess and J. Bagger, *Supersymmetry and Supergravity.* Princeton University Press, 2nd edition ed., 1992.

[71] J. Polchinski, *Dirichlet-Branes and Ramond-Ramond Charges*, Phys. Rev. Lett. **75** (1995) 4724–4727, arXiv:hep-th/9510017.

[72] J. Polchinski, *Lectures on D-branes*, arXiv:hep-th/9611050.

[73] E. Witten, *Bound states of strings and p-branes*, Nucl. Phys. **B460** (1996) 335–350, arXiv:hep-th/9510135.

[74] R. G. Leigh, *Dirac-Born-Infeld Action from Dirichlet Sigma Model*, Mod. Phys. Lett. **A4** (1989) 2767.

[75] E. Witten, *Solutions of four-dimensional field theories via M- theory*, Nucl. Phys. **B500** (1997) 3–42, arXiv:hep-th/9703166.

[76] C. V. Johnson, *D-Branes*. Cambridge University Press, 2003.

[77] G. T. Horowitz and A. Strominger, *Black strings and p-branes*, Nuclear Physics B **360** (1991) 197–209.

[78] N. Beisert *et al.*, *Review of AdS/CFT Integrability: An Overview*, arXiv:1012.3982.

[79] T. Hooft, *A planar diagram theory for strong interactions*, Nuclear Physics B **72** (1974) 461–473.

[80] F. Rust, *In-medium effects in the holographic quark-gluon plasma*, Adv. High Energy Phys. **2010** (2010) 564624, arXiv:1003.0187.

[81] D. T. Son and A. O. Starinets, *Minkowski-space correlators in AdS/CFT correspondence: Recipe and applications*, JHEP **09** (2002) 042, arXiv:hep-th/0205051.

[82] J. M. Figueroa-O'Farrill, *BUSSTEPP lectures on supersymmetry*, arXiv:hep-th/0109172.

[83] N. Beisert, *The dilatation operator of N = 4 super Yang-Mills theory and integrability*, Phys. Rept. **405** (2005) 1–202, arXiv:hep-th/0407277.

[84] I. R. Klebanov, *Testing the AdS/CFT Correspondence*, AIP Conf. Proc. **1031** (2008) 3–20.

[85] V. Balasubramanian and P. Kraus, *Spacetime and the holographic renormalization group*, Phys. Rev. Lett. **83** (1999) 3605–3608, arXiv:hep-th/9903190.

[86] P. Breitenlohner and D. Z. Freedman, *Positive Energy in anti-De Sitter Backgrounds and Gauged Extended Supergravity*, Phys. Lett. **B115** (1982) 197.

[87] P. Breitenlohner and D. Z. Freedman, *Stability in Gauged Extended Supergravity*, Ann. Phys. **144** (1982) 249.

[88] P. K. Townsend, *Positive energy and the scalar potential in higher dimensional (super)gravity theories*, Phys. Lett. **B148** (1984) 55.

[89] S. Lee, S. Minwalla, M. Rangamani, and N. Seiberg, *Three-point functions of chiral operators in D = 4, N = 4 SYM at large N*, Adv. Theor. Math. Phys. **2** (1998) 697–718, arXiv:hep-th/9806074.

[90] K. G. Wilson, *Confinement of quarks*, Phys. Rev. D **10** (Oct, 1974) 2445–2459.

[91] J. M. Maldacena, *Wilson loops in large N field theories*, Phys. Rev. Lett. **80** (1998) 4859–4862, arXiv:hep-th/9803002.

[92] S.-J. Rey and J.-T. Yee, *Macroscopic strings as heavy quarks in large N gauge theory and anti-de Sitter supergravity*, Eur. Phys. J. **C22** (2001) 379–394, arXiv:hep-th/9803001.

[93] E. Witten, *Anti-de Sitter space, thermal phase transition, and confinement in gauge theories*, Adv. Theor. Math. Phys. **2** (1998) 505–532, arXiv:hep-th/9803131.

[94] A. K. Das, *Topics in finite temperature field theory*, arXiv:hep-ph/0004125.

[95] S. M. Carroll, *Spacetime and Geometry*. Adison Wesley, 2004.

[96] S. W. Hawking and D. N. Page, *Thermodynamics of Black Holes in anti-De Sitter Space*, Commun. Math. Phys. **87** (1983) 577.

[97] V. E. Hubeny and M. Rangamani, *A holographic view on physics out of equilibrium*, Adv. High Energy Phys. **2010** (2010) 297916, arXiv:1006.3675.

[98] S.-J. Rey, S. Theisen, and J.-T. Yee, *Wilson-Polyakov loop at finite temperature in large N gauge theory and anti-de Sitter supergravity*, Nucl. Phys. **B527** (1998) 171–186, arXiv:hep-th/9803135.

[99] A. Karch and E. Katz, *Adding flavor to AdS/CFT*, JHEP **06** (2002) 043, arXiv:hep-th/0205236.

[100] J. Erdmenger, N. Evans, I. Kirsch, and E. Threlfall, *Mesons in Gauge/Gravity Duals - A Review*, Eur. Phys. J. **A35** (2008) 81–133, arXiv:0711.4467.

[101] M. Grana and J. Polchinski, *Gauge / gravity duals with holomorphic dilaton*, Phys. Rev. **D65** (2002) 126005, arXiv:hep-th/0106014.

[102] M. Bertolini, P. Di Vecchia, M. Frau, A. Lerda, and R. Marotta, *N = 2 gauge theories on systems of fractional D3/D7 branes*, Nucl. Phys. **B621** (2002) 157–178, arXiv:hep-th/0107057.

[103] F. Bigazzi *et al.*, *D3-D7 Quark-Gluon Plasmas*, JHEP **11** (2009) 117, arXiv:0909.2865.

[104] F. Bigazzi, A. L. Cotrone, J. Mas, D. Mayerson, and J. Tarrio, *D3-D7 Quark-Gluon Plasmas at Finite Baryon Density*, JHEP **04** (2011) 060, arXiv:1101.3560.

[105] S. Kobayashi, D. Mateos, S. Matsuura, R. C. Myers, and R. M. Thomson, *Holographic phase transitions at finite baryon density*, JHEP **02** (2007) 016, arXiv:hep-th/0611099.

[106] K. Skenderis, *Lecture notes on holographic renormalization*, Class. Quant. Grav. **19** (2002) 5849–5876, arXiv:hep-th/0209067.

[107] A. Karch, A. O'Bannon, and K. Skenderis, *Holographic renormalization of probe D-branes in AdS/CFT*, JHEP **04** (2006) 015, arXiv:hep-th/0512125.

[108] J. Babington, J. Erdmenger, N. J. Evans, Z. Guralnik, and I. Kirsch, *Chiral symmetry breaking and pions in non-supersymmetric gauge / gravity duals*, Phys. Rev. **D69** (2004) 066007, arXiv:hep-th/0306018.

[109] V. G. Filev, C. V. Johnson, R. C. Rashkov, and K. S. Viswanathan, *Flavoured large N gauge theory in an external magnetic field*, JHEP **10** (2007) 019, arXiv:hep-th/0701001.

[110] J. Erdmenger, R. Meyer, and J. P. Shock, *AdS/CFT with Flavour in Electric and Magnetic Kalb-Ramond Fields*, JHEP **12** (2007) 091, arXiv:0709.1551.

[111] J. Polchinski and M. J. Strassler, *The string dual of a confining four-dimensional gauge theory*, arXiv:hep-th/0003136.

[112] H. Liu, J. McGreevy, and D. Vegh, *Non-Fermi liquids from holography*, arXiv:0903.2477.

[113] J. D. Bekenstein, *Black hole hair: Twenty-five years after*, arXiv:gr-qc/9605059.

[114] S. S. Gubser, *Breaking an Abelian gauge symmetry near a black hole horizon*, Phys. Rev. **D78** (2008) 065034, arXiv:0801.2977.

[115] M. N. Chernodub and A. S. Nedelin, *Phase diagram of chirally imbalanced QCD matter*, arXiv:1102.0188.

[116] M. Tinkham, *Introduction to Superconductivity*. McGraw-Hill Kogakusha, Ltd., 1975.

[117] V. L. Ginzburg and L. D. Landau, *On the Theory of superconductivity*, Zh. Eksp. Teor. Fiz. **20** (1950) 1064–1082.

[118] K. Maeda and T. Okamura, *Characteristic length of an AdS/CFT superconductor*, Phys. Rev. **D78** (2008) 106006, arXiv:0809.3079.

[119] H.-B. Zeng, Z.-Y. Fan, and H.-S. Zong, *Superconducting Coherence Length and Magnetic Penetration Depth of a p-wave Holographic Superconductor*, Phys. Rev. **D81** (2010) 106001, arXiv:0912.4928.

[120] O. Aharony, O. Bergman, D. L. Jafferis, and J. Maldacena, *N=6 superconformal Chern-Simons-matter theories, M2-branes and their gravity duals*, JHEP **10** (2008) 091, arXiv:0806.1218.

[121] R. C. Myers, *Dielectric-branes*, JHEP **12** (1999) 022, arXiv:hep-th/9910053.

[122] A. Karch and A. O'Bannon, *Holographic Thermodynamics at Finite Baryon Density: Some Exact Results*, JHEP **11** (2007) 074, arXiv:0709.0570.

[123] J. Erdmenger, M. Kaminski, P. Kerner, and F. Rust, *Finite baryon and isospin chemical potential in AdS/CFT with flavor*, JHEP **11** (2008) 031, arXiv:0807.2663.

[124] A. O'Bannon, *Toward a Holographic Model of Superconducting Fermions*, JHEP **01** (2009) 074, arXiv:0811.0198.

[125] M. Ammon, J. Erdmenger, M. Kaminski, and A. O'Bannon, *Fermionic Operator Mixing in Holographic p-wave Superfluids*, JHEP **05** (2010) 053, arXiv:1003.1134.

[126] S. K. Rama, S. Sarkar, B. Sathiapalan, and N. Sircar, *Strong Coupling BCS Superconductivity and Holography*, arXiv:1104.2843.

[127] S. S. Gubser and S. S. Pufu, *The gravity dual of a p-wave superconductor*, JHEP **11** (2008) 033, arXiv:0805.2960.

[128] S. S. Gubser, *Colorful horizons with charge in anti-de Sitter space*, Phys. Rev. Lett. **101** (2008) 191601, arXiv:0803.3483.

[129] P. Basu, J. He, A. Mukherjee, and H.-H. Shieh, *Hard-gapped Holographic Superconductors*, Phys. Lett. **B689** (2010) 45–50, arXiv:0911.4999.

[130] R. Manvelyan, E. Radu, and D. H. Tchrakian, *New AdS non Abelian black holes with superconducting horizons*, Phys. Lett. **B677** (2009) 79–87, arXiv:0812.3531.

[131] V. Balasubramanian and P. Kraus, *A stress tensor for anti-de Sitter gravity*, Commun. Math. Phys. **208** (1999) 413–428, arXiv:hep-th/9902121.

[132] S. de Haro, S. N. Solodukhin, and K. Skenderis, *Holographic reconstruction of spacetime and renormalization in the AdS/CFT correspondence*, Commun. Math. Phys. **217** (2001) 595–622, arXiv:hep-th/0002230.

[133] N. Iqbal, H. Liu, M. Mezei, and Q. Si, *Quantum phase transitions in holographic models of magnetism and superconductors*, Phys. Rev. **D82** (2010) 045002, arXiv:1003.0010.

[134] D. B. Kaplan, J.-W. Lee, D. T. Son, and M. A. Stephanov, *Conformality Lost*, Phys. Rev. **D80** (2009) 125005, arXiv:0905.4752.

[135] G. T. Horowitz and M. M. Roberts, *Zero Temperature Limit of Holographic Superconductors*, JHEP **11** (2009) 015, arXiv:0908.3677.

[136] C. P. Herzog and S. S. Pufu, *The Second Sound of SU(2)*, JHEP **04** (2009) 126, arXiv:0902.0409.

[137] C. P. Herzog, *An Analytic Holographic Superconductor*, Phys. Rev. **D81** (2010) 126009, arXiv:1003.3278.

[138] P. Basu, J. He, A. Mukherjee, and H.-H. Shieh, *Superconductivity from D3/D7: Holographic Pion Superfluid*, JHEP **11** (2009) 070, arXiv:0810.3970.

[139] P. Koerber and A. Sevrin, *The non-abelian D-brane effective action through order alpha'**4*, JHEP **10** (2002) 046, arXiv:hep-th/0208044.

[140] A. A. Tseytlin, *On non-abelian generalisation of the Born-Infeld action in string theory*, Nucl. Phys. **B501** (1997) 41–52, arXiv:hep-th/9701125.

[141] A. Hashimoto and W. Taylor, *Fluctuation spectra of tilted and intersecting D-branes from the Born-Infeld action*, Nucl. Phys. **B503** (1997) 193–219, arXiv:hep-th/9703217.

[142] N. R. Constable, R. C. Myers, and O. Tafjord, *The noncommutative bion core*, Phys. Rev. **D61** (2000) 106009, arXiv:hep-th/9911136.

[143] R. C. Myers and M. C. Wapler, *Transport Properties of Holographic Defects*, JHEP **12** (2008) 115, arXiv:0811.0480.

[144] D. Mateos, S. Matsuura, R. C. Myers, and R. M. Thomson, *Holographic phase transitions at finite chemical potential*, JHEP **11** (2007) 085, arXiv:0709.1225.

[145] D. Mateos, R. C. Myers, and R. M. Thomson, *Thermodynamics of the brane*, JHEP **05** (2007) 067, arXiv:hep-th/0701132.

[146] J. Erdmenger, M. Kaminski, and F. Rust, *Holographic vector mesons from spectral functions at finite baryon or isospin density*, Phys. Rev. **D77** (2008) 046005, arXiv:0710.0334.

[147] A. Karch and S. L. Sondhi, *Non-linear, Finite Frequency Quantum Critical Transport from AdS/CFT*,. Comments: 16 pages.

[148] A. O'Bannon, *Holographic Thermodynamics and Transport of Flavor Fields*, arXiv:0808.1115.

[149] S. S. Gubser and A. Yarom, *Linearized hydrodynamics from probe-sources in the gauge- string duality*, arXiv:0803.0081.

[150] C. P. Herzog, P. Kovtun, S. Sachdev, and D. T. Son, *Quantum critical transport, duality, and M-theory*, Phys. Rev. **D75** (2007) 085020, arXiv:hep-th/0701036.

[151] S. A. Hartnoll and P. Kovtun, *Hall conductivity from dyonic black holes*, Phys. Rev. **D76** (2007) 066001, arXiv:0704.1160.

[152] S. A. Hartnoll, P. K. Kovtun, M. Muller, and S. Sachdev, *Theory of the Nernst effect near quantum phase transitions in condensed matter, and in dyonic black holes*, Phys. Rev. **B76** (2007) 144502, arXiv:0706.3215.

[153] S. A. Hartnoll and C. P. Herzog, *Ohm's Law at strong coupling: S duality and the cyclotron resonance*, Phys. Rev. **D76** (2007) 106012, arXiv:0706.3228.

[154] J. Erdmenger, M. Haack, M. Kaminski, and A. Yarom, *Fluid dynamics of R-charged black holes*, JHEP **01** (2009) 055, arXiv:0809.2488.

[155] N. Banerjee *et al.*, *Hydrodynamics from charged black branes*, JHEP **01** (2011) 094, arXiv:0809.2596.

[156] D. T. Son and P. Surowka, *Hydrodynamics with Triangle Anomalies*, Phys. Rev. Lett. **103** (2009) 191601, arXiv:0906.5044.

[157] A. Karch and A. O'Bannon, *Chiral transition of N = 4 super Yang-Mills with flavor on a 3-sphere*, Phys. Rev. **D74** (2006) 085033, arXiv:hep-th/0605120.

[158] I. Kirsch, *Generalizations of the AdS/CFT correspondence*, Fortsch. Phys. **52** (2004) 727–826, arXiv:hep-th/0406274.

[159] K. Ghoroku, T. Sakaguchi, N. Uekusa, and M. Yahiro, *Flavor quark at high temperature from a holographic model*, Phys. Rev. **D71** (2005) 106002, arXiv:hep-th/0502088.

[160] D. Mateos, R. C. Myers, and R. M. Thomson, *Holographic phase transitions with fundamental matter*, Phys. Rev. Lett. **97** (2006) 091601, arXiv:hep-th/0605046.

[161] T. Albash, V. G. Filev, C. V. Johnson, and A. Kundu, *A topology-changing phase transition and the dynamics of flavour*, Phys. Rev. **D77** (2008) 066004, arXiv:hep-th/0605088.

[162] C. Hoyos-Badajoz, K. Landsteiner, and S. Montero, *Holographic Meson Melting*, JHEP **04** (2007) 031, arXiv:hep-th/0612169.

[163] T. Albash, V. G. Filev, C. V. Johnson, and A. Kundu, *Finite Temperature Large N Gauge Theory with Quarks in an External Magnetic Field*, JHEP **07** (2008) 080, arXiv:0709.1547.

[164] A. O'Bannon, *Toward a Holographic Model of Superconducting Fermions*, JHEP **01** (2009) 074, arXiv:0811.0198.

[165] R. M. Wald, *General Relativity*,. Chicago, Usa: Univ. Pr. (1984) 491p.

[166] R. A. Janik and R. B. Peschanski, *Asymptotic perfect fluid dynamics as a consequence of AdS/CFT*, Phys. Rev. **D73** (2006) 045013, arXiv:hep-th/0512162.

[167] M. P. Heller and R. A. Janik, *Viscous hydrodynamics relaxation time from AdS/CFT*, Phys. Rev. **D76** (2007) 025027, arXiv:hep-th/0703243.

[168] J. Abajo-Arrastia, J. Aparicio, and E. Lopez, *Holographic Evolution of Entanglement Entropy*, JHEP **11** (2010) 149, arXiv:1006.4090.

[169] T. Albash and C. V. Johnson, *Evolution of Holographic Entanglement Entropy after Thermal and Electromagnetic Quenches*, New J. Phys. **13** (2011) 045017, arXiv:1008.3027.

[170] V. Balasubramanian *et al.*, *Thermalization of Strongly Coupled Field Theories*, arXiv:1012.4753.

[171] V. E. Hubeny, H. Liu, and M. Rangamani, *Bulk-cone singularities and signatures of horizon formation in AdS/CFT*, JHEP **01** (2007) 009, arXiv:hep-th/0610041.

[172] D. Z. Freedman, S. D. Mathur, A. Matusis, and L. Rastelli, *Correlation functions in the CFT(d)/AdS($d+1$) correspondence*, Nucl. Phys. **B546** (1999) 96–118, arXiv:hep-th/9804058.

[173] K.-c. Chou, Z.-b. Su, B.-l. Hao, and L. Yu, *Equilibrium and Nonequilibrium Formalisms Made Unified*, Phys. Rept. **118** (1985) 1.

[174] N. P. Landsman and C. G. van Weert, *Real and Imaginary Time Field Theory at Finite Temperature and Density*, Phys. Rept. **145** (1987) 141.

[175] K. Skenderis and B. C. van Rees, *Real-time gauge/gravity duality*, Phys. Rev. Lett. **101** (2008) 081601, arXiv:0805.0150.

[176] K. Skenderis and B. C. van Rees, *Real-time gauge/gravity duality: Prescription, Renormalization and Examples*, JHEP **05** (2009) 085, arXiv:0812.2909.

[177] B. C. van Rees, *Real-time gauge/gravity duality and ingoing boundary conditions*, Nucl. Phys. Proc. Suppl. **192-193** (2009) 193–196, arXiv:0902.4010.

[178] F. G. Tricomi, *Integral equations*. Dover, New York, USA, 1985.

[179] T. Banks, M. R. Douglas, G. T. Horowitz, and E. J. Martinec, *AdS dynamics from conformal field theory*, arXiv:hep-th/9808016.

[180] V. Balasubramanian and S. F. Ross, *Holographic particle detection*, Phys. Rev. **D61** (2000) 044007, arXiv:hep-th/9906226.

[181] R. A. Janik and R. B. Peschanski, *Gauge / gravity duality and thermalization of a boost- invariant perfect fluid*, Phys. Rev. **D74** (2006) 046007, arXiv:hep-th/0606149.

[182] W. Israel, *Singular hypersurfaces and thin shells in general relativity*, Nuovo Cim. **B44S10** (1966) 1.

[183] W. Zhuxi and G. Dunren, *An introduction to special functions*. Chinese Scientific, Beijing China, 2000.

[184] I. S. Gradshteyn and I. M. Ryzhik, *Tables of integrals, series and products*. Academic Press, Boston, USA, 7 ed., 2007.

[185] E. Barnes, D. Vaman, C. Wu, and P. Arnold, *Real-time finite-temperature correlators from AdS/CFT*, Phys. Rev. **D82** (2010) 025019, arXiv:1004.1179.

Lebenslauf

Persönliche Daten

Vor- und Zuname	Hai, Ngo Thanh
Geboren am	19. Februar 1981 in Hanoi, Vietnam
Staatsangehörigkeit	Vietnamesisch
Familienstand	verheiratet, eine Tochter

Ausbildung

09/1986 – 02/1996	Schulbesuch in Hanoi, Vietnam
03/1996 – 08/1998	Besuch der Mittelschule-Ost in Werdau, Sachsen
09/1998 – 07/2001	Besuch des Alexander v. Humboldt-Gymnasiums in Werdau
10/2001 – 07/2004	Physikstudium an der Humboldt-Universität zu Berlin
08/2004 – 06/2005	Physikstudium an der 'University of Illinois at Urbana-Champaign', USA
07/2005 – 12/2007	Physikhauptstudium an der Humboldt-Universität zu Berlin
11/2007	Diplomarbeit: "Wilson loops and the static quark-antiquark potential in the AdS/CFT correspondence"
05/2008 – 05/2011	Promotionsstudium an der Ludwig-Maximilians-Universität und am Max-Planck-Insitut für Physik in München
05/2011	Dissertation: "Gauge/gravity duality: From quantum phase transitions towards out-of-equilibrium physics"